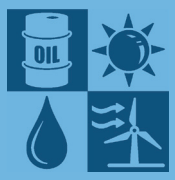

Groundwater Quantity and Quality

Edited by

John A. Luczaj and Dallas Blaney

Printed Edition of the Special Issue Published in *Resources*

www.mdpi.com/journal/resources

John A. Luczaj and Dallas Blaney (Eds.)

Groundwater Quantity and Quality

This book is a reprint of the Special Issue that appeared in the online, open access journal, *Resources* (ISSN 2079-9276) from 2015–2016 (available at: http://www.mdpi.com/journal/resources/special_issues/groundwater).

Guest Editors
John A. Luczaj
Department of Natural & Applied Sciences University of Wisconsin
USA

Dallas Blaney
Challenge Aspen
USA

Editorial Office
MDPI AG
Klybeckstrasse 64
Basel, Switzerland

Publisher
Shu-Kun Lin

Assistant Editor
Qian Jiao

1. Edition 2016

MDPI • Basel • Beijing • Wuhan • Barcelona

ISBN 978-3-03842-235-8 (Hbk)
ISBN 978-3-03842-205-1 (PDF)

Table of Contents

List of Contributors

Sana'a Al-Zyoud: Applied Earth and Environmental Sciences Department, Institute of Earth and Environmental Sciences, Al al-Bayt University, P.O. Box 130040, Mafraq 25113, Jordan.
Muhammad Basharat: International Waterlogging and Salinity Research Institute (IWASRI), Water and Power Development Authority (WAPDA), Lahore 54000, Pakistan.
Carmelo Bellia: National Institute of Advanced Industrial Science and Technology (AIST), Geological Survey of Japan, 1-1-1 Higashi, Tsukuba, Ibaraki 305-8561, Japan.
Kevin Erb: University of Wisconsin-Extension Environmental Resources Center, 1150 Bellevue St, Green Bay, WI 54302, USA.
Ehsan Forootan: Institute of Geodesy and Geoinformation, Bonn University, Nussallee 17, Bonn 53115, Germany.
Adrian H. Gallardo: Argentina National Scientific and Technical Research Council (CONICET), FCFMyN, Department of Geology, San Luis National University, Ejercito de los Andes 950, San Luis 5700, Argentina.
Gary M. Gold: The University of Texas at Austin, 204 E. Dean Keeton Street, Stop C2200, Austin, TX 78712, USA.
Marja-Liisa Hänninen: Department of Food and Environmental Hygiene, Faculty of Veterinary Medicine, University of Helsinki, P.O.Box 66, Helsinki 00014, Finland.
Eija Isomäki: Finnish Environment Institute, P.O.Box 140, Helsinki 00251, Finland.
Tiina Juselius: Department of Food and Environmental Hygiene, Faculty of Veterinary Medicine, University of Helsinki, P.O.Box 66, Helsinki 00014, Finland.
Kohei Kazahaya: National Institute of Advanced Industrial Science and Technology (AIST), Geological Survey of Japan, 1-1-1 Higashi, Tsukuba, Ibaraki 305-8561, Japan.
Anna-Liisa Kivimäki: Finnish Environment Institute, P.O.Box 140, Helsinki 00251, Finland; The Water Protection Association of the River Vantaa and Helsinki Region, Asemapäällikönkatu 12 B, Helsinki 00520, Finland.
Jill B. Kjellsson: Department of Civil, Architectural and Environmental Engineering, The University of Texas at Austin, 204 E. Dean Keeton St. Stop C2200, Austin, TX 78712, USA.
Vikram Koundinya: University of Wisconsin-Extension Environmental Resources Center, 445 Henry Mall, Madison, WI 53706, USA.
Kirsti Lahti: The Water Protection Association of the River Vantaa and Helsinki Region, Asemapäällikönkatu 12 B, Helsinki 00520, Finland.
Bakhshal Khan Lashari: Institute of Water Resources Engineering and Management, Mehran University of Engineering and Technology (MUET), Jamshoro 76062, Pakistan.
John Luczaj: Department of Natural & Applied Sciences, University of Wisconsin-Green Bay, Green Bay, WI 54311, USA.
Kevin Masarik: Center for Watershed Science and Education, University of Wisconsin-Stevens Point, Stevens Point, WI 54481, USA.
Ilkka T. Miettinen: National Institute for Health and Welfare, P.O.BOX 95, Kuopio 70701, Finland.

Mark W. Piersol: Department of Geological Sciences, University of Idaho, Moscow, ID 83844-3022, USA.
Tarja Pitkänen: National Institute for Health and Welfare, P.O.BOX 95, Kuopio 70701, Finland.
Eric Ronk: University of Wisconsin-Extension, 206 Court Street, Chilton WI 53014, USA.
Wolfram Rühaak: Department of Geothermal Science and Technology; Darmstadt Graduate School of Excellence Energy Science and Engineering, Technische Universität Darmstadt, Jovanka-Bontschits-Straße 2, Darmstadt D-64287, Germany.
Ingo Sass: Department of Geothermal Science and Technology; Darmstadt Graduate School of Excellence Energy Science and Engineering, Technische Universität Darmstadt, Jovanka-Bontschits-Straße 2, Darmstadt D-64287, Germany.
Kenneth F. Sprenke: Department of Geological Sciences, University of Idaho, Moscow, ID 83844-3022, USA.
Matti Valve: Finnish Environment Institute, P.O.Box 140, Helsinki 00251, Finland.
Frank van Steenbergen: MetaMeta Research, Hertogenbosch 5211EA2, The Netherlands.
Michael E. Webber: Department of Mechanical Engineering, The University of Texas at Austin, 204 E. Dean Keeton St. Stop C2200, Austin, TX 78712, USA.
Elizabeth Wheat: Department of Public and Environmental Affairs (Political Science), University of Wisconsin-Green Bay, 2420 Nicolet Drive, MAC B327, Green Bay, WI 54311, USA.
Hartmut Wittenberg: Institute of Ecology, Leuphana Universität, C13.015, Scharnhorststr. 1, Lueneburg D21335, Germany.
Masaya Yasuhara: National Institute of Advanced Industrial Science and Technology (AIST), Geological Survey of Japan, 1-1-1 Higashi, Tsukuba, Ibaraki 305-8561, Japan.

About the Guest Editors

John Luczaj a Professor of Geoscience in the Department of Natural and Applied Sciences at the University of Wisconsin-Green Bay, Wisconsin (USA). Luczaj holds his doctorate in Geology from Johns Hopkins University (2000). His research focuses on groundwater quality, water–rock interaction, fluid inclusions in minerals, and sedimentary geology. He is author or coauthor of several refereed articles, a geologic map, and coauthor of the textbook *Earth System History* (4th ed.).

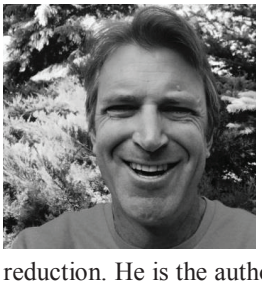

Dallas Blaney serves as the Operations Manager for Challenge Aspen, an adaptive recreation program based in Snowmass Village, Colorado (USA). Formerly, Blaney was an Assistant Professor of Political Science in the Department of Public and Environmental Affairs at the University of Wisconsin-Green Bay. His research focuses on the topic of global environmental politics, with a specific emphasis in global water politics and disaster risk reduction. He is the author of several refereed articles and is currently serving as the technical advisor for a documentary film about the Arkansas River.

Preface

Dear Colleagues,

The world's population is facing a water crisis, which is expected to worsen dramatically during the 21st century. Problems due to over-exploitation of groundwater, as well as from natural and anthropogenic contamination are major challenges facing humanity. This Special Issue on "Groundwater Quantity and Quality" contains a broad selection of eleven articles addressing many different aspects of groundwater quantity and quality, along with an introductory editorial. The research articles and case studies cover many different geographic regions and include examples from both developed and developing nations. The research articles are strong contributions that were selected after a rigorous peer-review process in which not all articles were accepted. We would like to thank the contributors and we hope that the Special Issue of *Resources* will stimulate an interest in groundwater issues.

John A. Luczaj and Dallas Blaney
Guest Editors

Editorial

John Luczaj

Abstract: The world's population is facing a water crisis, which is expected to worsen dramatically during the 21st century. Problems due to over exploitation of groundwater, as well as from natural and anthropogenic contamination are major challenges facing humanity. This Special Issue contributes a selection of topics on groundwater quantity and quality issues that face different parts of the world.

Reprinted from *Resources*. Cite as: Luczaj, J. Groundwater Quantity and Quality. *Resources* **2016**, *5*, 10.

1. Introduction

Groundwater plays an important role in supplying water to much of the global population for use in agriculture, drinking water, and industrial purposes. Physical and/or economic water scarcity occurs on all of the populated continents [1], with some parts of the world facing a genuine water crisis e.g., [2,3]. Water quality problems are both natural and anthropogenic in nature, with emerging contaminants playing an increasing role [1]. Groundwater quantity and quality problems constitute a major set of challenges facing the world during this century.

This Special Issue on Groundwater Quantity and Quality contains a broad selection of eleven articles addressing several different aspects of groundwater quantity and quality. The research articles cover many different geographic regions of the world (Table 1) and include examples from both developed and developing nations. Research articles were selected after a rigorous peer-review process.

Table 1. Geographic locations addressed by articles in this Special Issue.

Geographic Region	Topic	References
Pakistan	Management in Mega-Irrigation Systems	[4]
Jordan	Over Exploitation	[5]
Northwestern U.S.A.	Sustained Drought	[6]
Germany	Groundwater Abstraction; Low-Flow Impact	[7]
Texas, New Mexico, U.S.A.	Case Study of Legal Issues	[8]
Wisconsin, U.S.A.	Groundwater Quality in Karst	[9]
Finland	Groundwater Quality in Public Wells	[10]
Mt. Etna, Italy	Groundwater Quality in a Volcanic System	[11]
Texas, U.S.A.	Energy-Water Nexus	[12,13]
Wisconsin, U.S.A.	Groundwater Issues in a Water-Rich Region	[14] [1]

Note: [1] Review Article.

2. Contributions

The selected papers contained in this Special Issue are described in this section. They fall broadly into three categories: those focused on groundwater quantity, management, legal issues, and over exploitation (five papers); those focused primarily on groundwater quality (three papers); and those focused on the intersection of water resources and renewable energy (two papers). An additional review article provides insight into both quantity and quality challenges facing a water-rich region of the world in the Great Lakes region of United States of America.

2.1. Groundwater Quantity, Management, Legal Issues, and Over Exploitation

Five articles [4–8] examine various aspects of groundwater quantity by addressing groundwater management, legal issues, and over exploitation of groundwater.

The article by van Steenbergen *et al.* [4] presents a regional overview of water issues in the Lower Indus region of Pakistan. They describe the need for updated policies and conjunctive management of surface water and groundwater resources in an area with limited groundwater usage. This need arises for several reasons including the need to reduce waterlogging, increase crop yields, protecting public health, and to improve drinking water conditions in areas with saline groundwater. They supply rationale for reallocating water resources and improving water management policies to more efficiently meet the water requirements of agriculture, domestic, and industrial needs.

A contribution by Al-Zyoud *et al.* [5] provides an updated status of the water crisis in Jordan by illustrating the continued over exploitation of groundwater resources in the Amman Zarqa Basin that has occurred since the 1960s. They list new data about groundwater levels for the past 15 years for wells in the basin, along with an evaluation of GRACE satellite data. The results add to a growing body of evidence that the groundwater resources in the basin are not being used at a sustainable rate, and that significant policy changes are needed to secure enough water resources for future generations.

Piersol and Sprenke [6] illustrate the use of geophysical data and numerical groundwater modeling to better understand aquifer recharge pathways and to predict aquifer water levels. Their study area focused on a portion of the Palouse basin in a semi-arid region of the northwestern continental United States, which is located in the Columbia River Basalt Group and is an important source of water throughout much of the Pacific Northwest region. The article furnishes a better understanding of parts of the aquifer system that should lead to improved groundwater models and management in times of sustained drought.

Wittenberg [7] delivers a multiple regression analysis of how groundwater abstraction for irrigation has impacted low flows of the Ilmenau River in northern Germany. Distinguishing and quantifying the influence of climatic and anthropogenic variables such as precipitation, temperature, and groundwater withdrawal on annual low flows shows that groundwater abstraction for irrigation accounted for an average decrease of low flows of about 25 percent over the past 50 years. The decline of groundwater levels and decreasing low flow conditions have been influenced by the cumulative effect of higher irrigation during drier years.

An article by Wheat [8] contributes a case study of legal issues regarding water apportionment in Texas and New Mexico (United States). At the center of the analysis is a case currently before the U.S. Supreme Court, *Texas v. New Mexico and Colorado* (2013) [15]. The article examines the case involving the Rio Grande Compact and each state's legal obligations for managing and sharing water of the Lower Rio Grande, along with potential impacts of a Supreme Court decision. Texas claims that New Mexico is violating both the Compact and Rio Grande Project Act by using water in excess of its apportionment through its allowance of diversions of surface water and groundwater. The water quantity issues in the region are a major issue due to combined population growth on both sides of the Mexico-United States border, severe drought projections, and increased water demand.

2.2. Groundwater Quality

Three articles [9–11] focused primarily on groundwater quality issues. They were from three distinctly different geographic regions in different geologic settings.

The article by Erb *et al.* [9] focuses on a karst aquifer setting in the Western Great Lakes region of North America. The central issue of their paper was an analysis of the effectiveness of implementing recommendations of a regional "Karst Task Force" report on improving groundwater quality in the region. Four counties were analyzed for changes in water quality (e.g., brown water incidents, detections of bacteria) by comparing years before and after the 2007 report. The two counties in the study that adopted winter manure spreading restrictions on frozen or snow-covered ground showed statistically significant reductions in the instances of BWIs and other well water quality problems. The counties that only promoted education and training, but lacked regulatory action, showed no changes.

An article by Pitkänen *et al.* [10] examines the microbiological and chemical water quality of drinking water in 20 small water supply wells in Finland. They analyzed for enteric pathogens (*i.e.*, *Giardia*, *Cryptosporidium*, *Campylobacter*, noroviruses) and various indicator microbes. Detection of some fecal indicator bacteria and enteric pathogens, including *Giardia*, has revealed a surface water interaction in some of the wells. Their study is significant because most water supplies in the country distribute drinking water without disinfection treatment.

The article by Bellia *et al.* [11] provides a thorough geochemical and isotopic description of a groundwater system in at Mt. Etna Volcano (Sicily, Italy) to better define the groundwater characteristics of its aquifers. Their study found that the geochemical composition varied in parts of the volcano, with most of the groundwater being the Na-Mg ± Ca-HCO_3^- ± (SO_4^{2-} or Cl^-) type. Precipitation is the dominant source of recharge to the aquifers, although seawater mixing is important in coastal areas. Diffusion of gases appears controlled by tectonic structures in the volcano, and the ascent of deep brines also plays a role.

2.3. The Energy-Water Nexus

A pair of articles [12,13] involve the "Energy-Water Nexus" and its application to desalination of brackish groundwater resources.

First, the article by Kjellsson and Webber [12] presents an analysis of the potential for desalinating brackish groundwater using solar energy in Texas, United States. The analysis involves both geographic and depth distributions of brackish waters, along with solar radiation data, to determine the locations with best potential for integrating solar energy with brackish water desalination. Their results predicted that the northwestern region of Texas has the best potential for this application.

The article by Gold and Webber [13] involved a model using both wind and solar energy for reverse-osmosis desalination of brackish groundwater. They analyzed four different power generation models and presented cost analyses for an integrated model using wind and solar energy as part of a grid-connected desalination facility. Their results show that integrating desalination with renewable power can significantly reduce operational costs of water treatment.

2.4. Review Article and Insights from a Water-Rich Region

Also included in this issue is a review article describing the groundwater quantity and quality issues facing a water-rich part of the world in the western Great Lakes region of the United States [14]. Luczaj and Masarik present a comprehensive overview of this topic for the state of Wisconsin. Despite the fact that the region contains some of the world's most abundant surface and groundwater supplies, residents of this state face some significant groundwater quantity and quality challenges. Over exploitation of both confined and unconfined aquifers have led to significant drawdown in some areas, with unconfined aquifer drawdown affecting surface water resources. Water quality concerns are generally a more significant problem, but vary in origin and severity throughout the state. Naturally occurring contaminants include radium, arsenic and associated heavy metals, fluoride, strontium, and others. Anthropogenic contaminants include nitrate, bacteria, viruses, *etc.* The broad coverage of groundwater quantity and quality issues in the article will allow it to serve as a solid foundation reference for researchers in the region.

3. Conclusions

Eleven articles have been selected for this Special Issue. The contributions provide timely assessments of a wide variety of groundwater related problems over a broad geographic range. The coalition of papers should contribute significantly to the fields of groundwater quality and groundwater quantity research.

Acknowledgments: The author of this paper wishes to thank the coeditor of this special issue, the journal editors, and the authors for submitting manuscripts for publication. Referees and editors provided valuable judgment and feedback on the manuscripts, which allowed for substantial improvement in quality in some cases, and rejection of unsuitable manuscripts in other cases.

Conflicts of Interest: The author declares no conflict of interest.

References

1. United Nations Department of Economic and Social Affairs. International Decade for Action. "Water for Life" 2005–2015. Available online: http://www.un.org/waterforlifedecade/scarcity.shtml (accessed on 16 December 2015).
2. USA Today—Pumped Dry: The Global Crisis of Vanishing Groundwater. Available online: http://www.usatoday.com/pages/interactives/groundwater/ (accessed on 16 December 2015).
3. Bigas, H. *The Global Water Crisis: Addressing an Urgent Security Issue*; Papers for the InterAction Council, 2011–2012. UNU-INWEH: Hamilton, Canada, 2012. Available online: http://inweh.unu.edu/wp-content/ uploads/2013/05/WaterSecurity_The-Global-Water-Crisis.pdf (accessed on 16 December 2015).
4. Van Steenbergen, F.; Basharat, M.; Lashari, B.K. Key Challenges and Opportunities for Conjunctive Management of Surface and Groundwater in Mega-Irrigation Systems: Lower Indus, Pakistan. *Resources* **2015**, *4*, 831–856.
5. Al-Zyoud, S.; Rühaak, W.; Forootan, E.; Sass, I. Over Exploitation of Groundwater in the Centre of Amman Zarqa Basin—Jordan: Evaluation of Well Data and GRACE Satellite Observations. *Resources* **2015**, *4*, 819–830.
6. Piersol, M.W.; Sprenke, K.F. A Columbia River Basalt Group Aquifer in Sustained Drought: Insight from Geophysical Methods. *Resources* **2015**, *4*, 577–596.
7. Wittenberg, H. Groundwater Abstraction for Irrigation and Its Impacts on Low Flows in a Watershed in Northwest Germany. *Resources* **2015**, *4*, 566–576.
8. Wheat, E. Groundwater Challenges of the Lower Rio Grande: A Case Study of Legal Issues in Texas and New Mexico. *Resources* **2015**, *4*, 172–184.
9. Erb, K.; Ronk, E.; Koundinya, V.; Luczaj, J. Groundwater Quality Changes in a Karst Aquifer of Northeastern Wisconsin, USA: Reduction of Brown Water Incidence and Bacterial Contamination Resulting from Implementation of Regional Task Force Recommendations. *Resources* **2015**, *4*, 655–672.
10. Pitkänen, T.; Juselius, T.; Isomäki, E.; Miettinen, I.T.; Valve, M.; Kivimäki, A.; Lahti, K.; Hänninen, M. Drinking Water Quality and Occurrence of *Giardia* in Finnish Small Groundwater Supplies. *Resources* **2015**, *4*, 637–654.
11. Bellia, C.; Gallardo, A.H.; Yasuhara, M.; Kazahaya, K. Geochemical Characterization of Groundwater in a Volcanic System. *Resources* **2015**, *4*, 358–377.
12. Kjellsson, J.B.; Webber, M.E. The Energy-Water Nexus: Spatially-Resolved Analysis of the Potential for Desalinating Brackish Groundwater by Use of Solar Energy. *Resources* **2015**, *4*, 476–489.
13. Gold, G.M.; Webber, M.E. The Energy-Water Nexus: An Analysis and Comparison of Various Configurations Integrating Desalination with Renewable Power. *Resources* **2015**, *4*, 227–276.
14. Luczaj, J.; Masarik, K. Groundwater Quantity and Quality Issues in a Water-Rich Region: Examples from Wisconsin, USA. *Resources* **2015**, *4*, 323–357.
15. Texas *v.* New Mexico and Colorado. Available online: www.scotusblog.com/case-files/cases/texas-v-new- mexico-and-colorado (accessed on 29 January 2016).

Key Challenges and Opportunities for Conjunctive Management of Surface and Groundwater in Mega-Irrigation Systems: Lower Indus, Pakistan

Frank van Steenbergen, Muhammad Basharat and Bakhshal Khan Lashari

Abstract: This paper focuses on the scope of conjunctive management in the Lower Indus part of the Indus Basin Irrigation System (IBIS), and the contribution this could make towards food security and socio-economic development. The total Gross Command Area (GCA) of the Lower Indus is 5.92 Mha, with a cultivable command area (CCA) of 5.43 Mha, most of which is in Sindh Province. There is a limited use of groundwater in Sindh (about 4.3 Billion Cubic Meter (BCM)) for two reasons: first, there is a large area where groundwater is saline; and second, there is a high surface irrigation supply to most of the canal commands, e.g., average annual supply to rice command is 1723 mm, close to the annual reference crop evapotranspiration for the area, while there is an additional annual rainfall of about 200 mm. These high irrigation allocations, even in areas where groundwater is fresh, create strong disincentives for farmers to use groundwater. Consequently, areas are waterlogged to the extent of 50% and 70% before and after the monsoon, respectively, which contributes to surface salinity through capillary rise. In Sindh, about 74%–80% of the available groundwater recharge is lost in the form of non-beneficial evaporation. This gives rise to low cropping intensities and yields compared to fresh groundwater areas elsewhere in the IBIS. The drought of 1999–2002 has demonstrated a reduction in waterlogging without any corresponding reduction in crop yields. Therefore, in order to efficiently meet current water requirements of all the sectors, *i.e.*, agriculture, domestic and industrial, an *ab initio* level of water reallocation and efficient water management, with consideration to groundwater quality and its safe yield, in various areas are recommended. This might systematically reduce the waterlogged areas, support greater cropping intensity than is currently being practiced, and free up water for horizontal expansion, such as in the Thar Desert.

Reprinted from *Resources.* Cite as: van Steenbergen, F.; Basharat, M.; Lashari, B.K. Key Challenges and Opportunities for Conjunctive Management of Surface and Groundwater in Mega-Irrigation Systems: Lower Indus, Pakistan. *Resources* **2015**, *4*, 831–856.

1. Introduction

The Indus Basin Irrigation System (IBIS) is described as the world's single largest "mega" irrigation system—covering a total area of 17.2 Mha. The IBIS consists of The Indus River, itself falling ultimately to Arabian Sea, and the tributaries Kabul, Jhelum, Chenab, Ravi, Beas and Sutlej. However, for the latter three rivers, India has full rights under the Indus Water Treaty (IWT) of 1960. Furthermore, for river water storage and diversion, the IBIS comprises three major reservoirs, 16 barrages, two head-works, two siphons across major rivers, 12 inter river link canals, and 44 canal irrigation systems (normally called canal commands), of which 23 are in Punjab, 14 in Sindh, five in Khyber Pakhtunkhwa (KP), and two in Baluchistan (Figure 1).

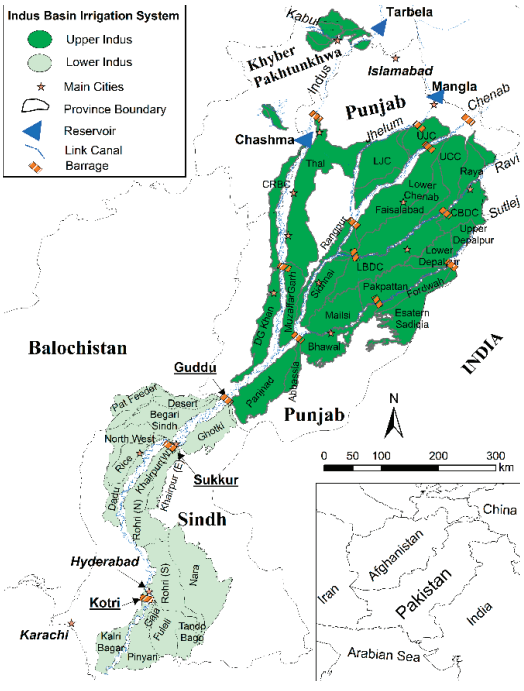

Figure 1. Indus Basin Irrigation System (IBIS), including rivers, link canals, barrages and canal commands.

With increased supplies from Mangla and Tarbela reservoirs, agricultural water supply has improved greatly, but, at the same time, this has contributed towards increased recharge of the groundwater. This increased recharge was utilized for supplementing crop water requirements in Punjab. However, in Lower Indus, the groundwater has not been developed in comparison to this increasing rate of groundwater recharge. This changing water balance has caused permanently waterlogged conditions, especially during and immediately after the Kharif season, with the result of low cropping intensities and obviously lower crop yields than the potential, especially in the Rabi season. Furthermore, while the water management approach being followed is heavily outdated, the population has increased over time. The people in Thar are constantly facing food and water shortages. The drought of 1999–2002 presented the best demonstration for the Indus system, especially the Lower Indus, in the form of reduced waterlogging without any reduction in crop yields [1].

At present, the water management is still based on per/post-independence historic allocations, without any logic to justify over or under allocations amongst different areas, with persistent and heavily waterlogged areas in many of the canal commands in the Lower Indus part of the IBIS [2,3]. Similarly, a World Bank paper [4] pointed out that "the realistic water requirements of the canals are required to be re-calculated, keeping in view of various factors under the present situation". This means that water allowances are, therefore, required to be revised accordingly [5]. Also, it has been projected that urban water requirement for the 25 major cities of Pakistan would be 6.34 and

8.67 BCM, respectively, for the years 2030 and 2050, against the current supply of about 4.0 BCM [6]. Therefore, the current situation of increasing water demands, calls for integration of water demand and supply across and within all the water use sectors. In this context, this paper demonstrates for the Lower Indus that the groundwater has considerably higher potential that it is largely unexplored, due to ample availability of canal water and, in several areas, the high salt content.

2. Study Area

Sindh Province forms the southern part of the Indus Plain that lies below Guddu, forming the narrowest width of the Indus Plain below the confluence of the Punjnad River with the Indus (Figure 1). The climate of Sindh is hot and arid, and the maximum temperature in summer exceeds 40 °C. Evaporation in Sindh is higher than anywhere else in Pakistan. Mean annual precipitation ranges from about 100 to 200 mm in parts of the Lower Indus Plain, whereas lake evaporation stands at 2800 mm at Thatta [7]. The Indus enters Sindh province at an elevation of 75 m (246 ft) above mean sea level (amsl). Gradients are very flat in the area and have an average rate of 12.5 cm/km (eight inches/mile). The river lies on a slight ridge, which slopes away in lateral direction up to Larkana. Thus, it has an influent behavior and loses water to the underlying aquifer. Some of the flow drains towards the desert in the east. Another part flows towards the Khirthar Hills. In the Rabi season, when the flow in the river below Sukkur Barrage is almost zero, the river receives groundwater, especially from the left bank.

The Indus River provides irrigation to a major portion of Sindh (about 41 percent) through the canals taking off from the three Barrages in Sindh: Guddu, Sukkur and Kotri. A very small part of Balochistan Province is also irrigated through the Pat Feeder Canal from Guddu Barrage and the Kirthar Branch from North West Canal, taking off from Sukkur Barrage. The total Gross Command Area (GCA) of the Lower Indus plain (Sindh and Baluchistan, Figure 1) is 5.92 Mha with a culturable command area (CCA) of 5.43 Mha. The major crops in the area are wheat, cotton, rice, and sugarcane, which utilize 68 percent of the total cropped area. Sindh also produces horticultural crops: mangoes, bananas, dates and chilies. Sindh has a diversion capacity of 111 Billion Cubic Meter (BCM), which is equivalent to 90 Million Acre Feet (MAF); but, as per the Water Accord 1991, Sindh's share is 60.15 BCM (48.76 MAF) of surface water. In addition, annual groundwater use is about 4.3 BCM [8], but it is unregulated and unplanned.

Groundwater Use in Lower Indus Plain—A Contrast to Upper Indus

Compared to the situation in the Upper Indus, groundwater use in the Lower Indus is very modest; yet waterlogging (groundwater within 1.5 meter of the soil surface) is common and has been assessed to prevail over 1.5 to 3.5 Mha. While in Punjab groundwater use at field scale is equivalent to canal water use in various canal commands [9,10], in Sindh this is not the case. For example, for the Lower Bari Doab Canal, based on the 2005 tube well survey data, total groundwater abstraction was estimated as 4674 MCM (million cubic meter) [11]. On the basis of the same data, the Halcrow [12] consultants for LBDC (Lower Bari Doab Canal) calculated the revised estimates of groundwater abstraction for the year 2005 as 4796 MCM, against annual

average canal supplies of 4849 MCM (3.93 MAF) diverted to the LBDC at its head [9]. Thus, canal and ground water use in the LBDC irrigation system are at par with each other. In addition, there is no waterlogging in the command, which means that whatever is recharged to the aquifer from the irrigation and rainfall is again pumped for meeting deficit supplies from the irrigation system.

In Punjab, the number of tube wells was 944,649 in 2009–2010 [13], and is now over 1,000,000. This growth in the number of tube wells has made higher crop intensity and precision farming possible. In comparison, the estimated number of tube wells in Sindh was 95,921 in 2010–2011 [14]. This includes a small number of public fresh water drainage tube wells. Out of 4100 of such so-called "SCARP (Salinity Control and Reclamation Project)" tube wells installed since the mid-1960s, less than 10% are operational—often under *de facto* joint farmer management. Tube well densities in different canal commands are in the order of two to three private tube wells per 100 ha [15,16]. However, in the command areas of the canals that start from Guddu Barrage (Begari, Ghotki and Desert), wells are virtually non-existent, with the exception of the tail reaches and the higher lands, even though the shallow groundwater in many areas is fresh.

A look into how things could be if surface water supplies were not overabundant can be seen in the groundwater exploitation in the Kunner—2 Minor (near Hyderabad), where tube well density is 6.6 per 100 hectares—related to relatively better groundwater qualities and the proximity to a major market. Another example is the higher lands in Pano Aqil in the Ghotki command areas, where canal supplies are inadequate and tube well densities exceed 15 per 100 ha. In general, even in some fresh groundwater zones, tube well densities are low and there is also evidence of fresh SCARP tube well water being routed directly to disposal canals and not being used in agriculture. Low tube well densities are also seen in saline zones; hardly any tube wells are present there. However, in comparable saline groundwater areas in Punjab, the number of tube wells is considerably higher. The basic reason is that the water allowance in Punjab varies from 2.73 to 4.2 cusec/1000 acres, whereas in Sindh the water allowance ranges from 8 to 17 cusecs/1000 acres. Thus, farmers are forced to supplement their deficit canal supplies with groundwater pumping.

The most recent assessment of overall groundwater abstraction in Sindh was 4.3 BCM [8]. Another study from the same period by the IWMI (International Water Management Institute) estimated the discharge through tube wells to be even lower, *i.e.*, at 2.15 BCM (about 2 MAF) [17]. In other words, groundwater use stands at about 4%–8% of surface water use in Sindh, whereas in the canal areas of Punjab, the use of surface and groundwater at farm level are approximately 50:50 [10]. These figures may need to be updated, but in general, groundwater is an underutilized resource in the canal-irrigated areas of Sindh. A large part of the groundwater use in Sindh is in the riverine areas where there are no irrigation canals and the soils are relatively sandy. In contrast, there is relatively limited use of groundwater in the canal command areas due to the high surface water allocations.

In addition, because of widespread waterlogging, water productivity in Sindh is also considerably less than Punjab. For the different canal commands in Sindh, it ranges between 0.32 and 1.15 kg per m^3 for wheat, whereas in Punjab, the median is 1.08 kg per m^3. In the Indian Punjab, it is 1.42 kg per m^3, being again 35% higher than in Pakistani Punjab [18]. Variations in water

productivity in different command areas under the Sindh Irrigation System as well as overall productivity are shown in Table 1.

Table 1. Overall water productivity (WP) in various canal commands in Sindh [18].

AWB/Command Area	Eta (mm)	BIO (kg/ha)	WP (kg/m^3)
Khairpur West	1281	14,820	1.15
Rice	1225	12,380	1
Rohri	1203	12,153	0.98
Ghotki	1083	10,622	0.96
Khairpur East	1105	10,530	0.9
Pat Feeder	1004	8437	0.8
Begari	1148	8359	0.71
Desert	1152	8303	0.7
Dadu	1042	7657	0.69
Northwest	1130	7961	0.68
Nara	1098	7009	0.61
Gaja Branch (Old Fuleli)	1371	7760	0.55
Fuleli	1287	5791	0.44
Lined (TandoBago)	1304	5437	0.41
Pinyari	1277	5178	0.39
Kalri	1228	4192	0.32

3. Data Sources and Methods

Managing surface irrigation in an extensive system such as that in Sindh, with extremely long canals, a flat gradient, pre-dominant saline groundwater and widespread alkaline and saline soils is a huge and daunting challenge, to say the least, and in the management of the canal system in Sindh some things have not gone well. This is because water management on a scientific basis has never been evaluated for the Lower Indus area. Here, we analyzed the situation with an extensive and comprehensive literature review and data analysis regarding different water management challenges, *i.e.*, groundwater quality, drainage facilities and their requirements, irrigation water supplies, the resulting waterlogging and surface salinity conditions, and their impact on crop yields on temporal and spatial scales. Based on this comprehensive insight of the issues being faced in the area, we recommend a set of integrated approaches that can offer a comprehensive and long-term solution for conjunctive water management and also result in consequent increased crop output from the area.

4. Water Management Challenges Being Faced in Lower Indus

The amount of annually renewable groundwater available in Sindh is estimated to be 22 to 27 BCM (18 to 22 MAF); yet only a fraction of this is used—with the groundwater discharge now leading to waterlogging and soil salinity. There is a need to make better use of groundwater in Sindh. One of the reasons for this concerns the challenge of climate change: with more extreme hydrological situations, the buffering role of groundwater becomes important. Another reason is the

expected reduced availability of surface water due to sedimentation of the current large storage reservoirs. Over the years, three main water reservoirs in Pakistan have been constructed, Tarbela, Mangla and Chashma, with a total live storage of 20 BCM (16.29 MAF). However, as a result of sedimentation, the effective gross capacity of these reservoirs has been reduced by 5.4 BCM (4.37 MAF) (28%) as of 2012 [19]. Moreover, it is expected that the process of sedimentation will continue and gross surface storage loss would reach 7.18 BCM (5.82 MAF) (37%) by 2025 [20]. This calls for better management of groundwater reservoirs.

At present, the groundwater buffer is not well managed, with waterlogging being the main manifestation. This suppresses farm yields and keeps cropping intensity relatively low. In Sindh, these cropping intensities have increased significantly over the original intensities. They are, however, considerably lower than they are in Punjab, varying from 116.7% in Sindh Cotton Wheat zone (SCWS) to 234.0% in Punjab Sugarcane Wheat zone (PSW) [21]. The impacts are not only limited to agriculture but also extend beyond. Thus, the area is facing multifaceted water management challenges that are interlinked and acting in combination to produce various ill effects regarding water management and the ensuing crop and soil environment. These water management challenges are discussed in detail as follows.

4.1. Groundwater Salinity

Groundwater salinity in Sindh is widespread. In 1959, a program of investigations was started by Water and Power Development Authority (WAPDA) by the name of Lower Indus Project (LIP). Bore holes, varying from 30 to 90 m deep, were drilled in the Guddu, Sukkur and Kotri Barrage commands, to determine aquifer characteristics and the quality of groundwater in horizontal and vertical scales [22]. The general pattern of groundwater distribution in the Lower Indus Plains is one of good quality water immediately adjacent to the river, with increasing salinity as we move away from the river (Figure 2). A lesser quantity of good quality water is available on the right bank of the river than on the left [23]. This is due to the proximity of limestone hills on the right bank as well as the poor aquifers associated with piedmont plains. Another feature of importance is the complete absence of usable groundwater in the deltaic area south of Hyderabad, with the exception of some shallow pockets in the recently abandoned riverbeds of the Gaja Command.

Throughout the region, the salinity of groundwater increases with depth and no case has been recorded in Sindh where saline water overlies fresh water. Based on the assessments of LIP, it is estimated that 71% of Sindh's irrigated area has groundwater that is too saline (>1500 ppm) for irrigation [24]. However, the picture improves if one looks at shallower depths (<15 m), where salinity is less widespread. According to Ahmad [23], there are many sites where shallow useable groundwater exists. The total fresh groundwater zones at shallow depth (15 m) are tentatively estimated as spreading over 46% of the area [3]. However, further detailed groundwater investigations are needed for precise assessment of different groundwater qualities at shallow depths.

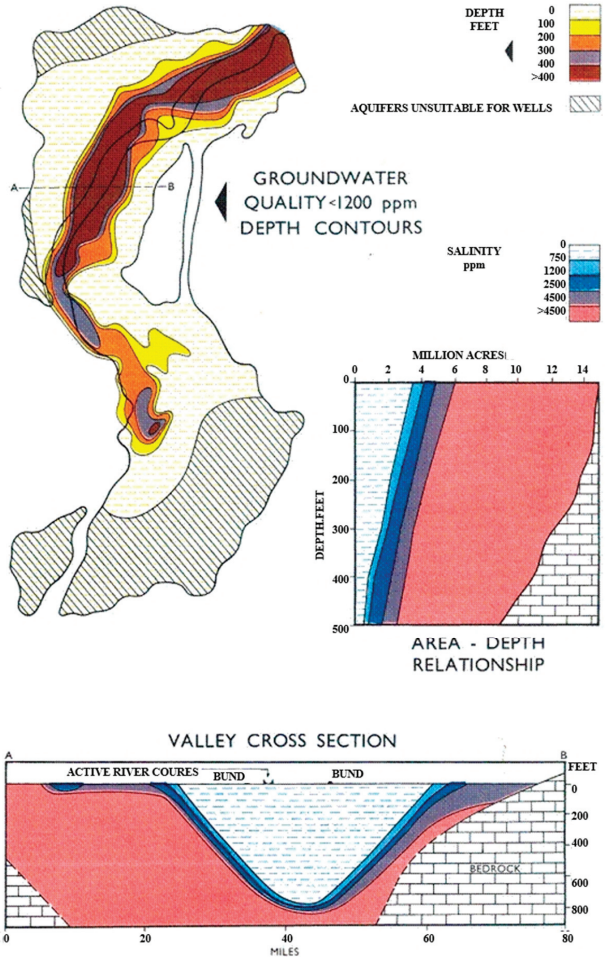

Figure 2. Vertical and horizontal extent of groundwater salinity in Lower Indus (Developed from [23]).

4.2. High Irrigation Supplies and Waterlogging

The most prominent element explaining the limited use of groundwater in Lower Indus is the high surface irrigation allowances in several of the canal commands in Sindh (8 to 17 cusecs per 1000 acres). The situation of high allowance is more amplified because in several canal commands, water is diverted in excess of the allowances. The picture is further distorted within the canal commands by unregulated direct outlets, tampered off-takes or in some areas, extensive canal seepage, creating local overabundance of water.

These high surface water deliveries have given rise to widespread waterlogging. In October 2011, for instance, 36% of the command area had a depth to water table of less than 1.0 m, and another 33.6%, a water table within the range of 1.0 to 1.5 m. Thus, in about 70% of the command area in the province, the root zone is waterlogged (Figure 3). This means only about 30.4% area

was not waterlogged during October 2011 [3]. The extent of waterlogging conditions usually only drops off just before monsoon, due to less canal supplies during the Rabi season. In acreage, the affected area is colossal: 2.19 M ha in post monsoon 2011, with major impacts on the sowing of Rabi crops, especially wheat (Figure 4).

Figure 3. Vast agricultural lands lying barren with ponded water in Rice Canal Command (13 December 2013).

(**a**) (**b**)

Figure 4. Patchy wheat crop germination due to waterlogging and salinity in Mirpur Khas (**a**); and Dadu (**b**) districts (pictures taken on 11–12 December 2013).

There is a wide variety of irrigation allocations in the canal systems in Sindh. These are not necessarily based on any water management logic, but on a series of historic decisions. Basharat *et al*. [3] analyzed canal water supplies per cultivable canal area for the different canal systems in Sindh and Balochistan. The depth of water (mm) over the CCA differs widely (Figure 5). The Rice and Kalri command areas are entitled to the highest allowances. Annual average supplies to the Rice command is 1723 mm, almost close to the annual reference crop evapotranspiration in the area, and with an additional annual rainfall of about 200 mm.

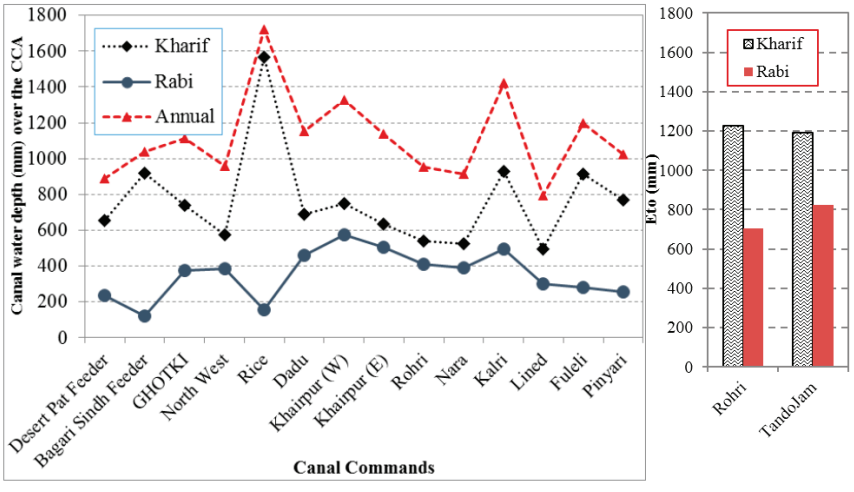

Figure 5. Comparison of canal water supplies amongst the irrigation systems in Lower Indus [3].

An example of an area with larger surface water availability and a limited use of its fresh groundwater is the Jalbani Distributary, which takes-off from North West Canal and has a command area of 8642 acres [1]. The irrigation duty for the Distributary is high—12.15 cfs/1000 acre (84 L/s/100 ha). The actual water delivery per acre is even higher, as not more than 50% of the command areas are used in any season, due to the rest being waterlogged. Even during the drought period of 1999 to 2002, surface water supplies—despite being reduced by 5% to 10%—remained abundant. There was more (though still limited) interest among farmers to compensate for the lower supplies by developing shallow wells. The drought helped to lower water tables, as observed from SMO (SCARP Monitoring Organization). In the observation wells, water table had deepened from 1 to 1.5 m deep in the normal years to 1.5 to 2 m in drought period (1999–2002). In several areas, this was beneficial for wheat cultivation in the Rabi season.

The overgenerous surface irrigation supplies, especially in some canal commands, reduce the need for additional groundwater irrigation [25]. Several studies have also argued that in many areas of Northern Sindh, a layer of fresh water is present over the more saline water that could be exploited more extensively by skimming wells. Some small tube wells and dug wells already use these lenses along canals and distributaries in several parts of Sindh, where water is relatively short in supply (canal tail ends in the area with low surface irrigation supplies). In many areas, however, surface water supplies in the canals fed from Guddu Barrage are so high that there is little incentive to pump. In the post-monsoon period the entire area is waterlogged, as shown in Figure 6 [1]. Moreover, within the canal commands, there is no difference in water allowance for fresh and saline areas, which can encourage groundwater pumping.

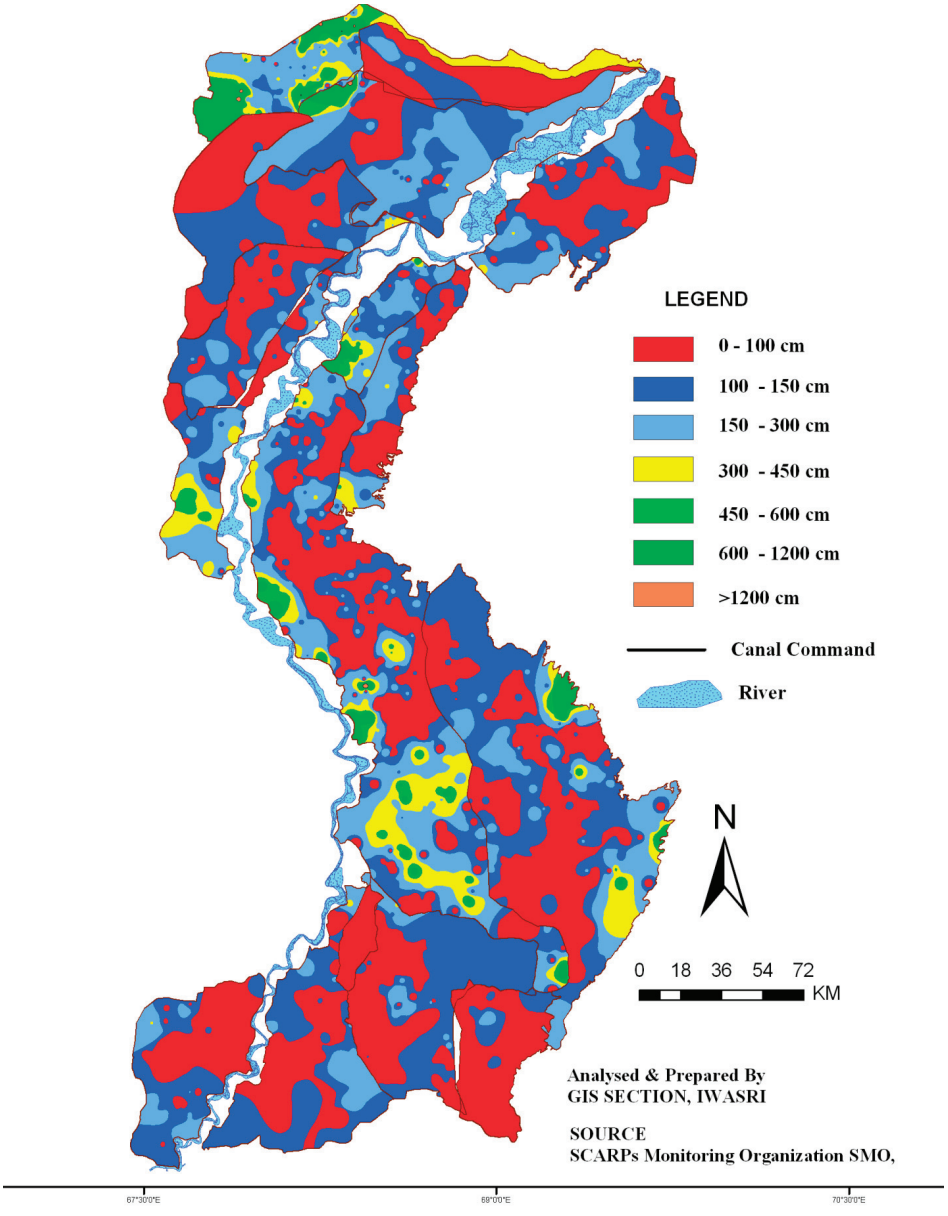

Figure 6. Depth to water table map of Lower Indus, post monsoon 2011 [3].

Thus, the main cause for this extensive waterlogging and low cropping intensities is the high and generally outdated surface irrigation allocations. Waterlogging appears to be particularly persistent in the areas served by non-perennial canals. These canals receive copious supplies in the Kharif season, causing the water table to rise significantly, but to fall again in the winter season, when the canals are not flowing. Rice Canal in District Larkana Area is one of the main examples of this phenomenon, where the water table fluctuates between one and three meters during Kharif

(summer) and Rabi (winter) seasons. This annual cycle of rise and fall of water table has brought the salts to the upper soil strata [26]. By regulating the flow after the commissioning of the Tarbela and Mangla Dams, made 24% more water available for irrigation and some canals are now converted officially or unofficially to perennial canals. Canal duties were, however, not officially recalibrated after this additional water became available. The problems in the perennial channels in Sindh are different from those in the non-perennial channels. In the former, the water duties are generally lower (though still higher than elsewhere in the subcontinent). Here, salinity is concentrated in areas with deficient surface water supplies, as there is not enough water for leaching accumulated salts. This often concerns the tail reaches of the channels.

4.3. Surface Salinity

Closely linked to high water tables and widespread waterlogging, the Lower Indus also has extensive surface salinity. Such surface salinity is caused by capillary rise in areas with high water tables [27], particularly common in areas with reduced dry season supplies or low irrigation supplies in general, or in lands surrounded by heavily waterlogged lands. Farmers respond by planting kalar grass or Sesbania, deep plowing, and adding press mud or organic manure. Figure 7 gives an overview based on the latest available surface salinity survey (2002–2003) by IWASRI (International Waterlogging and Salinity Research Institute).

A comparison of the 2002–2003 survey for Sindh and Balochistan with the earlier main survey of 1976–1979 shows that soil salinity in the Lower Indus had increased from 46% to 51% (Table 2). In the same period, the trend in the Upper Indus was opposite and surface salinity reduced from 14% to 7%. This was caused by the lowered ground water table in Punjab that was the result of intense use of shallow groundwater for irrigation purposes.

Table 2. Trends in Surface Salinity in Lower Indus Irrigation Systems (Sindh and Balochistan).

Soil Class	ECe (dS/m) at 25 °C	Salt (%)	1976–1979 (%)		2001–2003 (%)	
Non Saline	Less than 4	Less than 0.2	54		49	
Slightly Saline	4–8	0.2–0.5	19		20	
Moderately Saline	8–15	0.5–1.0	10	46	10	51
Strongly Saline	More than 15	More than 1.0	17		21	

4.4. L\ack of Field Drainage

In addition to higher canal supplies, there are other reasons for waterlogging too, e.g., almost 50% of the cultivable command area does not have drainage facilities. Although 18 different drainage projects consisting of surface and sub-surface drainage, covering an area of 2.3 Mha, were completed from 1963 to 1990s, afterwards no major attention was paid to their operation and maintenance (Table 3). The present surface drainage density is usually not more than 3–7 m/ha. This leaves much of the land without a drainage system. Thus, root zone drainage is almost entirely ignored. The waterlogging is further aggravated because over the years main natural drains have been blocked by the private encroachment and construction of roads and other infrastructure.

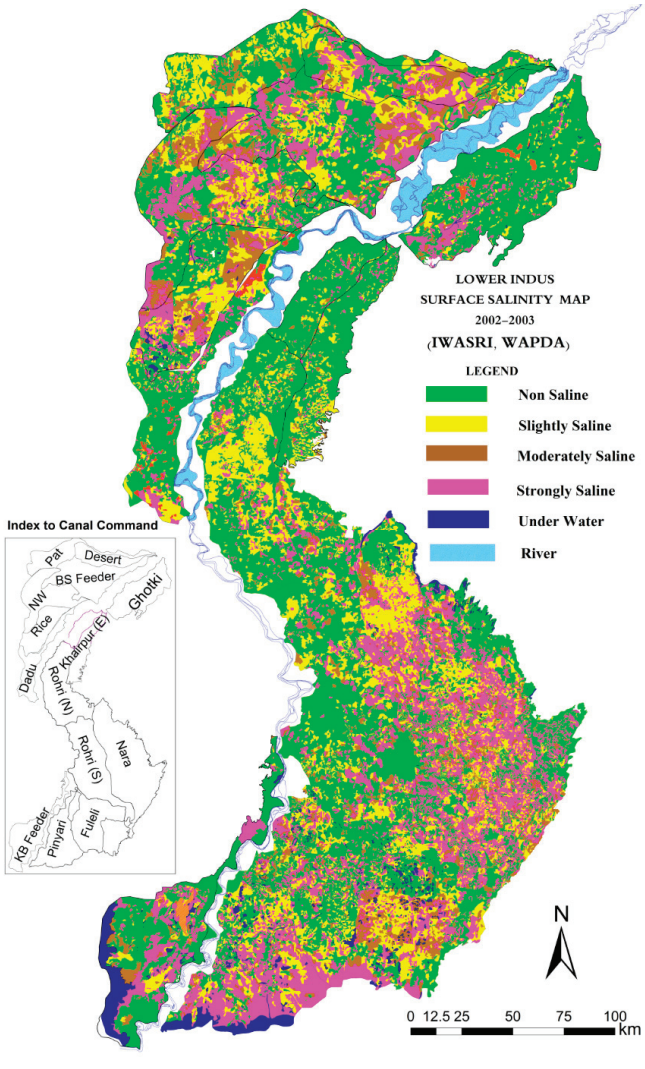

Figure 7. Soil surface salinity in Lower Indus [3].

Table 3. Drainage facilities in Pakistan—up to June 2001 [28].

Province	Gross Area (Ma)	CCA (Ma)	Surface Drains (km)	Subsurface Drainage					
				Tube wells (Numbers)			Interceptor Drains (km)	Tile Drainage	
				FGW *	SGW **	ScW ***		Length (km)	Area (Ma) GCA	Area (Ma) CCA
Punjab	10.357	9.220	3402	8065	1985	–	6	2810	0.235	0.164
Sindh	6.732	5.710	9031	4190	1587	361	154	2046	0.105	0.089
KPK	0.884	0.884	971	491	–	–	–	7756	0.658	0.137
Balochistan	0.177	0.161	322	–	–	–	–	–	–	–
Total	18.150	15.793	13726	12746	3572	361	160	12612	0.998	0.390

Notes: * Fresh groundwater; ** Saline groundwater; ***Scavenger well.4.6. Other Consequences of Poor Water Management.

A massive investment in drainage facilities was made under the Left Bank Outfall Drain starting from the 1990s. The investment concerned a surface drainage network and vertical drainage systems. The non-functionality, however, is very high: more than 70% of drainage pumping stations do not work properly, according to assessments done for the recent Left Bank Drainage Master Plan.

4.5. Flooding Hazards

Flooding has always been an issue in the Indus Basin. The Lower Indus part of the basin sustained enormous physical and financial losses during the super flood of 2010. The disaster was then repeated in 2011. The floods in 2011 were only due to abnormal rainfall in the Lower Indus plains. It was estimated that 14.7 billion rupees would be required for restoration of the damages caused by the floods in Sindh [2]. Apart from these major floods, there have been at least three distinct minor flood events in the last decade.

Due to waterlogging conditions in the area, a major part of such floodwater immediately becomes excess and the area is increasingly less equipped to accommodate inevitable unusual rainfall events. The massive Left Bank Outfall Drainage System for instance was designed to remove the saline effluent, not to drain the storm water, and apart from that, suffers from high non-functionality. The problems are worsened by the encroachment and blockage of natural drains and waterways. When the floods develop, the situation is further worsened by breaches in the drains and deliberate cuts in canals, drains and roads. The floods are made worse by the high groundwater tables—meaning that the excess water has nowhere to go but to transform into runoff. If water tables were lower, there would have been the capacity to absorb part of the excess rainfall. Therefore, the frequent floods in Sindh are an additional imperative for rethinking the prevailing water management.

Waterlogging also creates public health problems, due to the difficulty of developing rural sanitation facilities in waterlogged areas and the large prevalence of human and animal diseases related to standing water. These are areas with very high saline groundwater at present, foreclosing the use of groundwater for drinking purposes. In this respect, the lower Left Bank areas of the Indus (Badin and Thatta) are the premier problem spot and a “water management disaster” area even by international standards. The high saline groundwater here is very much in the root zone and waterlogging and salinity continue to persist. This is caused by the high erratic irrigation supplies (often during the Kharif season when there is less demand elsewhere) and the flat topography of this area, along with the worsened natural drainage due to tidal effect having moved upstream after the scouring out of the Tidal Link. The impact does not only concern agricultural productivity but also basic drinking water supplies. With groundwater levels being as high as they are—no fresh/brackish water lens can form in the area that would at least provide some relief. The main source of drinking water is the highly polluted water in the three main irrigation canals running in the area. The situation in Badin and Thatta was further worsened by the 2010 floods—consolidating and further spreading the high water tables.

Furthermore, outside the Indus Plains, there is scope to improve groundwater management. The Thar Desert is one of the most densely populated deserts in the world. As one moves towards the south of the desert, annual rainfall increases considerably, reaching 350 mm/year. The rainfall

pattern, however, is highly variable and characterized by spells of dry years, causing outmigration as even drinking water sources fail. The groundwater in Thar Desert is mainly saline—with salinity of water in terms of electrical conductivity in 86% of the area—ranging between 2000 and 10,000 μS/cm. Generally, this is unfit for consumption, but under duress water quality up to 5000 μS/cm can be considered. It may be argued that there is scope to develop groundwater resources in the Thar in a more systematic manner, particularly in the dune zone, where coal bearing sedimentary units and basement formation have remarkable potential. Moreover, recharge of the aquifers is immediate and the quality of deep groundwater can improve after a long period of pumping.

5. The Lessons Learned

The situation in Lower Indus could have been very different with proper water management, as the lessons from the 1999–2002 drought show (as well as the drought year of 1988). In 1999–2002, the El Nino effect caused rainfall to reduce by more than 50% and releases from Tarbela to drop by 9% and from Mangla by 37%. This translated in lower canal deliveries in the country. Overall, there was 12%–25% less canal supply compared to preceding years [1]. Interestingly, in this period, crop production did not suffer. If anything, across the board it even increased. Area under crops such as wheat, rice, cotton and sugarcane increased by 0.8%, 6%, 4% and 6%, respectively, during the drought period (1999–2002) compared to before the drought period (1989–1998). Wheat, rice, cotton and sugarcane crop yields increased by 18%, 15%, 9% and 4%, respectively, during the drought (1999–2002) compared to before the drought (1989–1998), particularly in areas with uniform high groundwater tables, such as Badin and Thatta. The increase in production was not uniform in areas with limited surface supplies (higher land and tail reaches) and no possible access to fresh groundwater yields had a set back. In this period there was also a spectacular increase in yields in areas where the massive Left Bank Outfall Drain drainage system was completed and became operational—such as in Mirpurkhas and Sanghar District. The yield increases, however, also extended to areas that were not served by the new drainage network.

The waterlogged area in fact fluctuates enormously from year to year (Figure 8). This is because of the reduction in the percentage of the waterlogged areas in the drought years due to the reduced inflows, the increased groundwater use and the more economical use of canal water by the farmers. Particularly, in low-lying areas with heavy soils, waterlogging and salinity disappeared (for instance in Badin and Mirpurkhas). The summary of Figure 9 follows.

- Waterlogged area increased from 62.14% in 1990 to 68.73% in 1992, responding to canal diversions of 55.12 BCM in 1990 to 64.08 in 1992.
- Waterlogged areas dropped to 61.12% in 1993, as the surface water supplies reduced to 55.2 BCM.
- Due to drastic reduction in available supplies in 2001 and 2002, the waterlogged area reduced to 45.48 and 34.98%, respectively; however, a part of this could also be attributed to the commissioning of the new drainage facilities under LBOD project.

- Again in 2011, canal supplies and waterlogged areas increased; part of this waterlogging could also be attributed to excess rainfall and deterioration in performance of the drainage system, as pointed out by Basharat *et al*. [3].
- Hence, there is a very strong case for reevaluating the surface water allocation in Sindh in normal years, because, at present, normal years bring huge increases in waterlogging and reduced crop production. Monitoring under the SCARP Transition Project showed no indication of groundwater-induced secondary salinization in Moro and Sakrand, but instead suggests that in recent years soil salinity has improved, due to increased private tubewell development and the leaching this made possible [29]. This suggests that it is worthwhile to look into the option of draining saline water to create more storage for fresh water recharge.
- In addition, there is an evident benefit to be gained from drainage facilities, provided they can be kept operational.

The same finding is repeated in a more detailed analysis of a number of canal commands and distributaries in Sindh. Figures 9 and 10 show the reduction of pre-monsoon waterlogging for North West Canal and Rohri Canal.

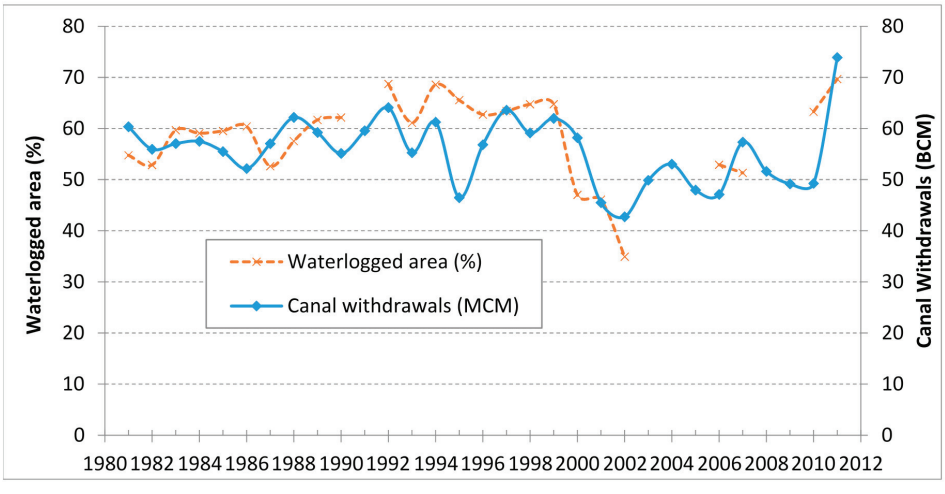

Figure 8. Waterlogging and canal supplies in Sindh (1980–2012).

A water management system with high waterlogging entails enormous water losses. For Sindh, 74%–80% of the available groundwater recharge is lost in the form of non-beneficial evaporation. These water losses, resulting from canal seepage and irrigation returns, could have been productively used as potential recharge. It occurs over both the fresh groundwater zones and saline groundwater zones of the province, in the ratio of 25:75 by area. Groundwater balance for the province, in broad terms and considering average rainfall and canal flows, is given in Table 4 [8].

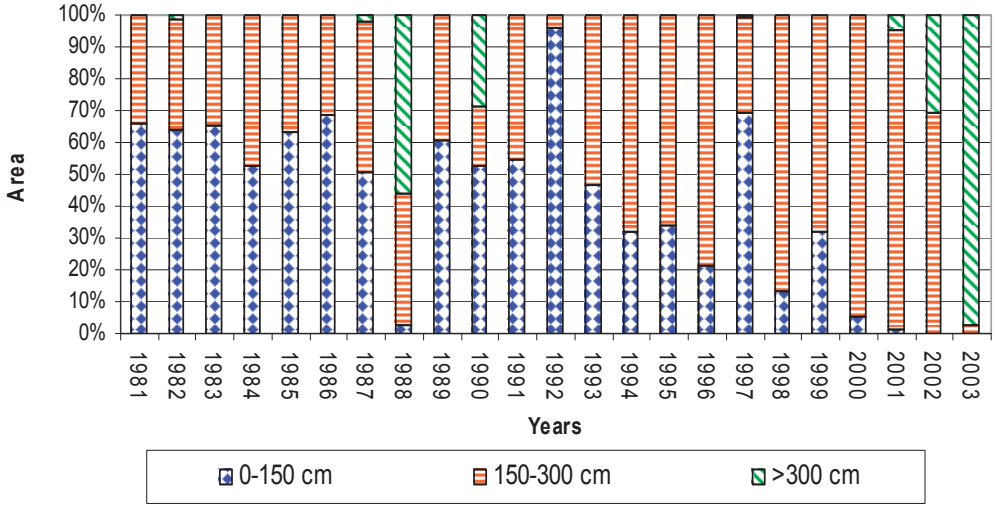

Figure 9. Pre-Monsoon Areas under Different Watertable Depths in North West Canal Command [1].

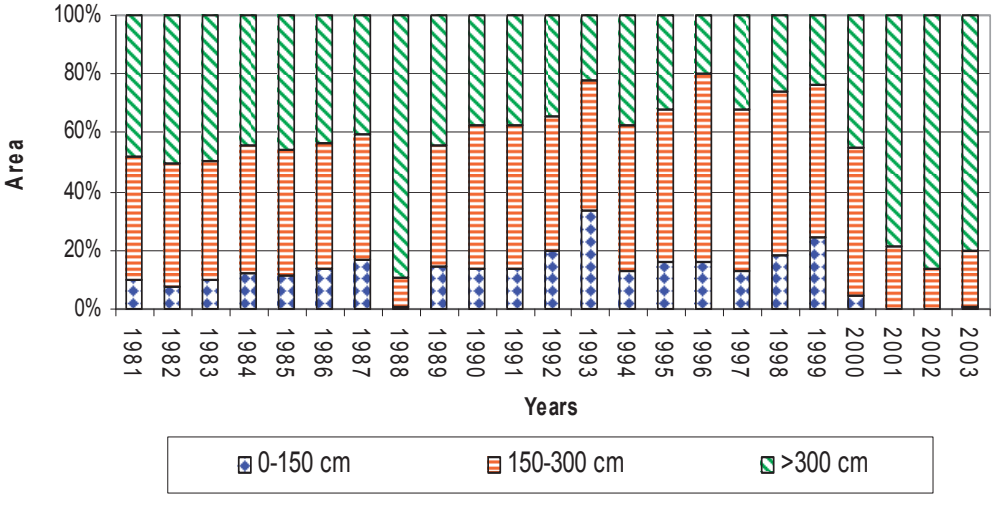

Figure 10. Pre-Monsoon Area under Different Water table Depths in Rohri Canal Command [1].

The above figures indicate the order of magnitude. The budget shows colossal amounts of non-beneficial evapotranspiration of around 17 BCM, which can be saved partly by lowering water tables or reducing seepage from canals system and even canal supplies in certain areas and also by using groundwater of fresh-to-marginal quality through adjustment of the cropping pattern and introduction of fish ponds.

Table 4. Groundwater balance for Sindh.

Recharge/Discharge Components in BCM	Normal Year
Recharge Components	
Recharge from Rainfall	2.42
Recharge from Canal System @ 15% of 56 BCM	8.34
Return flow from Irrigation system @ 22.5% of net flow	10.58
Return flow from GW Abstraction @ 22.5%	0.97
Recharge from Rivers	0.37
Total	**22.68**
Discharge Components	
Groundwater Abstraction (Public + Private)	4.30
Non-beneficial ET losses	16.96
Base flow to rivers	1.42
Total	**22.68**

6. Enabling Environment for Conjunctive Water Management

There is an urgent need for action to improve water productivity in Sindh in order to keep up with the increasing population and the need to better capture the opportunities in agricultural markets. Better conjunctive water management of surface water and groundwater will also improve drinking water availability, public health and the ability to store run-off from high rainfall events and hence prevent flooding.

Given the specific characteristics of Sindh, in particular the salinity of the groundwater (more so at greater depth), the flat gradient and the high surface water allocation, introducing conjunctive management would require six main interventions:

- Rationalize irrigation duties;
- Increase and intensify the irrigated areas;
- Improve field water use efficiency;
- Selective drainage investments;
- Make use of storm water;
- Adapt to saline conditions in some areas.

6.1. Rationalize Irrigation Duties

The first step is to properly manage the shallow groundwater resource and put an end to the widespread waterlogging by learning from the positive impacts of drought years (1999–2002). This should be done primarily by adjusting current canal supplies and irrigation duties and preparing area-specific conjunctive water management plans. At present, the irrigation duties amongst canal command are highly variable and defy prevailing water management logic. Some canals have extremely high duties (Figure 5). The supplies to different areas become even further unbalanced, as significantly more water is diverted to certain areas than the designed discharges. An example is Ghotki Feeder, which already has high duties of 6.6 cusec per 1000 acres but on top of this receives as much as 30%–40% more supplies.

The result of these high duties is waterlogging and large volumes of non-beneficial evaporation, which reduces productivity, worsens public health and stands for the overall loss of water. In such high supply areas, canal tail end or higher lands at times have higher crop yields than the waterlogged head reaches. The irrigation duties should be set so as to develop an optimum balance between surface water supplies and groundwater availability, and usage and guidelines may be developed in support of this. This requires that:

(a) Surface water seepage is equivalent to groundwater use in combination with beneficial evaporation.
(b) Surface water supplies are set at an optimum scarcity so that they encourage groundwater pumping as a complementary source.
(c) Where groundwater is of marginal quality, the mixing of supplied surface water and pumped groundwater results in useable water quality.

In a number of areas, the supply of surface water may need to be curtailed, not only to encourage supplementary groundwater irrigation but to reduce the area that is waterlogged and cannot be used productively. The reduction of surface water supplies should go hand in hand with the introduction of water saving farming techniques (such as greenhouses, use of mulches, soil amendments (e.g., press mud), micro-irrigation and the introduction of other less water demanding crops). In other areas, surface supplies may be increased to have more recharge through canal seepage. This is particularly true for low-lying water-short areas in tail sections with fresh groundwater. Shifting excess water to such areas may achieve a higher level of balance in these areas, where the additional ground and surface water serve to support higher intensities—as in the lower section of Rohri Canal. In Rohri Canal, high water tables occur in patches due to seepage from the canal, the large number of direct outlets in places or blocked natural drainage, but in other areas water availability is low. Particularly in fresh groundwater areas, a reallocation of water from areas that are oversupplied would increase productivity by canal supplies and pumped groundwater.

To grow rice and sugarcane in the very flat lands of Sindh without adequate drainage results in waterlogging, with ill-effects on water productivity and public health. In areas with highly saline groundwater, the lowering of the water table will create space so that fresh water lenses can form on top of the saline water tables, fed by seepage and rainfall. This will at least make it possible to improve the availability of drinking water in such areas. This is what happened in the Drainage IV area where the drainage project made it possible for such fresh/brackish water lenses to develop and this was a major boost for local drinking water supply. If the fresh water lenses are thick enough, they can also be accessed for agriculture by dug wells or properly spaced skimming wells.

IWMI and Global Water Partnership [30] have very rightly concluded that by considering groundwater availability and quality when allocating surface water, water managers could improve the equity, sustainability and productivity of irrigated systems. In areas with fresh or marginal groundwater, the canal supplies should be adjusted in such a way that a balance is achieved between using surface water and groundwater. Surface water supplies from canals need to ensure the right mixes of water qualities and to have water left for recharge. Canal supplies should be lowered so as to encourage groundwater pumping, especially in areas with fresh groundwater. The

use of groundwater also makes it possible to have more precise agriculture and leads to much higher water productivity by providing a psychological cushion for the farmers for water use as and when required.

The management of the surface water in conjunction with groundwater requires political courage and leadership to take this on, as well as water balance models for the different canal commands to study its sustainability. A broad agenda for the six main commands in Lower Indus is given in Table 5.

Table 5. Agenda for the six main commands in Sindh.

Area	Water Management Priorities	Investment Priorities	Agricultural Priorities
Guddu Right Command	Rationalize irrigation duties	Restore surface drainage	Introduce more efficient rice irrigation
Guddu Left Command	Rationalize irrigation duties	Restore surface drainage	Use fresh water zones for high value crops
Sukkur Right Command	Rationalize irrigation duties for improved filed irrigation	Restore surface drainage	Introduce more efficient rice irrigation
Sukkur Left Command	Relocate/ increase supplies especially to fresh groundwater areas	Selective rehabilitation of saline drainage wells, escapes structures, lining of drainage section that are in fill	–
Kotri Right Command	–	Restore surface drainage	Reconsider cropping pattern to low delta crops
Kotri Left Command	Rationalize irrigation duties	Flap gates at tail of drains to prevent sea water intrusion and selected drainage investments	Reconsider cropping pattern to low delta crops. Introduce biosaline agriculture and aquaculture Introduce more efficient rice irrigation

6.2. Increase and Intensify the Irrigated Areas

This leads to the second agenda item: the better buffer management in the canal command areas by revisiting the irrigation duties will save enough water within the provincial quota to consider developing/expanding the command areas and even developing new canals in Sindh (4.3 Mha of Thar has no access to surface water). There are areas where expansion is possible on either bank—preferably the areas chosen must have relatively fresh or marginal quality groundwater and relatively sandy soils, so that highly conjunctive systems can be developed right from the start. Going by the experience of the drought period, it may be possible to develop an additional area of 500,000 ha. At present, some of these expansions are already happening in an uncontrolled manner, with water in drains being fresh due to the large excess flows, which leads to its pumping by farmers. In reassessing the irrigation duties, the current reuse from drain may need to be considered and regularized.

Moreover, better use of shallow groundwater will also make it possible to intensify and extend the cropped areas through more groundwater irrigation by:

- The promotion of shallow irrigation wells in general.
- Promoting and regulating the collection and reuse of drainage water and creating special buffers in some areas that have heavy soils.
- Particularly in the part of the province where fresh water overlays saline water, there is a need to carefully promote multi-strainer skimming wells that exploit water at a very shallow depth. In several such areas, groundwater is exploited by conventional tube wells and local up-coning of saline water is a tangible risk. There is a need for better guidance on the sustainable use of groundwater and the benefits of skimming wells. Combined with a rationalization of surface irrigation supplies, this can create a safe and productive way of exploiting thin fresh water buffers in the areas with shallow fresh groundwater and deeper saline groundwater. Presently, the occurrence of skimming wells is sparse. In some areas, they are common and even jointly owned, but in other areas they are relatively unknown. Their popularity in some areas is related to the fact that simpler drilling technology could be used for low depth low diameter multiple strainers, *i.e.*, the same technology that is used for hand pumps.

Some crops with high water demands, such as sugarcane, are grown in areas such as the sandy riverine tract, primarily by using groundwater. Therefore, the financial feasibility of this type of agriculture is proven. However, costs of pumping may further be reduced by the application of water saving measures (see the next section), the introduction of fuel saving measures on the pump sets and the application of solar or wind energy.

6.3. Improve Field Water Use Efficiency

In close relation to that discussed in the previous section, it is important to look at field water management practices too. An improvement in the agriculture system is needed, particularly in the rice–wheat system in Sindh. Methodologies such as precise land leveling and mechanized operation have shown a boost in agriculture production and water saving of up to 50%. Direct seeding, the introduction of the System of Rice Intensification or other methods of alternate drying and wetting and growing rice in areas with saline groundwater, have the potential of saving water and increasing yields at the same time. In general, the rice–wheat system has much room for improvement [27]: a large effort in ensuring equitable and reliable supplies (so as to avoid excessive water being monopolized in certain areas at the cost of reliable supplies elsewhere); restoration of the main irrigation systems and learning from the programs currently being implemented; the introduction of alternate drying and wetting, at least after panicle initiation; better irrigation scheduling; direct seeding; and the development of better field bunds so as to retain and control water better at standing depth.

There are several other examples of farmers applying water saving techniques and achieving high yield as well as avoiding the waterlogging that is all-pervasive in the land around them. Some examples are the systematic use of mulch (from banana or mango leaves) that reduces evaporation

and increases the organic matter in the soil, the application of press mud from sugar mills and the use of low cost greenhouses.

Furthermore, the wasteful "pancho" system, whereby standing water in rice fields is drained before applying fresh water, and rice, more or less, grows in flowing water (as is practiced in the rice growing areas), would need to be discontinued. This will require investment in constructing additional field channels, so that each field can be served separately, as well as investment in drainage for low-lying areas.

6.4. Selective Drainage Investment

The fourth point is the need for a well-targeted initiative for a selective drainage investment program. The high non-functionality of all drainage systems (70%–90%), including the recently constructed Left Bank Outfall Drain (LBOD), gives a clear message to be very judicious in drainage investment. Moreover, the experience from LBOD also showed that due to the uncertainties in establishing the drainage coefficient in some areas, "too much" drainage facilities were foreseen and even before all facilities were operational, the system was in balance again. It is important to make a clear distinction between drainage for storm water removal (only surface drains) and root zone drainage (tube wells, tile drainage and surface drains).

There are a number of guiding principles for storm water drainage:

- Priority should be given to unblocking surface drains closed by roads and railway tracks and making adequate cross drainage on new and old infrastructure compulsory.
- In some cases, local dugouts may serve to lower groundwater tables, and also as local freshwater storage—such as borrow pits from construction.
- Care should be taken not to "over drain" and make sure that water tables are lowered but not too much, so that the beneficial effects on soil moisture from water tables are safeguarded.

Additionally, in root zone drainage:

- The main aim is to create enough storage space in the upper soil layers to ensure adequate soil aeration for crop growth and ideally, in saline areas, to allow the development of fresh water lenses that can be used for local drinking water systems. In addition, this root zone aeration would help to avoid rainfall flooding, as was observed in 2011 on left bank areas.
- There is no reason at all to develop or maintain public drainage facilities in fresh groundwater zones, as normally most of the drainage requirement would be taken care of by private pumping in such areas. Such private pumping may be further stimulated by curtailing and rationalization of surface supplies, as described above.
- Ideally, where root zone drainage is provided, there should be the possibility of flexibility in water levels and non-uniformity: some crops (rice) can tolerate high water tables, while for other crops, sub-irrigation is beneficial. It is better to have a controlled drainage system that accommodates the different requirements.
- There should be constructive cooperation between farmers and government. By now, there are several examples of farmers maintaining and even investing in drainage facilities. Joint

agreement and support in the provision of sophisticated Operation and Maintenance (O&M) is permanently needed.

- Finally, biological drainage—in particular, the promotion of eucalyptus tree stands—needs to be more systematically promoted. At present, farmers often do not replant their eucalyptus trees because of the effect of the trees and leaves on the soil fertility. This requires the introduction of other eucalyptus varieties and the promotion of local concentrated eucalyptus forests rather than isolated stands.

The current generation of water professionals has the large responsibility to do better. In general, the response to waterlogging and salinity in Sindh has not been to prevent the problems and use the excessive water supplies into a potential level of production as argued above, but to respond to the problems by investment in watercourse lining or drainage investments. Investment in drainage, however, is the measure of last resort targeted at the areas that most need it. Where possible, the problem should be prevented by better managing surface supplies, which is the cheapest solution. In addition, there is an urgent need to restore natural drainage paths that are now often blocked by road and railway development or urban expansion.

6.5. Make Use of Storm Water

A fifth related agenda item in an overhauled water system is to turn the menace of floods into an opportunity and overhaul the storm water drainage system in order to create overflow areas in the dry regions. These areas should be chosen in such a way that the floods that are spread and infiltrated can be used to build up soil fertility and recharge shallow groundwater. This will further increase the agricultural potential of Sindh. In addition, a lowered groundwater table will help to better absorb flood events when they arrive. Some use of excess water is already made by some of the farmers in the tail areas by constructing small multifunctional storage ponds, which are also used by herdsmen and their livestock.

6.6. Adapt to Saline Conditions in Some Areas

Finally, a larger effort should be made to adapt to the saline conditions that are natural in Sindh, both the extensive occurrence of saline groundwater (in 70% of the land) as well as the soil salinity (affecting 20% of the land). There are several strategies that can help to adapt to salinity. An important one is the introduction of bio-saline agriculture and brackish pond fisheries. Bio-saline agriculture can make use of salt-tolerant halophytes and special varieties [31], such as sesbania, that can yield high biomass fodder at 7.5 t/ha.

In addition, recent research indicates that even existing varieties of common crops (wheat, sorghum, sugar-beet, potatoes, *etc.*) can, after selection, adapt surprisingly well to the use of brackish water, particularly on free draining soils. In fact, a number of farmers are using locally selected wheat varieties. Other promising adaptation measures concern crop agronomy—from planting on ridges to using special salt-tolerant microbial agents.

To start this process, it is important to have an up to date understanding of groundwater quality at shallow and deeper depth, soil conditions, shallow stratigraphy and water levels. All these

factors will contribute to the optimum conjunctive water use model for the concerned part of the command areas. The monitoring of water tables and groundwater quality needs to be fully resumed and extended to non-SCARP areas. The changes in water management require considerable discussion with farmers and rural leaders, but as this is more or less a win-win situation, it seems to be possible. There is also a need for action and study in a number of areas such as:

- assessment of optimum water duties for different command areas and sections thereof, with the highest value cropping patterns;
- developing local water buffering and water storage strategies;
- promotion and improvement of techniques such as skimming wells and biological drainage;
- addressing the issue of bringing down pollution in the drains, particularly from sugar mills; and
- explore the precise scope of saline agriculture in the coastal areas.

Moreover, there is a need to get the process going at practical levels as well, with pilot activities at the level of minors and distributaries in different parts of the province. In a world of increased demand for agricultural products, Sindh has much potential to develop into an important source area. Situated close to good shipping lines in a region with impressive economic growth, Sindh cannot afford to deny itself the ample conjunctive opportunities within its own land and water resource system.

7. Conclusions and Recommendations

Keeping in view the increasing water demands and varying groundwater depth and quality in irrigated areas, the conjunctive use of surface and subsurface reservoirs needs to be pursued systematically in the Lower Indus. Basharat *et al*. [5] has highlighted a similar requirement for well-planned and integrated management approach in Punjab, stressing upon canal water reallocation amongst different canal commands.

There is a need to rethink and consider the introduction of conjunctive management of surface and groundwater in Sindh for a number of reasons:

- It can reduce waterlogging and hence contribute to higher yields and better public health.
- It can improve drinking water conditions, especially in areas with high saline groundwater tables, by creating the space for fresh water lenses.
- It will improve sanitary conditions, as an unsaturated zone above the water table is maintained, which would prevent the sewerage to be in direct contact with the shallow groundwater being used by rural population.
- It will make high value precision agriculture possible and introduce “on demand” irrigation within the canal systems, as farmers would be able to irrigate as and when required.
- It can free up canal water and make it possible to expand the area under cultivation or intensification in Sindh or to have water available for environmental flows.
- It will be possible to store frequent floods, especially generated by rainfalls, by creating more storage space in the shallow aquifers.

Therefore, in order to efficiently meet the water requirements of all sectors, *i.e.*, agriculture, domestic and industrial, an *ab initio* level of water re-allocations and efficient water management in consideration of groundwater quality and its safe yield in various areas is recommended, as discussed in detail in Section 6. This would certainly provide relief from the prevailing water management issues to all water use sectors and stakeholders in the area.

Acknowledgments

This paper was prepared with the support of the UKAID Research Grant Climate Resilience and Groundwater in the Indo-Gangetic Basin.

Acknowledged are the important contributions to an earlier version of this paper by the following persons: Habib Ursani, Shamshad Gohar, Mustafa Ujjan, Zarif Khero, Naseer Memon, Sukru Esin, Abdul Wasay Sheikh, Mir Aijaz, Hussain Mahar, Afsheen Bashir, Ghazala Channar, Arshad Hussain, Munir Amed Mangrio, Shafi Muhamemed Kori, Ghulam Hussain Wagan, Shah Nawaz Chandio, Atta Muhammed, Mansoor Ahmed, Ali Ahmed Detho, Agha Akhtar Mehmood, Kousar Ali, Amber Jawad, Abdul Wahid, Shakir Habib Memon, Afshan Mallah, and Cecilia Borgia.

Author Contributions

This paper is the joint effort of the three authors. The ideas were developed jointly and the data come from various research activities that the individual authors were involved with.

Conflicts of Interest

The authors declare no conflict of interest

References

1. Saeed, M.; Khan, N.M.; Rafiq, M.; Bhutta, M.N. *Change in Waterlogging due to Drought in the Indus Basin and Its Impact on Crop Yields*; Pakistan Water & Power Development Authority (WAPDA): Lahore, Pakistan, 2009.
2. Ali, A.I.; Bokhari, J.I.; Siddiqui, Q.T.M. *An Appraisal of 2011 Rain/Flood Damages in Sindh*; Pakistan Engineering Congres: Lahore, Pakistan, 2012.
3. Basharat, M.; Hassan, D.; Bajkani, A.A.; Sultan, S.J. *Surface Water and Groundwater Nexus: Groundwater Management Options for Indus Basin Irrigation System*; Pakistan Water & Power Development Authority (WAPDA): Lahore, Pakistan, 2014.
4. Blackmore, D.; Hasan, F. Water Rights and Entitlements. In *Pakistan's Water Economy Running Dry*; Briscoe, J., Qamar, U., Eds; Oxford University Press: Oxford, UK, 2005; pp. 201–253. Available online: http://www-wds.worldbank.org/external/default/WDSContentServer/WDSP/IB/2010/02/01/000333037_20100201014523/Rendered/PDF/529140WP0Box341University0Press2006.pdf (accessed on 22 March 2015).

5. Basharat, M.; Ali, S.; Azhar, A.H. Spatial variation in irrigation demand and supply across canal commands in Punjab: A areal integrated water resources management challenge. *Water Policy J.* **2014**, *16*, 397–421.
6. Basharat, M.; Sultan S.J.; Malik, A.S. *Groundwater Management in Indus Plain and Integrated Water Resources Management Approach*; Pakistan Water & Power Development Authority (WAPDA): Lahore, Pakistan, 2015.
7. Ahmad, N. *An Estimate of Water Loss by Evaporation in Pakistan*; Irrigation Drainage and Flood Control Research Council; Planning and Coordination Cell: Lahore, Pakistan, 1982.
8. Halcrow-ACE. *Exploitation and Regulation of Fresh Groundwater-Main Report*; ACE-Halcrow JV Consultants: Lahore, Pakistan, 2003.
9. Basharat, M. Spatial and temporal appraisal of groundwater depth and quality in LBDC command: Issues and options. *Pak. J. Eng. Appl. Sci.* **2012**, *11*, 14–29.
10. Habib, Z. Policy and Strategic Lessons from the Evolution of Water Management in the Indus Basin Pakistan. Available online: https://www.researchgate.net/publication/258688640_Policy_and_Strategic_Lessons_from_the_evolution_of_Indus_Basin (accessed on 22 March 2015).
11. National Engineering Services Pakistan (Pvt) Limited (NESPAK). *Punjab Irrigated Agriculture Development Sector Project*; NESPAK: Lahore, Pakistan, 2005.
12. Halcrow 2006. *Punjab Irrigated Agriculture Development Sector Project, Final Report Annex 5—Groundwater Management*; Halcrow Pakistan (PVT) Ltd: Lahore, Pakistan, 2006.
13. Government of the Punjab. *Punjab Development Statistics—2012*; Bureau of Statistics; Government of the Punjab: Lahore, Pakistan, 2012.
14. Government of Pakistan. *Agricultural Statistics of Pakistan*. Statistics Division: Islamabad, Pakistan, 2012.
15. Lashari, B.; Memon, Y. Use of shallow groundwater in water-short period: The case study of Dhoro Naro Minor, Nawabshah. In Proceedings of the Regional Groundwater Management Seminar, Islamabad, Pakistan, 9–11 October 2000.
16. Van Steenbergen, F.; Oliemans, W. A review of policies in groundwater management in Pakistan 1950–2000. *Water Policy* **2002**, *4*, 323–344.
17. Qureshi, A.S.; Shah, T.; Akhtar, M. *The Groundwater Economy of Pakistan; IWMI Working Paper No. 64*; International Water Management Institute: Colombo, Sri Lanka, 2003; p. 23.
18. Bastiaanssen, W.G.M.; Miltenburg, I.J.; Zwart, S.J. *Modelling and Mapping Global Water Productivity of Wheat, Maize and Rice*; WaterWatch: Wageningen, The Netherlands, 2010.
19. Pakistan Institute of Legislative Development and Transparency (PILDAT). *Inter-Provincial Water Issues in Pakistan*; PILDAT: Islamabad, Pakistan, 2011.
20. Ahmad, I.; Sufi, A.B.; Hussain, T. *Water Resources of Pakistan*; Pakistan Engineering Congress: Lahore, Pakistan, 2012.
21. Mirza, G.M.; Latif, M. Assessment of current agro-economic conditions in Indus Basin of Pakistan. In Proceedings of International Conference on Water, Energy, Environment and Food Nexus: Solutions and Adaptations under Changing Climate, Lahore, Pakistan, 4–5 April 2012.
22. WAPDA. *Lower Indus Project, Part One and Two*; Hunting Technical Services Ltd.: London, UK, 1966.

23. Ahmad, N. *Groundwater Resources of Pakistan (Revised)*; Shahzad Nazir: Lahore, Pakistan, 1995.
24. MacDonald; National Engineering Services Pakistan (Pvt) Limited (NESPAK). *Water Sector Investment Planning Study: Guide to the Indus Basin Model Revised*; World Bank: Washington, DC, USA, 1990.
25. Ahmad, M.; Kutcher, G.P. *Irrigation Planning with Environmental Considerations. A Case Study of Pakistan's Indus Basin*; Technical paper 166; World Bank: Washington, DC, USA, 1993.
26. Mukarram, A.S. *Water Logging and Salinity Problems in the Irrigated Areas of Sindh with Special Reference to the Left Bank Outfall Drain Project*; Pakistan Water & Power Development Authority (WAPDA): Hyderabad, Pakistan, 1984.
27. Aslam, M. *Improved Water Management Practices for the Rice-Wheat System in Sindh*; International Irrigation Management Institute: Lahore, Pakistan, 1998.
28. International Waterlogging and Salinity Research Institute (IWASRI). *Master Drainage Plan of Pakistan—Drainage Vision—2025, Pre-Feasibility*; Pakistan Water & Power Development Authority (WPADA): Lahore, Pakistan, 2004.
29. Government of Sindh, Pakistan. *Second SCARP Transition North Rohri Pilot Project (SSTNRPP)*; Government of Sindh: Hyderabad, Pakistan, 1997.
30. IWMI; Global Water Partnership. Water Policy Briefing, Issue 13: Reducing Poverty through Integrated Use of Groundwater and Surface Water. Available online: http://www.iwmi.cgiar.org/publications/briefs/water-policy-briefs/iwmi-water-policy-briefing-13/ (accessed on 5 April 2015).
31. Louis Berger Group; Indus Consultants. *Bio-Saline Agriculture in Badin and Thatta Districts*; Government of Sindh: Hyderabad, Pakistan, 2012.

Over Exploitation of Groundwater in the Centre of Amman Zarqa Basin—Jordan: Evaluation of Well Data and GRACE Satellite Observations

Sana'a Al-Zyoud, Wolfram Rühaak, Ehsan Forootan and Ingo Sass

Abstract: Jordan faces a sincere water crisis. Groundwater is the major water resource in Jordan and most of the ground water systems are already exploited beyond their estimated safe yield. The Amman Zarqa Basin is one of the most important groundwater systems in Jordan, which supplies the three largest cities in Jordan with drinking and irrigation water. Based on new data the groundwater drawdown in the Amman Zarqa Basin is studied. This basin is the most used drainage area in Jordan. Groundwater drawdown in eight central representative monitoring wells is outlined. Based on almost continuous data for the last 15 years (2000–2015) an average drawdown for the whole basin in the order of 1.1 $m \cdot a^{-1}$ is calculated. This result is in accordance with results of previous studies in other areas in Jordan and shows that, until now, no sustainable water management is applied. Groundwater management in such a basin presents a challenge for water managers and experts. The applicability of satellite data for estimating large-scale groundwater over exploitation, such as gravity products of the Gravity Recovery and Climate Experiment (GRACE) mission, along with supplementary data, is discussed. Although the size of the basin is below the minimum resolution of GRACE, the data generally support the measured drawdown.

Reprinted from *Resources*. Cite as: Al-Zyoud, S.; Rühaak, W.; Forootan, E.; Sass, I. Over Exploitation of Groundwater in the Centre of Amman Zarqa Basin—Jordan: Evaluation of Well Data and GRACE Satellite Observations. *Resources* **2015**, *4*, 819–830.

1. Introduction

Aim of this study is to present new data about the groundwater depletion in the Amman Zarqa Basin in Jordan during 2000–2015. In addition to scattered and relatively sparse well data observations, GRACE satellite data are evaluated to find out if a general groundwater loss is reflected in these gravity measurements.

1.1. Study Area

The Jordanian part of Amman Zarqa Basin (Figure 1) covers an area of 3739 km^2 compared to 310 km^2 in Syria [1]. This basin represents the transitional area between western hills and eastern desert. The climatological conditions change from humid to arid leading to different land use patterns. The western hilly areas are relatively densely populated, whereas the southeast areas are deserts and almost without population. More than 60% of the population of Jordan [2] is located inside the basin. In the areas of upper Zarqa, Baqa'a, Dhulail, and Jerash the groundwater is mainly used for irrigation. According to [3] different agriculture products exist (cereals, vegetables, fruit trees).

According to [4] in 2010 22% of the land cover are urban, mixed rain-fed areas sum up to 37% and irrigated areas sum up to 2.4%.

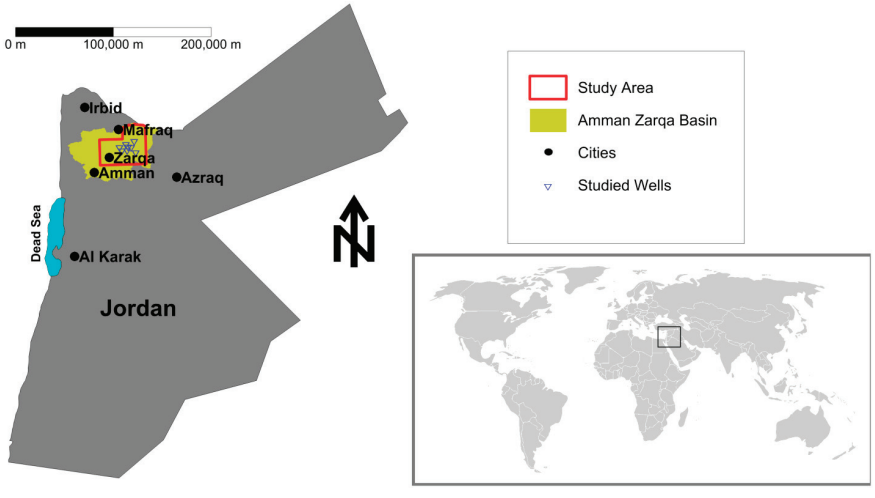

Figure 1. A simplified map of Jordan showing the location of the study area, the Amman Zarqua Basin, and of the studied wells.

The three main aquifers in the Amman Zarqa Basin are formed by (1) a basaltic eruption at the top, (2) a limestone aquifer in the middle, and (3) a sandstone aquifer at the bottom. The upper two aquifers are hydraulically connected. They are underlain by a 20–35 m thick marl formation. The limestone formation, called Amman—Wadi As Sir (B2/A7), is the most important aquifer in the basin. It has a large and continuous extent together with a high hydraulic conductivity. It is considered as the main source of fresh water for domestic, as well as irrigated agricultural, uses. The Amman Zarqa Basin is underlain by the sandstones of the Kurnub-Ram Formations, which form a deeper aquifer system. The Ajlun marl aquitard separates the sandstones from the Basalt Aquifer Complex [5].

The uppermost basaltic aquifer which is formed by highly vesicular lava flows has, based on pumping tests, transmissivity values in the range from 5.0×10^{-5} to 5.4×10^{-1} $m^2 \cdot s^{-1}$, the average is about 8×10^{-2} $m^2 \cdot s^{-1}$, corresponding to a mean hydraulic conductivity of 2.3×10^{-4} $m \cdot s^{-1}$. The transmissivity of the limestone aquifer (B2/A7) varies between 5.4×10^{-5} and 2.5×10^{-2} $m^2 \cdot s^{-1}$, the average is about 5×10^{-3} $m^2 \cdot s^{-1}$, corresponding to a mean hydraulic conductivity of 8.1×10^{-5} $m^2 \cdot s^{-1}$ [6].

Mean discharge rate values in different areas of the basin are between 1 and 40 $m^3 \cdot h^{-1}$ corresponding with transmissivity values of shallow basalt aquifer between 3.47×10^{-4} and 1.50×10^{-2} $m^2 \cdot s^{-1}$.

The basalt sequence has a thickness of 100 m–300 m. Transmissivity values are estimated at around 1.0×10^{-2} $m^2 \cdot s^{-1}$ with corresponding mean hydraulic conductivity of 2×10^{-4} to 6×10^{-4} $m \cdot s^{-1}$ [5].

1.2. Water Availability

Water availability is an important factor controlling human's wealth and prosperity, especially in arid and semi-arid regions [7]. Jordan has a water scarcity probably more serious than other countries in the Middle East [8,9]. This shortage is due to many reasons, such as low rainfall of 100–150 mm·a^{-1} [9,10] with an annual rainfall decrease at an average rate of 1.2 mm [9], uneven water distribution, high water volume losses due to evaporation, and an increasing demand on drinking and agricultural water due to population growth [11]. Surface water resources are very limited in Jordan; therefore, groundwater is the main water resource [6]. As a result, extensive groundwater pumping is taking place in the Jordanian groundwater systems with the use of public and private wells. Rimawi and Al Ansari [12] found that groundwater salinity in the upper aquifer complex in the north-eastern part of the Al Mafraq area (Figure 1) has increased in the last decades. This is due to intensive exploitation of groundwater for irrigation purposes. Salameh [13] showed the lowering trend for some selected wells within the Jordanian area. He concluded that the major Jordan basins may be beyond restoration.

El-Naqa *et al.* [14] found that Azraq Basin (the southeastern neighbor basin of Amman Zarqa Basin) is suffering from groundwater drawdown due to extensive overexploitation. Bajjali *et al.* [15] found that, in the central part of Amman Zarqa Basin, the groundwater level is declining approximately one meter per year.

Ta'any *et al.* [1] applied geostatistics to analyze the spatial and temporal variations of groundwater level fluctuations in 33 wells scattered in the Amman Zarqa Basin. They have been analyzed for the period of 2001–2005. The annual drawdown in wells of [1] is ranging from 0.47 to 1.68 m. Five wells of this study are common with the work of Ta'any *et al.* [1].

New groundwater level data from eight wells in the Amman Zarqa Basin have been studied. The study area is about 28 km NE of Zarqa city (Figure 1), the second largest city in Jordan. Many industrial infrastructures are located in the basin, such as the Jordanian Free Zone Areas, the refinery of Jordan, and the Al Hussain power station; the main power station in Jordan. It is the largest industrial city in Jordan. It is considered the most polluted area in Jordan.

In general, the water level is declining in almost all wells in the basin. The Ministry of Water and Irrigation [16] reported that the declines in water level of the limestone aquifer (B2/A7) range between 0.67 m and 2.0 m per year. Al Mahamid [6] predicted that the maximum accumulative drawdown will reach more than 70 m in the year 2025. He forecasted that some wells between Al Khalidiyya and Umm Al Jimal—located in the middle basin area—will become completely dry. Margane *et al.* [17] reported, too, that the exploitation of the limestone aquifer (A7/B2) has increased over the past decade, so that water levels are rapidly declining in about 2 m·a^{-1}.

The following recent data show that a continuous water level decline is happening in the upper basaltic aquifer of Amman Zarqa Basin.

Remote sensing is a powerful technique for studying groundwater at regional scales [18]. In this study the result of the field data is compared with GRACE satellite data.

2. Methods and Data

2.1. Well Data

The wells discussed in the following are located in the northeastern Jordanian desert in the center of the Amman Zarqa Basin (Figure 1). Their records refer to the water level of the upper aquifer in Amman Zarqa Basin. As this aquifer is an unconfined aquifer, a dropping water level, therefore, reflects an actual decrease in reserves.

Eight monitoring wells which have complete water level records (Ministry of Water and Irrigation MWI [19]) over the last fifteen years (Table 1) were selected in the area (Figures 1 and 2).

The wells are located in the central part of the basin under the largest unprotected industrial zone in Jordan. The data were gathered for the last 15 years (2000–2015) and give detailed information about the condition and operation of the wells.

Table 1. Groundwater drawdown in the studied wells.

Well Name	Total Cumulative Drawdown (m)	Well Observation Period	Total Time (a)	Mean Annual Drawdown from 2000 Till 2015 (m)
AL 1043	31.11	01/2000–03/2015	15.17	2.05
AL 1926	28.09	01/2000–02/2015	15.10	1.86
AL 2698	18.25	01/2000–02/2015	15.10	1.21
AL 3384	14.28	01/2000–02/2015	15.10	0.95
AL 1022	10.98	03/2000–01/2014	13.83	0.79
AL 3387	10.75	06/2001–03/2015	13.80	0.78
AL 1041	59.79	01/2000–01/2013	13.00	4.60
AL 1040	11.33	01/2000–05/2013	13.30	0.85

2.2. Remote Sensing

Since March 2002, the Gravity Recovery and Climate Experiment (GRACE) is routinely providing satellite-based estimates of changes in total water storage (TWS, known as a vertical integration of water changes due to vegetation changes, surface water, soil moisture, and groundwater changes) within the Earth's system. Using GRACE data it is possible to quantify amounts of groundwater usage [20]. GRACE monthly gravity products have been recently used in few studies to explore hydrological patterns within the Middle East. For instance, Longuevergne *et al.* [21] and Voss *et al.* [22] showed a pattern of water storage loss over a large area of Northwest Asia, including the Tigris River Basin (Iraq and Syria), extending to Northwestern Iran, including the Urmia Basin. Forootan *et al.* [23] showed that the extension of groundwater changes can be estimated using GRACE and complementary products within a joint inversion technique. The proposed method is adopted in this study to estimate the large-scale extension of groundwater drawdown over the study area.

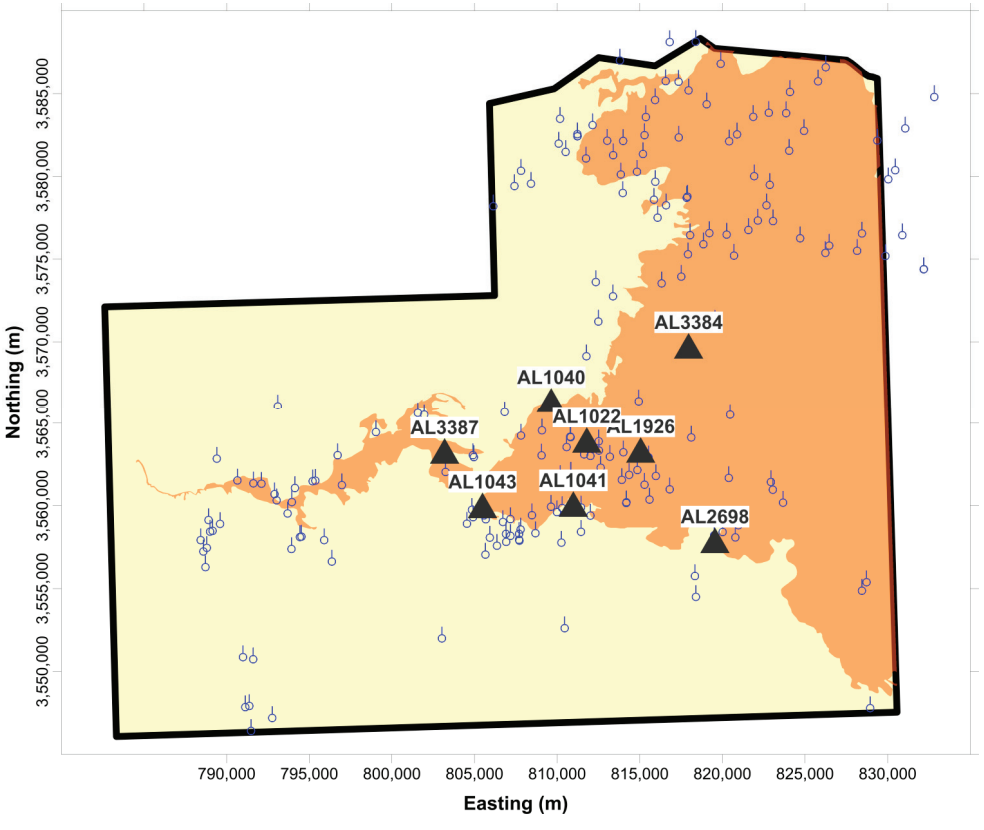

Figure 2. A simplified geological map of the upper aquifer of the Jordanian Harrat basalt showing the long-term monitoring wells discussed in this study, together with all other available wells (coordinates UTM 36 North).

Total water storage (TWS) data within a rectangular box (between 28° to 34° N and 34° to 40° E) that includes Jordan, is extracted from each monthly GRACE-TWS map, which was computed using the Release 5 products of the Center for Space Research (CSR, University of Texas, Austin), over January 2003 to July 2014, following the approach in [24]. Degree one and two coefficients have been replaced by the satellite laser ranging products following the advice given by the GRACE team [25,26]. Correlated errors in GRACE-derived TWS products were reduced using the de-correlation filter of DDK3 [27]. The signal damping due to the application of the DDK3 filter was accounted by computing a single scale factor (4/3 in this study) that is derived as the ratio of the spatial average of a homogenous TWS field (filled by 1 mm within the box area) to the spatial average of the same field after application of the DDK3 filter. Figure 3 shows the linear rate of TWS changes over January 2003 to July 2014. Please note that the scale of TWS changes is 1 mm in a 100 km × 100 km area; thus, the vertical changes cannot be directly compared to the estimated groundwater changes from *in situ* wells.

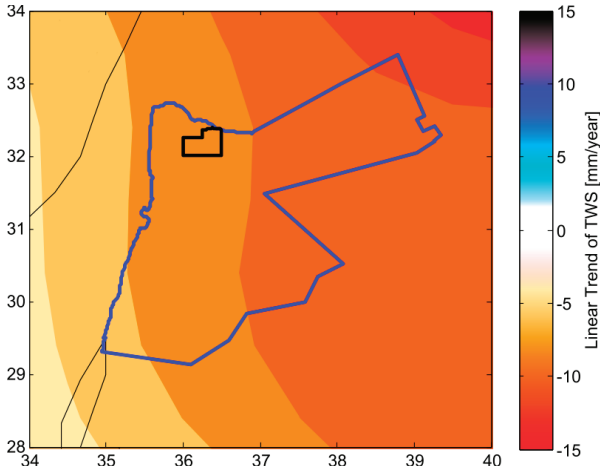

Figure 3. Linear trend over January 2003 to July 2014 derived from GRACE-TWS maps (geographic coordinates).

Over the same period, gridded altimetry data (representing surface water storage changes) derived from the Environmental Research Division's Data Access Program, while the terrestrial water storage changes, including the summation of canopy and soil moisture changes, were derived from the output of the Global Land Data Assimilation System (GLDAS [28]). The dominant independent patterns of altimetry (including the Dead Sea and the Mediterranean Sea) and GLDAS were estimated using the independent component analysis technique [29] and the spatial patterns were introduced as known (base-functions) to separate GRACE-TWS maps in a least squares adjustment (LSA) procedure (similar to [23]). This procedure makes the best use of all available datasets in a LSA framework and reduces the leakage impact due to the implementation of mandatory filtering. Once the base-functions (from altimetry and GLDAS) were adjusted to GRACE-TWS observation, they were used to remove the contribution of surface and terrestrial water storage changes from TWS time-series and compute groundwater changes. The inversion step adopts temporal variability of GLDAS to what is likely reflected in GRACE-TWS. Therefore, it accounts for the resolution mismatch between GLDAS and GRACE data. It should be mentioned here that the steric level changes in the Mediterranean Sea was accounted for using sea surface temperature (SST) data as in [22], therefore, the steric changes due to salinity changes was neglected. No SST was found over the Dead Sea; thus, the estimated volume changes were considered as mass variability.

Groundwater signal estimated from GRACE observations might be contaminated with signals originating from regions outside the region of interest, or the signal of the target area might be moved out as a result of filtering that is used to post process GRACE estimations. Both effects are known as the spatial leakage problem in GRACE related studies. However, various studies indicate that GRACE observations can be used over small regions when care is taken of this leakage problem (see e.g., [30]). In this study, a new methodology was applied, which allows one to mitigate the possible effect of leakage by inversion. This method has already been used to study

water storage changes over the Middle East and the results have been evaluated with groundwater observations [23].

3. Study Results

3.1. Well Data

The groundwater level change shown in Figure 4 and Table 1 extends from different dates where the pumping has started up to early of 2015. The average drawdown was calculated to be 1.64 m·a^{-1} in the last 15 years.

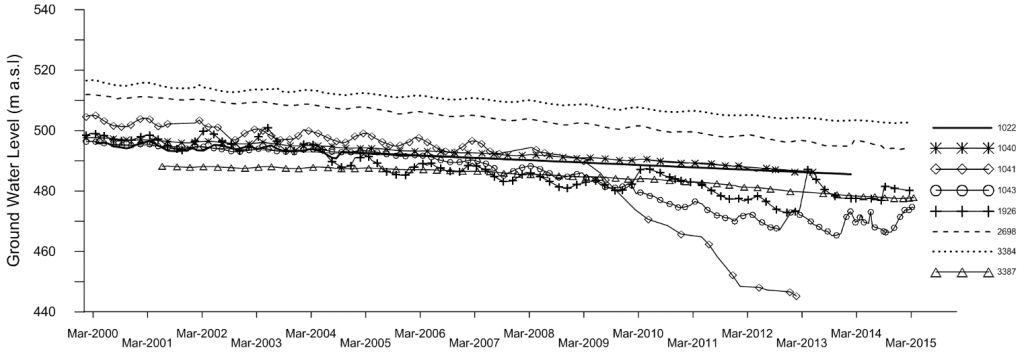

Figure 4. Groundwater drawdown in all studied wells from January 2000 until April 2015.

The report of the Ministry of Water and Irrigation [16] shows that since the early 1960s groundwater levels are declining in this basin. Each well shown in Figure 4 shows a clear water level declination.

According to [6] recharge from rainfall is approximately 45 × 10^6 m^3·a^{-1} and approximately 62 × 10^6 m^3·a^{-1} from lateral subsurface inflow. Accordingly, the outflow is in the order of 66 × 10^6 m^3·a^{-1} into Azraq Basin (neighboring in the south-east [31]) and 3.4 × 10^6 m^3·a^{-1} into Yarmouk Basins (neighboring to the north [31]). The leakage into the lower aquifer is about 12 × 10^6 m^3·a^{-1}. In Mafraq and the Dhuleil—Hallabat area in the central Amman Zarqa Basin it was found that the groundwater is transferred laterally and vertically from the basalts to the lower Amman Wadi Sir limestone [32]. In addition there is an amount of 27 × 10^6 m^3·a^{-1} underflow towards the Zarqa River.

The average drawdown trend observed at the studied wells with 1.64 m·a^{-1} for 15 years should not be considered as the representative trend for the Amman Zarqa Basin, since they are concentrated on the central basin. Furthermore, the hydrogeological settings of the Amman Zarqa Basin are complex due to numerous large fault systems.

However, the presented results are in good agreement with previous data [1,5,6,13–17,33]. In average all these studies stated an annual groundwater level drawdown in the order of 0.65 m to 2.0 m.

3.2. Remote Sensing

Figure 5a shows the linear trend from GRACE adjusted terrestrial water storage (including soil moisture and vegetation changes) during January 2003 to July 2014. The results indicate a decrease

in soil moisture (approximately −15 mm per year in water column) over the country, which is dominated mainly over the northeastern and western regions. A linear trend of groundwater is shown in Figure 5b), which indicates a decline of groundwater at the rate of up to approximately −10 mm per year in the water column concentrated over the study area. This value is equivalent with approximately 160 mm per year in groundwater change concentrated over the model area.

It should be mentioned here that GRACE has usually been used for basins larger than 100,000 km^2 [34]; thus, for basins such as the one studied here, estimations of terrestrial water storage might include a significant level of uncertainty. However, the results in Figure 5 are consistent with those of previous studies [23].

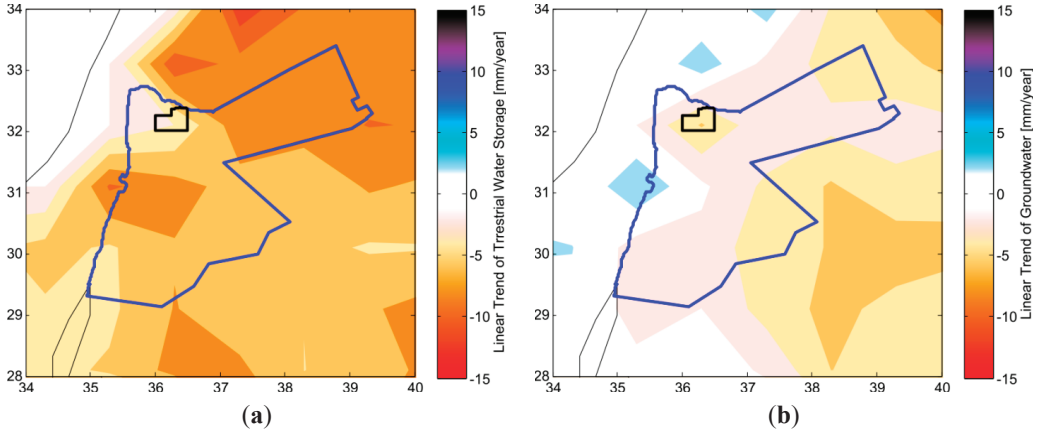

Figure 5. Linear trend over January 2003 to July 2014 derived from GRACE observations and complimentary data (compare with Figure 3). (**a**) From GRACE-adjusted terrestrial water storage products (showing the variability in soil moisture and biomass); and (**b**) side from groundwater storage maps (geographic coordinates).

4. Discussion

The groundwater resources in the Amman Zarqa Basin in Jordan are overused. The basin safe yield is 87.5 million·m^3, while the actual pumping is 156.3 million m^3, resulting in a groundwater depletion of 68.8 million·m^3 by the end of 2013 [35]. Numerous wells in the basin document for the evaluated 15 years an average annual groundwater drawdown of 1.64 m·a^{-1}.

In addition to the over-usage of the groundwater, rainfall has notably declined since 1995 [9]. However, as no precise data of the total pumping exist and recharge rates are estimated [3], no valid hydrological water balance can be calculated.

Although the basin's size is beyond the resolution of the GRACE data, which inhibits detailed predictions, these satellite data also indicate severe groundwater depletion.

Another indication for groundwater depletion, which can be detected by satellites, is subsidence. InSAR or GPS data (e.g., [36,37]) could be evaluated, even if the occurring subsidence may be in the order of the detection limit.

5. Conclusions

Decision-makers should finally recognize the serious groundwater overexploitation status in this area, which has not changed since the last data were published. The groundwater table is still slowly depleting. The urge to find more appropriate solutions for the groundwater management in Jordan is seriously needed.

The major Jordan basins may have become beyond restoration. In any case groundwater extraction should be limited to yield the remaining groundwater resources of the basin.

Measures have to be taken that the access to enough water resources is guaranteed for future generations. To preserve the groundwater resource for future generations all reasons for the groundwater depletion have to be studied carefully. The urgency to implement the necessary measures is, again, proven by this study which should be understood as a part within a framework of national and international investigations.

Acknowledgments

This work is partly supported by the Alliance of Science Organizations in Germany (DFG) in the framework of the Excellence Initiative, Darmstadt Graduate School of Excellence Energy Science and Engineering (GSC 1070).

Author Contributions

The authors have contributed in several ways. Ingo Sass initiated this study, Sana'a Al-Zyoud evaluated the well data and the literature about the regional hydrogeology, Ehsan Forootan evaluated the GRACE data set, Wolfram Rühaak initiated the combination of field data with satellite data and compiled the paper. All authors contributed to the text.

Conflicts of Interest

The authors declare no conflict of interest.

References

1. Ta'any, R.; Tahboub, A.; Saffarini, G. Geostatistical analysis of spatiotemporal variability of groundwater level fluctuations in Amman Zarqa basin, Jordan: A case study. *Environ. Geol.* **2009**, *57*, 525–535.
2. DOS Jordan Department of Statistics 2010. Available online: http://www.dos.gov.jo/sdb_pop/sdb_pop_e/ehsaat/alsokan/2010/2-2.pdf (accessed on 3 November 2015).
3. Al-Abed, N.; Al-Sharif, M. Hydrological modeling of Zarqa River Basin—Jordan using the hydrological simulation program—FORTRAN (HSPF) model. *Water Resour. Manag.* **2008**, *22*, 1203–1220.
4. Al-Bakri, J.T.; Salahat, M.; Suleiman, A.; Suifan, M.; Hamdan, M.R.; Khresat, S.; Kandakji, T. Impact of climate and land use changes on water and food security in Jordan: Implications for transcending "the tragedy of the commons". *Sustainability* **2013**, *5*, 724–748.

5. *UN-ESCWA and BGR (United Nations Economic and Social Commission for Western Asia*; *Bundesanstalt für Geowissenschaften und Rohstoffe)*; Inventory of Shared Water Resources in Western Asia: Beirut, Lebanon, 2013.
6. Al Mahamid, J. Integration of water resources of the upper aquifer in Amman—Zarqa basin based on mathematical modeling and GIS, Jordan, Freiberg Online Geology, Germany, 2005, Available online: http://citeseerx.ist.psu.edu/viewdoc/download?doi=10.1.1.225.991&rep=rep1&type=pdf (accessed on 6 August 2015).
7. Sidiropoulos, P.; Mylopoulos, N.; Loukas, A. Optimal management of an overexploited aquifer under climate change: The Lake Karla case. *J. Water Resour. Manag.* **2013**, *27*, 1635–1649.
8. Al-Weshah, R. Jordan's water resources: Technical perspective. *Water Int.* **1992**, *17*, 124–132.
9. Rahman, K.S.M.; Gorelick, P.J.; Dennedy-Frank, J.; Yoon, B. Rajaratnam, declining rainfall and regional variability changes in Jordan. *Water Resour. Res.* **2015**, *51*, doi:10.1002/2015WR017153.
10. Jordan Meteorological Department. *Department Data Base*; JMD: Amman, Jordan, 2015.
11. Al-Kharabsheh, A.; Al-Mahamid, J. Optimizing pumping rates of Hallabat-Khalidiya Wellfield using finite-difference model: A case study for evaluating over pumped aquifers in arid areas (Jordan). *J. Arid Environ.* **2002**, *52*, 259–267.
12. Rimawi, O.; Al-Ansari, N. Groundwater degradation in the northeastern part of Mafraq area, Jordan. In *Freshwater Contamination*, Proceedings of Rabat Symposium S4; April–May 1997; IAHS Publ.: Oxfordshire, UK, pp. 235–243.
13. Salameh, E. Over-exploitation of groundwater resources and their environmental and socio-economic implications: The case of Jordan. *Water Int.* **2008**, *33*, 55–68.
14. El-Naqa, A.; Al-Momani, M.; Kilani, S.; Hammouri, N. Groundwater deterioration of shallow groundwater aquifers due to overexploitation in northeast Jordan. *Clean Soil Air Water* **2007**, *35*, 156–166.
15. Bajjali, W.; Al-Hadidi, K.; Ismail, M. Water quality and geochemistry evaluation of groundwater upstream and downstream of the Khirbet Al-Samra wastewater treatment plant/Jordan. *J. Appl. Water Sci.* **2015**, doi:10.1007/s13201-014-0263-x.
16. *Outline Hydrogeology of the Amman—Zarqa Basin, Report: Water Resources Policy Support*; MWI Ministry of Water and Irrigation: Amman, Jordan, 2000.
17. Margane, A.; Hobler, M.; al Momani, M.; Subah, A. *Contributions to the Hydrogeology of Northern and Central Jordan—Geologisches Jahrbuch C 68*; Schweizerbart Science Publishers: Stuttgart, Germany, 2002; p. 52.
18. Becker, M.W. Potential for satellite remote sensing of ground water. *Ground Water* **2006**, *44*, 306–318.
19. *MWI Files and Personal Communications*; MWI Ministry of Water and Irrigation: Amman, Jordan, 2010.
20. Richey, A.S.; Thomas, B.F.; Lo, M.-H.; Reager, J.T.; Famiglietti, J.S.; Voss, K.; Swenson, S.; Rodell, M. Quantifying renewable groundwater stress with GRACE. *Water Resour. Res.* **2015**, *51*, 5217–5238.

21. Longuevergne, L.; Wilson, C.R.; Scanlon, B.R.; Crétaux, J.-F. GRACE water storage estimates for the Middle East and other regions with significant reservoir and lake storage. *Hydrol. Earth Syst. Sci. Discuss.* **2012**, *9*, 11131–11159.
22. Voss, K.A.; Famiglietti, J.S.; Lo, M.-H.; de Linage, C.; Rodell, M.; Swenson, S.C. Groundwater depletion in the Middle East from GRACE with implications for transboundary water management in the Tigris-Euphrates-Western Iran region. *Water Resour. Res.* **2013**, *49*, doi:10.1002/wrcr.20078.
23. Forootan, E.; Rietbroek, R.; Kusche, J.; Sharifi, M.A.; Awange, J.; Schmidt, M.; Omondi, P.; Famiglietti, J. Separation of large scale water storage patterns over Iran using GRACE, altimetry and hydrological data. *Remote Sens. Environ.* **2014**, *140*, 580–595.
24. Wahr, J.; Molenaar, M.; Bryan, F. Time variability of the Earth's gravity field: Hydrological and oceanic effects and their possible detection using GRACE. *J. Geophys. Res.* **1998**, *103*, 30205–30229.
25. Jet Propulsion Laboratory, Geocenter-Degree 1. Available online: http://grace.jpl.nasa.gov/data/get-data/geocenter/ (accessed on 26 September 2015).
26. Jet Propulsion Laboratory, Spherical Harmonic coefficients of Degree 2. Available online: http://grace.jpl.nasa.gov/data/get-data/oblateness/ (accessed on 26 September 2015).
27. Kusche, J.; Schmidt, R.; Petrovic, S.; Rietbroek, R. Decorrelated GRACE time-variable gravity solutions by GFZ, and their validation using a hydrological model. *J. Geod.* **2009**, *83*, 903–913.
28. Rodell, M.; Houser, P.R.; Jambor, U.; Gottschalck, J.; Mitchell, K.; Meng, K.; Arsenault, K.; Cosgrove, B.; Radakovich, J.; Bosilovich, M.; *et al.* The global land data assimilation system. *Bull. Am. Meteorol. Soc.* **2004**, *85*, 381–394.
29. Forootan, E.; Kusche, J. Separation of global time-variable gravity signals into maximally independent components. *J. Geod.* **2012**, *86*, 477–497.
30. Longuevergne, L.; Scanlon, B.R.; Wilson, C.R. GRACE hydrological estimates for small basins: Evaluating processing approaches on the High Plains Aquifer, USA. *Water Resour. Res.* **2010**, *46*, doi:10.1029/2009WR008564.
31. Goode, D.J.; Senior, L.A.; Subah, A.; Jaber, A. Groundwater-Level Trends and Forecasts, and Salinity Trends, in the Azraq, Dead Sea, Hammad, Jordan Side Valleys, Yarmouk, and Zarqa Groundwater Basins, Jordan; Open-File Report 2013–1061; U.S. Department of the Interior: Washington, DC, USA; U.S. Geological Survey: Reston, VA, USA, 2013.
32. Abu Sharar, R. Water chemistry of the Dhuleil aquifer (Jordan) as influenced by long term pumping. *J. Hydrol.* **1993**, *149*, 49–66.
33. Bajjali, W.; Al-Hadidi, K. Recharge origin, overexploitation, and sustainability of water resources in an arid area from the Azraq basin, Jordan: Case study. *Hydrol. Res.* **2006**, *37*, 277–292.
34. Swenson, S.; Wahr, J.; Milly, P. Estimated accuracies of regional water storage variations inferred from the Gravity Recovery and Climate Experiment (GRACE). *Water Resour. Res.* **2003**, *39*, doi:10.1029/2002WR001808.

35. MWI Ministry of Water and Irrigation Web Site, Jordan Water Sector Facts and Figures 2013. 2014. Available online: http://www.mwi.gov.jo/sites/en-us/Documents/W.%20in%20Fig.E%20FINAL%20E.pdf (accessed on 6 August 2015).
36. Amelung, F.; Galloway, D.L.; Bell, J.W.; Zebker, H.A.; Laczniak, R.J. Sensing the ups and downs of Las Vegas: In SAR reveals structural control of land subsidence and aquifer-system deformation. *Geology* **1999**, *27*, 483–486.
37. Abidin, H.Z.; Andreas, H.; Gamal, M.; Wirakusumah, A.D.; Darmawan, D.; Deguchi, T.; Maruyama, Y. Land subsidence characteristics of the Bandung Basin, Indonesia, as estimated from GPS and InSAR. *J. Appl. Geod.* **2008**, *2*, 167–177.

A Columbia River Basalt Group Aquifer in Sustained Drought: Insight from Geophysical Methods

Mark W. Piersol and Kenneth F. Sprenke

Abstract: Aquifers within the Columbia River Basalt Group (CRBG) provide a critical water supply throughout much of the Pacific Northwest of the United States. Increased pumping has resulted in water level declines in this region. Recharge into this aquifer system is generally not well understood. Recent suggestions of probable decades-long droughts in the 21st century add to this problem. We show that geophysical methods can provide useful parameters for improved modeling of aquifers in a primary CRBG aquifer located on the eastern edge of the Columbia Plateau. Groundwater models depend in part on the area, thickness, porosity, storativity, and nature of confinement of this aquifer, most of which are poorly constrained by existing well information and previous stress tests. We have made use of surface gravity measurements, borehole gravity measurements, barometric efficiency estimates, earth tidal response, and earthquake seismology observations to constrain these parameters. We show that the aquifer, despite its persistent drawdown, receives a great deal of recharge annually. Much of the recharge to the aquifer is due to leakage from overlying flows, ultimately tied to precipitation, an important result for future aquifer management in times of sustained drought.

Reprinted from *Resources*. Cite as: Piersol, M.W.; Sprenke, K.F. A Columbia River Basalt Group Aquifer in Sustained Drought: Insight from Geophysical Methods. *Resources* **2015**, *4*, 577–596.

1. Introduction

The Columbia River Basalt Group (CRBG) in the Pacific Northwest of the United States hosts a regional aquifer system that extends from the foothills of the northern Rocky Mountains in west-central Idaho into the Columbia Basin of Washington and Oregon (Figure 1). In many locations within the region, it is the only water source for communities, residences, industry, agriculture, and aquaculture [1]. The CRBG aquifer system is a significant concern to water resources managers because of long-term water level decline and a general lack of knowledge about natural recharge.

A recent study has suggested that in the western states, drought risk in the 21st century will likely exceed the driest centuries of the past millennia, leading to unprecedented drought conditions [2]. Much of the inland Pacific Northwest is characterized by an arid to semiarid climate. The majority of surface water in this region originates as upland precipitation. The causes of past and future drought will not be identical but the paleoclimatic record demonstrates the plausibility of extensive, severe droughts [3]. In the past half century, the up-dip areas of the Columbia Basin abutting the northern Rocky Mountains region have experienced a substantial decline in peak snow water equivalent [4]. A recent USGS study of the Columbia Basin suggests that climate change will result in a drop in water levels across the region with resultant degradation and disappearance of aquatic ecosystems [5]. Water managers in the Columbia Basin need to understand the nature of recharge into the aquifer system and the effect a sustained drought will have on aquifer system productivity.

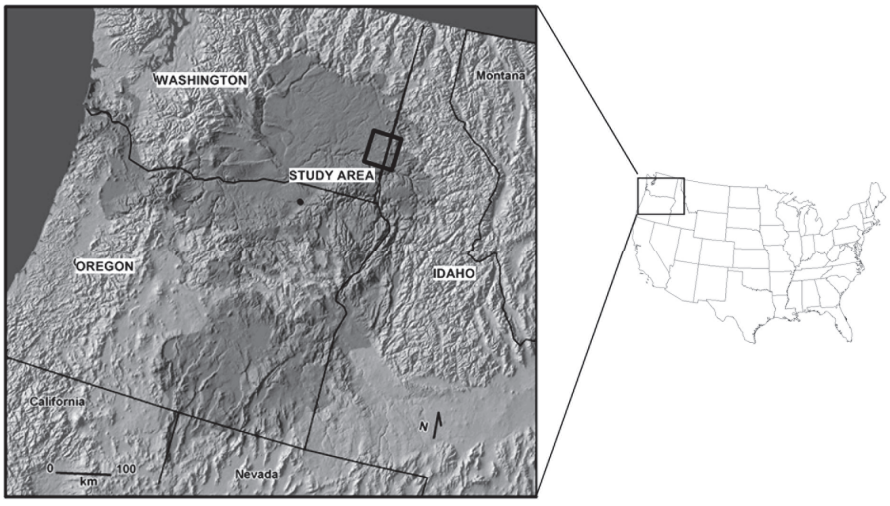

Figure 1. The darkly shaded area is the CRBG regional aquifer system in the Pacific Northwest of the contiguous United States. The rectangle on the left map shows the location of the general study area, the Palouse basin.

Recharge, if any, of the deeper CRBG aquifers is generally inferred to occur (1) from groundwater movement originating around the edge of the Columbia Basin in up-dip areas where units pinch out; and (2) from vertical leakage through younger more shallow flows via open faults and tectonic fractures. Both of these sources are intimately related to precipitation and ultimately climate change. The general area of this study (the Palouse basin), lies at the eastern up-dip edge of the CRBG in good position to study the nature of CRBG recharge (Figure 1). Furthermore, excellent records of pumping volumes and historic records of annual water level declines are maintained by the Palouse Basin Aquifer Committee [6].

The key to understanding the nature of recharge in the study area is to have an adequate groundwater model that explains the dynamics of the aquifer system. However, previous groundwater models [7,8] for the study area have neither predicted the annual drop in water levels within the aquifer system nor have they provided any useful insight into the nature of recharge. We believe the lack of success of these models was at least in part the result of incorrect parameters employed, particularly with respect to the area, thickness, porosity, storativity, and nature of confinement of the aquifer system. The purpose of this study is to show that geophysical methods including surface gravity measurements, borehole gravity measurements, barometric efficiency estimates, earth tidal response, and earthquake seismology observations can be useful to better constrain these parameters for future groundwater models.

1.1. CRBG Aquifers

Numerous studies of CRBG aquifers have been conducted within the Columbia Basin to better understand their hydrogeology [9–17]. One of the most significant findings of these studies is the similarity of the hydrogeological characteristics, properties, and behavior of the CRBG aquifers

across the region. These general characteristics include: (1) simple sheet flows of basalt 10 to >100 m thick of great lateral extent that act as aquitards; (2) intraflow structures such as vesicular flow-tops, rubble zones, and sedimentary interbeds that act as aquifers; (3) control of lateral continuity of the aquifers by erosion, flow pinchouts, folds, faults and dikes; (4) flow pathways dominantly sub-horizontal down-dip; (5) limited vertical groundwater movement. These similar characteristics allow for the application of the knowledge of the general hydraulic characteristics and behavior of the CRBG aquifers in one area to be applied to CRBG aquifers in other areas [18].

1.2. Study Area

Our general study area (Figure 2) is the Palouse basin of western Idaho and eastern Washington abutting the crystalline rocks of the northern Rockies foothills. The Palouse is an important dryland agricultural region, with a semi-arid climate and topography dominated by rolling hills composed predominantly of windblown loess. A larger amount of precipitation falls in the mountainous terrain which bounds the study area to the east, southeast, and north [19]. The Palouse River, its tributaries, and other local streams drain the area and flow towards the northwest to eventually join the Snake River. Some 800 water wells have been cataloged in the Palouse basin [20] which covers an area of 1280 km^2. Most are shallow, very-low productivity domestic wells hosted in the loess soil cover or in the crystalline rocks of the surrounding highlands.

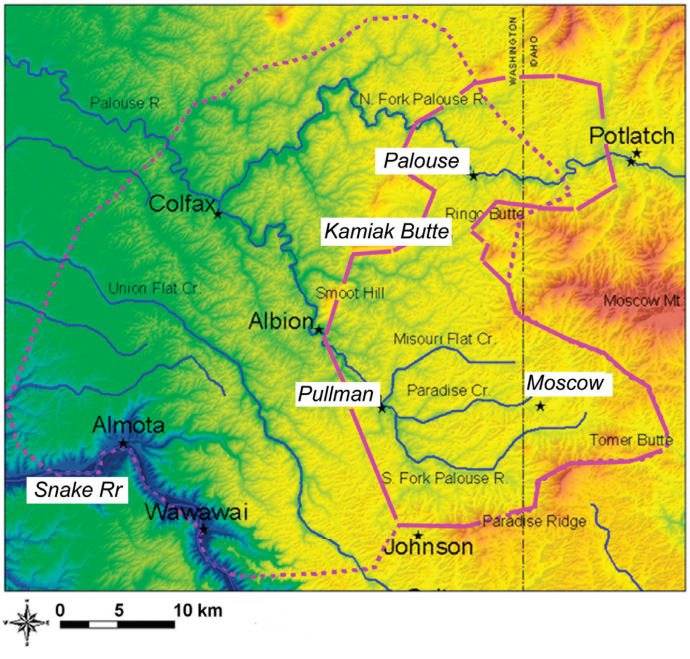

Figure 2. The Palouse basin general study area. See Figure 1 for location. The specific study area, the Moscow-Pullman basin is indicated by the solid purple line. The dashed line is the boundary of the larger area under the political jurisdiction of the Palouse Basin Aquifer Committee.

1.3. The Moscow-Pullman Basin

Based on the very similar piezometric elevations and historic water level declines, the primary aquifer system that serves the cities of Pullman and Moscow appears to be restricted to an area referred to as the Moscow-Pullman basin (Figure 2) which is partially hydraulically isolated from the larger Palouse basin and the main body of the CRBG regional ground-water flow system. This is a lava embayment of the CRBG Grande Ronde Formation which flowed into the area during Miocene time from the southwest following a pre-basalt stream system cut into the western slope of the northern Rockies. The Moscow-Pullman basin has an area of 420–660 km^2 and encompasses the cities of Pullman, Washington and Moscow, Idaho plus multiple smaller communities and rural areas, as well as two large universities. This basin is part of the much larger Palouse basin, also shown on Figure 2.

A geological section (Figure 3) through Moscow and Pullman illustrates the general stratigraphy in the Moscow-Pullman basin. Beneath a loess soil cover are the Saddle Mountain, Wanapum, Grande Ronde, and Imnaha basalt formations of the Miocene CRBG, each of which is composed of multiple flows. Interspersed between flows are sedimentary interbeds collectively called the Latah Formation. The pre-basalt rocks are Cretaceous granites and Precambrian crystalline metasediments.

As shown in Figure 4, hydrographs are available for about 30 wells in the Moscow-Pullman basin. Fairly common are wells 30–40 m deep, hosted in the Wanapum Formation. These wells account for 10% of the water produced in the basin. The primary aquifer system (known locally as the "lower" or "Grande Ronde" aquifer system) is completely contained within the Grande Ronde Formation. The high yield municipal and university wells tap the Grande Ronde Formation typically at depths of 90–120 m. The Grande Ronde Formation accounts for 90% of the 2.45 billion gallons (62.4 × 10^6 m^3) pumped annually in the Palouse basin [6].

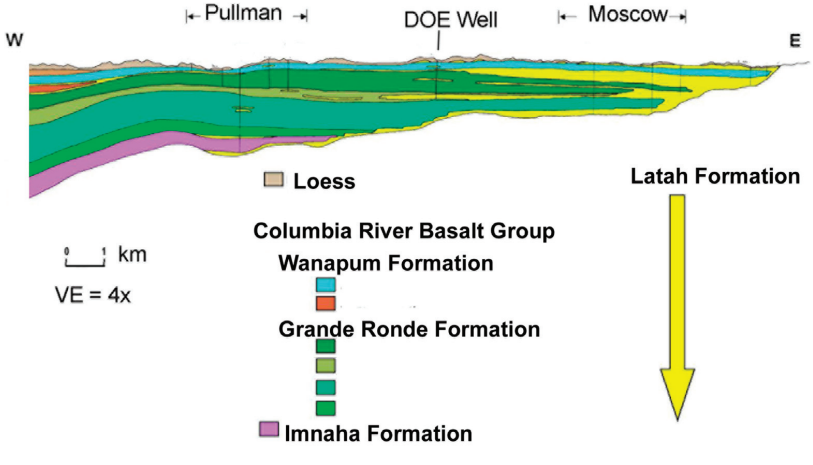

Figure 3. Diagrammatic west to east geological cross section through Pullman to Moscow showing the basalt stratigraphy of the study area.

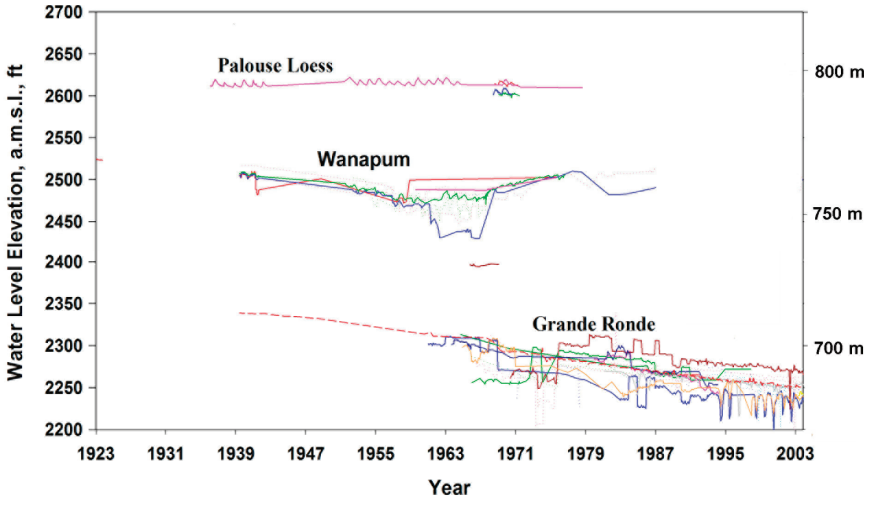

Figure 4. Composite hydrograph of 30 water wells in the Palouse basin. Modified from [20].

Except at the entrance to the basin, the aquifer system is largely bounded by crystalline rocks of the surrounding highlands. The entrance to the Moscow-Pullman basin near Pullman coincides with a ground water divide apparent on the piezometric surface of the primary aquifer system (Figure 5).

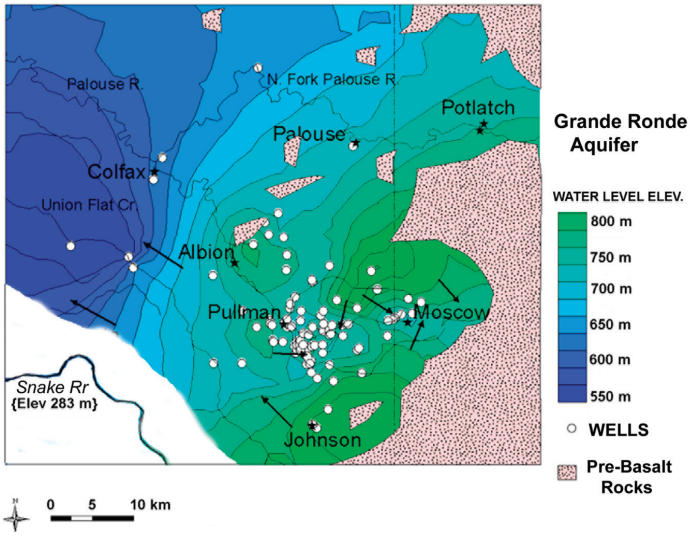

Figure 5. Piezometric map of the primary aquifer. Arrows indicate postulated flow directions of groundwater.

To the southwest of Pullman, a poorly understood barrier to groundwater flow [7] prevents groundwater from flowing down the steep gradient to the elevation of the Snake River, lying in a deep canyon some 500 m in elevation below the Moscow-Pullman basin (Figure 5). Geochemical observations [21] have shown that groundwater does not seep into the Snake Canyon. It has also been

noted that there is a conspicuous lack of large springs on the walls of the Snake River canyon [22]. Generally to the west of the Moscow-Pullman basin piezometric elevations fall off more moderately toward Colfax, dropping some 135 m. As shown in the stratigraphic and hydrogeological cross-section (Figures 3 and 6), the top of the Grande Ronde drops in elevation east towards Moscow and west and northwest away from Pullman.

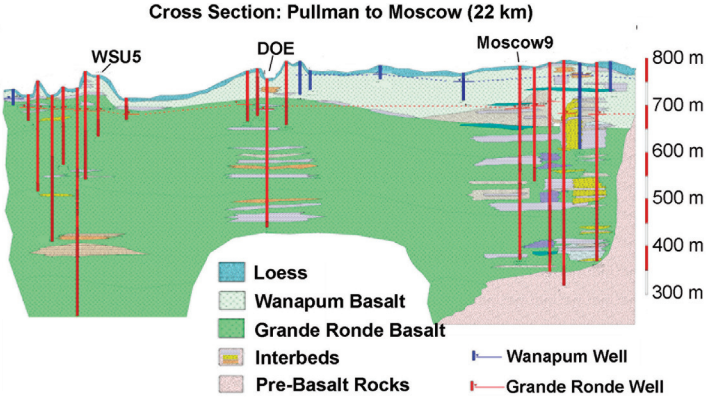

Figure 6. Diagrammatic hydrogeological cross-section from the Pullman wells on the left (west) to the Moscow wells on the right (east).

1.4. The Primary Aquifer System

At Pullman, the top of the Grande Ronde Formation is at a relatively high elevation; the depth to the Grande Ronde Formation top is less than 15 m in places (Figure 6). Here, water-level elevations are essentially the same in wells completed deep in the aquifer system and in more shallow open wells. At Moscow and Palouse, however, the primary aquifer system is definitely confined. The Grande Ronde Formation is more than 130 m deep at Moscow, yet the piezometric surface rises to the same level as at Pullman. Wells completed in the overlying Wanapum aquifer system have higher ground-water levels as compared to wells completed in the primary aquifer system (Figures 4 and 6). This strong downward hydraulic gradient suggests that the Wanapum aquifer system, might leak into the primary aquifer system. However, no hydraulic connection has ever been observed between the Wanapum aquifer system and the Grande Ronde aquifer system in the Moscow area.

Four predominant studies using isotopic concentrations in groundwater have been completed in the Moscow-Pullman basin [23–26]. The apparent radiocarbon ages of water in the Pullman-Moscow area range from 11,000 to 26,000 year in the primary aquifer and from modern to 10,000 year in the overlying units [25,26]. For stable oxygen isotopes, the $\delta^{18}O$ values range from −16% to −17.5% in the primary aquifer and from −16% to −14.8% in the overlying units [24,26]. These numbers suggest that the majority of the water in the Grande Ronde was recharged during ice age conditions in the Pleistocene. On the other hand, tritium concentrations, no older than 60 years, have been detected in the upper part of primary aquifer indicating that modern recharge is mixing with the Pleistocene water in the Grande Ronde [26].

In the Moscow-Pullman basin, recharge, if any, to the primary aquifer system comes from either the mountains on edges of the basin where the basalt flows pinch out against the crystalline rocks of the highlands or from vertical leakage from overlying more shallow aquifers perched between flows above the regional aquifer system [27]. It is of critical importance for future management of the aquifer system to determine if there is any recharge to the primary aquifer system and whether it is generated in the surrounding highlands at flow pinchouts or by vertical leakage throughout the basin. If there is no recharge, then new sources of water need to be found for future development, such as a pipeline to the Snake River, some 20 km south and 500 m in elevation below the study area. If there is recharge, then the optimum locations of recharge galleries need to be determined.

The rational approach to understanding the nature of recharge is to develop a ground water model based on a sound hydrogeological conceptual model consistent with pumpage records and the history of water level declines. Previous groundwater models [7,8] of the study area have failed in all these regards. Below we show how geophysical methods have provided better parameters for future groundwater models.

2. Methods

Groundwater models depend in part on the porosity, area, thickness, storativity, and nature of confinement of the aquifer. These parameters, in the Moscow-Pullman basin, are poorly constrained by existing well information and previous stress tests. We have made use of geophysical measurements, including surface gravity measurements, borehole gravity measurements, barometric efficiency estimates, earth tidal response, and earthquake seismology observations to constrain these parameters.

2.1. Porosity of the Aquifer System

The porosity of the CRBG strata exhibits a bimodal distribution due to the difference between the dense, massive interiors of flows (aquitards) and the intraflow structures (aquifers). To better quantify this porosity difference, we made use of extraordinarily detailed borehole gravity data that have been carried out in CRBG strata in three wells at the Hanford site in central Washington State as part of the design process for a new waste treatment plant [28]. The Hanford Site is a mostly decommissioned nuclear production complex sitting on CRBG bedrock operated by the United States federal government on the Columbia River in the U.S. state of Washington. This borehole gravity survey is stated to include the longest section (approximately 1280 m in the three wells) of measurements data taken at such a small station spacing (3 m).

The borehole gravity meter tool has a very large horizontal depth of investigation so it is not influenced by washouts and borehole construction. The survey goal at Hanford was to provide CRBG rock densities with an estimated error of ±0.05 g/cm^3 or less. We plotted the 302 CRBG basalt density determinations from the Hanford survey as a histogram in Figure 7. The distribution is clearly bimodal indicating the dichotomy between the massive flows and the porous intraflow zones encountered in the section of CRBG strata surveyed. As also shown in Figure 7, we fit the histogram with two Gaussian curves [29]. The higher peak is at a density 2.80 ± 0.12 mg/cm^3 which we take as the mean density of the massive flows. The lower peak is at density 2.02 ± 0.17 g/cm^3 which we

interpret as the density of the intraflow zones. The density contrast between the massive flow zones and the intraflow units is 0.78 ± 0.20 g/cm^3. If we treat the massive flows as having no effective porosity, but with an unconnected vesicle volume typical of basalt (7.8%) [30], we find the mean porosity of the intraflow zones is 0.355 ± 0.04.

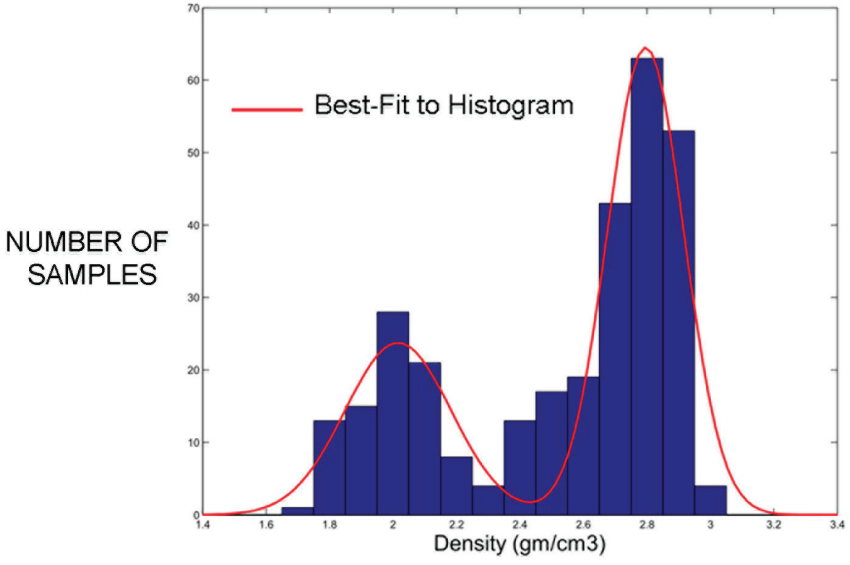

Figure 7. Histogram of basalt densities found from a borehole gravity survey [28]. The survey densities were binned in 0.1 g/cm^3 increments and then fitted to a bimodal curve using the EzyFit toolbox [29]. The lower density peak is modeled as 2.02 ± 0.17 g/cm^3 and the higher density peak as 2.80 ± 0.12 g/cm^3.

2.2. Area of the Aquifer System

The area of the main Grande Ronde aquifer system that should be included in a groundwater model of the Moscow-Pullman basin is quite controversial. By area in this regard, we mean the areal extent to which aquifer parameters determined from well tests in the deep city wells should be applied. In some studies the southwest boundary of the Moscow-Pullman aquifer system is thought to be bounded by the Snake River [8,31], however, geochemical studies have shown that Moscow-Pullman basin ground water does not seep into the Snake River Canyon [21]. It appears likely that northwest trending folds paralleling the Union Flat Creek restrict groundwater movement towards the Snake River Canyon, instead channeling it northwest [7,20,32–37].

Another controversy concerns whether the Grande Ronde aquifer system hydrologically connects the southern cities of Pullman and Moscow to the northern city of Palouse. A break in the crystalline rocks within the basin, called the Kamiak Gap, occurs between Pullman and Palouse immediately east of Kamiak Butte (Figure 2). Hydraulic connection between Palouse and the rest of the basin through the Kamiak Gap has been investigated on a geophysical basis by several researchers [38,39]. A magnetotelluric study [38] suggested continuity of the Grande Ronde Formation through the gap. On

the other hand, gravity methods [39] initially suggested that the Grande Ronde was interrupted by a saddle of crystalline basement rock obstructing aquifer conductivity south of Palouse. However, new test well data [40], providing much needed control on the elevations of formation tops, has allowed us to reinterpret these gravity data. Gravity readings were taken along four lines in the Kamiak Gap (Figure 8) [39].

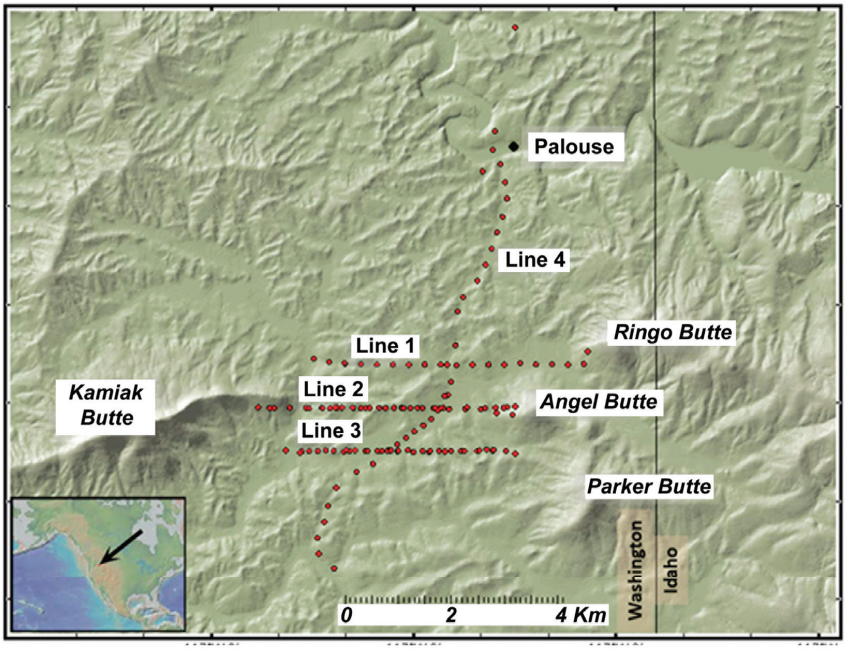

Figure 8. Gravity survey area in the Kamiak Gap [39]. See Figure 2 for location of Kamiak Butte within the study area. Lines 1, 2, and 3 are east-west transects of gravity stations across the gap and Line 4 meanders approximately north-south crossing the other three lines. Figure generated with GeoMapApp [41].

The stratigraphy of the DOE Butte Gap well, drilled at the latitude of the southernmost east-west transect, is remarkably similar to the stratigraphy of the Palouse City #3 well drilled to the north of the Kamiak Gap [40]. Using these constraints we propose a new geophysical model (Figure 9) suggesting that the Grande Ronde basalts are indeed continuous through the Kamiak Gap with a net thickness in excess of 100 m. Thus, Kamiak Gap should not create a hydraulic barrier to north-south groundwater flow.

Thus, for improved ground-water models, the total area of the primary aquifer system that directly affects the Moscow-Pullman basin should be about 620 km^2, with 420 km^2 south of Kamiak gap, and 200 km^2 north of the gap.

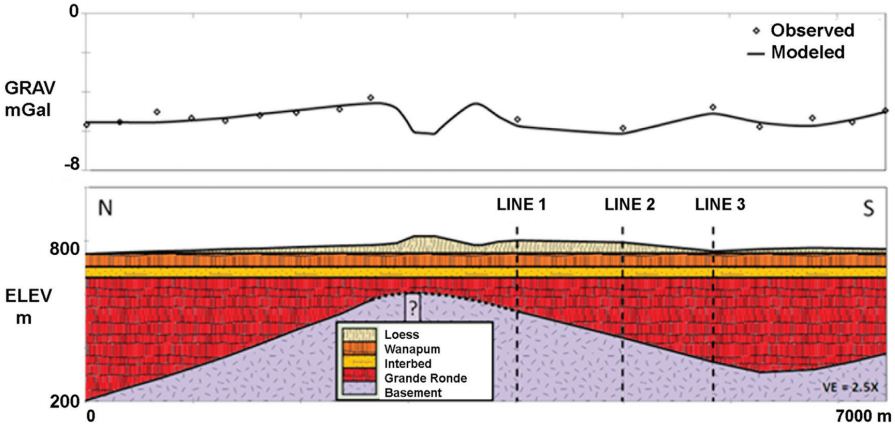

Figure 9. Gravity model through the Kamiak Gap from north to south. Modeled thickness of Grande Ronde at intersection of Line 1 (Figure 8) is 125 m, at intersection of Line 2 is 224 m, and at intersection of Line 3 is 316 m. The dashed line between basement and Grande Ronde north of Line 1 below the topographic divide indicates uncertainty in the model as there is approximately 1.35 km between survey point locations.

2.3. Thickness of the Aquifer System

Comparing the areas of the two normal curves of the histogram of borehole gravity data from CRBG strata at the Hanford site (Figure 7), we find that 29% of the basalt section there is aquiferous intraflow units; the remainder is massive basalt with negligible effective porosity. Based on the logs from deep wells in the Moscow area (Figure 6), a previous study [42] estimates that 25% of the Grande Ronde section consists of intraflow zones. A well construction report [34] for the DOE well (Figure 6) logged where water was seen in the drill core. About 28% of the core length contained water. Producing zones from the Grande Ronde in the Moscow-Pullman basin lie between elevations of 350 m and 716 m above sea level (Figure 6), a net thickness of 365 m. Thus, we estimate the effective thickness of the primary aquifer to be 25% to 29% of 365 m or 100 ± 2 m.

2.4. Specific Storage from Barometric Efficiency

Specific storage can be estimated from barometric efficiency if the porosity of the aquifer is known.

$$S_S = \frac{\eta \gamma_w}{E_w BE} \quad (1)$$

where η is porosity; γ_w is the unit weight of water in N/m^3; E_w is the elastic modulus of water (2.2×10^9 Pa); BE is barometric efficiency; and S_S is aquifer specific storage in m^{-1}. The barometric efficiency of aquifers in the CRBG is high because of the strength of the massive nearly impermeable flow interiors that separate the confined intraflow aquiferous zones. In the Grande Ronde aquifer system of the Moscow-Pullman basin, previous studies [43,44] have shown that BE ranges from

0.9 to 1.0. As described above, we estimate the mean porosity of the intraflow zones to be 0.355 ± 0.04. Using this value in Equation (1) above, along with the known BE of 0.95 ± 0.05, we find that the specific storage S_s of the aquiferous intraflow zones is $1.67 \times 10^{-6} \pm 0.18 \times 10^{-6}$ m^{-1}.

2.5. Specific Storage from Earthquake Seismology

Seismological theory [45–47] predicts that S_s for a confined aquifer can be found by comparing, as the Rayleigh waves from distant large earthquakes roll by, earthquake seismograms to water level oscillations as illustrated in Figure 10. To determine specific storage, the borehole amplification factor has to be known for the well. This factor depends on oscillation frequency, the borehole radius, initial height of the water column, screened aquifer thickness, transmissivity of the aquifer, and, to a minor extent, S_s [46]. Because our quantity to be determined, S_s is involved in the calculation of the borehole amplification factor, the method requires an iterative procedure for its solution. An initial guess of S_s is used to generate successively better approximations. However, because S_s has only a minor effect on the borehole response, convergence is quickly obtained.

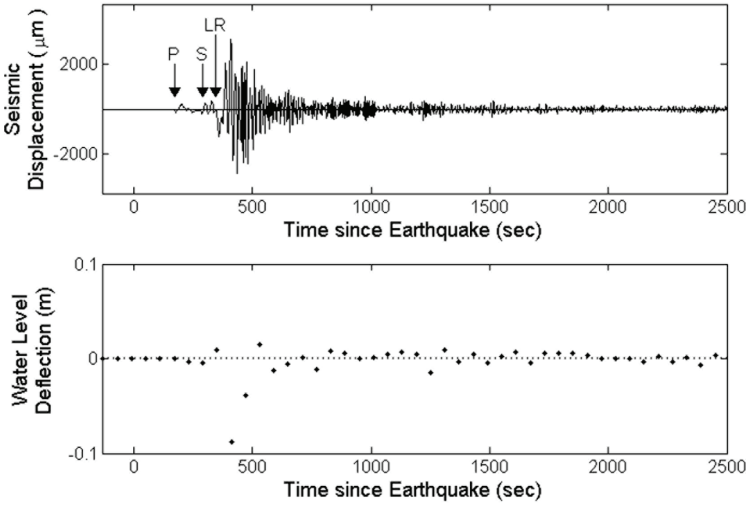

Figure 10. Water level oscillations observed in a water well near Moscow, Idaho while seismic waves from the 2012 M7.8 Haida Gwaii Earthquake passed through the aquifer.

The seismic Rayleigh wave response of municipal well Moscow 9 (see Figure 6 for location) was evaluated. This important supply well was shut down temporarily for pump repair for several months in 2012, giving an opportunity for the installation of a data logger. The well is cased except for 27 m of screen adjacent to several interconnected highly permeable flow top units within the Grande Ronde aquifer. The top of the aquifer is at a depth of 198 m below land surface. The static level of the water rises to a height of 104 m above the top of this confined artesian aquifer. The borehole diameter above the screened intervals is 0.22 m. A transmissivity estimate from previous well tests was used [48]. Rayleigh waves from three moderately large 2012 earthquakes (magnitude >7.7) with epicenters in Haida Gwaii, Okhotsk, and the Philippines were observed. During the same time

intervals as the Rayleigh wave were passing, the data logger in well Moscow 9 was collecting measurements at one minute intervals (Figure 10). Twenty water level measurements immediately after the Rayleigh wave first arrival for each of three separate earthquakes were used to find S_s.

Combining the data from the earthquakes, S_s was found to be $1.5 \times 10^{-6} \pm 0.2 \times 10^{-6}$ m^{-1}. However, this optimistic figure does not take into account sources of error that are difficult to quantify. The method assumes the aquifer is confined, uniformly porous, and free of heterogeneities.

2.6. Specific Storage from Earth Tides

Gravity theory predicts that earth tides (Figure 11) will result in harmonic subsurface dilatations within a few hundred meters of the earth's surface [46,49]. At inland sites, the lunar diurnal (O1) and lunar semi-diurnal (M2) are the most affected by the local hydraulic characteristics of the formations open to the wells [46]. On the other hand, the solar harmonics, K1 and S2, at periods of 1.0 and 0.5 days, contain the influence of atmospheric-pressure oscillations. At latitude θ, the resulting water level deflections for the O1 and M2 earth tides in an open water well in a confined aquifer are given by

$$A_{O1} = 1.56 \times 10^{-8} \sin(\theta) \cos(\theta)/S_s \text{ and } A_{M2} = 1.89 \times 10^{-8} \cos(\theta) \cos(\theta)/S_s \quad (2)$$

where A_{O1} and A_{M2} are the amplitudes at periods of 1.0758 and 0.5376 days [46,49].

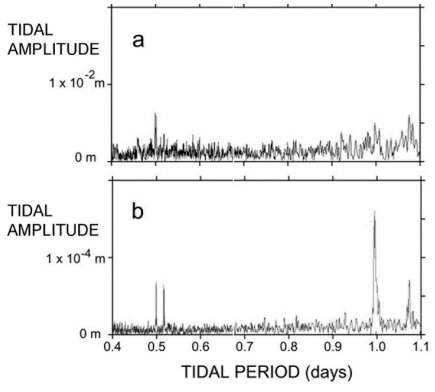

Figure 11. Water level deflections caused by earth tides in (**a**) DOE well and (**b**) WSU5 well. See Figure 6 for locations. The O1 and M2 harmonics have periods of 1.0758 and 0.5376 days. Note that the DOE tidal amplitudes are 50 times higher than those in Pullman well WSU5, suggesting that the primary aquifer system near Pullman is partially unconfined.

The DOE well, located midway between Moscow and Pullman (Figure 3), was the site of an experiment to measure earth tides in the study area. Groundwater levels were sampled at 10 min intervals for an entire year to produce the spectrum shown in Figure 11. The spectrum is noisy because of interference from nearby pumping wells. To agree with the S_s from barometric efficiency, the equations above predict that A_{M2} would be less than 0.001 m, an amplitude lost in the background noise apparent in Figure 11a On the other hand, we found A_{O1} at 0.0054 m to be five times above the

background noise, resulting in a S_s of $1.44 \times 10^{-6} \pm 0.14$ m^{-1}, a value in agreement with our estimate from barometric efficiency.

2.7. Pressure State of the Aquifer System

Figure 11 also shows the earth tide response of well WSU5 (see Figure 6 for location) in Pullman. The amplitude of A_{O1} in this well was 7.0×10^{-5} m, 50 times smaller than the O1 amplitude in the DOE well. The amplitude A_{M2} was 6.4×10^{-5} m. The calculated S_s values from Equation (2) are 1.1×10^{-4} m^{-1} and 1.4×10^{-4} m^{-1} for the O1 and M2 harmonics respectively, far too large if the aquifer at this location is confined. Earth tides can occur in partially confined aquifers, and the strength of the response depends on the distance to the exposed phreatic water table [50]. The low tidal response of WSU5 compared to DOE is consistent with the idea that the primary aquifer system is unconfined at places near Pullman.

2.8. Storativity of the Aquifer System

Estimates of the storativity of the primary aquifer system based on previous well tests and ground water models in the Moscow-Pullman basin have ranged over six orders of magnitude (Figure 12). To better constrain this parameter, we made use of our estimates stated above of specific storage and effective thickness. In Moscow, where the aquifer system is clearly confined, these yield consistent values of specific storage of $1.5 \times 10^{-6} \pm 0.2 \times 10^{-6}$ m^{-1}. Multiplying the specific storage by the effective aquifer thickness of 100 m, we obtain a storativity of $1.5 \times 10^{-4} \pm 0.2 \times 10^{-4}$, a value that falls in the range of previously determined storativity values from well tests (Figure 12).

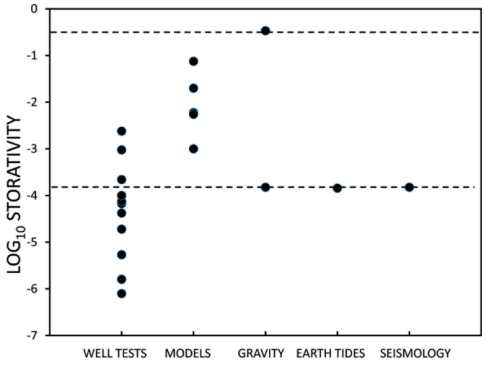

Figure 12. Values of storativity found by previous well tests [43] and groundwater models [7,8,31,43] compared to the values found using three geophysical methods described in the text. The dashed lines show the preferred values for storativity found in this study. The upper line is for the unconfined areas of the aquifer system and the lower value is for the confined units.

In Pullman, where the aquifer system is apparently unconfined at places, we suggest that the annual decrease in water levels is the result of extraction of water from storage in the aquiferous

intraflow units with a storativity equal to the specific yield, which would be about 0.35 based on the results above. As shown in Figure 12, this storativity for the unconfined areas is much higher than values used in previous groundwater models of the primary aquifer system.

In summary, where the aquifer is confined, the storativity was found to be near 1.5×10^{-4}; where unconfined, 3.5×10^{-1}. Thus, for the same drop in hydraulic head, very little water is produced by water expansion from the confined units compared to the amount of water extracted from the unconfined area. For each m^3 of water produced from the confined units by expansion, more than 350 m^3 are extracted from storage in the uppermost unconfined aquiferous unit.

3. Synthesis with Pumpage and Records of Water Level Decline

3.1. Water Budget Model

The goal of this study was to employ geophysical methods to provide better estimates of certain parameters needed for future comprehensive groundwater models of the Moscow-Pullman basin. For the present study, however, we do employ a simple single cell model to test the sensitivity of the basin's recharge budget to our parameters. Single cell models employ infinite transmissivity, but finite storativity, and are commonly used in economic hydrology [51]. On an annual basis, we treat the Moscow-Pullman basin as a single cell with boundary conditions such that:

$$V_p = V_r + S\,A\,(\Delta h) \tag{3}$$

where V_p in m^3/year is the annual volume of water pumped; V_r in m^3/year is the annual volume of water replenished from outside the cell; S is the dimensionless storativity of the cell; A is the area of the cell in m^3; and Δh in m/year is the annual decline in water level. Two of the variables V_p and Δh in the above relation are well known from records kept by the Palouse Basin Aquifer Committee [6]. For the storativity and area of the cell, we use the estimates provided by the geophysical methods described above.

The annual volume of replenishment has two components: (1) that driven by Δh; and (2) that not directly associated with Δh [43]. In the first category are head-related changes in influx to the cell from the surrounding region. Also in this category are any changes in flux from overlying units due to the increased vertical hydraulic gradient. In the second category is decreased recharge due to depletion of the overlying hydraulically connected source (overlying leaky aquifers or surface streams). To better understand the effect a sustained drought may have on replenishment, it is useful to separate these two components. In our simple model, we employ a linear approximation such that:

$$V_r = S_c\,\Delta h + V_0 \tag{4}$$

where S_c in m^2/year is an annual volume replenished per unit annual drop in head for head-related sources and V_0 in m^3/year is the volume of annual recharge not directly head-related. Combining the above two equations and taking into account the possibility that the aquifer is unconfined in places:

$$Vp = (S_c + S\,A_c + S_y\,A_u)\,\Delta h + V_0 \tag{5}$$

where S and S_y are the storativities and A_c and A_u are the areas of the confined and unconfined portions, respectively. Thus, our simple model predicts a linear relationship between annual volume

pumped and annual drop in water level, with an intercept equal to V_0 and a slope associated with storativity, area, and head-related replenishment.

Figure 13 shows a cross-plot of annual water volume pumped as a function of annual drop in water level for the primary aquifer in the study area as provided by the Palouse basin Aquifer Committee [6]. The data points (modified from [32]) are for years 1968–2010. The solid line in the cross-plot is the best-fit line to the data. The correlation coefficient (r^2) is 0.52, showing that the data can be reasonably fit by a straight line with slope of $30.6 \times 10^6 \pm 4.4 \times 10^6$ m and intercept of $58.34 \times 10^6 \pm 1.55 \times 10^6$ m^3/year.

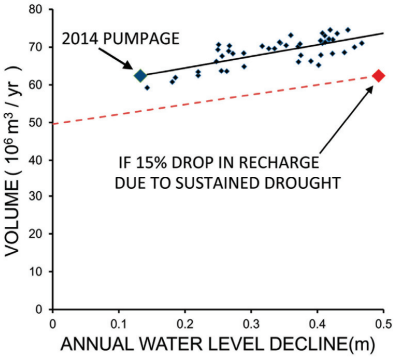

Figure 13. Annual water level decline *vs.* pumped volume for the Grande Ronde aquifer system. The data points show the historic data since 1968 along with a best-fit line. The large blue diamond is the current state. The red dashed line is the predicted state of the aquifer system in the event of a sustained drought causing a 15% drop in recharge. The red diamond indicates the expected annual water level decline if the current pumpage is maintained during the drought.

3.2. Model Results

We can make several inferences from the simple model. All the parameters in Equation (5) controlling the slope of the best-fit line are not known, so we consider a number of possibilities.

First of all, we find that the water budget is relatively insensitive to the parameters which we have derived by the geophysical methods described above. Regardless of values used for storativity, aquifer area, or head-related replenishment, there is a large amount of annual recharge unrelated to head ($V_0 = 58.34 \times 10^6 \pm 1.55 \times 10^6$ m^3/year), accounting for 93.5% ± 2.6% of the current pumped volume, but unfortunately not enough to stop long term-water level declines. It is clearly impossible to model the aquifer without invoking a considerable amount of annual recharge.

Second, if the primary aquifer is in fact confined everywhere, then, from our geophysical results above, we can set $S = 1.5 \times 10^{-4} \pm 0.2 \times 10^{-4}$ and $A_c = 620$ km^2 in Equation (5), leading to $S_c = 30.51 \pm 0.01$ m^2/year, a result very insensitive to our uncertainty in storativity. In this scenario, only 0.02% of the current pumped volume of 62.4 m^3/year, comes from storage. 6.5% comes from head-related replenishment, and the remainder from recharge. The relatively low percentage of

head-related replenishment compared to recharge suggests that constant-head boundary conditions should be used with caution in future numerical models of the confined system. Also, the value of storativity in the confined system is unimportant and could be off by an order of magnitude without affecting the water balance by more than one per cent.

Third, if the primary aquifer is partly unconfined as the geophysical data suggest, we can estimate the maximum area of the phreatic water table. For this case, using our geophysical results, we can set $S = 1.5 \times 10^{-4} \pm 0.2 \times 10^{-4}$, $S_y = 0.355 \pm 0.04$, $S_c = 0$, $A_c = 620$ km^2 A_u, leading to an A_u of at most 86 ± 8 km^2 or 14% of the area of the Moscow-Pullman basin. Under this scenario, 6.5% of the current water being pumped comes from storage. Recharge accounts for 58.3×10^6 m^3/year, independent of head; the remaining 3.1×10^6 m^3/year of the water pumped is produced from storage almost entirely by gravity drainage of the uppermost aquiferous unit. In future models involving a phreatic water table, specific yield does become a relevant parameter, but, nonetheless, a very small contributor compared to recharge.

Fourth, the actual situation could well be a combination of the previous two scenarios, with a phreatic water surface over a smaller area releasing water from storage along with the drop in head inducing more recharge into the deeper aquifer systems from overlying units or decreasing the flux out of the study area to the west. However, these effects on a numerical model will all still be minor compared to head-unrelated recharge.

Finally, we can use our simple model to predict the response of the primary aquifer to a sustained drought (Figure 13). If we assume for example, that annual replenishment to the aquifer system is reduced by 15% as a result of an episode of continued low annual precipitation, the model shows that the annual water level decline would increase four-fold over the current value if current levels of pumpage were maintained.

4. Conclusions

This study clarifies a number of issues about the primary aquifer system within the Palouse basin and should lead to better numerical groundwater models, and more rational planning for the future not only for this aquifer system but for any CRBG aquifer should the 21st century prove to be as dry as predicted. The storativity of the deeper aquiferous basalt intraflow units is, in fact low, 1.5×10^{-4}, a value within the range of the many well tests that have taken place, but an order of magnitude or more below the values used for these units in previous groundwater models of the aquifer system. While the primary aquifer system is generally confined, in the vicinity of Pullman it is apparently unconfined with a phreatic water table and a storativity of 0.35, a value far higher than that used in previous groundwater models. Thus, the water that is derived from storage throughout the basin is at a cost of the lowering of the phreatic water table near Pullman and a general depressurization of the primary aquifer system throughout the Moscow-Pullman basin.

The derived values of aquifer thickness, area, and storativity derived from geophysical methods in this study will improve future groundwater models of the primary aquifer, but they will have only a second-order effect. The first order unknown is recharge. Although the mechanism remains elusive, currently more than 90% of the water pumped annually is replenished by recharge unrelated to head. Should that replenishment be halted by a prolonged drought, water level decline would accelerate.

Furthermore, if the aquifer system is in fact, partially unconfined, water level drops may be sudden as the phreatic table encounters different units at depth. There is no guarantee that the primary aquifer system would continue to operate as a unified system as horizontal intraflow pathways get cut off as water levels decline.

Current studies of possible recharge galleries for the Moscow-Pullman basin are focused on the eastern side of the basin in hopes of recharging, not the primary aquifer system, but the overlying Wanapum system [27]. But this system provides only 10% of the net water supply, mostly in Moscow, and it is not clear that replenishing the Wanapum in Moscow will affect the primary aquifer. The geophysical results presented here suggest that the most logical location for future recharge galleries may be in the Pullman vicinity where the primary aquifer system appears to be unconfined and where its phreatic groundwater table is shallow. Two tributaries of the Palouse River have a confluence at Pullman. Redirecting the spring runoff in those tributaries into the aquifer system could restore historical water levels at Pullman and re-pressurize the confined units throughout the Moscow-Pullman basin.

Acknowledgments

We thank Steve Robischon and the Palouse Basin Aquifer Committee for providing much of the hydrological data used in this paper; and John Bush, Dean Garwood, and the Idaho Geological survey for providing geological data. Comments by three anonymous reviewers have greatly improved this manuscript.

Conflicts of Interest

The authors declare no conflict of interest.

References

1. U.S. Geological Survey. *Ground-Water Availability Assessment for the Columbia Plateau Regional Aquifer System, Washington, Oregon, and Idaho*; 2008. Available online: http://pubs.usgs.gov/fs/2008/3086/ (accessed on 22 July 2015).
2. Cook, B.I.; Ault, T.R.; Smerdon, J.E. Unprecedented 21st century drought risk in the American Southwest and Central Plains. *Sci. Adv.* **2015**, *1*, doi:10.1126/sciadv.1400082.
3. Woodhouse, C.A.; Meko, D.M.; MacDonald, G.M.; Stahle, D.W.; Cook, E.R.A. 1200-year perspective of 21st century drought in southwestern North America. *Proc. Natl. Acad. Sci. USA* **2010**, *107*, 21283–21288.
4. Pederson, G.T.; Gray, S.T.; Woodhouse, C.A.; Betancourt, J.L.; Fagre, D.B.; Littell, J.S.; Graumlich, L.J. The unusual nature of recent snowpack declines in the North American Cordillera. *Science* **2011**, *333*, 332–335.
5. Vaccaro, J.J. Potential impacts of climate change on groundwater resources of the Columbia River basin. In Proceedings of the Pacific Northwest Science Conference, Portland, OR, USA, 16 June 2010; pp. 1–18.

6. Palouse Basin Aquifer Committee, 2013. Available online: http://www.webpages.uidaho.edu/pbac/ (accessed on 27 February 2015).
7. Barker, R.A. Computer simulation and geohydrology of a basalt aquifer system in the Pullman-Moscow basin, Washington and Idaho. Available online: https://fortress.wa.gov/ecy/publications/documents/wsb48 (accessed on 22 July 2015).
8. Lum, W.E.; Smoot, J.L.; Ralston, D.R. Geohydrology and numerical model analysis of ground-water flow in the Pullman-Moscow area, Washington and Idaho. Available online: http://pubs.usgs.gov/wri/1989/4103/report.pdf (accessed on 22 July 2015).
9. Bauer, H.H.; Hansen, A.J. Hydrogeology of the Columbia Plateau regional aquifer system, Washington, Oregon, and Idaho. Available online: http://pubs.usgs.gov/wri/1996/4106/report.pdf (accessed on 22 July 2015).
10. Kahle, S.C.; Olsen, T.D.; Morgan, D.S. Geologic setting and hydrogeologic units of the Columbia Plateau Regional Aquifer System, Washington, Oregon, and Idaho. Available online: http://pubs.usgs.gov/sim/3088/pdf/sim3088.pdf (accessed on 22 July 2015).
11. Burns, E.R.; Snyder, D.T.; Haynes, J.V.; Waibel, M.S. Groundwater status and trends for the Columbia Plateau Regional Aquifer System, Washington, Oregon, and Idaho. Available online: http://pubs.er.usgs.gov/publication/sir20125261 (accessed on 22 July 2015).
12. U.S. Department of Energy. *Site characterization plan, Reference Repository Location, Hanford Site, Washington-consultation draft*; Office of Civilian Radioactive Waste Management: Washington, DC, USA, 1988.
13. Reidel, S.P.; Fecht, K.R.; Hagood, M.C.; Tolan, T.L. The geologic evolution of the central Columbia Plateau. In *Volcanism and Tectonism in the Columbia River flood-Basalt Province*; Reidel, S.P., Hooper, P.R., Eds.; Geological Society of America: Washington, DC, USA, 1989.
14. Drost, B.W.; Whiteman, K.J. Surficial geology, structure, and thickness of selected geohydrologic units in the Columbia Plateau, Washington. Available online: http://pubs.usgs.gov/wri/1984/4326/report.pdf (accessed on 22 July 2015).
15. Drost, B.W.; Whiteman K.J.; Gonthier J.B. Geologic Framework of the Columbia Plateau Aquifer System, Washington, Oregon, and Idaho. Available online: http://pubs.usgs.gov/wri/1987/4238/report.pdf (accessed on 22 July 2015).
16. Steinkampf, W.C.; Hearn, P.P., Jr. Ground-Water Geochemistry of the Columbia Plateau Aquifer System, Washington, Oregon, and Idaho. Available online: http://pubs.usgs.gov/of/1995/0467/report.pdf (accessed on 22 July 2015).
17. Vaccaro, J.J. Summary of the Columbia Plateau Regional Aquifer-System Analysis, Washington, Oregon, Idaho. Available online: http://pubs.usgs.gov/pp/1413a/report.pdf (accessed on 22 July 2015).
18. Tolan, T.; Lindsey, K.; Porcello, J. A Summary of Columbia River Basalt Group Physical Geology and its Influence on the Hydrogeology of the Columbia River Basalt Aquifer System: Columbia Basin Ground Water Management Area of Adams, Franklin, Grant, and Lincoln Counties, 2009. Available online: http://www.cbgwma.org/pdf/GWMA_Geology-Hydrogeology%20of%20CRBG_TEXT_June%202009.pdf (accessed on 27 February 2015).
19. McNab, W.H.; Avers, P.E. Ecological Subregions of the United States. 1996. Available online: http://www.fs.fed.us/land/pubs/ecoregions/ (accessed on 22 July 2015).

20. Leek, F. *Hydrogeological Characterization of the Palouse Basin Basalt Aquifer System, Washington and Idaho*; Washington State University: Pullman, WA, USA, 2006.
21. Hopster, D. *A Recession Analysis of Springs and Streams in the Moscow-Pullman Basin*; University of Idaho: Moscow, ID, USA, 2003.
22. Walters, K.L.; Glancy, P.A. *Reconnaissance of Geology and of Ground-Water Occurrences and Development in Whitman County, Washington*; Water-Supply Bulletin 26; 1969. Available online: https://fortress.wa.gov/ecy/publications/documents/wsb26.pdf (accessed on 22 July 2015).
23. Crosby, J.W., III; Chatters, R.M. *Water Dating Techniques as Applied to the Pullman-Moscow Ground-Water Basin*; Washington State University: Pullman, WA, USA, 1965.
24. Larson, K.R. *Stable Isotopes in the Pullman-Moscow Basin, Eastern Washington and North Idaho: Implications for the Timing, Magnitude, and Distribution of Groundwater Recharge*; Washington State University: Pullman, WA, USA, 1997.
25. Douglas, A.A. *Radiocarbon Dating as a Tool for Hydrogeological Investigations in the Palouse Basin*; University of Idaho: Moscow, ID, USA, 2004. Available online: http://www.webpages.uidaho.edu/pbac/Theses/Douglas_Thesis_Age_Dating_2004.pdf (accessed on 22 July 2015).
26. Carey, L.R. *Evaluation of Oxygen and Hydrogen Isotopes in Groundwater of the Palouse Basin and Moscow Sub-Basin*; University of Idaho: Moscow, ID, USA, 2011.
27. Fairley, J.P.; Solomon, M.D.; Hinds, J.J.; Grader, G.W.; Bush, J.H.; Rand, A.L. Latah County Hydrologic Characterization Report. Available online: http://www.researchgate.net/publication/262260160_Latah_County_Hydrogeological_Characterization (accessed on 22 July 2015).
28. MacQueen, J.D.; Mann, E. Borehole Gravity Meter Surveys at the Waste Treatment Plant, Hanford, Washington. Available online: http://www.pnl.gov/main/publications/external/technical_reports/PNNL-16490.pdf (accessed on 22 July 2015).
29. Moisy, F. Discover Ezyfit: A Free Curve Fitting Toolbox for Matlab. Available online: http://www.mathworks.com/matlabcentral/fileexchange/10176-ezyfit-2-40/content/ezyfit/demo/html/efdemo.html#1 (accessed on 27 February 2015).
30. Hyndman, R.D.; Drury, M.J. Physical properties of basalts, gabbros, and ultramafic rocks from DSDP Leg 37. *DSDP* **1977**, *37*, 395–401.
31. Smoot, J.L.; Ralston, D.R. *Hydrogeology and Mathematical Model of Ground-Water Flow in the Pullman-Moscow Region, Washington and Idaho*; Idaho Water Resources Research Institute, University of Idaho: Moscow, ID, USA, 1987. Available online: http://digital.lib.uidaho.edu/cdm/ref/collection/idahowater/id/310 (accessed on 22 July 2015).
32. Moran, K. Evaluation of the relationship between pumping and water level declines in the Grande Ronde Aquifer of the Palouse Basin. Available online: http://www.webpages.uidaho.edu/pbac/Presentations/2011/110915_Moran_WL_Pumping_Relationships_report.pdf (accessed on 22 July 2015).
33. Foxworthy, B.L.; Washburn, R.L. *Ground Water in the Pullman Area, Whitman County, Washington*; Geological Survey Water-Supply Paper 1655; 1963. Available online: http://pubs.usgs.gov/wsp/1655/report.pdf (accessed on 22 July 2015).

34. Brown, J.C. *Well Construction and Stratigraphic Information: Pullman Test and Observation Well, Pullman, Washington*; Washington State University: Pullman, WA, USA, 1976; pp. 1–35.
35. Teasdale, E.W. *Hydrogeologic Basins in the Palouse Area of Idaho and Washington*; University of Idaho: Moscow, ID, USA, 2002.
36. Bush, J.H.; Garwood, D.L. Interpretation and use of well data in the Columbia River Basalt Group, Pullman, Washington. In Proceedings of 2003 Seattle Annual Meeting, Seattle, WA, USA, 2–5 November 2003.
37. Bush, J.H. *The Columbia River Basalt Group of the Palouse Basin with Hydrological Interpretations, western Latah County, Idaho and eastern Whitman County, Washington*; Report to Palouse Basin Aquifer Committee: Moscow, ID, USA, 2005.
38. Klein, D.P.; Sneddon R.A.; Smoot J.L. Magnetotelluric study of the thickness of volcanic and sedimentary rock in the Pullman-Moscow Basin of eastern Washington. Available online: http://pubs.usgs.gov/of/1987/0140/report.pdf (accessed on 22 July 2015).
39. Holom, D. *Ground Water Flow Conditions Related to the Pre-Basalt Basement Geometry Delineated by Gravity Measurements near Kamiak Butte, Eastern Washington*; University of Idaho: Moscow, ID, USA, 2006.
40. Conrey, R.; Beard, C.; Wolff, J. Columbia River Basalt flow stratigraphy in the Palouse Basin Department of Ecology test wells. Available online: http://www.webpages.uidaho.edu/pbac/pubs/2013_Conrey_Beard_Stratigraphy_in_Palouse_Basin_DOE_test_Wells.pdf (accessed on 22 July 2015).
41. Ryan, W.B.F.; Carbotte, S.M.; Coplan, J.O.; O'Hara, S.; Melkonian, A.; Arko, R.; Weissel, R.A.; Ferrini, V.; Goodwillie, A.; Nitsche, F.; *et al.* Global Multi-Resolution Topography synthesis. *Geochem. Geophys. Geosyst.* **2009**, *10*, doi:10.1029/2008GC002332.
42. Ducar, S. *Properties of the Grande Ronde Aquifer in the Vicinity of Moscow, Idaho from the Synthesis of Aquifer Test Results with Seismic Groundwater Response*; Department of Geological Science, University of Idaho: Moscow, ID, USA, 2014.
43. Moran, K. *Interpretation of Long-Term Grande Ronde Aquifer Testing in the Palouse Basin of Idaho and Washington*; University of Idaho: Moscow, ID, USA, 2011.
44. Sokol, D. *Interpretation of short term water level fluctuations in the Moscow Basin, Latah County, Idaho*; Pamphlet No. 137; 1966. Available online: http://www.idahogeology.org/PDF/Pamphlets_(P)/P-137.pdf (accessed on 22 July 2015).
45. Cooper, H.H.; Bredehoeft, J.D.; Papadopulos, I.S.; Bennett, R.R. The response of well-aquifer systems to seismic waves. *J. Geophys. Res.* **1965**, *70*, 3915–3926.
46. Bredehoeft, J.D. Response of well-aquifer systems to earth tides. *J. Geophys. Res.* **1967**, *72*, 3075–3087.
47. Shih, D.C.F. Storage in confined aquifer: Spectral analysis of groundwater responses to seismic Rayleigh waves. *J. Hydrol.* **2009**, *374*, 83–91.
48. Folnagy, A.J.; Osiensky, J.L.; Kobayashi, D.; Sprenke, K.F. Specific storage from sparse records of groundwater response to seismic waves. *J. Hydrol.* **2013**, *503*, 22–28.

49. Merritt, M.L. Estimating Hydraulic Properties of the Floridan Aquifer System by Analysis of Earth-Tide, Ocean-Tide, and Barometric Effects, Collier and Hendry Counties, Florida. Available online: http://pubs.usgs.gov/wri/wri034267/wri03_4267.pdf (accessed on 22 July 2015).
50. Rojstaczer, S.; Riley, F.S. Response of the water level in a well to earth tides and atmospheric loading under unconfined conditions. *Water Resour. Res.* **1990**, *26*, 1803–1817.
51. Brown, G.; Deacon, R. Economic optimization of a single-cell aquifer. *Water Resour. Res.* **1972**, *8*, 557–564.

Groundwater Abstraction for Irrigation and Its Impacts on Low Flows in a Watershed in Northwest Germany

Hartmut Wittenberg

Abstract: Low flows of the Ilmenau River (1434 km^2) in northwest Germany have decreased by about 25% over the last 50 years. In the same period, moderate climate changes have taken place and annual groundwater abstractions for sprinkler irrigation have increased by up to 50 hm^3 (million m^3), with a strong variation due to the respective prevailing weather conditions. Time-series analyses with multiple regression analysis allow detecting and quantifying different influences on low flows. It is also shown that farmers allocate irrigation water volumes carefully according to seasonal precipitation and temperatures. Decline of groundwater levels in summer and the low flow situation are aggravated by the cumulative effect of higher irrigation in drier years. Groundwater recharge and recovery of the water table have been observed subsequently during the winter season.

Reprinted from *Resources*. Cite as: Wittenberg, H. Groundwater Abstraction for Irrigation and Its Impacts on Low Flows in a Watershed in Northwest Germany. *Resources* **2015**, *4*, 566–576.

1. Introduction

In spite of their high impact on environment, forestry, agriculture, waste water disposal, power plants, waterways, *etc.*, drought periods in Central Europe were seldom the focus of public attention. The hot and dry 1990s, and in particular the drought year 2003, changed this situation as it became clear that in spite of its temperate climate, Germany can be hit severely by low flows and drought [1], stimulating hydrological research, e.g., [2]. Like other hydrological processes and water balances of river basins, low flows are not only subject to climate variability and catchment characteristics [3], but also anthropogenic impacts. Due to the superposition of various influences in hydrological data, the effect of single factors is not easily quantified. The present study aims at establishing relationships between the variation and decrease of low flows in a river in northern Germany, meteorological data, and groundwater abstractions for irrigation.

2. The Study Area

The Ilmenau River in the north German lowlands (Figure 1) is the largest river of the Lueneburg Heath and a tributary of the Elbe River, which drains into the North Sea. Daily average flows have been recorded since 1956 at the Bienenbüttel gauging station. The catchment area of 1434 km^2 corresponds roughly to the county of Uelzen. The town of Uelzen is situated in its center at approximately 53° N, 10.5° E, and 35 m a.s.l. The landscape was shaped by the Saale glaciation, with sandy and loamy soils and a slightly hilly topography with altitudes between 20 and 136 m a.s.l. With annual temperature means of around 9 °C and precipitation of about 700 mm (see also in paragraph 5), the climate is temperate and humid. Snow in winter melts at the latest in the early spring and has no direct impact on low flows in summer. Mean flow is 9.2 m^3/s (runoff depth

202 mm) and is mainly fed by the shallow groundwater aquifer. The region is characterized by agriculture with wheat, potatoes, and sugar beets as the main crops. A large sugar factory is located in Uelzen.

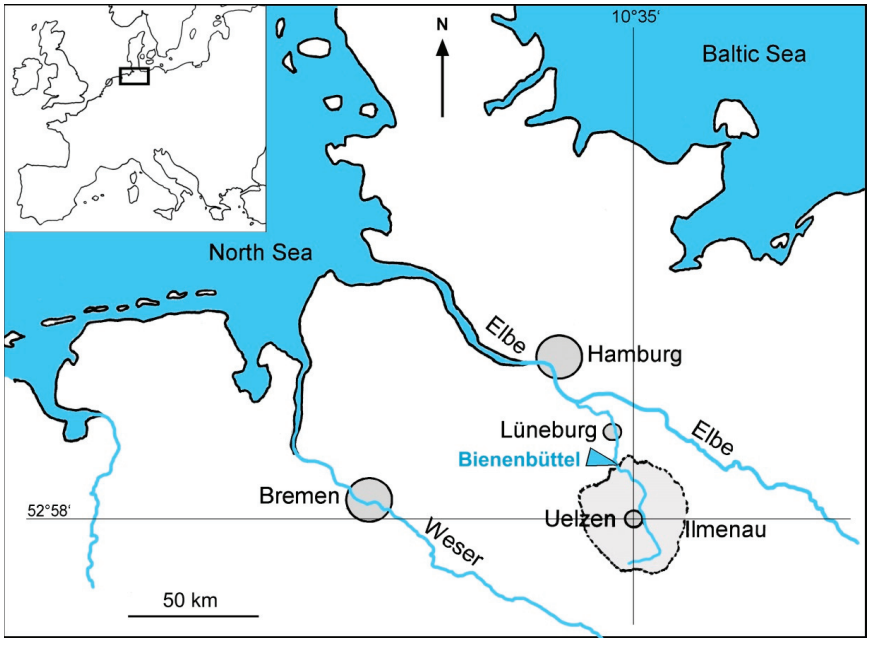

Figure 1. Map of northwest Germany with the Ilmenau River basin and Bienenbüttel gauging station.

To ensure high crop yields in dry years, sprinkler irrigation was introduced in the 1950s [4]. Because of the low water retention capacity of the soils and sometimes scarce summer rainfalls, irrigation is necessary for agricultural production [5]. With an average annual low flow in the Ilmenau River of more than half of the mean flow, there is no indication of a serious water shortage affecting the biosphere. Nevertheless, the public is very attentive and irrigation farmers find themselves generally suspected of wasting water. The quantitative and temporal analysis of irrigation as it is actually carried out by farmers in the area is therefore a further aim of this study.

3. Irrigation in the Ilmenau Basin

Sprinkler irrigation introduced in the 1950s is still considered by farmers to be the most suitable and economical method for growing crops under regional conditions [6]. It is typically performed by turntable machines with rain-gun trolleys. The trolley is pulled along the irrigation track by its PE (polyethylene) hose, which is wound up by the drum. Slow rotation is provided by a turbine driven by the irrigation water. Field strips of several hundred meters in length and about 30 m width can be irrigated in one application with a typical depth of 30 mm. Figure 2 shows a unit in operation.

Figure 2. Sprinkler irrigation with pipe drum and rain-gun trolley.

Water is taken from the Quaternary aquifer at a depth of about 100 m by pumping stations owned and operated by the farmers. All wells, groundwater withdrawals, and irrigated areas need permission from the local environmental and water authorities [7]. Applications must be backed by hydro-geological expertise. The irrigation water depth for the respective areas is limited to 70 mm per summer over a seven-year average, *i.e.*, higher abstractions in dry years can be compensated by lower ones in wetter summers. Nearly 700 km^2 (50%) of the county is farmland. Since the 1950s, when irrigation was introduced, irrigated areas were enlarged to about 550 km^2. The irrigation depth of 70 mm would then need a volume of 38.5 hm^3 per year. Depending on the summer weather, the actual volumes varied in the observed years between less than 10 and about 50 hm^3. For the catchment area of 1434 km^2 the maximum abstraction corresponds to a 35 mm depth, which is about 5% of mean annual basin precipitation (1955–2012) or more than a quarter of the precipitation in a very dry summer (May–October 1959: 131 mm). Effects on low flows and groundwater storage must be expected. Figure 3 shows the development of registered areas and of the groundwater abstractions for irrigation 1977–2012.

With the objective of ensuring a sustainable management of water resources, the water and environmental authorities observe this development. The chamber of agriculture initiated an interdisciplinary study of irrigation possibilities for different climate change scenarios and adapted technologies [8].

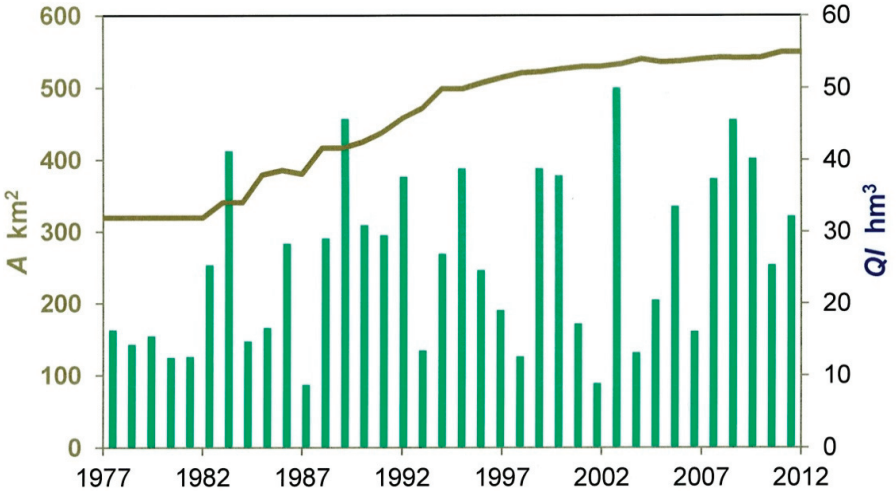

Figure 3. Development of irrigation areas and groundwater abstraction in the catchment; registration of areas and groundwater abstractions began in 1977, data: County of Uelzen.

4. Low Flows, Climate, and Groundwater Abstractions

At the Bienenbüttel gauging station, daily flows have been recorded since 1956. In assessing low flows and water levels, the absolute minima of each year are of little significance. Since the damage potential of low flow events also depends on their duration, the lowest arithmetic mean LQ_{xd} of x consecutive daily flow values of every year is used as the assessment variable. The annual values LQ_{xd} are determined for durations of typically x = 3, 7, 20 days for each water budget year. In northern Germany, the relevant low flow events are to be expected in the summer months (May–October).

The time series 1956–2012 of annual low flows LQ_{20} at the Bienenbuettel/Ilmenau gauging station in Figure 4 reveals a significant (t-test) linear downward trend. The strong fluctuations can be interpreted as a sequence of different negative and positive trends. It seems that after a decline until the end of the 1970s, there is no further clear trend, but instead there is a high variability in annual low flows. The physical causes of these variations and inconsistencies of the low flow hydrograph can be due to both weather processes and anthropogenic influences. Mean annual basin precipitation is also depicted in Figure 4, derived by the Thiessen polygon method using the data of 13 stations in and around the catchment. It increased statistically by about 100 mm during the observation period while evapotranspiration was stimulated by the warming of mean summer temperatures of about 1 K. In Germany, the hydrological year is divided into the winter half-year (November to April) and the summer half-year (May to October). The latter represents roughly the vegetation season. Mean values of catchment precipitation and air temperatures in the two seasons in Lueneburg are given in Table 2. Essential impacts are to be expected from groundwater

abstractions for irrigation, which are recorded by water meters at all irrigation wells. Annual total values for the catchment expressed in m^3/s are also shown in Figure 4.

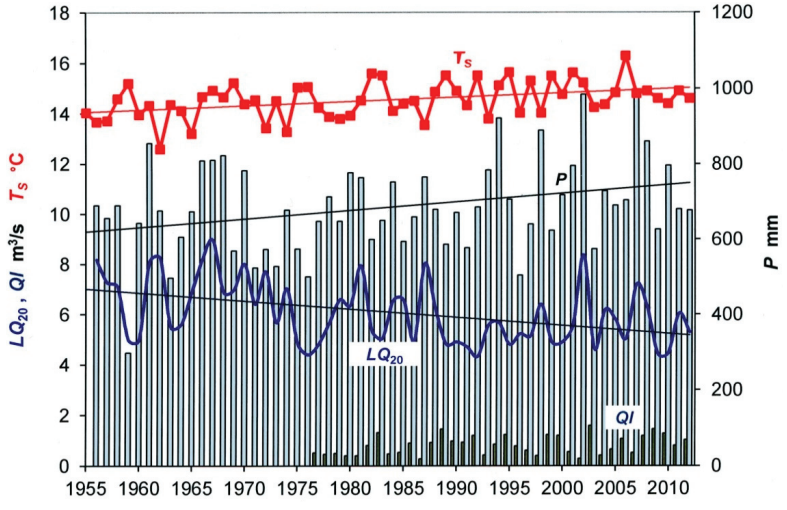

Figure 4. Annual basin precipitation *P*, summer temperature *Ts*, 20-day low flows LQ_{20}, and groundwater abstractions *QI*, Ilmenau Basin at Bienenbüttel, 1977–2012.

5. Multiple Regression Analysis—Low Flows

Multiple regression is a classic method of data analysis [9] but is rarely used in contemporary hydrology. Even state-of-the-art studies on low flows [2] mostly use regression only in its simple version and for trend analysis. Unlike the simple trend analysis of low flows which relates all changes to time, multiple regression enables the assessment of statistical associations among the response variable and primarily independent multiple covariates. The relationship established in Equation (1) assumes annual low flows:

$$LQx_t = LQ_0 + a \cdot PW_t + b \cdot PS_t + c \cdot PJ_{t-1} + d \cdot TW_t + e \cdot TS_t + f \cdot QI_t \quad (1)$$

where,

LQx_t: *x* days low flow in the year *t* in m^3/s;
LQ_0: base value of low flow in m^3/s;
PW_t: winter precipitation in the year *t* in mm;
PS_t: summer precipitation in the year *t* in mm;
PJ_{t-1}: precipitation of preceding water year in mm;
TW_t: mean air temperature, winter of year *t* in °C;
TS_t: mean air temperature, summer of year *t* in °C;
QI_t: groundwater abstraction for irrigation in year *t* in mm.

With the data set of 1977–2012, there is an over-determined system of 36 equations. Reducing the system by the Gauss-Jordan algorithm determines the seven unknowns, *i.e.*, the base value and

the six coefficients *a* to *f*, according to the least squares criterion. For the 20-day period, low flows are obtained:

$$LQM_{20t} = 4.48 + 0.0030\ PW_t + 0.00094 PS_t + 0.0033 PJ_{t-1} + 0.022\ TW_t - 0.049 TS_t - 0.102 QI \qquad (1a)$$

The coefficients, factors, or weights represent the sensitivity of low flow values to unit changes of the variables. Table 1 shows the correlation coefficients of the variables to one another and to the dependent variable low flow. Correlations with $|R| > 0.33$ are significant at the 95% level. In addition, the coefficients concerning the registered irrigation areas *AI* are listed. These values are expected to have an influence on the assessment of applied water volumes in Section 7.

Table 1. Partial correlation coefficients of variables, time series 1977–2012.

variable	*PW*	*PS*	*PJt-1*	*TW*	*TS*	*QI*	*AI*
PW	1						
PS	0.127	1					
Pt-1	0.194	−0.092	1				
TW	0.490	0.168	−0.020	1			
TS	0.186	−0.194	0.181	0.336	1		
QI	0.033	**−0.618**	0.320	0.199	**0.472**	1	
Ai	0.096	0.259	0.312	0.222	0.310	0.324	1
LQ_{20}	0.265	**0.578**	0.116	−0.059	−0.317	**−0.735**	−0.220

The overall correlation coefficient between the $n = 36$ calculated values and the data is $R = 0.865$ ($R^2 = 0.75$). As expected, it is considerably higher than all partial coefficients and thus demonstrates the advantage of multiple regression over simple regression analysis. The coefficient of variation, *i.e.*, the average deviation between data and values by Equation (1a), is 9%.

The groundwater abstraction for irrigation *QI* has a significant negative correlation with summer precipitation *PS* and a positive one with summer temperature *TS*, an indication for disciplined and frugal water allocation by the farmers. Higher rainfall reduces the need for irrigation, while higher temperatures increase evaporation and irrigation requirements.

As indicated by the correlation coefficients, the information of the values *PS* and *TS* with relevance for low flows seems to be largely included in the time series *QI*. The influence of winter temperature *TW* on low flows is negligible (see Equation (1a)). Therefore, a further multiple regression for LQ_{20} with variables as in Equations (1) and (1a), but without *PS*, *TW*, and *TS* was performed:

$$LQ_{20t} = 4.22 + 0.0032\ PW_t + 0.0033\ PJ_{t-1} - 0.1092\ QI \qquad (1b)$$

The correlation coefficient between the observed and calculated low flows is $R = 0.863$ and the coefficient of variation is $CV = 9.2\%$. Thus, the result is practically the same as for Equation (1a) and the assumption is confirmed.

Table 2 contains the mean values from 1977 to 2012 of the input variables in the first line. By multiplying with their coefficients or weights according to Equations (1a) and (1b), respectively, their contribution to the total value of the low flow is obtained (following lines).

First of all, the coefficients are statistical weights that do not necessarily represent partial physical flows. However, since the coefficients of the three parameters used in both Equations (1a) and (1b) have similar to equal values, it is concluded that the computed partial flows are not purely mathematical regressive values but do stand for real water flows. It is worth noting the high contributions of winter and the previous year's precipitation to low flows because of their importance for groundwater recharge.

Table 2. Coefficients and partial flows of LQ_{20} according to Equations (1a) and (1b).

variable	LQ_0	PW	PS	$Pj\text{-}1$	TW	TS	QI	$\Sigma\, LQ_{calc}$
	m^3/s	mm	mm	mm	°C	°C	mm	m^3/s
mean values		336	376	708	3.79	14.7	18.1	
coefficients 1a		0.0030	0.00094	0.0033	0.022	−0.0494	−0.1023	
flow	4.48	1.01	0.35	2.34	0.08	−0.73	−1.85	5.68
coefficients 1b		0.0032	-	0.0033	-	-	−0.1092	
flow	4.22	1.08	-	2.34	-	-	−1.98	5.68

In this study, one focus is on the influence of groundwater abstraction. As shown in Table 2, the respective average annual reduction of low flow LQ_{20} is about 1.9 m^3/s or 25%. Observed low flows from 1977 to 2012 and values computed by Equation (1b) are depicted in Figure 5. Annual amounts of groundwater abstraction are shown for comparison. By omitting the last term of Equation (1b), the influence of groundwater abstraction QI is eliminated and a time series of hypothetical uninfluenced low flows obtained. The resulting hydrograph is also shown in Figure 5.

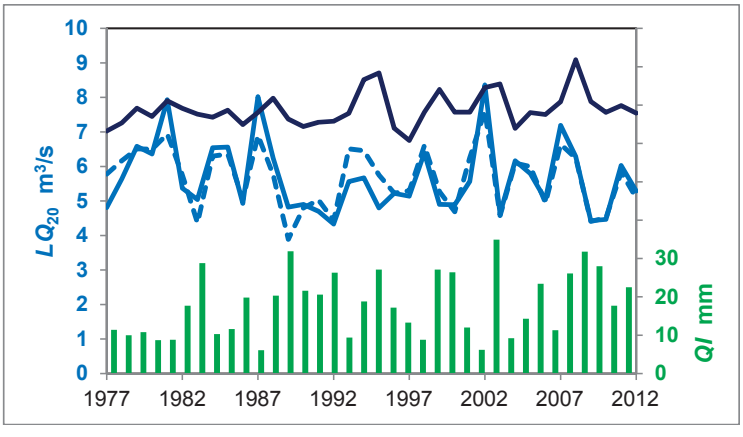

Figure 5. Observed and computed (Equation (1b), dashed line) annual low flow values, computed low flows uninfluenced by abstractions (above, dark blue), and groundwater abstractions QI.

As reflected by the above equations, the reduction of annual low flows is higher in drier years with more groundwater withdrawal than in moderate years. This is also shown by the empirical probability curves in Figure 6. These curves were determined according to the method of "plotting

positions". Data and the computed uninfluenced low flows are respectively sorted in decreasing order, and statistical return intervals T are determined for every value according to Equation (2):

$$T = (n+1)/(n+1-m) \tag{2}$$

with

T: return interval in years;
n: number of data, length of data set;
m: ranking from 1 (greatest value) to n (lowest value).

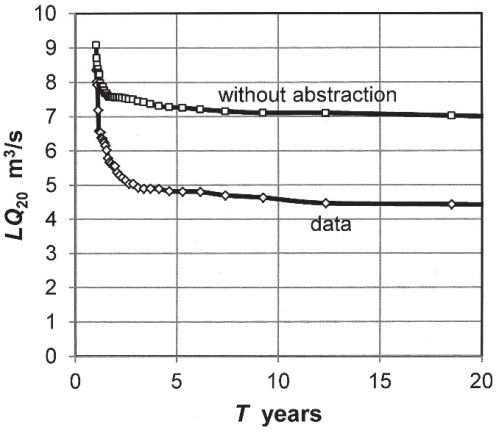

Figure 6. Frequency analysis of 20-day low flows.

The difference between probable low flows with and without groundwater abstraction increases with the recurrence interval T. The regressions and calculations described above were also carried out for time series of low flows of three- and seven-day durations. Comparable results and relationships following the same pattern have been obtained.

6. Groundwater Impacts

Low flow occurs when direct runoff has ceased and the river only carries baseflow, *i.e.*, groundwater outflow from the adjacent aquifer. Therefore, the lowest annual low flow coincides with the lowest groundwater level. Groundwater withdrawal lowers the level but also reduces the outflow, preserving, in a sense, the aquifer. At the end of the irrigation period, with lower evapotranspiration in the autumn, rainfall leads to a recharge and recovery of the aquifer. The respective hydrographs of monthly precipitation P and abstraction QI and daily groundwater levels GWL for a sub-catchment of the Ilmenau Basin in the summer season of 1994 are shown in Figure 7. Daily values of mobile groundwater storage GWS obtained in another study [10] are also depicted. These values were computed from baseflow separated from total flow by using a nonlinear reservoir algorithm.

In the same study, it was found that, under regional conditions, only about 70% of irrigation water is lost for the groundwater, since 30% infiltrates back or prepares the soil for infiltration of the next rainfalls. These findings match the results obtained in a different approach [11].

While low flows are lowered by groundwater abstractions, the long-term volumes and water levels of the aquifer are little affected. Depressions are only observed at some places at higher parts of the watershed. Water quantity does not pose substantial problems. However, the preservation of long-term groundwater quality by a careful use of fertilizers and agrochemicals remains an important issue [12].

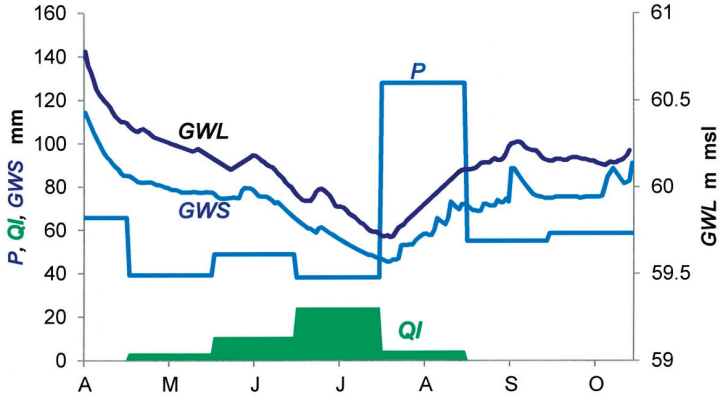

Figure 7. Monthly rainfall *P*, groundwater abstraction *QI*, daily values of groundwater level *GWL*, and computed mobile groundwater storage *GWS*, Eisenbach catchment, summer 1994.

7. Multiple Regression—Groundwater Abstraction

Except for some smaller test areas, groundwater abstraction data are available per irrigation season (April–October) of every year, while precipitation and temperature data are available monthly and per season. As given in Table 1, groundwater abstraction *QI* is significantly correlated with summer rainfall *PS*, summer temperature *TS*, and irrigated areas *AI*. The corresponding regression had the following result:

$$QI_t = -11.6 - 0.0743\, PS_t + 2.56\, TS_t + 0.000434\, AI_t \qquad R = 0.82 \tag{3a}$$

While the correlation coefficient is high, the coefficient of variation, *i.e.*, the mean deviation of calculated values from abstraction data, is 26% and thus not quite satisfying. This is mainly due to a fuzziness of the term summer rainfall (April–October). For irrigation requirements and management, it makes a big difference whether rains fall early in the growing period rather than during or even after harvest. A first step to improving the relationship was the substitution of the values of total summer precipitation (April–October) with those of the main irrigation period (May–August). A correlation coefficient of $R = 0.86$ and a mean deviation of 23% were obtained.

However, rainfall depth has more or less importance depending on the month of the irrigation period. Monthly data of groundwater uptake in some smaller test areas in the watershed [13] from 1990 to 2011 showed the following temporal distribution of volumes: April 3%, May 17%, June 30%, July 29%, August 15%, September 4%, and October 2%. Monthly rainfalls were multiplied by the percentages. The sum of these products for every year represents a weighted mean value for replacing the total summer rainfall. Indeed, the partial correlation of groundwater abstraction with the new variable is closer (R = −0.73) than with summer rainfall (R = −0.62; Table 1). The improved relationship is:

$$QI_t = -9.02 - 0.419\ Pwei_t + 2.48\ TS_t + 0.0004\ AI_t \qquad R = 0.89 \tag{3b}$$

The result is shown in Figure 8. The annual weighted means of seasonal rainfall P_{wei} are plotted for comparison. The mean deviation between data and computed values is 21%. This seems high, but it must be seen in the context that the variation coefficient (standard deviation/mean) of the annual abstractions is more than double (47%). It is also noticeable that this variation is essentially preserved in the computed series of QI (42%), though they are based on variables with much lower variation coefficients, P_{wei} (23%), TS (4%), and AI (19%). Other than with single regression, where variation is determined (and damped) by the independent variable, this is possible by the superposition effects of multiple regression.

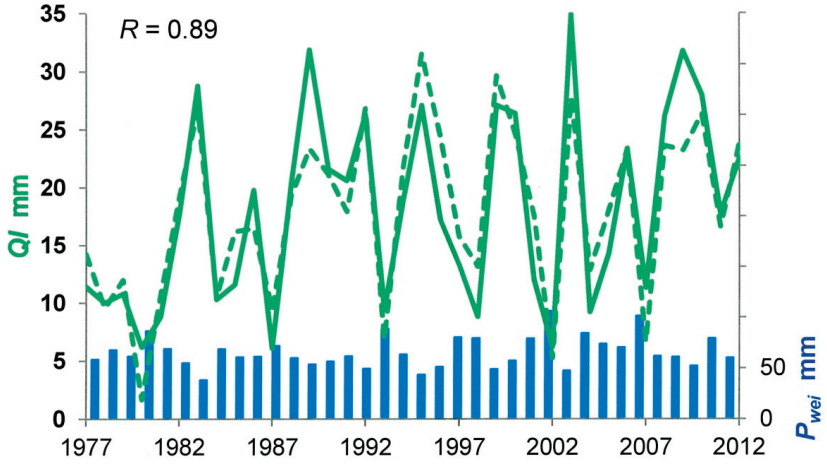

Figure 8. Recorded and computed (Equation (3b), dashed line) annual groundwater abstractions QI, weighted means of seasonal rainfall P_{wei}.

8. Conclusions

Multiple regression analysis allows distinguishing and quantifying the influence of different climatic and man-made variables such as precipitation, temperature, and groundwater withdrawal on annual low flows. It was found that groundwater abstraction for irrigation in the Ilmenau Basin accounts for an average decrease of low flows of about 25%. The groundwater levels and long-term

volumes recover during the winter season. The annual abstraction volume is highly correlated with rainfall depth in the vegetation season, summer air temperature, and irrigation area. It is thus evident that groundwater abstractions in the Ilmenau Basin are based closely on actual irrigation requirements.

Acknowledgments

Thanks go to the Water Authority Landkreis Uelzen (Claudia Boik and Carolin Kuschel) for groundwater abstraction data and advice, to the water autority NLWKN Lüneburg (Daniel Gauglitz) for flow data and to Ulrich Ostermann, District Association of Water and Soil Associations Uelzen, for advice and communication about the temporal water distribution.

Conflicts of Interest

The author declares no conflict of interest.

References

1. Droughts Germany. Available online: http://www.climateadaptation.eu/germany/droughts/ (accessed on 20 June 2015).
2. Hisdal, H.; Stahl, K.; Tallaksen, L.; Demuth, S. Have streamflow droughts in Europe become more severe or frequent? *Int. J. Climatol.* **2001**, *21*, 317–333.
3. Van Loon, A.F.; Laaha, G. Hydrological drought severity explained by climate and catchment characteristics. *J. Hydrol.* **2015**, *526*, 3–14.
4. Brühmann, G. Untersuchung des Wasserhaushaltes im Uelzener Becken (Water balance investigation in the Uelzen Basin). *Wasser Boden* **1982**, *2*, 51–57.
5. Riediger, J.; Breckling, B.; Nuske, R.; Schröder, W. Will climate change increase irrigation requirements in agriculture of Central Europe? A simulation study for Northern Germany. *Environ. Sci. Eur.* **2014**, *26*, doi:10.1186/s12302-014-0018-1.
6. FAO Sprinkler Irrigation. Available online: www.fao.org/docrep/s8684e/s8684e06.htm (accessed on 20 June 2015).
7. Ostermann, U. Grundwasserentnahme für landwirtschaftliche Beregnung aus Sicht einer Unteren Wasserbehörde (Groundwater abstraction for agricultural irrigation from the perspective of a water authority). *Mitt. NNA* **1998**, *3*, 47–50.
8. LWK, Landwirtschaftskammer (Chamber of Agriculture) Niedersachsen. *No Regret—Genug Wasser für die Landwirtschaft?! (Enough Water for Agriculture?!)*; Schulz, E., Ed.; LWK Niedersachsen: Uelzen, Germany, 2008.
9. Gauss, C.F. *Theoria Combinationis Observationum Erroribus Minimis Obnoxiae (Theory of Combination of the Observations Subject to Smallest Errors)*; H. Dieterich: Göttingen, Germany, 1823; pp. 1–58.
10. Wittenberg, H. Effects of season and man-made changes on baseflow and flow recession: Case studies. *Hydrol. Process.* **2003**, *17*, 2113–2123.

11. Wessolek, G.; Renger, M. Einfluss der Beregnung auf den regionalen Wasserhaushalt (Influence of irrigation on the regional water balance). *Wasser Boden* **1987**, *3*, 112–114.
12. Lewandowski, J.; Meinikmann, K.; Nützmann, G.; Rosenberry, D. Groundwater—The disregarded component in lake water and nutrient budgets. Part 2: effects of groundwater on nutrients. *Hydrol. Process.* **2015**, *29*, 2922–2955.
13. Ostermann, U. Water and Soil Association, Uelzen, Germany. Personal Communication, 2014.

Groundwater Challenges of the Lower Rio Grande: A Case Study of Legal Issues in Texas and New Mexico

Elizabeth Wheat

Abstract: In 1938, Texas, New Mexico, and Colorado signed the Rio Grande Compact, establishing terms of apportionment for some of the water from the Rio Grande for the three states. Following congressional approval in 1939, this compact governs water allocation in a region with a variable climate and frequent drought conditions and established the Rio Grande Compact Commission, comprised of a commissioner from each state and one from the federal government, to enforce the compact. With an increasing population and declining surface water supply, the Compact has been tested among the parties and within the states themselves. In a case currently before the U.S. Supreme Court, *Texas v. New Mexico and Colorado* (2013), Texas claims New Mexico is violating the Compact and Rio Grande Project Act by using water in excess of its apportionment through its allowance of diversions of surface and groundwater. The issue is further compounded by disputes within Texas over separate legal regimes for groundwater and surface water. Combined with growing scarcity issues, the allocation of water in the Lower Rio Grande presents a timely natural resource challenge. This review explores legal issues involved in the case as well as growing challenges of population growth, agricultural development needs, and water shortages.

Reprinted from *Resources*. Cite as: Wheat, E. Groundwater Challenges of the Lower Rio Grande: A Case Study of Legal Issues in Texas and New Mexico. *Resources* **2015**, *4*, 172–184.

1. Introduction

The Rio Grande flows 1900 miles from the San Juan Mountains in Colorado before reaching the Gulf of Mexico [1]. It is the fifth longest river in the United States and forms a 1255-mile border with Mexico. Both countries share the Rio Grande/Bravo watershed of 335,000 square miles, necessitating international cooperation on the river's supply and health [2]. On the United States side, 75% of the water is allocated for agriculture, which means many of the disputes over water rights involve competing economic decisions [2]. This article will look at a current case before the U.S. Supreme Court between Texas, New Mexico, and Colorado over the Rio Grande Compact ("Compact") and each state's legal obligations for managing and sharing water of the Lower Rio Grande. To help the reader understand the context of the case before the Supreme Court I begin with a summary of the Compact and then discuss state water regimes in Texas and New Mexico. Colorado's state water laws are omitted because the Supreme Court case is primarily a dispute between Texas and New Mexico; Colorado is only listed because it is a party to the original Compact.

2. Discussion

2.1. Development of the Rio Grande Compact

Historically, groundwater availability in the Southwest became a point of contention as the region's population grew due to mining and agricultural development, placing a greater strain on available water resources. These land uses shaped the development of several water doctrines that varied by region or state, and created a complicated legal regime in which the federal government began working to address the water challenges and needs of the expanding country [3]. These legal regimes of riparian rights and prior appropriation will be discussed in greater depth in Section 2.3.

To address these water needs, President Roosevelt signed the National Reclamation Act in 1902 to use revenue from public land sales for large-scale irrigation projects that would store, divert, and maintain water in the arid states. This ushered in the Big Dam era of the 1930s, with peak construction from 1950 to 1980 [3,4]. Dam advocates promised these structures would generate rapid change, help with forest fire responses, and improve irrigation, navigation, and water storage. Opponents argued there were less expensive options for taxpayers and cautioned about the unknown environmental effects [5]. A "water bureaucracy" between the Army Corps of Engineers, Bureau of Reclamation, and Tennessee Valley Authority was tasked with facilitating these water projects with the states. As part of the dam construction, large reservoirs were also created and these become an integral point in the dispute between Texas and New Mexico.

While the United States is expanding dams during the Progressive Era, challenges with the country's neighbor to the South arose. In the late 1800s, the United States enacted an embargo on development of reservoirs on federal lands. The embargo was part of a dispute between the U.S. and Mexico, resulting in a 1906 treaty to lift the embargo, but it was only the beginning of disagreements between the two countries or between the states involved. The Harmon Doctrine states a country is sovereign over the international waters within its borders, but the U.S. has never followed it in practice and instead chose to consider Mexico's needs in managing this international watercourse on the United States side [6]. The U.S. government then reinstated the embargo and instructed Colorado, Texas, and New Mexico to develop the Rio Grande Compact where each state would receive an adequate water supply along the Rio Grande. The agreement placed a limit on water use for each state using a credit and debit system [7,8].

Congress approved the Compact in 1939. It applies to use of waters of the Rio Grande above Fort Quitman, Texas, delivery of water from Colorado to New Mexico near the state line, and from New Mexico to Texas above the Elephant Butte Reservoir [9]. The Elephant Butte Reservoir's construction occurred between 1911 and 1916, with the fill beginning in 1915. It can store up to 2,056,010 acre-feet of water and supplies irrigation water supply for 178,000 acres of land and electric power for surrounding communities [10–12]. As of January 2015, the Elephant Butte Reservoir is approximately thirteen percent full, but the ongoing drought and increased temperatures in the Southwest will further complicate water available for irrigation and obligations for New Mexico under the Compact [13,14]. During a drought period, farms must pump from underground water sources to sustain their crops instead of water from the Elephant Butte or Percha Dams. New Mexico river flows are projected to decrease and scientists warn that if existing water use patterns

do not change, the state will run a deficit for its required Compact contributions [15]. In many parts of Texas, heavy groundwater pumping for agriculture is rapidly depleting available groundwater resources. For example, the Ogallala Aquifer's pumping rate is six times greater than its recharge rate and this aquifer supplies a majority of the state's groundwater supplies [16]. The urgency of these water problems and forecasts of a worsening drought demonstrate the importance of resolving the current Compact dispute.

2.2. Requirements of the Compact

For the Colorado portion of the Compact, there are four index stations located at the Rio Grande headwaters and a schedule of water deliveries. A credit and debit system allows for water to be stored in the Elephant Butte and Caballo Reservoirs [9]. According to Craig Cotton, the Colorado Division Engineer from the Rio Grande Division, the Compact requires the state deliver water from the Rio Grande (approximately 27%–28% of average flow) and its main tributary, the Conejos River (approximately 38% of average flow) [7]. This is measured by hydrologic flow curves that account for conveyance losses. The challenging aspect for the state is it must project its water needs in advance of actual need. For low flow periods, Colorado's projections are prioritized, but in high flow periods the state's delivery obligations increase. One hundred percent of excess water must be sent to New Mexico and Texas during extremely high flow periods and farmers are prohibited by the state from diverting water that flows by their property [7].

New Mexico must deliver a set amount of water to the Elephant Butte Reservoir, approximately 105 miles north of the Texas state line. The Bureau of Reclamation then allocates water between the Elephant Butte Irrigation District (EBID) and El Paso County Water Improvement District (EPCWID) No. 1 [17]. EBID is an 8500-member irrigation district that delivers river water in the southern area of Sierra County and Doña Ana County [18]. It receives 57% of the reservoir water and the EPCWID receives 43%.

2.3. State Water Regime: Texas

Texas' legal system divides water into several classes—surface, groundwater, atmospheric—each of which is governed by separate legal systems. For surface water, Texas is a dual doctrine state, recognizing both riparian and prior appropriation legal regimes. A majority of the state's water law focuses on surface water, with very little on groundwater or atmospheric moisture [19]. It is important to note surface water rights are considered property rights in Texas [20]. Surface water is defined in the Texas Water Code (§11.021) as "water of the flow underflow and tides of every flowing river, natural stream, lake, bay, arm of the Gulf of Mexico, and stormwater, floodwater or rain water of every river, natural stream, canyon, ravine, depression, and watershed in the state" [20].

Riparian doctrine governs surface waters, giving rights to the water based on ownership of land adjacent to a natural river or stream [21]. An individual's water rights are directly connected to the land owned and may be freely exercised as long as the use is reasonable [21]. Riparian rights originated from Hispanic legal principles during Spanish settlements and continued with the Mexican government and through the Republic of Texas until 1840 when the state's Congress adopted English

common law [19]. Under common law, courts develop rules for riparian owners based on cases over water conflicts. Realizing the problematic nature of riparian doctrine for arid areas where water and riparian land are both limited, the prior appropriation doctrine was adopted around 1900 and water rights must be acquired from the state through statutory processes.

Under prior appropriation (Texas Water Code §11.027), the first person receiving a permit has senior water rights to any subsequent permit holders. In contrast to the case-based nature of the riparian doctrine, prior appropriation is based on statutes and rights are acquired by complying with these statutes [21]. This "first in time, first in right" approach can be altered by the Texas Commission on Environmental Quality (TCEQ) if there is an imminent threat to public health or safety through an emergency permit, order, or amendment to an existing permit under Texas Water Code §11.139. Compensation must be made to the water right holder for water taken to address the emergency [20].

Since the appropriation doctrine was adopted, state water agencies faced administrative challenges recognizing and protecting these new rights while remnants of the riparian system remained law. Conflicting records and duplicate allocation of waters under both systems greatly complicated management of the state's surface water [19]. Following the failure of a judicial resolution for state water rights in the *State v. Hidalgo County Water Control and Improvement District No. 18* (1967) case, Texas passed the Water Rights Adjudication Act. This statute merged the riparian rights system into the prior appropriation system, creating an adjudication procedure administered by the Texas Water Commission, now known as the Texas Natural Resource Conservation Commission [19]. This adjudication process has been upheld as constitutional and a comparatively more efficient system of permits and allocation of water rights exists because there is now a unified water system instead of two competing regimes [21].

For groundwater, Texas law divides it into two classes: percolating groundwater and water flowing in well-defined underground streams [19]. All groundwater is presumed to be percolating unless otherwise proven and is governed by the rule of capture, granting landowners rights to capture water beneath their property [21]. Based on the Texas Supreme Court case *Houston & T.C. Ry. V. East* (1904) upholding English common judge-made law, a landowner can pump and use the water on his/her land with few restrictions, regardless of the impact on adjacent landowners [19,22]. Groundwater provides 60% of the 16.1 million acre-feet of water used in the state of Texas with 80% of the groundwater used for crop irrigation [16,23]. Comparable usage statistics for the entire Lower Rio Grande are difficult to obtain with the United States Geological Survey's most recent data published in 1985. At that point in time, 77% (900,000 acre-feet) of the groundwater drawn from the Rio Grande aquifer was used for agricultural purposes and 15% (180,000 acre-feet) was used for public supply primarily in Albuquerque, Las Cruces, and Sante Fe [24]. Statistics from the Bureau of Reclamation project a shortfall of 592,084 acre-feet of water per year in addition to 86,438 acre-feet needed due to climate change, for a projected total demand of 678,522 acre-feet in the year 2060 [25].

In 1949, Texas passed a law to create local groundwater conservation districts (GCDs) for underground water and to exert controls over groundwater uses by landowners. Texas manages much of its groundwater through these Groundwater Conservation Districts (GCDs) created by the legislature under Article XVI §59 of the Texas Constitution or by the TCEQ, which has primary

jurisdiction of state groundwater regulations [26,27]. Each GCD is mandated to have a groundwater management plan (GMP), regulate spacing and well production, and monitor conditions of the district's aquifers. The Texas Water Development Board must approve the groundwater management plans of these districts and as of December 2014, there are 96 confirmed districts and all management plans for these districts have received approval [28]. GCDs are authorized to regulate the amount of water withdrawn from the aquifers with little process for appeal [29]. According to the Texas Administrative Code §356.52, a GMP must specify the district's ground water goals which include the following: "The most efficient use of groundwater, controlling and preventing waste of groundwater, controlling and preventing subsidence, addressing conjunctive surface water management issues, addressing natural resource issues, addressing drought conditions, addressing conservation, groundwater recharge, and desired future aquifer conditions" [27]. There are also Groundwater Management Areas (GMAs), required as of 2005, to develop desired future conditions (DFCs) for aquifers crossing political boundaries. Six regional aquifer alliances exist in Texas and the Texas Water Development Board (TWDB) acts as the overseeing state actor [30]. The TWDB's responsibilities include conducting groundwater studies, monitoring water levels and quality, reviewing the GMPs, and conducting investigations to help policymakers and legislators [16]. Local governments may also receive grants from the TWDB for water supply projects. Most central to the legal water rights issues discussed in this paper, the TWDB administers the Texas Water Bank to facilitate the transfer, sale, and lease of water rights in the state [31].

The proposed development and sale of groundwater by private companies looking to expand their businesses and revenue illustrates one challenge Texas faces with groundwater allocation and managing increasing water shortages. The Val Verde Water Company proposes pumping 16 billion gallons a year for sale to cities in need of water such as San Antonio or San Angelo. The San Antonio Water System (SAWS) solicited private sector company proposals for developing new water supplies in the area, but announced in February 2014 that the three pumping projects in the final round of consideration would be tabled and SAWS would instead pursue desalination plans for brackish water [32]. SAWS President Richard Puente said, "Groundwater law in Texas leaves too much uncertainty and risk for the private and public sectors. I hope that the proposers and cities across the state will join SAWS in calling for the Legislature to change the law so Texans can build projects to meet growing future demand" [32]. Opponents are concerned increased groundwater pumping proposals such as Val Verde's, would jeopardize water from Devils Lake which feeds into Lake Amistad on the Texas-Mexico border and the Lower Rio Grande. The importance of this proposal is to show the growing demand and need for water and willingness of private companies to step in and provide services for the government. If Texas chooses to contract for these kinds of plans, it will become critical for the GCDs and TCEQ to closely monitor the pumping and greater environmental risks of brackish groundwater pumping [33].

For the third and final class of Texas water regimes, the state's courts have taken the unique approach of finding water rights for atmospheric moisture since interest in weather modification grew post-World War II. While it is not the only state recognizing such rights, Texas affords more rights than any other state in the country [19]. In *Southwest Weather Research, Inc. v. Duncan* (1958), the court said, "We believe that the landowner is entitled…to such rainfall as may come from clouds

over his own property that nature in her caprice may provide" [19]. Following the Weather Modification Act of 1967, the Texas Water Development Board gained control of weather modification and the Texas Water Commission issues licenses and permits for modification operations [19]. This class of rights will not factor into the Supreme Court dispute, but it is important to briefly discuss and provide the reader with a full picture of water classes in the state.

2.4. State Water Regime: New Mexico

New Mexico's water law can be divided into state law, interstate law (such as the Compact), federal law, and Native American historic use water rights. The state is party to several water allocation arrangements, including settlement agreements with First Nations through the New Mexico Office of the State Engineer, but the Compact will be the primary focus since it is at the center of the Supreme Court dispute [22]. New Mexico Statutes Annotated (NMSA) §72-1-1 (1907) recognizes surface-water rights, later extended by the legislature in 1941 to include underground waters defined as "underground streams, channels, artesian basins, lakes, and reservoirs having 'reasonably ascertainable boundaries'" [34]. Article XVI, §3 of the state Constitution describes the state's doctrine of prior appropriation and defines beneficial use for New Mexico. Implementation of this doctrine in New Mexico resembles the Texas surface water approach prior to their unified water system, with the first user (senior appropriator) having the right to take and use the water over a junior appropriator in times of drought [34].

In contrast to Texas treating surface and groundwater separately, New Mexico administers its water regime through a conjunctive water management approach established by the decision in *City of Albuquerque v. Reynolds* (1962) [35,36]. Conjunctive water use looks at the hydrologic connection between surface water and groundwater, and develops a system of timing by shifting when and where water is stored based on availability. Conjunctive water management uses this water use approach, but adds monitoring, evaluation of the monitoring data, and works to develop local management plans [37]. New Mexico's Supreme Court has upheld this management approach and recognizes the State Engineer as having jurisdiction over the Lower Rio Grande Basin [38]. The New Mexico Environmental Improvement Board (NMEIB) and the New Mexico Water Quality Control Commission (NMWQCC) hold the responsibility for adopting regulations and setting groundwater standards, with the NMWQCC is the official water pollution control agency in the state [34]. There is ongoing litigation in New Mexico over surface and groundwater rights in the state such as the Aquifer Science LLC or Augustin Plains Ranch cases, but for the purposes of this article, the Supreme Court case is the primary focus [39,40].

2.5. Case before the Supreme Court

The TCEQ argues New Mexico's groundwater pumping is reducing the flow of the Rio Grande and therefore violates terms of the Compact [41]. Texas claims New Mexico's issuance of permits for 2500 wells between the Elephant Butte Reservoir and state line are reducing the amount of water Texas receives [17,12]. The state does not dispute that New Mexico is delivering the required amount of water to the reservoir, but alleges the Compact's purpose or intent is violated by water diversion

prior to delivery to Texas [42]. The suit states, "The Rio Grande Compact is predicated on the understanding that delivery of water at the New Mexico-Texas state line would not be subject to additional depletions beyond those that were occurring at the time the Rio Grande Compact was executed" [13]. In *Texas v. New Mexico and Colorado* (2013), Texas is asking the Court to stop New Mexico's diversions, compensate the state for water it has removed through the diversions, and specify the amount of water Texas is entitled under the Compact [17,42]. The state has allocated $5 million for litigation in this case based on the FY 2014 budget [13].

New Mexico's response to the depletion claims is that the Compact does not mandate a specific amount of water to be delivered to Texas-New Mexico state line and only requires a certain amount be delivered into the reservoir. Additionally, New Mexico contends the area between the reservoir and Texas state line falls under New Mexico law. Governor Susana Martinez stated New Mexico "will not cede one inch of New Mexico water to Texas" [17] Attorney General Gary King said he felt Texas is "trying to rustle New Mexico's water and is using a lawsuit to extort an agreement that would only benefit Texas while destroying water resources for hundreds of thousands of New Mexicans" [13].

EBID, at the center of the dispute, is under New Mexico law for groundwater, but is combined with Texas under the Compact for river water regulation. In 2008, EBID signed an Operating Agreement with the federal government and its Texas counterpart, EPCWID, in El Paso to share water and avoid a legal battle between the states [1]. The agreement allowed water to be carried over from one year to the next. EBID believes this agreement has been successful, potentially distancing the district from the state's Compact dispute with Texas [43]. When it comes to the Supreme Court dispute, EBID Manager Gary Esslinger said, "We'll not necessarily be taking New Mexico's side or taking Texas' side" [18]. Esslinger notes the 2008 agreement guarantees farmers in Texas receive their share of river water and the success of the agreement positions EBID well before the Supreme Court in the current case. The New Mexico State Engineer then sued Texas to overturn this Operating Agreement in *New Mexico v. United States, EBID, EPWCID#1* (2011), but the lawsuit was stayed by Justice Browning, pending the Supreme Court case that is the focus of this research [12].

Texas v. New Mexico and Colorado (2013) proceeded directly to the United States Supreme Court because the Court has original jurisdiction in disputes between two or more states under Article 3 §2 of the Constitution [44]. For this type of case, a state is required to file a motion seeking permission to file the complaint and submit a brief explaining why the Supreme Court should hear the dispute [42]. Original jurisdiction cases can proceed directly to the Supreme Court without going through the lower federal courts and the justices do not have to provide an explanation as to why they accept or deny a given case. Texas filed the required motion for this case in January 2013 [45]. The Court will consider three factors in making the decision whether to hear the case: if the case is really between states (and not state agencies), seriousness of the dispute, and whether there is an alternative forum to hear the dispute [42].

The case centers on Texas and New Mexico and their pumping next to the Rio Grande, but as a party to the Compact, Colorado is implicated [7]. A complicating factor to the Compact and case is that Texas does not treat surface and groundwater as part of the same water system, meaning it does not use a conjunctive water management approach, though both its 1969 and revised 1984 water

plans specify conjunctive water management as a desirable goal [28]. Texas landowners have the right to capture which gives them the ability to use the groundwater on their land [30]. The Compact, Texas, and Colorado all have separate legal regimes for surface water and groundwater, with Texas placing very few restrictions on water use and New Mexico as the only state operating a conjunctive water management system. When trying to reach a judicial resolution for Compact disputes, this wide variation of legal doctrines makes it difficult [7].

In January 2014, the Supreme Court issued an order explaining that it may have jurisdiction in the dispute between Texas and New Mexico, but also suggested New Mexico file a motion to dismiss the action. Gary King, Attorney General for the State of New Mexico described this order in saying, "Clearly, I was hoping for a different outcome, however, I am not surprised. I am confident that the Court takes such state to state disputes very seriously and we look forward to being able to tell New Mexico's side of the story and to have our day in Court" [15].

On 9 July 2014 the Supreme Court distributed this case for the 29 September 2014 conference. This indicates the court is considering the petition to hear the case, but not yet decided whether it will hear oral arguments and issue a ruling. On 3 November 2014, the court appointed a Special Master to do the following: fix the time and conditions for the filing of additional pleadings, to direct subsequent proceedings, to summon witnesses, to issue subpoenas, and to take such evidence as may be introduced and such as he may deem it necessary to call for [46]. As of the time this article was submitted for publication, a 29 January 2015 deadline has been set for all parties to file motions. Thus far, the following parties have filed amicus briefs: Hudspeth County Conservation and Reclamation District No. 1, El Paso County Water Improvement District No.1, City of El Paso, Texas, City of Las Cruces, and the Solicitor General of the United States.

2.6. Potential Impacts of a Supreme Court Decision

One possible effect of a Supreme Court ruling in favor of Texas are groundwater pumping limitations for crops grown in New Mexico such as pecan, chile, and onion. Pecans depend on a constant reliable supply of water and pumping limitations could harm these crops and in turn reduce property values of farmers owning orchards [15]. In contrast to large-scale farming operations, pecan farms in the state are often family businesses and thus farmers face greater risks for pumping limitations and are less able to absorb rising costs of obtaining more water or smaller crops. Pecans generate over $100 million annually to New Mexico and account for one-third of the country's pecan production combined with California and Arizona [47]. The New Mexico Pecan Growers (NMPG) [48] worked with the EBID to formulate an equitable settlement of water rights for all crops [49]. The final settlement went beyond pecans to specify water allocations for all crops in the Lower Rio Grande basin in compliance with the Compact. Until this agreement is appealed or the Supreme Court rules on the allocation, water rights will be appropriated as agreed [50,51].

Whereas high use crops like pecans need larger amounts of water, often in excess of the standard allotment, vegetable crops can use less water but it must be more frequent and of a higher quality [34]. New Mexico's strong chile industry generates over $400 million annually for the state's economy and sustains more than 4000 jobs. The cities of Deming and Hatch, self-proclaimed "Chile Capital of the World," and homes to much of the state's chile crop, have received rain recently, but depend

on a heavy snowpack from the northern mountains into the Rio Grande to sustain water supplies [52]. Chile and pecan farmers received twice as much water for irrigation in 2014 as they did in 2013, but this is allotment is lower than their normal water amount. Some farmers argue groundwater is preferable for crop irrigation because it is comparatively cleaner and has fewer plant diseases, but it can be more saline and costly. Using groundwater for irrigation can also be more time-consuming compared to irrigation from river water [53]. As the drought reduces river water, wells pump less and become limited as to how much can be pumped for a single irrigation. Reduced single irrigation can decrease a chile crop yield by 5%, but the reduction for crops like onions could be as high as 30% yield reduction [54]. Without the recharge into the Rio Grande and thus into Elephant Butte Lake and the Caballo Reservoir, the underground water supply and irrigation for cities such as Hatch could be jeopardized, placing economically valuable crops at risk.

A challenge for all three states involved is maintaining water flow to designated critical habitats along the Rio Grande for endangered species under 16 U.S.C. §1533 of the Endangered Species Act (ESA). The ESA's purpose is to protect at-risk species from extinction and from being harassed or harmed. Harm is defined as "An act which actually kills or injures wildlife. Such act may include significant habitat modification or degradation where it actually kills or injures wildlife by significantly impairing essential behavioral patterns, including breeding, feeding or sheltering" [55]. In July 2014, Wild Earth Guardians filed suit in federal district court against the Middle Grande Conservancy District, claiming Article 9 ESA violations for the District's diversion of water from the Rio Grande at four separate dams along the river. Wild Earth Guardians claim this diversion has harmed the critical habitat and essential behavioral patterns of the endangered Rio Grande silvery minnow and the Southwestern willow flycatcher [56]. Any resolution to water disputes of the Rio Grande will have to answer ESA situations such as these or face additional litigation.

3. Conclusions

Combined with population growth on both sides of the Mexico-United States border, severe drought projections, increased demand for water, agricultural needs, and the added pressure these all place on the Rio Grande, resolving the allocation issues of the Compact will become increasingly urgent for all states involved. The legal dispute before the Supreme Court may take years and millions of dollars to resolve, including the possibility of the Supreme Court declining to issue a ruling, but the drought and water shortages are pressing problems which New Mexico, Texas, and Colorado need to address soon in order to avoid greater problems in the future.

Conflicts of Interest

The authors declare no conflict of interest.

References

1. Drought Fuels Water War Between Texas and New Mexico. Available online: http://newswatch.nationalgeographic.com/2013/01/18/drought-fuels-water-war-between-texas-and-new-mexico (accessed on 30 June 2014).

2. U.S. International Boundary & Water Commission. Available online: http://www.ibwc.gov/crp/riogrande.htm (accessed on 30 June 2014).
3. U.S. Department of the Interior-Bureau of Reclamation; Army Corps of Engineers; U.S. Department of the Interior-National Park Service. The History of Large Federal Dams: Planning, Design, and Construction. Available online: http://www.usbr.gov/history/HistoryofLargeDams/LargeFederalDams.pdf (accessed on 6 March 2015).
4. Poff, N.L.; Hart, D.D. How dams vary and why it matters for the emerging science of dam removal. *Bioscience* **2002**, *52*, 659–668.
5. Babbitt, B. What goes up, may come down. *Bioscience* **2002**, *52*, 656–658.
6. McCaffrey, S.C. The Harmon Doctrine One Hundred Years Later: Buried, Not Praised. Available online: http://lawschool.unm.edu/nrj/volumes/36/4/13_mccaffrey_harmon.pdf (accessed on 1 March 2015).
7. McFadden, A. Rio Grande! Available online: http://duwaterlawreview.com/rio-grande/ (accessed on 30 June 2014).
8. Rio Grande River Compact 37-66-101. Available online: http://water.state.co.us/DWRIPub/Documents/riograndecompact.pdf (accessed on 15 July 2014).
9. Rio Grande Compact. Available online: http://wrri.nmsu.edu/wrdis/compacts/Rio-Grande-Compact.pdf (accessed on 5 January 2015).
10. Bureau of Reclamation. Elephant Butte Powerplant. Available online: http://web.archive.org/web/20060926130025/http://www.usbr.gov/power/data/sites/elephant/elephant.html (accessed on 5 January 2015).
11. Michaelson, A.M.; Dowell, T.; Sheng, Z.; Lacewell, R.; Hurd, B.; American Water Resources Association. In Proceedings of the Annual Conference Texas *v*. New Mexico Supreme Court Water Case: Issues, Process, and Interpretation, Vienna, VA, USA, 3–6 November 2014. Available online: http://www.awra.org/meetings/Annual2014/doc/pdfs/ANL_S65_Michelsen_Ari.pdf (accessed on 5 January 2015).
12. Elephant Butte Irrigation District: Litigation on the Lower Rio Grande. Available online: http://www.ebid-nm.org/legalUpdates/legalUpdates/Legal_Issues_Affecting_EBID.pdf (accessed on 5 January 2015).
13. Galbraith, K. Texas Allocates $5 Million for New Mexico Lawsuit. Available online: http://texasclimatenews.org/wp/?p=7901 (accessed on 30 June 2014).
14. Water Data for Texas. Available online: http://www.waterdatafortexas.org/reservoirs/individual/elephant-butte (accessed on 20 October 2014).
15. Fleck, J. U.S. Supreme Court Allows Texas Water Suit Against New Mexico to Proceed. Available online: http://www.abqjournal.com/343679/abqnewsseeker/u-s-supreme-court-allows-texas-water-suit-against-new-mexico-to-proceed.html (accessed on 30 June 2014).
16. Texas Water Development Board. Available online: www.twdb.state.tx.us/groundwater (accessed on 30 June 2014).
17. Dowell, T. States' Water Dispute Could Reach the U.S. Supreme Court. Available online: http://www.progressivecattle.com/news/industry-news/6035-states-water-dispute-could-reach-us-supreme-court (accessed on 30 June 2014).

18. Bryan, S.M. Texas to Proceed with Water Lawsuit Against NM. Available online: http://www.lcsun-news.com/las_cruces-news/ci_25002335/texas-proceed-water-lawsuit-against-nm (accessed on 30 June 2014).
19. Templer, O.W. Water Law, Handbook of Texas Online. Available online: http://www.tshaonline.org/handbook/online/articles/gyw01 (accessed on 7 December 2014).
20. Texas Water: Basics of Surface Water Law. Available online: http://agrilife.org/texasaglaw/2013/09/30/texas-water-basics-of-surface-water-law/ (accessed on 29 December 2014).
21. Texas A & M University. Texas Water Law. Available online: http://texaswater.tamu.edu/water-law (accessed on 4 March 2015).
22. New Mexico Office of State Engineer. Interstate Stream Commission. Available online: www.ose.state.nm.us/Legal/settlements_IWR.php (accessed on 27 February 2015).
23. Texas Groundwater Basics. Available online: http://texaslivingwaters.org/groundwater/groundwater-in-texas/ (accessed on 30 June 2014).
24. United States Geological Service. Groundwater Atlas of the United States—Arizona, Colorado, New Mexico, Utah HA 730-C. Available online: http://pubs.usgs.gov/ha/ha730/ch_c/C-text4.html (accessed on 6 March 2015).
25. United States Bureau of Reclamation. Lower Rio Grande Basin Study Executive Summary. Available online: http://www.usbr.gov/WaterSMART/bsp/docs/finalreport/LowerRioGrande/LowerRioGrandeExecutiveSummary.pdf (accessed on 5 March 2015).
26. Groundwater Conservation District (GCD) FAQs. Available online: http://www.twdb.state.tx.us/groundwater/faq/index.asp (accessed on 1 October 2014).
27. Texas Groundwater Protection Committee. Joint Groundwater Monitoring and Contamination Report—2013. Available online: https://www.tceq.texas.gov/assets/public/comm_exec/pubs/sfr/056-13.pdf (accessed on 10 October 2014).
28. Groundwater Conservation Districts. Available online: www.twdb.state.tx.us/groundwater/conservation_districts/ (accessed on 29 December 2014).
29. Desalination Opportunities Expanded in Texas from Brackish Groundwater. Available online: https://www.waterworld.com/articles/2014/02/brackish-groundwater-allows-saws-to-go-big-with-desalination.html (accessed on 30 June 2014).
30. Groundwater Resources. Available online: www.hillcountryalliance.org/HCA/Groundwater (accessed on 18 October 2014).
31. Texas Water Development Board. About Texas Water Development Board. Available online: http://www.twdb.texas.gov/about/index.asp#twdb-history (accessed on 1 March 2015).
32. San Antonio Shelves Groundwater Projects. Available online: http://smmercury.com/2014/02/07/san-antonio-shelves-groundwater-projects/ (accessed on 30 June 2014).
33. Satija, N. Brackish water abounds, but using it isn't simple. Available online: www.texastribune.org/2014/01/08/plenty-brackish-water-underground-still-elusive/ (accessed on 26 February 2015).

34. Terracon; John Shomaker & Associates, Inc.; Livingston Associates, LLC, Inc.; Zia Engineering and Environmental, Inc.; Sites Southwest. The New Mexico Lower Rio Grande Regional Water Plan—August 2004. Available online: http://wrri.nmsu.edu/lrgwuo/rwp/LowerRioGrandeRegional WaterPlan.pdf (accessed on 23 March 2015).
35. Hazard, J.; Shively, D. Conjunctive Management of Surface and Ground Water Resources in the Western United States. Available online: dnrc.mt.gov/divisions/water/management/docs/clark-fork-task-force/policy-administrative_tools-shively.pdf (accessed on 30 December 2014).
36. Bryner, G.; Porcell, E. Groundwater Law Sourcebook of the Western United States. Available online: http://cacoastkeeper.org/document/groundwater-law-sourcebook-of-the-western-united-states.pdf (accessed on 4 January 2015).
37. Dudley, T.; Fulton, A. Conjunctive Water Management: What is it? Why Consider it? What are the Challenges? Available online: http://www.glenncountywater.org (accessed on 20 October 2014).
38. Office of the State Engineer of New Mexico. In the Matter of the Requirements for Metering Groundwater Withdrawals in the Lower Rio Grande Watermaster District, New Mexico. Available online: http://www.ose.state.nm.us/PDF/ActiveWater/LowerRioGrande/LRG_ MeterRequirementsOrder.pdf (accessed on 1 October 2014).
39. Massey, B. New Mexico High Court Asked to Decide Dispute over Pecos River. Available online: http://lubbockonline.com/filed-online/2013-04-29/new-mexico-high-court-asked-decide-dispute-over-pecos-river#.VKrwyEu4mFI (accessed on 4 January 2015).
40. New Mexico Environmental Law Center. Cases-Water. Available online: nmelc.org/cases-water (accessed on 4 January 2015).
41. Satija, N. Rio Grande Water Users Fear Groundwater Pumping Project. Available online: http://www.texastribune.org/2014/01/29/groundwater-pumping-project-could-hurt-rio-grande/ (accessed on 30 June 2014).
42. Texas Water Wars: Texas *v*. New Mexico. Available online: http://agrilife.org/texasaglaw/ 2013/09/18/texas-water-wars-texas-v-new-mexico/ (accessed on 30 June 2014).
43. Texas to Proceed with Lawsuit against New Mexico. Available online: http://dfw.cbslocal.com/ 2014/01/27/texas-to-proceed-with-water-lawsuit-against-nm/ (accessed on 30 June 2014).
44. Federal Judicial Center. Original, Supreme Court- History of the Federal Judiciary. Available online: www.fjc.gov/history/home.nsf/page/jurisdiction_original_supreme.html (accessed on 27 February 2015).
45. State of Texas *v*. State of New Mexico and State of Colorado. Available online: http://sblog.s3. amazonaws.com/wp-content/uploads/2013/04/1-7-13-Texas-v-NM-booklet.pdf (accessed on 1 October 2014).
46. Texas *v*. New Mexico and Colorado. Available online: www.scotusblog.com/case-files/cases/texas-v-new-mexico-and-colorado (accessed on 30 December 2014).
47. Dan Frosch. New Mexico is Reaping a Bounty in Pecans as Other States Struggle. Available online: http://www.nytimes.com/2014/03/28/us/new-mexico-reaps-pecan-bounty-as-other-states-struggle.html?_r=2 (accessed on 18 October 2014).

48. New Mexico Pecan Growers Association. Available online: http://www.nmpecangrowers.us (accessed on 18 October 2014).
49. New Mexico Pecan Growers Association. Agreement on Settlement in Principle. Available online: http://www.nmpecangrowers.us/Water%20Issue/STREAM_ISSUE_101_SETTLEMENT_AGREEMENT_6.11.pdf (accessed on 30 June 2014).
50. Rister, M.E.; Sturdivant, A.W.; Lacewell, R.D.; Michelsen, A.M. Water Litigation in the Lower Rio Grande. Available online: http://uttoncenter.unm.edu/pdfs/Water-Matters-2013/Water%20Litigation%20in%20the%20Lower%20Rio%20Grande%20.pdf (accessed on 30 July 2014).
51. EBID Agreement. Available online: http://www.ose.state.nm.us/PDF/HotTopics/EBID-Agreement/SS-97-101-FinalJudgment.pdf (accessed on 30 June 2014).
52. Carcamo, C. New Mexico's Dwindling Chile Crop Has Farmers Anxious. Available online: http://www.latimes.com/nation/la-na-ff-new-mexico-chiles-20141012-story.html (accessed on 18 October 2014).
53. Hawkes, L. More Water Available this Year for New Mexico Chile Pepper Growers. Available online: http://southwestfarmpress.com/vegetables/more-water-available-year-new-mexico-chili-pepper-growers (accessed on 30 June 2014).
54. Soular, D.A. New Mexico Chile Acreage Hits Four-Decade Low. Available online: http://www.lcsun-news.com/las_cruces-news/ci_25469929/new-mexico-chile-acreage-hits-four-decade-low (accessed on 30 June 2014).
55. 50 C.F.R. §17.3. Available online: http://www.ecfr.gov/cgi-bin/searchECFR?idno=50&q1=17&rgn1=PARTNBR&op2=and&q2=&rgn2=Part (accessed on 18 October 2014).
56. Wild Earth Guardians. Notice of Intent to Sue the Middle Rio Grande Conservancy District for Violations of the Endangered Species Act. Available online: http://www.wildearthguardians.org/site/DocServer/8.20.14_MRGCD_NOI_Final.pdf?docID=14502 (accessed on 18 October 2014).

Groundwater Quality Changes in a Karst Aquifer of Northeastern Wisconsin, USA: Reduction of Brown Water Incidence and Bacterial Contamination Resulting from Implementation of Regional Task Force Recommendations

Kevin Erb, Eric Ronk, Vikram Koundinya and John Luczaj

Abstract: In the Silurian Dolostone region of eastern Wisconsin, the combination of thin soils and waste application (animal manure, organic waste) has led to significant groundwater contamination, including Brown Water Incidents (BWIs—contamination resulting in a color or odor change in well water) and detections of pathogen indicator bacteria such as *E. coli* and others. In response, a Karst Task Force (KTF) was convened to identify risks and recommend solutions. This article looks at the impact eight years after the 2007 Karst Task Force report—both the actions taken by local resource managers and the changes to water quality. We present the first regional analysis of the 2007 Karst Task Force report and subsequent regulatory changes to determine if these regulations impacted the prevalence of wells contaminated with animal waste and the frequency of BWIs. While all of the counties in the KTF area promoted increased awareness, landowner/manager and waste applicator education alone did not result in a drop in BWIs or other water quality improvements. The two counties in the study that adopted winter manure spreading restrictions on frozen or snow-covered ground showed statistically significant reductions in the instances of BWIs and other well water quality problems.

Reprinted from *Resources*. Cite as: Erb, K.; Ronk, E.; Koundinya, V.; Luczaj, J. Groundwater Quality Changes in a Karst Aquifer of Northeastern Wisconsin, USA: Reduction of Brown Water Incidence and Bacterial Contamination Resulting from Implementation of Regional Task Force Recommendations. *Resources* **2015**, *4*, 655–672.

1. Introduction

Karst regions are widespread across the world, and approximately 20%–25% of the global population depends on groundwater resources obtained directly from karst aquifers [1]. Karst aquifers are particularly vulnerable to microbial pathogens and other introduced substances resulting from surface land use activities due to a lack of filtration in the aquifer and short subsurface residence times [2]. Microbial pathogens include bacteria, viruses, and protozoan parasites. Conduits, such as sinkholes and swallow holes, provide direct access points that connect water in the surface environment to the karst aquifer below, often bringing with it contaminants that would not normally enter the aquifer by diffuse recharge, such as phosphate, pesticides, and pathogens [2]. Regions of karst bedrock with little or no soil or unconsolidated sediment cover are especially vulnerable.

Impacts to karst aquifers from pathogens and nitrates have been reported in karst aquifers from many parts of the world (e.g., [2–6]), and contamination from multiple sources, including animal waste, are well documented in parts of Wisconsin and the Midwestern United States where a regional Paleozoic karst aquifer is present (e.g., [7–13]), In Wisconsin, contamination from

pathogenic indicator bacteria is often associated with “brown water” incidents (BWIs), resulting in a color or odor change in well water. BWIs have occurred for decades throughout northeast Wisconsin, often in the spring during snowmelt after application of bovine (dairy) manure on agricultural fields. Between 2006 and mid-2014, sixty-four well replacements were subsidized throughout Wisconsin due to confirmed contamination by livestock manure [7]; three-quarters of those wells were located in areas rated as having a significant to extreme vulnerability to groundwater contamination related to karst-type landscape features (e.g., sinkholes, disappearing streams, surface carbonate rock outcrops, and fracture traces) [13].

Thin soils are a particular risk factor for microbial impact and nitrate contamination of karst aquifers (e.g., [13,14]), Risk for groundwater contamination in karst aquifers as a result of manure application is higher when manure is liquid (< ~12% solids); surface applied outside the normal growing season to wet, frozen, or bare frozen soils; applied to a wet snowpack ready to melt, or immediately prior to significant rainfall [14]. Ronk and Erb [15] noted that in Wisconsin, a majority of animal waste surface water contaminations due to runoff occur in the late winter runoff period. In particular, land application of manure on frozen soils in the Midwestern United States has seen increased attention because of concerns of the negative effects on surface water and groundwater quality [13,16].

This article focuses on a four-county region in northeastern Wisconsin, USA (Figure 1a). Luczaj [17] provides a more detailed description of the geology in the study area, but a basic description of the geology is included here as necessary context. Paleozoic age sedimentary rocks, including dolostone and shale, underlie the region and dip gently eastward toward the ancestral Michigan basin [17]. The landscape displays relatively moderate topography, except along the Niagara Escarpment, which locally has cliffs and steep slopes as high as 70 m. The escarpment occurs along and near the western edge of the Silurian dolostone in the region (Figure 1b) where the underlying Maquoketa shale has been preferentially removed by erosion. Bedrock across the entire study area is overlain by Pleistocene glacial till, glaciofluvial sediments and lacustrine sediments that range in thickness from <1 m to >100 m in buried bedrock valleys. The portions of this four-county area that are most heavily impacted by nitrates, pathogens and pathogenic indicators, and BWIs are located east of the Niagara Escarpment, typically in areas where the Silurian bedrock is mantled with thin soils or Pleistocene sedimentary cover [7,9]. West of the Niagara Escarpment, bedrock consists of Ordovician age shale and dolostone (Figure 1b), with generally thicker amounts of unconsolidated sedimentary cover [17]. Karst features are not typically observed west of the Niagara Escarpment in the four-county region identified in the study.

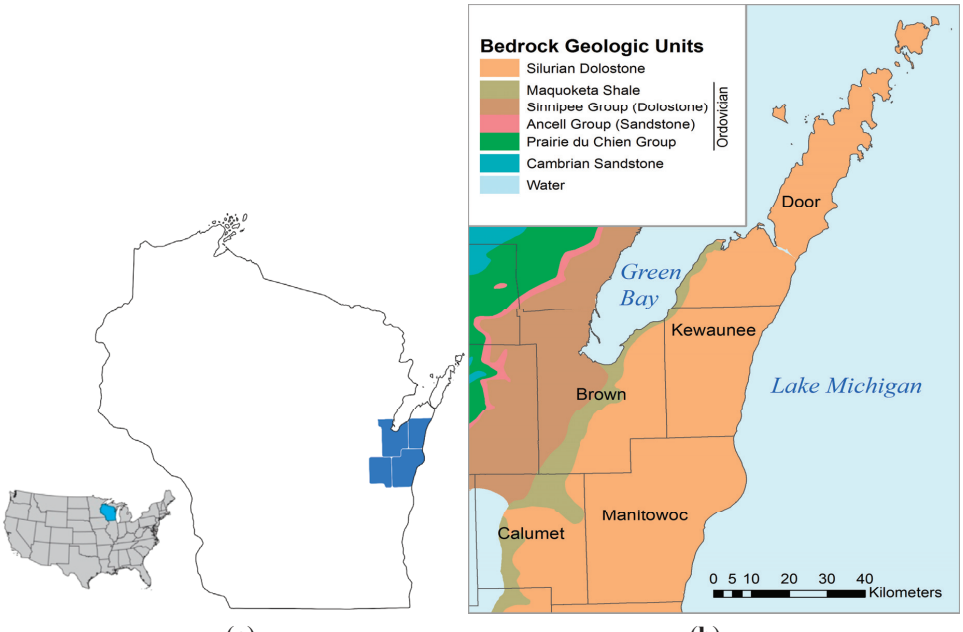

Figure 1. Maps showing the location of the four-county study area in Wisconsin, USA. (**a**) shows an inset map of the lower 48 contiguous United States along with an outline of the State of Wisconsin and counties (local units of government) for the study area highlighted; (**b**) is the bedrock geologic map showing geologic units for this portion of northeastern Wisconsin with names of counties in the region. Bedrock map after [18].

The Silurian bedrock east of the Niagara Escarpment displays significant karst development, albeit heavily modified by Pleistocene age glacial activity (Figure 1). Many karst features are exposed, such as sinkholes, solution-enlarged joints, and caves, which act as preferential recharge points to the aquifer. Most karst features are concealed beneath a variably thick mantle of sediment, but exposed areas of Silurian dolostone bedrock are common within about 15 km of the escarpment edge. Thin to moderate soils (defined for this region as <15.25 m of soil over the bedrock) are also common in this area (Figure 2).

Climatologically, the four-county study area (Figures 1 and 2) lies in a portion of the United States with a humid continental climate and cold winters. Mean annual precipitation (liquid equivalent) varies from about 75 to 84 cm (29.5 to 33 inches) [19], with about two-thirds of the precipitation falling during the growing season. Winter snowfall averages about 105 to 130 cm (41.3 to 51.4 inches) [19]. Average annual temperatures for the four-county study area range from about 6.6 to 7.4 °C (43.8° F to 45.3° F) [20]. The lowest mean monthly temperatures in the region occur during January, −9.4 to −7.2 °C (15 to 19° F), and the highest mean monthly temperatures occur during July, 20.0 to 21.7 °C (68–71° F) [20].

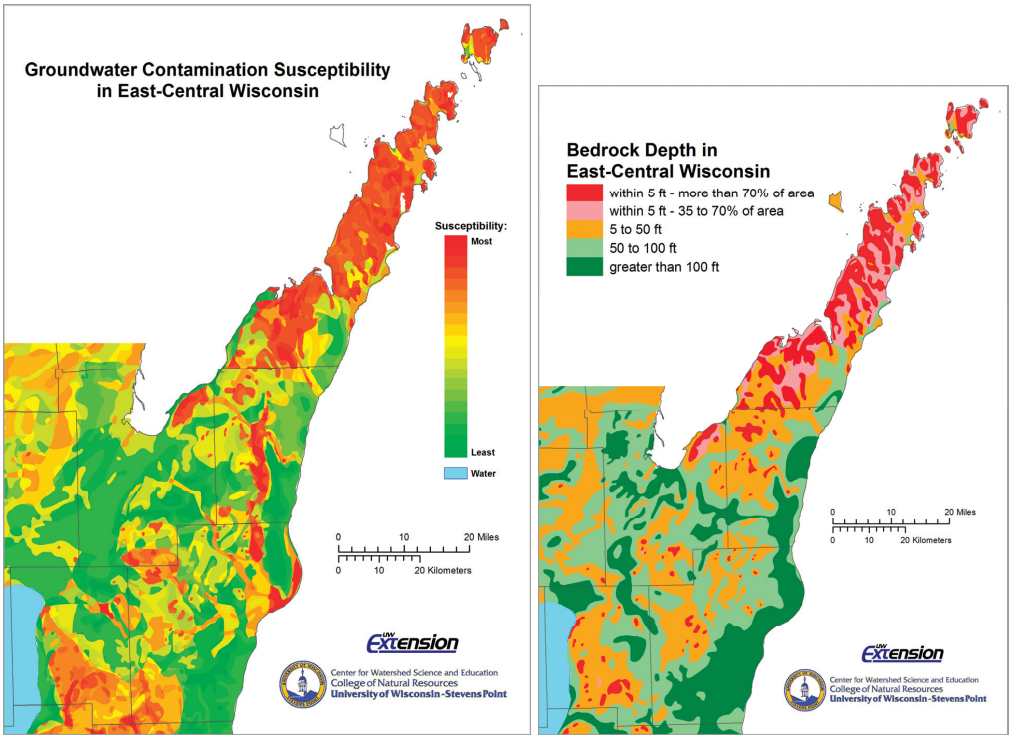

(**a**) (**b**)

Figure 2. Maps showing soil depth (or unconsolidated sediment depth) over bedrock (**a**) and groundwater contamination susceptibility (**b**), based on soil type and depth to bedrock [13]. Original depth to bedrock map was constructed with categories of <5 feet (1.5 m), 5 to 50 feet (1.5 to 15 m), 50 to 100 feet (15 to 30.5 m), and >100 feet (>30.5 m).

The presence or absence of seasonally frozen ground is an important climatological factor that can influence a number of groundwater quality indicators, including BWIs and variability in nitrates, chloride, alkalinity, and conductivity [9,14,16]. In the study area between 2006 and 2014, the average number of days of frozen ground per winter at Green Bay (Brown County) ranged from 78 to 134 days (average 109) while Manitowoc (Manitowoc County) ranged from 72 to 133 days (average 102) between 2003 and 2014. [21], In Kewaunee County, there were 120 days of frozen ground during the winter of 2013–2014 [9]. The average number of days with >2.5 cm (1 inch) of snow cover ranges from about 70 in the south along the Lake Michigan shoreline to about 90 in western Brown County [22].

The four-county study area includes Brown, Calumet, Kewaunee and Manitowoc counties (Figure 1). Land use in the study area is characterized by a mix of urban development, small rural communities and industries, including manufacturing, dairy (bovine) livestock production and agricultural field crops, but the majority of the study area is >75% cultivated land [23]. With the exception of areas near the Fox River and the Bay of Green Bay in Brown County, the region's municipal boundaries are largely based on the U.S. Public Land Survey System, in which Towns

(93.2 km^2 (36 mi^2)) are the most basic unit of local government in rural areas. Several towns, villages, and cities occur within counties.

The residents and manufacturing industries in the region rely on both ground and surface water [24], while the livestock production industry relies entirely on groundwater. In the four-county study area, only the City of Manitowoc in Manitowoc County and major municipalities near Green Bay in Brown County utilize surface water for municipal supplies. Rural regions making up most of the four-county study area depend on either domestic wells or municipal wells to provide potable water resources [7]. The vast majority of agricultural field crops rely on annual precipitation as their sole source of moisture [25–27].

The dairy industry in the four counties has recorded a 30% increase in milking cows between 2002 and 2012 (from 131,500 to 172,500) [25–27] and a corresponding increase of 5.2 million kiloliters to 6.53 million kiloliters of animal waste annually (Figure 3). In the study area, 100% of the animal waste (manure) is land applied. More than half of the waste is stored and applied seasonally (usually in the fall and spring months), however, year to year variations in weather result in some stored manure being land applied to frozen ground. Less than 5% of the volume is treated with anaerobic digestion prior to land application. The increase in bovine numbers, and associated increase in manure volume applied to the land increases the risk of manure contamination occurring.

Statewide, restrictions on the land application of manure (in both karst and non-karst areas) are based on the USDA NRCS 590 Nutrient Management Standard [28]. This technical standard is referenced in several state laws that govern manure and fertilizer application including ATCP 50 and NR 151.

A statewide survey in 1994 of 538 wells [29] showed positive detections for coliform bacteria in 23.3% of the state's wells, with *E. coli* in 2.5% of the wells, and 6.5% of wells exceeding 10 ppm nitrate-nitrogen. In the region, sediment and pathogen contamination of the shallow aquifer has long been a common occurrence. Concerns regarding coliform bacteria, *E. coli*, and nitrate in the region's wells became greater during the late 1990s and early 2000s, as the number of contaminated wells and the severity of the contamination continued to rise [13,30]. WDNR policy denotes any well with any detectable coliform, any type of *E. coli* or any pathogen as contaminated by a pathogenic indicator [30]. Wells over 2.0 ppm nitrate-nitrogen are also considered impacted by human activity, while those over 10 ppm are considered unsafe (above the WNDR heath standard) for sensitive populations (young children, pregnant women) [13,30].

Voluntary well testing programs in two to six townships in Calumet, Brown, Kewaunee, and Manitowoc counties documented between 20% and 30% of wells exceed the nitrate-nitrogen standard of 10 ppm [8,13]. Targeted testing programs of more than 1000 wells between 2002 and 2005 in Calumet County revealed that 35% of the samples were positive for coliform bacteria, and 4.6% were positive for *E. coli*. The testing also showed that 53% of wells had elevated levels of nitrate-nitrogen (2–10 ppm), with 25% above the health standard of 10 ppm for nitrate-nitrogen. Altogether, 47% of the wells tested were considered unsafe for either bacteria or nitrate, with 12% unsafe for both bacteria and nitrate [13].

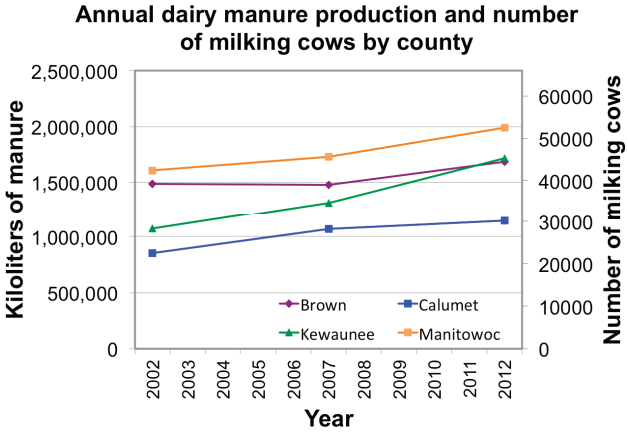

Figure 3. Estimates of annual dairy manure production by county (left axis) and the number of milking cows by county in the four-county study area (right axis). Values show increasing population trends and manure production volumes over time [25–27].

In Door County (adjacent to the study area with the same geologic, soil and climate features), a well sampling program (2000 samples) showed that on any given day, over one-third of the tests indicated the presence of coliform bacteria [2].

Each spring, snowmelt and rainfall are typical precursors to clusters of contaminated wells in the area, as documented by The Karst Task Force [13] and shown in Table 1. Weather events in February and March of 2006 resulted in both snowmelt and precipitation runoff carrying manure into shallow karst bedrock features and improperly abandoned wells, leading to coliform and *E. coli* detections in 78 of the 422 tested wells in the Town of Morrison [13]. Public pressure resulting from this event and previous clusters of contamination led to the formation of the Northeast Wisconsin Karst Task Force (KTF) [13].

Table 1. Example contamination cases [13,30].

Incident Location	Date	Impact
Town of Morrison, Brown County	February–March, 2006	78 wells tested unsafe for coliform bacteria and/or *E. coli*
Town of Franklin, Manitowoc County	2005	10 wells tested unsafe for coliform bacteria; 6 positive for *E. coli*
Town of Luxemburg, Kewaunee County	March, 2004	A single well contamination by manure that tested positive for *E. coli* resulted in severe illnesses and hospitalizations

The objective of this study was to evaluate groundwater quality changes that occurred in a four-county region of northeastern Wisconsin to determine whether or not implementation of recommendations from a regional task force had an impact on groundwater quality in the region. A brief description of the Karst Task Force results and regulatory/policy changes that resulted are presented below.

2. Results of the 2007 Karst Task Force (KTF)

2.1. Purpose and Justification

The KTF was charged with examining the available scientific data and with making recommendations on how to address the groundwater contamination problem. The Task Force consisted of researchers and experts from five University of Wisconsin institutions, resource managers from county Land and Water Conservation Departments, and the state environmental agencies (Wisconsin Department of Ag Trade and Consumer Protection and Department of Natural Resources (WDNR)), a crop consultant, farmer, a professional manure hauler, a USDA Natural Resources Conservation Service (NRCS) District Conservationist, and a well driller. Outside contributors included hydrogeologists from the Minnesota DNR, the University of Minnesota, and a private engineering consultant.

The Task Force focused on agricultural issues, as the primary land use in the karst area is livestock and cash crop agricultural production, and the trends noted in NASS [25] showed the number of livestock increasing and with a concurrent decrease in available cropland for manure application. Task Force members agreed that because of the aquifer type, overlying soils and land use practices, it would be impossible to prevent every instance of contamination, but that landowners can take significant steps to reduce the potential for animal and human waste, and other materials from entering the groundwater [13]. It also became clear that the physical environment cannot be characterized, understood, or protected by merely locating and managing karst features visible at the surface. Rather, the controlling factor is the underlying fractured carbonate bedrock and the pathways through which surface contaminants may enter the bedrock environment.

This task force created a set of recommendations, of which two counties chose to implement restrictions on the application of animal waste (manure) to reduce the risk of groundwater contamination in 2007. This article represents the first regional analysis of the KTF and subsequent regulatory changes to determine if these regulations impacted the prevalence of wells contaminated with animal waste and the frequency of BWIs. This paper is the first analysis of the impacts of the task force report and the effectiveness of actions taken by local resource managers that have been examined with regard to groundwater quality.

2.2. Regulatory and Policy Responses to the 2007 KTF Report

The two counties that implemented regulations varied in their approach. Manitowoc County was the stricter of the two, implementing both year-round and frozen soil restrictions on manure application [31–33] in 2007. Year round restrictions included (1) No application within 30.5 m of a known karst feature, (2) requiring incorporation (injecting or mixing into the soil) of animal manure within 48 h of application on any site (a) within 30.5–151.5 m of a known karst feature, and (b) any area that drained into a known karst feature. Seasonal (frozen soil) restrictions include no applications of liquid manure on slopes >6% when unable to incorporate within 48 h. Solid manure can be applied on slopes between 6% and 12% if at least 40% of the soil surface is covered with crop residue. Manitowoc County does not require pre-approval of application sites, but has

created maps of the above restrictions and made them available to livestock farmers, agronomic consultants and the general public. Exemptions are not granted for incorporation or setbacks. Violators may be fined $500 (US) plus fees. The county ordinance was voted on by each town in the county, and passed on a popular vote.

Regulations implemented in Brown County in 2007 [34] required the land manger to gain pre-approval for seasonal land application by submitting a winter manure spreading plan (WSP). The focus of the WSP is to prioritize fields from lowest to highest risk, with maps showing karst features provided to farmers and agronomic consultants. There are no mandatory additional incorporation requirements or setbacks from karst features. Manure application rates are pre-approved by the SWCD. Non-mandatory recommendations include limiting manure application to 46,670 L/hectare and 44,834 kg/hectare and encouraging larger setbacks from wells and karst features. The Brown County ordinance addresses only manure and not other waste applications.

Three other counties (Calumet, Door, Kewaunee) used the 2007 KTF report to begin building the case for additional setbacks and regulations, but did not make changes to their county regulations impacting manure and waste application. State regulations continued to be enforced in all five counties.

Calumet County's LWCD created a focused educational approach—identifying the areas of highest risk of contamination and working one on one with landowners and land managers in these areas to identify and map karst features and encourage better management. This was done on a volunteer basis because there were no revisions made to the ordinances, limiting any enforcement and incentive for landowners to change management practices [35–37].

Door County has also documented BWIs. The county did not make any ordinance changes as a result of the 2007 KTF. County Conservationist William Schuster, however, states that the KTF, by providing a solid scientific consensus, has eliminated debate over many issues and reaffirmed that contamination in the karst aquifer is a regional problem, and not just a county problem [38]. Recent (2014) BWIs have brought the issue to the forefront, and changes to manure and waste application regulations are likely to occur. In 2015, Door County is increasing enforcement of existing county ordinances surrounding manure application, however, these ordinances incorporate state rules by reference and do not include the additional winter restrictions that were adopted by Manitowoc and Brown counties [39].

Kewaunee County has continued to experience a high number of BWIs. While no regulatory changes were made in the years following the 2007 KTF, the KTF set the stage for a regional approach. Since the release of the KTF report, Kewaunee's past and current resource managers have focused their efforts on identifying features and implementing a detailed well water testing program to delineate the areas of concern. The county board approved detailed aquifer protection ordinance in 2014 and it passed with an 83% yes vote when placed on every municipal ballot in the county in April 2015. The ordinance prohibits animal waste application on both frozen/snow covered fields and applications between Jan 1 and April 15 on cropland fields with less than 6.1 m of soil over bedrock and those that drain to these areas [40].

All five counties implemented some aspects of the education recommendations made by the KTF by working with key people, such as for-hire manure applicators and consultants, who cross

county lines. The county SWCDs and The University of Wisconsin - Extension partnered to increase outreach and education to three key audiences: (1) Commercial Manure Applicators: Responsible for >60% of the manure applied in the target area, educational modules were added to their Level 1 and Level 2 certification program to provide basic and advanced training to manure applicators, (2) Nutrient Management Plan Writers: Task force members communicated recommendations directly to plan writers at their statewide conferences and at local meetings and (3) Farmers: Information and KTF recommendations were included in the farmer training sessions for those farms writing their own Nutrient Management Plans.

3. Methods

3.1. Data Sources and Statistical Analysis

Three sources of water quality data for domestic water wells were compiled during this study. These included state regulatory agency (Wisconsin Department of Natural Resources—WDNR) records, County health department (CH) records, and various county Land and Water/Soil and Water Conservation District (SWCD) records. Data were compiled from each source for as many years as records existed prior to 2007 (starting in 2002), and for the 2008–2014 timeframe. Data acquired from the sources included the date, well location, whether the color change in the water (BWI) was observed by a trained individual (WNDR, CH or SWCD staff), and the presence of a strong animal waste odor that would deter bathing or laundry (ODOR). As well testing is often suggested when a neighboring well is contaminated, data requested included either BWI or ODOR in that well or a nearby well along with a positive pathogenic indicator test, and lastly, a lack of either BWI or ODOR, but a nearby well had documented pathogenic indicators, ODOR or BWI. Data were received as Excel spreadsheets, and the data were then imported into SPSS (version 23.0) for statistical analysis. A Chi-Square test was computed to test for any statistically significant association between the treatments (year samples were taken (pre-2007 and post-2007) and frozen ground (presence or absence of frozen ground)) and the variables mentioned above.

WDNR records included staff investigations of homeowner-reported well contamination. Depending on the situation and the time between the initial report and staff visit, these may include records of visual documentation of BWIs, nasal detection of odors, laboratory detections of bacteria or nitrate, or if a specialized bacterial testing was conducted. A well was determined to be impacted by animal waste if trained staff sampled the well, followed WDNR or written CH QA/QC protocols, and one of the following tests produced conclusive results: (1) presence of *Rhodococcus corpophilus*, (2) presence of *E. coli* at levels higher than what would be attributable to human waste, and/or (3) presence of bovine *Bacteroides*, as determined by a Microbial Source Tracking (MST) analysis (post 2006) [41]. Data were summarized by WDNR staff at the authors' request. Reliable records were available from WDNR for the time period 2002–2014 for all counties except Door County; hence, it was excluded from this study.

The SWCD records from each county included staff investigations of homeowner-reported well contamination. The SWCD staff collaborated with WDNR and/or CH staff to conduct well water quality sampling. SWCD records closely paralleled the records of WDNR. WDNR records were

provided to SWCD staff, who then compared them to their records and information they had on file from CH to complete missing data (such as visual verification of BWIs) or provide well testing results. Thoroughness of data tracking of reported well contamination varied between counties, with some having very complete records and others having no formalized tracking system [42–48].

The CH records included visual observations, along with *E. coli*, and *Rhodococcus coprophilus* test results. Counties with complete records were included in the dataset, either by the SWCD or by providing a copy of the WDNR data to the CH. Data from CH where no third party verification of BWI or odor existed for an incident, (such as where the well owner collected their own sample, or where it is unknown whether WDNR or CH QA/QC protocols were followed), were excluded from the dataset.

A total of 124 data points were included in the dataset. Sixty-two data points were from the 2002–2006 timeframe and 63 were from the 2008–2014 timeframe. Data from 2007 were excluded because Brown and Manitowoc Counties implemented their regulations during 2007. Twenty-nine of the data points were from Brown County, 12 were from Calumet, 22 were from Kewaunee, and 61 were from Manitowoc County. Multiple instances of contamination were documented in some wells during the studied time period. Multiple events of contamination that occurred within a 14-day period were counted as one contamination. If contamination occurred and the water clarity returned to normal or all pathogenic indicator tests were negative within 14 days and then re-occurred after the initial 14 day period, it was treated as a second instance.

Frozen ground has been identified as a critical factor in BWIs and well water contamination [49,50]. When the ground is frozen, snowmelt and/or precipitation infiltrate more slowly, as some of the pores between soil particles that normally allow for infiltration are filled with frozen water. This decrease in infiltration results in an increase in the volume of water leaving via surface flow. In some years, “concrete frost” or “dense frost” has developed, where a very high percentage of soil pores are filled with ice. This results in a much lower infiltration rate, higher runoff volumes, and has been tied to spikes in well water contamination [49].

For this study, the presence or absence of frozen ground was determined by using the National Oceanic and Atmospheric Administration’s (NOAA) Cooperative Observer Database (COD) hosted by UW Madison [21]. A central location was chosen in each county, and for each well contamination event where a month and date of contamination was available, the COD data for that date was accessed. For the purposes of the data analysis, a central location for each county was selected to determine the presence or absence of frozen ground. A central location was selected to avoid the climate mitigating affects of Lake Michigan on the data analysis.

3.2. Data Limitations

The data presented in this article represent the most complete data available in the study area. However, the authors recognize several limitations to the dataset. Because the sampling of wells is triggered by an event and well user observations, not all instances of contamination will be documented. Pathogens or other microbial contamination can be present in water with no visual or other indication of problems that would trigger sampling. Illnesses caused by pathogens in well water may be misinterpreted as seasonal gastrointestinal illnesses or food poisoning by the well

owner, and not necessarily connected to a well contamination problem. Asymptomatic illness and locally acquired immunity are further limitations in the context of illness as an indicator of water quality. All of our data providers [30,37,40,44,48,51–53] noted that some well owners are hesitant to report problems to avoid disrupting neighbor relations, or because of the additional expense of replacing a well or adding a treatment system. By requiring a third party verification of odor or BWI issues, and only including well samples where trained individuals following QA/QC protocols and the same analysis methods were used, our data represent the most reliable instances of positive well contamination indicators. Cow numbers and, as seen in Figure 3, did not hold steady, but increased during the entire study period [25–27].

The majority of human waste in rural areas of Wisconsin is discharged to septic systems with drain fields designed to allow for infiltration of liquids on a continual basis. While some instances of human pathogens in groundwater have been documented in the region (see [7] for details), analysis of human waste is beyond the scope of this paper, and septic system design and installation practices are not likely to have changed significantly during the study period.

The well water quality data gathered in the region are limited by the fact that there is not a scheduled or randomized testing program in place to document BWIs, ODORS or pathogenic indicators in rural wells. While it is clear that such contamination events occur, the true frequency and severity of these events remain unknown.

In addition, an ongoing WDNR well replacement subsidy program [7] and decisions by individual homeowners not participating in the subsidy program have resulted in numerous wells to be replaced in the karst region of the state. While this is a potential confounding factor, it is unlikely to be significant for the observed water quality changes because many of these wells were replaced in the two counties that did not adopt regulatory changes restricting winter spreading. If well replacement was the first-order cause of water quality improvement, we expect that this response should be seen in all four counties analyzed.

The 2007 KTF report focused on reducing BWIs in 5 counties. A combination of factors led us to exclude Door County from the analysis. Most importantly, complete datasets for 2002–2014 were not available from WDNR and SWCD for Door County. The WDNR was also unable to provide a complete dataset for this county as a result of staffing issues [54]. The SWCD stated [38] that they have not historically tracked BWIs and contamination, as it is considered to be a common occurrence. They noted that they are actively working with the Door County Health Department and landowners to address the problem.

4. Results

Our results revealed that no statistically significant changes occurred in counties that only had education and training for manure application in a karst setting. However, in all scenarios tested, at least one statistically significant association occurred with counties that implemented regulatory changes as a result of the 2007 KTF report (Brown County, Manitowoc County, or both). Implementing seasonal restrictions on waste application has had a positive impact on ground water quality in the four counties in our study by reducing bacterial contamination from 35 documented cases (pre-2007) to 15 (post-2007) in the four county area, a fifty-seven percent decrease. Twenty-eight

cases were documented in the two counties (pre-2007) that implemented regulations before implementation and eight after regulations were implemented (post 2007). The same number of cases was documented in the two non-regulated counties (7 total) in the pre and post 2007 timeframes. For BWIs, there was a 38% increase (from 5 to 8) in the counties with regulations, but a 70% increase (from 10 to 17) in the counties without. Since almost half of the data points originated in Manitowoc County due to a more aggressive testing program implemented by the County Health Department, the increased numbers are not unexpected.

4.1. Restrictions on Frozen Ground Spreading

The statistical analysis showed that the implementation of restrictions on winter (frozen ground) spreading of animal waste has likely had an impact on the documented instances of well contamination. In almost every variable examined, at least one of the regulated counties (Brown or Manitowoc) showed a statistically significant difference when the pre-regulation period (2002–2006) was compared to the post regulation period (2008–2014).

For BWIs, the Chi-Square analysis determined significance at the 0.01 level. The analysis showed Manitowoc County was statistically significant ($p = 0.003$), but not significant for the other three counties (Brown ($p = 0.204$), Calumet ($p = 0.377$) and Kewaunee ($p = 1.00$)). For a confirmed ODOR, significance was at the 0.01 level. The data were significant for Manitowoc County ($p = 0.003$), with non-significance for the other three counties (Brown ($p = 0.204$), Calumet ($p = 0.190$) and Kewaunee ($p = 0.35$)).

Where BWI and/or ODOR was present, and a pathogenic indicator test produced conclusive results with the presence of *Rhodococcus coprophilus*, presence of *E. coli* at levels higher than what would be attributable to human waste, and/or presence of bovine *Bacteroides*, as determined by a Microbial Source Tracking (MST) analysis, significance was at the 0.05 level. The data were statistically significant for Brown County ($p = 0.017$), with non-significance for the other three counties (Manitowoc County ($p = 0.06$), Calumet County ($p = 0.855$) and Kewaunee County ($p = 0.448$)).

In cases where the well owner did not have a BWI or ODOR, but the well was sampled because a neighboring well did, significance was at the 0.01 level. Both Brown ($p = 0.000$) and Manitowoc counties ($p = 0.020$) were significant, but the other two counties were not significant (Calumet ($p = 0.345$) and Kewaunee ($p =$ number not recorded as there was only one level of this variable for this county and is hence a constant)). In cases where the well had a positive pathogenic indicator test with or without BWI or ODOR, significance occurs at the 0.01 level. Significant for Brown County ($p = 0.000$), but not significant for the other three counties (Calumet ($p = 0.554$), Kewaunee ($p = 0.448$) and Manitowoc ($p = 0.945$)).

4.2. Presence or Absence of Frozen Soil

The statistical analysis shows that the presence or absence of incidents involving spreading of animal waste on frozen ground likely had an impact on the documented instances of well

contamination. In almost every variable examined, at least one of the regulated counties (Brown, Manitowoc) showed a statistically significant difference compared to the non-regulated counties.

For BWIs, significance occurs at the 0.01 level. Results were significant for Manitowoc County ($p = 0.001$), but not significant for the other three counties (Brown ($p = 0.842$), Calumet ($p = 0.490$) and Kewaunee ($p = 0.211$)). For confirmed strong manure odor (ODOR), Significance occurred at the 0.01 level. The results were significant for Manitowoc County ($p = 0.001$), but not significant for the other three counties (Brown ($p = 0.842$), Calumet ($p = 0.301$) and Kewaunee ($p = 0.061$)).

In cases with a positive pathogenic indicator test and either BWI or ODOR in the well or a neighboring well, the Chi-Square test showed a statistically significant difference ($p = <0.05$). Values for each county were: Brown ($p = 0.045$), Calumet ($p = 0.490$), Kewaunee ($p = 0.377$) and Manitowoc ($p = 0.13$). In cases with a positive pathogenic indicator test and BWI or ODOR, Significance occurs at the 0.05 level. The results were significant for Manitowoc County ($p = 0.015$), but not significant for the other three counties (Brown ($p = 0.152$), Calumet ($p = 0.325$) and Kewaunee ($p = 0.371$)).

In cases where the well did not have BWI or ODOR but was sampled because of neighbor's well did, significance occurs at the 0.01 level. The results were significant for Brown County ($p = 0.000$), but not significant for the other three counties ((Calumet ($p = 0.490$), Kewaunee and Manitowoc counties (p = number not recorded as there was only one level of this variable for these counties and is hence a constant)). In cases where the well tested positive for a pathogenic indicators, regardless of other factors, significance occurred at the 0.01 level. The results were significant for Brown County ($p = 0.000$) and Manitowoc County ($p = 0.005$), but not significant for the other two counties (Calumet ($p = 0.175$), Kewaunee ($p = 0.371$)).

5. Discussion

The objective of this study was to evaluate groundwater quality changes that occurred in a four-county region of northeastern Wisconsin to determine whether or not implementation of recommendations from a regional task force had an impact on groundwater quality in the region. By comparing the pre-regulation and post-regulation statistics, the counties that implemented WSPs had a statistically significant impact in one or both regulated counties on reducing the number of BWIs, ODORS, and pathogenic indicator bacteria in groundwater. This study also verifies that the presence of frozen ground and implementing the WPSs reduced BWIs, ODORS and pathogenic indicator bacteria in groundwater.

The data showed an overall decrease in the number of pathogenic indicator bacteria in the counties that implemented regulations, with 28 recorded incidents in the pre-2007 period and 8 in the post 2007 period. Pathogenic indicator bacteria remained constant (7) in the other two counties that did not implement regulations. BWIs showed a lower rate of increase (38%) in regulated counties (5 pre/8 post) *versus* 70% in non-regulated counties (10 pre/17 post). The increase in manure volume (Figure 3) applied in the target area may or may not be a factor, and was beyond the scope of this study.

The average snowfall totals, number of days with snow cover, and number of days with frozen ground were higher during the second half of the study due to decadal-scale climate anomalies. [20,55];

Manitowoc recorded an average of 93 days frozen ground in the first part of the study and 107 in the second. Only one year of frozen ground data prior to 2007 was available for Green Bay. [21]. However, it is unlikely that these variables had a strong influence on the observed trends for two principal reasons. First, increased snowfall would be expected to produce increased spring runoff and greater groundwater quality impacts during the 2008–2014 period, which was not observed. Second, and more importantly, these inter-annual climatological variations would not be expected to impact only Brown and Manitowoc counties, rather, if significant they should have impacted all four analyzed counties. What is more likely important for limiting spring infiltration is the percentage of ice-filled soil pores, which is a complex function of freeze-thaw cycles and winter rain precipitation events [49]. Therefore, we feel that these potential confounding factors were not likely of first-order importance in the observed changes in water quality.

6. Future Trends

Within the past year, Kewaunee County passed a winter spreading ordinance that is more restrictive than either the Brown or Manitowoc ordinances [40]. Starting in 2015, this regulation prohibits the land application of animal waste during the frozen ground months and extends into the thawed period (15 April). Future study will be needed to determine the impact of this regulation on well water.

On a statewide level, the proposed revisions to the USDA NRCS 590 Nutrient Management Standard [56–58] includes the designation of "Silurian Dolomite" soils as "areas where Silurian dolomite bedrock is present within 1.52 m (60 inches) of the surface." It is clear that the 2007 KTF report is reflected in the current draft of the WI NRCS 590 practice standard including: the immediate (subsurface) incorporation of manure within 24 h in areas known to deliver surface water runoff to direct conduits to groundwater and no winter application of liquid manure in February and March when soils are frozen or snow covered [57].

7. Conclusions

The combination of the geology of northeastern Wisconsin and the seasonal spreading of animal waste (manure) on frozen soil are contributing factors to the detection of pathogen indicator bacteria in the aquifer and Brown Water Incidents (BWIs). The implementation of seasonal winter manure spreading restrictions on these sensitive areas did not eliminate the contamination, but did significantly reduce the risk of both pathogen contamination and BWIs, resulting in improved aquifer water quality.

Acknowledgments

We are very grateful to the many individuals cited in this article that provided water quality data and other information, without which this study could not have been completed. Steve Buan (NOAA) and Rick Wayne (UW Madison) helped with finding some of the climatological data used in the study. Dave Mechenich (UW Stevens Point Center for Watershed Science and Education) and Sarah Congdon (UW Extension Environmental Resources Center) provided drafting and

graphics assistance. Jenna Klink helped review some of the statistical analysis results. We are also grateful to three anonymous reviewers, whose comments and suggestions greatly enhanced this paper.

Author Contributions

Kevin Erb was responsible for the data collection, and worked with WDNR, CH and SWCD staff in four counties to gather the data and coordinating the writing of the paper. Eric Ronk's contribution includes early data gathering and summarization of contamination issues in the region (prior to his current position) researching and meeting with Calumet County LWCD staff to draft and update part of the results, as well as the data on the trends in the dairy industry in the region. Vikram Koundinya performed the statistical analyses. John Luczaj provided information on geological and climatological data, and assisted in the development of the project, as well as edited the figures and tables.

Conflicts of Interest

The authors declare no conflict of interest.

References

1. Ford, D.; Williams, P. *Karst Hydrogeology and Geomorphology*, 2nd ed.; John Wiley & Sons Ltd.: West Sussex, UK, 2007; pp. 1–562.
2. Coxon, C. Chapter 5, Agriculture and Karst. In *Karst Management*, 1st ed.; van Beynen, P.E., Ed.; Springer: New York, NY, USA, 2011; pp. 103–138
3. Guo, F.; Yuan, D.; Qin, Z. Groundwater Contamination in Karst Areas of Southwestern China and Recommended Countermeasures. *Acta Carsologica* **2015**, *32*, 389–399.
4. Worthington, S.R.H.; Smart, C.C.; Ruland, W.W. Assessment of Groundwater Velocities to the Municipal Wells at Walkerton. In *Ground and Water: Theory to Practice*; Proceedings of the 55th Canadian Geotechnical and 3rd Joint IAH-CNC and CGS Groundwater Specialty Conferences, Stolle, D., Piggott, A.R., Crowder, J.J., Eds.; Niagara Falls, ON, USA, 20–23 October 2002; pp. 1081–1086.
5. Celico, F.; Musilli, I.; Naclerio, G. The impacts of pasture- and manure-spreading on microbial groundwater quality in carbonate aquifers. *Environ. Geol.* **2004**, *46*, 233–236. doi:10.1007/s00254-004-0987-2.
6. Hrudey, S.E.; Payment, P.; Huck, P.M.; Gillham, R.W.; Hruday, E.J. A fatal waterborne disease epidemic in Walkerton, Ontario: Comparison with other waterborne outbreaks in the developed world. *Water Sci. Technol.* **2003**, *47*, 7–14.
7. Luczaj, J.A.; Masarik, K. Groundwater Quantity and Quality Issues in a Water-Rich Region: Examples from Wisconsin, USA. *Resources* **2015**, *4*, 323–357.
8. Center for Watershed Science and Education (CWSE) WI Well Water Viewer. University of Wisconsin-Stevens Point. Available online: http://www.uwsp.edu/cnr-ap/watershed/Pages/WellWaterViewer.aspx (accessed on 29 June 2015).

9. Bonness, D.; Masarik, K. *Investigating Intra-annual Variability of Well Water Quality in Lincoln Township*; Final Report; June 2014; pp. 1–42. Available online: http://www.uwsp.edu/cnr-ap/watershed/Documents/Lincoln_FinalReport.pdf (accessed on 2 July 2015).
10. Bauer, A.C.; Wingert, S.; Fermanich, K.J.; Zorn, M.E. Well water in karst regions of northeastern Wisconsin contains estrogenic factors, nitrate, and bacteria. *Water Environ. Res*. **2013**, *85*, 318–326.
11. Borchardt, M.A.; Bradbury, K.R.; Alexander, E.C., Jr.; Kolberg, R.J.; Alexander, S.C.; Archer, J.R.; Braatz, L.A.; Forest, B.M.; Green, J.A.; Spencer, S.K. Norovirus outbreak caused by a new septic system in a dolomite aquifer. *Ground Water* **2011**, *49*, 85–97.
12. Borchardt, M.A.; Bertz, P.D.; Spencer, S.K.; Battigelli, D.A. Incidence of enteric viruses in groundwater from household wells in Wisconsin. *Appl. Environ. Microbiol.* **2003**, *69*, 1172–1180.
13. Erb, K.R.; Stieglitz, R. *Final Report of the Northeast Wisconsin Karst Task Force*; University of Wisconsin—Extension: Madison, WI, USA, 2007; pp. 1–46.
14. Czymmek, K.; Geohring, L.; Lendrum, J.; Wright, P.; Albrecht, G.; Brower, B.; Ketterings, Q. *Manure Management Guidelines for Limestone Bedrock/Karst Areas of Genesee County*, *New York: Practices for Risk Reduction*; Animal Science Publication Series No. 240; Cornell University: Ithaca, NY, USA, 2011; pp. 1–9. Available online: http://nmsp.cals.cornell.edu/publications/files/Karst_2_15_2011.pdf (accessed on 8 August 2015).
15. Ronk, E.; Erb, K. A Preliminary Analysis of 300 Manure Incidents in Wisconsin. In Proceedings of the 2010 Wisconsin Crop Management Conference, Madison, WI, USA, 12–14 January 2010.
16. Gupta, S.; Munyankusi, E.; Moncrief, J.; Zvomuya, F.; Hanewall, M. Tillage and Manure Application Effects on Mineral Nitrogen Leaching from Seasonally Frozen Soils. *J. Environ. Qual*. **2004**, *33*, 1238–1246.
17. Luczaj, J.A. Geology of the Niagara escarpment in Wisconsin. *Geosci. Wis.* **2013**, *22*, 1–34. Available online: http://wgnhs.uwex.edu/pubs/gs22a01/ (accessed on 2 July 2015).
18. Mudrey, M.G., Jr.; Brown, B.A.; Greenberg, J.K. *Bedrock Geologic Map of Wisconsin*; University of Wisconsin-Extension, Geological and Natural History Survey: Madison, WI, USA, 1982; scale= 1:1,000,000.
19. NOAA—National Weather Service, Index of Climate Images for Wisconsin. Available online: http://www.crh.noaa.gov/images/mkx/climate/ (accessed on 2 July 2015).
20. Wisconsin State Climatology Office (WSCO). Statewide Wisconsin Climate Data. Available online: http://www.aos.wisc.edu/~sco/clim-history/state/ (accessed on 2 July 2015).
21. University of Wisconsin-Extension, Wisconsin Cooperative Observer Database, Wisconsin State Climatology Office (WSCO). Available online: http://agwx.soils.wisc.edu/uwex_agwx/weather/hyd (accessed on 7 July 2015).
22. Wisconsin State Climatology Office (WSCO). Wisconsin Winter Climate. Available online: http://www.aos.wisc.edu/~sco/seasons/winter.html#Snow (accessed on 2 July 2015).

23. Department of Agriculture, Trade and Consumer Protection (DATCP). Agricultural Chemicals in Wisconsin Groundwater (April 2008). Available online: http://datcp.wi.gov/uploads/Environment/pdf/ARMPub180.pdf (accessed on 20 August 2015).
24. Krohelski, J.T. *Hydrogeology and Ground-Water Use and Quality*, *Brown County*, *Wisconsin*; Wisconsin Geological and Natural History Survey: Madison, WI, USA, 1986; Volume 57, pp. 1–42.
25. United States Department of Agriculture, National Ag Statistics Service (UDSA, NASS). 2002 Census of Agriculture. Available online: http://www.agcensus.usda.gov/Publications/2002/ (accessed on 8 July 2015).
26. USDA, NASS. 2007 Census of Agriculture. Available online: http://www.agcensus.usda.gov/Publications/2007/ (accessed on 8 July 2015).
27. USDA, NASS. 2012 Census of Agriculture. Available online: http://www.agcensus.usda.gov/Publications/2012/ (accessed on 8 July 2015).
28. United States Department of Agriculture, Natural Resources Conservation Service. March 2005 Wisconsin NRCS 590 Standard. 4 July 2015. Available online: http://efotg.sc.egov.usda.gov/references/public/WI/590.pdf (accessed on 8 July 2015).
29. Warzecha C.; Gerhardt, R.; Kluender, S. *Wisconsin Private Well Water Quality Survey*; NGWIC Call Number GB1025.W6.W45; Wisconsin Department of Natural Resources: Madison, WI, USA, 2015.
30. Heinen, L. Drinking Water and Ground Water Specialist, Wisconsin Department of Natural Resources. Personal Communication, 7 April 2015.
31. Smith, T. Resource Conservationist, Manitowoc Soil and Water Conservation Department, Manitowoc, WI, USA. Personal Communication, 7 April 2015.
32. Riesterer, B. Resource Conservationist, Manitowoc Soil and Water Conservation Department, Manitowoc, WI, USA. Personal Communication, 7 April 2015.
33. Manitowoc County, Wisconsin. Ordinances, Chapter 19, Animal Waste Management. Available online: http://www.manitowoccounty.com/Upload/8/Chapter%2019%20-%202011-0118H.pdf (accessed on 5 May 2015).
34. Brown County, Wisconsin. Ordinances, Chapter 26, Animal Waste Management. Available online: http://www.co.brown.wi.us/i_brown/d/county_clerk/2013_web/chap026-updated_6-24-13.pdf?t=1373902597 (accessed on 5 May 2015).
35. Kleiber, A. Land Resource Specialist, Calumet County Land and Water Conservation Department, Chilton, WI, USA. Well water incidents. Personal Communication, 4 April 2015.
36. Reali, A. County Conservationist, Calumet County Land and Water Conservation Department, Chilton, WI, USA. Well water incidents. Personal Communication, 8 April 2015.
37. Santry, D. Water Resource Specialist, Calumet County Land and Water Conservation Department, Chilton, WI, USA. Well water incidents. Personal Communication, 8 April 2015.
38. Schuster, W. County Conservationist, Door County Soil and Water Conservation Department, Sturgeon Bay, WI, USA. Well water incidents. Personal Communication, 7 April 2015
39. Schuster, W. County Conservationist, Door County Soil and Water Conservation Department, Sturgeon Bay, WI, USA. Brown water incidents. Personal Communication, 27 June 2015

40. Bonness, D. County Conservationist, Kewaunee County, Wisconsin Land and Water Conservation Department, Luxemburg, WI, USA. Personal Communication, 7 April 2015.
41. Layton, A.; McKay, L.; Williams, D.; Garrett, V.; Gentry, R.; Sayler, G. Development of *Bacteroides* 16S rRNA Gene TaqMan-Based Real-Time PCR Assays for Estimation of Total, Human, and Bovine Fecal Pollution in Water. *Appl. Environ. Microbiol*. **2006**, *72*, 4214–4224, doi:10.1128/AEM.01036-05.
42. Wergin, A. RN BSN, Health Officer, Manitowoc County Health Department, Manitowoc, WI, USA. Karst Data. Personal Communication, 17 June 2015.
43. Kinnard, C. Registered Nurse, Public Health Director, Kewaunee County Health Department, Kewaunee, WI, USA. Karst Paper. Personal Communication, 18 May 2015.
44. Halverson, J. County Conservationist, Manitowoc County, Wisconsin Soil and Water Conservation Department, Manitowoc, WI, USA. Research Paper. Personal Communication, 5 May 2015.
45. Bonness, D. County Conservationist, Kewaunee County, Wisconsin Land and Water Conservation Department, Luxemburg, WI, USA. Personal Communication, 4 April 2015.
46. Jolly, J. County Conservationist, Brown County Land and Water Conservation Department, Green Bay, WI, USA Personal Communication, 3 April 2015.
47. Santry, D. Water Resource Specialist, Calumet County Land and Water Conservation Department, Chilton, WI, USA. Karst Data Request. Personal Communication, 14 April 2015.
48. Gollman, R. Environmental Lab Manager, Brown County (WI) Health Department, Green Bay, WI, USA. Personal Communication, 13 May 2015.
49. Komiskey, M.J.; Stuntebeck, T.D.; Frame, D.R.; Madison, F.W. Nutrients and sediment in frozen-ground runoff from no-till fields receiving liquid-dairy and solid-beef manures. *J. Soil Water Conserv.* **2011**, *66*, 303–312, doi:10.2489/jswc.66.5.303.
50. State of Wisconsin. *Final Report of the Manure Management Task Force*; Wisconsin Department of Ag, Trade and Consumer Protection: Madison, WI, USA, 10 March 2006.
51. Wergin, A. RN BSN, Health Officer, Manitowoc County Health Department, Manitowoc, WI, USA. Karst Data. Personal Communication, 17 June 2015.
52. Jolly, J. County Conservationist, Brown County Land and Water Conservation Department, Green Bay, WI, USA. Personal Communication, 3 April 2015.
53. Kinnard, C. Registered Nurse, Public Health Director, Kewaunee County Health Department, Kewaunee, WI, USA. Maps for paper. Personal Communication, 18 May 2015.
54. Merry, J. Water Supply Specialist, Hydrogeologist, WDNR, Green Bay, WI, USA. Current spreadsheet data. Personal Communication, 8 June 2015.
55. Wisconsin State Climatology Office (WSCO). Green Bay Climate—Number of Days of 1 Inch or More Now Cover Per Snow Season: Green Bay Airport (1949/1950–2013/2014 season). Available online: http://www.aos.wisc.edu/~sco/clim-history/stations/grb/GRB-AP-D-snwcv.gif (accessed on 2 July 2015).
56. USDA, NRCS. Draft March 2015 Wisconsin NRCS 590 Standard. Available online: http://socwisconsin.org/wp-content/uploads/2015/03/Draft590Standard_BroadReview.pdf (accessed on 15 April 2015).

57. USDA, NRCS. Draft March 2015 Wisconsin NRCS 590 Tech Note 1. Available online: http://socwisconsin.org/wp-content/uploads/2015/03/590TechNote_BroadReview1.pdf (accessed on 15 April 2015).
58. Murphy, P. State Resource Conservationist, United States Department of Agriculture Natural Resources Conservation Service, Madison, WI, USA. Personal Communication, 13 April 2015.

Drinking Water Quality and Occurrence of *Giardia* in Finnish Small Groundwater Supplies

Tarja Pitkänen, Tiina Juselius, Eija Isomäki, Ilkka T. Miettinen, Matti Valve, Anna-Liisa Kivimäki, Kirsti Lahti and Marja-Liisa Hänninen

Abstract: The microbiological and chemical drinking water quality of 20 vulnerable Finnish small groundwater supplies was studied in relation to environmental risk factors associated with potential sources of contamination. The microbiological parameters analyzed included the following enteric pathogens: *Giardia* and *Cryptosporidium*, *Campylobacter* species, noroviruses, as well as indicator microbes (*Escherichia coli*, intestinal enterococci, coliform bacteria, *Clostridium perfringens*, *Aeromonas* spp. and heterotrophic bacteria). Chemical analyses included the determination of pH, conductivity, TOC, color, turbidity, and phosphorus, nitrate and nitrite nitrogen, iron, and manganese concentrations. *Giardia intestinalis* was detected from four of the water supplies, all of which had wastewater treatment activities in the neighborhood. Mesophilic *Aeromonas salmonicida*, coliform bacteria and *E. coli* were also detected. None of the samples were positive for both coliforms and *Giardia*. Low pH and high iron and manganese concentrations in some samples compromised the water quality. *Giardia intestinalis* was isolated for the first time in Finland in groundwater wells of public water works. In Europe, small water supplies are of great importance since they serve a significant sector of the population. In our study, the presence of fecal indicator bacteria, *Aeromonas* and *Giardia* revealed surface water access to the wells and health risks associated with small water supplies.

Reprinted from *Resources*. Cite as: Pitkänen, T.; Juselius, T.; Isomäki, E.; Miettinen, I.T.; Valve, M.; Kivimäki, A.-L.; Lahti, K.; Hänninen, M.-L. Drinking Water Quality and Occurrence of *Giardia* in Finnish Small Groundwater Supplies. *Resources* **2015**, *4*, 637–654.

1. Introduction

Small drinking water supplies that provide water to small communities are an important public health issue because they are often vulnerable and may cause microbiological or chemical quality-associated health risks to the water consumers [1,2]. Even if the number of users in a supply is low, the total number of these supplies is high, and they often constitute the major water supplies, especially in rural areas. In 2001, there were 1359 water supplies in Finland, of which 61% distributed groundwater [3]. Estimates indicate that approximately 500 of these supplies serve fewer than 500 consumers in their distribution area and are, therefore, defined as small water supplies [4]. Most small water supplies are owned by cooperatives with operators who are often community members who work part-time, usually with no required professional training in the management of a water supply.

Small Finnish water supplies with fewer than 50 users (or with a water distribution of less than 10 m^3 per day) are controlled by local health authorities according to the Decree of the Finnish Ministry of Social Affairs and Health [5] governing small water supplies. Supplies with more than 50 consumers are controlled on the basis of Finnish regulations governing the quality demands and surveillance of household water based on criteria stated in European Union drinking water directive 98/83/EC [6,7]. The microbiological and chemical quality of tap water is monitored in certain periods according to the number of consumers or the quantity of water distributed, but at least once every three years.

Many small European supplies have been found to have occasional contamination by surface water associated with increased coliform counts, indicating that they are at risk for fecal contamination [2,8]. However, usually the microbiological quality of groundwater supplies in Finland meets the quality criteria of the legislation, and most of the supplies distribute drinking water without disinfection treatment. Moreover, the chemical quality generally meets the criteria, but some chemical parameters, such as low pH and high iron and manganese concentrations, degrade the technical quality of the water in small private wells, as well as in some large water abstraction plants [9,10].

Occasional waterborne outbreaks have been reported annually in Finland. The National Institute for Health and Welfare has reported in 1998–2009 a total of 67 waterborne outbreaks, which caused illness for more than 27,000 people [11]. Most of these outbreaks originated from contaminated small groundwater supplies [12]. The most important microbial agents in the outbreaks have been noroviruses and *Campylobacter jejuni* [13]. No outbreaks associated with protozoan parasites *Giardia* or *Cryptosporidium* were reported in Finland prior to 2007 when sewage contaminated tap water in the town of Nokia contained *Giardia* among other pathogens [14]. In a small number of the waterborne outbreaks, the causative agent remained unidentified [11].

The bedrock in Finland in dominated by Precambrian igneous rocks, the crust consisting mainly of plutonic and metamorphic rocks [15]. Although drilled wells utilizing deep groundwater flowing in the bedrock fractures are widely used in household water supply, the majority of municipal water supply relies on groundwater resources in shallow aquifers, *i.e.*, glaciofluvial and glacigenic deposits. Our aim was to study the microbiological quality, including the enteric pathogens (*Giardia* spp., *Cryptosporidium* spp., *Campylobacter* spp. and noroviruses), of small groundwater supplies and the association of microbiological quality with environmental risk factors that could increase the possibility of fecal contamination. In addition, we studied indicator bacteria and some chemical quality parameters of the small groundwater supplies. The supplies were selected on the basis of a recent history of coliform contamination or reported river or lake bank filtration, agricultural fields, household septic tanks or gravel mining pits close to the supply, potentially affecting groundwater quality in the studied shallow aquifers. The distance between the identified risk factors and the production wells ranged from less than 50 m to 200 m.

2. Results

2.1. Water Supplies

The characteristics of the 20 water supplies selected for the study are presented in Table 1. All studied water supplies were considered as small supplies since they served less than 500 inhabitants. The number of inhabitants in the area served by the water supplies varied from 38 to 450 (median 120 inhabitants). The average daily water intake was from 4 to 125 m^3/d (median 30 m^3/d) and the maximum water intake from 12 to 700 m^3/d (median 138 m^3/d). The majority of the studied wells derive groundwater from a shallow aquifer, the average thickness of a vadose zone being, in most cases, less than 5 m (Table 1). Only limited data on aquifer characteristics were available. These small groundwater supplies in Finland are prone to the surface water influence due to the insufficient depth of protective layers above the water table [2].

The water supplies were located around Finland and were regulated by the national Decree of the Finnish Ministry of Social Affairs and Health [5] when having fewer than 50 users or a water distribution of less than 10 m^3 per day or by Finnish regulations based on European Union drinking water directive [6] when having more than 50 consumers or a water distribution of more than 10 m^3 per day. Problems mentioned in the previous monitoring by the local public health protection authorities include the occasional detection of coliform bacteria (14 of the 19 water plants), low pH (11/19), and excess iron or manganese (7/19), or both. In six of the water supplies, the water was alkalized with either lye (NaOH), soda (Na_2CO_3), or limestone ($CaCO_3$), and in three supplies, excess iron or manganese was removed prior to distribution to consumers (Table 1). In three of the supplies, water was continuously disinfected with either UV light or sodium hypochlorite, in two supplies water was occasionally disinfected as reactive action to a contamination episode. In the majority of the water supplies (14/19), no disinfection procedure was performed. We have no information on the details of one supply.

The well maintenance category presented in the Table 1 is based on information gathered from the personnel of the water supplies through the questionnaire. The well maintenance category is based on estimated technical state of well structures, piping, as well as general groundwater protection measures in the surroundings of the production wells. Instead of exact locations of the drinking water supplies, we report, herein, the results using the anonymous water supply number codes 1–20. All the results exceeding the drinking water quality standards have been announced to the corresponding water supply operators and health protection authorities to enable their corrective actions.

Table 1. Characteristics of the studied water supplies.

Water Supply	Aquifer Type	Average Thickness of Vadose Zone (m)	Well Type [1]	Well Depth (m)	Well Maintenance [2]	Water Intake Constructed	Main Risk Factor	Water Treatment [3]
1	Glaciofluvial esker, unconfined, sand and gravel	7	Driven well	8	3	1998	Bank filtration	1
2	Glaciofluvial esker, semi-confined, silty till and sand	<5	Dug well	NA	3	1987	Bank filtration	1
3	Ablation moraine, semi-confined, sandy till	<5	Spring well	2	3	1963	Bank filtration	0
4	Glaciofluvial esker, unconfined, till and gravel	<5	Dug well	6	2	1978	Bank filtration	0
5	Deep bedrock aquifer, confined	NA	Drilled well	NA	1	1979	Agriculture, sewage	0
6	Glaciofluvial esker, confined, clay and sand	NA	Spring well	3	2	1960	Agriculture	0
7	Ablation moraine, semi-confined, sandy till	<5	Driven + dug well	185	3	NA	Agriculture	2
8	Glaciofluvial sand formation, confined, clay and sand	NA	Dug well	4	2	1988	Agriculture	3
9	Moraine, confined, clay and silty till	NA	Dug well	10	1	1983	Agriculture	3
10	Littoral sand, semi-confined, clay and till	NA	Dug + spring wells	3	3	1940	Agriculture	0
11	Glaciofluvial esker, unconfined, sand and silt	3	Driven well	7	2	1988	Agriculture	1
12	Glaciofluvial ice-marginal formation, semi-confined, sand and silt	3	Driven well	10	3	1986	Sewage	3

Table 1. *Cont.*

Water Supply	Aquifer Type	Average Thickness of Vadose Zone (m)	Well Type [1]	Well Depth (m)	Well Maintenance [2]	Water Intake Constructed	Main Risk Factor	Water Treatment [3]
13	Glaciofluvial interlobate formation, semi-confined, sand, gravel and till	NA	Dug well	3	1–2	1962	Sewage	0
14	Littoral sand, semi-confined, till and sand	2	Dug well	4	1	1978	Sewage	NA
15	Moraine, semiconfined, till and sand	3	Spring wells	5–6	3	1962	Sewage	0
16	Littoral sand, semi-confined, till and sand	1	Dug wells	2–4	1	1948	Gravel mining	0
17	Deep bedrock aquifer and moraine, confined, till and gravel	NA	Dug well	NA	3	1993	Gravel mining	1
18	Ablation moraine, semi-confined, sandy till and gravel	6	Spring well	4 *	1	1992	Gravel mining	1
19	Littoral sand, semi-confined, till and sand	<5	Dug wells	NA	1–2	NA	Surface water runoff	0
20	Moraine, confined, till and sand	NA	Spring well	NA	1–2	NA	Flooding	0

Notes: [1] Well type "Spring well" is a shallow dug well installed in close vicinity to a spring, the groundwater level reaching the ground surface; [2] Well maintenance categories based on information on well structures and piping plus the surroundings of the production wells: 1 = poor, 2 = moderate, 3 = good; [3] Treatment after sampling point before water distribution; 0 = no treatment, 1 = alkalization, 2 = reverse osmosis, 3 = disinfection. NA = not available. * Well is located in a pit where gravel layers have been removed during previous gravel mining.

2.2. Microbiological Quality

The results of the microbiological analyses appear in Table 2. *Giardia* cysts were detected in autumn in samples from four small groundwater supplies (Table 2). All were later identified as *Giardia intestinalis*. No *Cryptosporidium* oocycts, *Campylobacter* spp. or noroviruses were detected in any of the samples.

Table 2. Microbiological quality parameters of 20 small water supplies in spring and autumn 2005.

Water Supply	Risk Factor Category	Coliforms		*E. coli*		Intestinal Enterococci		HPC		*Aeromonas*		*Giardia*	
		CFUs/1000 mL		CFUs/1000 mL		CFUs/1000 mL		CFUs/mL		CFUs/1000 mL		cysts/100 L	
		Spring	*Autumn*	*Spring*	*Autumn*	*Spring*	*Autumn*	*Spring*	*Autumn*	*Spring*	*Autumn*	*Spring*	*Autumn*
1	1	-	-	-	-	-	-	<1	<1	-	-	-	1
2	1	-	-	-	-	-	-	2	0	-	-	-	-
3	1	-	-	-	-	-	-	<1	<1	-	-	-	-
4	1	-	830	-	-	-	-	<1	18	-	9	-	-
5	2	-	-	-	-	-	-	3	14	-	12	-	1
6	2	-	10	-	-	-	-	<1	<1	1	-	-	-
7	2	-	-	-	-	-	-	1	<1	-	-	-	-
8	2	-	-	-	-	-	-	83	1	33	5	-	-
9	2	-	10	-	2	-	-	3	5	-	2	-	-
10	2	-	-	-	-	-	-	6	<1	-	-	-	-
11	2	-	-	-	-	-	-	<1	1	-	-	-	-
12	3	-	50	-	40	-	-	<1	8	-	-	-	-
13	3	-	-	-	-	-	-	3	0	15	3	-	1
14	3	-	-	-	-	-	4	296	10	-	-	-	2
15	3	-	70	-	-	-	5	30	25	5	-	-	-
16	4	-	-	-	-	-	-	267	1	-	-	-	-
17	4	-	-	-	-	-	-	14	8	-	-	-	-
18	4	-	-	-	-	-	2	200	214	-	-	-	-
19	5	-	-	-	-	-	-	4	8	-	-	-	-
20	5	-	150	-	-	-	-	<1	45	-	-	-	-

Notes: Recognized environmental risk factors: 1 = bank filtration, river or lake; 2 = agricultural load; 3 = wastewater treatment plant/household septic tanks <100 m; 4 = sand/gravel mining; 5 = multiple threats to contamination. HPC = heterotrophic plate count, - not detected/below the detection limit.

Low CFUs of coliform bacteria (10–150 CFUs/1000 mL) were found in five samples and a relatively high CFU (830 CFUs/1000 mL) in one sample. In the spring sampling, no coliforms were detected in any of the plants and the difference between the coliform counts at spring and autumn can be considered statistically significant (p = 0.027, Wilcoxon signed rank test). Low CFUs of *Escherichia coli* were found in two samples in autumn (2/1000 mL and 40/1000 mL), but in none of the samples in spring. Intestinal enterococci were found in three 1000-mL samples (2–5 CFUs/1000 mL), and no *Clostridium perfringens* was detected in any of the samples.

The CFUs of heterotrophic aerobic bacterial counts varied in the range of <1 to 300 CFUs/mL in spring and <1 to 200 CFUs/mL in autumn. No significant differences (p = 0.795, Wilcoxon signed rank test) in heterotrophic CFUs were detected between the spring and autumn samples.

Aeromonas spp. was detected in spring samples from four supplies and in autumn samples from five supplies; two of the positive wells were the same (Table 2). Further identification at the genospecies level showed that all *Aeromonas* species were mesophilic *A. salmonicida* [16].

2.3. Chemical Parameters

The chemical parameters appear in Table 3. Water temperature was significantly lower at the spring samples compared to the autumn samples ($p < 0.001$, Wilcoxon signed rank test). The pH of the wells studied varied from 5 to 7.6, the TOC varied from 0.5 to 11 mg/L, and no significant differences in the levels between the spring and autumn samples were detected (pH; $p = 0.657$ and TOC; $p = 0.159$, Wilcoxon signed rank test). Color, which is supposed to be about 5 mg Pt/mL, was high (20–40 mg Pt/mL) in two water supplies (14, 15) independent of the season (Table 3). In one of those supplies (14), turbidity was also significantly higher than in other samples. The iron concentrations were relatively high, ranging from 20 to 780 µg/L. The high concentrations were found mostly in the same wells both in spring and autumn. Manganese concentrations were clearly above the recommended limits in two wells (up to 180 µg/L), and the same wells had high concentrations in both seasons (Table 3). The concentration of nitrogen compounds was low in all samples: nitrate nitrogen varied from below 1 to 8.7 mg/L and nitrite nitrogen from below 0.01 to 0.02 mg/L.

2.4. Association of Recognized Risk Factors with Microbiological and Chemical Parameters

At one groundwater supply (15), where the septic tank of a household and a subterranean sand filter were located in close proximity (<100 and <500 m) to the well, TOC and color were high, and intestinal enterococci, coliform bacteria and *Aeromonas* spp. were detected. Intestinal enterococci and coliform bacteria were detected in autumn and *Aeromonas* spp. in spring. Conductivity was high in both seasons, and TOC, total phosphorus, color, and the nitrate nitrogen content were the highest of all the water supplies studied.

In one water supply (14), located in the middle of a small rural village and close to a common road, some of the study parameters showed increased values. A septic tank and a subsurface sand filter were located <100 m from the water supply. Intestinal enterococci and *Giardia* were detected in autumn, while TOC, color and turbidity values were high.

Table 3. Chemical quality parameters of 20 small water supplies in spring and autumn 2005.

Water Supply	T (°C)		pH		EC (µS/cm)		TOC (mg/L)		Color mgPt/mL		Turbidity (FTU)		P (µg/L)		Fe (µg/L)		Mn (µg/L)	
	Spring	*Autumn*	*Spring*	*Autumn*	*Spring*	*Autumn*	*Spring*	*Autumn*	*Spring*	*Autumn*	*Spring*	*Autumn*	*Spring*	*Autumn*	*Spring*	*Autumn*	*Spring*	*Autumn*
1	7.1	10.2	5.6	6.2	92	93	1.7	2.0	5	5	0.50	1.10	7	11	440	780	25	32
2	2.2	8.4	6.1	6.5	48	53	5.7	1.0	5	<5	1.05	1.33	16	18	120	170	11	8.2
3	4.8	6.5	6.2	6.3	41	46	1.2	1.0	<5	<5	0.16	0.15	28	27	<20	<20	<5	<5
4	0.7	17.8	6.9	7.6	44	95	1.8	4.1	15	10	0.15	0.15	8	12	55	110	<5	56
5	7.5	7.3	7.5	6.9	328	337	1.1	1.2	<5	5	0.22	0.08	8	13	26	23	25	28
6	7.9	8.1	7.5	7.6	391	421	0.9	1.0	<5	<5	0.06	0.52	23	24	<20	<20	130	180
7	6.6	8.0	6.5	7.0	259 *	ns	1.2	1.3	<5	<5	0.06	0.04	9	11	<20	53	12	12
8	7.8	6.5	6.6	ns	178 *	ns	3.7	3.3	5	<5	0.69	0.35	11	12	150	83	79	46
9	6.8	5.7	6.5	ns	215 *	ns	1.3	1.2	<5	<5	0.80	0.70	14	9	71	126	<5	7
10	3.5	7.9	5.6	6.0	ns	ns	1.1	0.8	<5	<5	0.04	0.02	15	16	<20	<20	<5	<5
11	5.6	5.7	6.0	5.9	46	153	1.4	1.4	<5	<5	0.94	0.30	13	7	390	240	59	51
12	5.0	7.0	ns	6.5	148 *	150	0.8	0.9	<5	<5	0.52	0.92	5	11	38	220	<5	<5
13	5.2	8.0	7.0	6.9	214	196	1.0	1.0	5	<5	0.39	0.26	10	15	35	31	<5	<5
14	5.4	8.5	ns	5.4	12	202	5.3	5.2	20	20	3.7	3.46	20	21	440	120	<5	<5
15	4.3	8.5	6.1	6.0	231	479	11.0	10.8	40	40	0.73	0.79	182	108	180	150	100	110
16	1.5	9.7	5.5	5.9	ns	30	3.5	2.8	10	5	0.15	0.12	8	9	<20	<20	<5	<5
17	3.3	7.4	7.2	6.3	150	148	1.7	1.2	<5	<5	0.20	0.24	15	15	<20	<20	<5	<5
18	4.7	6.9	6.2	6.3	81	79	0.5	0.6	<5	<5	0.16	0.16	21	12	<20	<20	<5	<5
19	4.0	6.1	6.3	5.1	173	ns	1.8	1.5	<5	<5	0.18	0.16	16	15	31	29	<5	<5
20	3.5	7.1	5.1	5.0	ns	ns	1.8	1.8	<5	<5	0.12	0.15	12	13	<20	21	<5	<5

Notes: EC = Electrical Conductivity; TOC = Total Organic Carbon; ns = not defined; * = measured only in laboratory.

Giardia intestinalis was also detected in a water supply (1) in which no indicator bacteria were detected. Of the chemical parameters, only iron was high. The recognized risk factor in the supply was bank filtration, floodwater also had access to the well, and a wastewater treatment system was situated at a distance of 200–500 m.

The *Giardia*-positive well (5) also tested positive for *A. salmonicida* in autumn. Of the chemical parameters, conductivity was high (337 µs/cm). The identified potentially contaminating risk factor was agricultural load, but a wastewater treatment system was also located 200–500 m, and a wastewater drain 100–200 m, from the well.

Giardia intestinalis was also detected in a well (13), where *Aeromonas* spp. was detected in both spring and autumn samples, though no other indicators or pathogens were detected. The principal recognized threat to water safety was waste water treatment, and indeed the septic tank of a household was situated 50–100 m from the plant. Surface water also had access to the well.

Coliforms (830/1000 mL) were detected in an autumn sample from a well (4) located on a narrow isthmus between two lakes where bank filtration is substantial. The difference in the water temperature of the well between spring and autumn samplings was marked and suggests the close impact of large water bodies of the nearby lakes.

In one water supply (12), coliforms (50/1000 mL) and *E. coli* (40/1000 mL) were detected in autumn, though UV light disinfection was in use after the point of sampling. A septic tank as well as an oil tank, gravel pit, and a cultivated field were situated <50 m from the well.

Some of the water quality parameters associated with the recognized environmental risk factor categories. Heterotrophic CFUs were significantly higher in the supplies at gravel mining category compared to the bank filtration category supplies (p = 0.020, Kruskal-Wallis test). Electrical conductivity and manganese concentrations were more elevated at supplies close to agricultural fields than supplies with other risk factors (p = 0.005 and 0.009, respectively, Kruskal-Wallis test). Elevated water color and turbidity associated with supplies in close proximity of septic tanks (p = 0.022–0.023, Kruskal-Wallis test). The iron concentration was lower at the supplies associated with gravel mining than supplies in other risk factor categories (p = 0.005, Kruskal-Wallis test).

2.5. Associations within Microbiological and Chemical Parameter Results at Spring and Autumn

Coliform bacteria, *E. coli*, intestinal enterococci and *Giardia* findings were occasional and originated solely from the autumn samples (Table 2). Physico-chemical parameters pH, TOC, color, turbidity, and the concentrations of phosphorus, iron, and manganese were more stable and showed significant relation between the spring and autumn samples in the correlation analysis (Spearman correlation coefficient, $r_S > 0.719$, $p = 0.001$).

As regards associations between the microbiological parameters, intestinal enterococci counts associated with heterotrophic CFUs ($r_S = 0.319$, $p = 0.045$) when all samples were considered ($n = 40$) in the Spearman correlation analysis. The associations between the chemical parameters were strong: TOC associated with color ($r_S = 0.693$, $p < 0.001$) and iron concentration ($r_S = 0.418$, $p = 0.007$) and the iron concentration was also associated with color ($r_S = 0.413$, $p = 0.008$) and turbidity of the water ($r_S = 0.727$, $p < 0.001$). Manganese concentration was associated with the electrical conductivity of the water ($r_S = 0.468$, $p = 0.008$).

Overall, the associations between microbiological and chemical parameters were rare. When analyzing the autumn samples (n = 20), there was a weak association between the water color and the detection of *Giardia* (r_S = 0.463, p = 0.040) and when all samples were considered, water temperature associated with the *Giardia* counts (r_S = 0.377, p = 0.016). Furthermore, *Aeromonas* counts were associated with the water pH (r_S = 0.420, p = 0.011) and electrical conductivity (r_S = 0.438, p = 0.014).

3. Discussion

The definition of a small drinking water supply varies in Europe and in the United States. In the USA, a small supply is one that supplies drinking water to fewer than 10,000 people. In the EU the DWD (Drinking Water Directive 98/83/EC) [7] does not require reporting from the supplies which either provide water to fewer than 50 users or which distribute less than 10 m^3/d. The EU research program WEKNOW collected data from European small and very small water supplies and defined a small supply as one which provides water to fewer than 5000, but more than 50 people, and distributes 10–1000 m^3/d [8]. The small water supplies in our study had 38 to 450 users and were thus not totally within any of the EU definitions mentioned above. Of the 20 Finnish small groundwater supplies studied, 4 contained *Giardia intestinalis* in autumn samples. The detected *Giardia* cyst counts were low (1–2 cysts/100 L). Due to the lack of exact recovery rates of the method used, we cannot rule out the possibility of false negative results in the *Giardia* and *Cryptosporidium* analysis. However, the detection of *Giardia* in these samples was proved and can be considered as a reliable result. No other studied enteric pathogens, *Campylobacter* spp. or noroviruses were detected. In addition, intestinal enterococci, coliforms and *E. coli* were detected in 8 of the 20 wells. All these results indicate that these water supplies are at increased risk for fecal contamination, thus extending the results of the studies of Corkal *et al*. [17] from Canada and of Rutter *et al*. [18] as well as those of Richardson *et al.* [1] from England and Wales. In our study, a trend emerged in which indicator organisms were detected more often in autumn samples than in spring samples, suggesting the impact of weather. Spring 2005 was dry, and occasional rain was common in autumn.

Giardiasis, as an endemic disease in Finland, has most likely been underestimated. Hörman *et al.* [19] estimated on the basis of their meta-analysis study that there could be as many as 4664 unregistered symptomatic *Giardia* cases per 100,000 general population compared to 5.38 registered symptomatic cases per 100,000 general population (ratio 1:867). In our previous studies, we identified *Giardia* cysts in Finnish surface water samples [20] as well as in municipal wastewater samples [21] and in tap water contaminated with sewage [14]. Our present study is the first Finnish study to identify *Giardia* cysts in a small drinking water supply. No data were available on potential asymptomatic carriers or symptomatic *Giardia* cases among the water users. If contaminated water caused the human illness, the number of patients was most likely so low that they remained undetected. The impact of small water supplies as source of *Giardia* infections in humans requires further study. *Giardia intestinalis* is a zoonotic pathogen, thus the contamination source of the supplies can be of either human or animal origin.

Only three of the water supplies distributed disinfected tap water, revealing that in most cases there were no preventive barriers between the aquifer and consumers' taps. The *Giardia* positive wells (Supplies 1, 5, 13, and 14) seem to be unprepared for the microbiological risk as there was no advanced water treatment or disinfection in place after the sampling point. The *E. coli* positive wells were better prepared presumably due to the earlier noncompliance with the microbiological water quality standards as the supplies 9 and 12 had disinfection in use. Fecal contamination of drinking water increases the risk for enteric illness among users even if no such documented data are available from our study region. Small supplies have been shown to be frequently prone to fecal contamination in Finland [2,11] and elsewhere. Richardson *et al.* [1] analyzed the microbial quality of 11,233 private drinking water supplies within England and found that *E. coli* was detected in at least one sample from 32.4% of the water supplies. In accordance with the increased risk for fecal contamination of small water supplies, analysis of the distribution of waterborne outbreaks in England and Wales showed that small supplies were associated with 36% of all drinking water outbreaks even though they serve only 0.5% of the entire population [22]. The impact of small supplies on the disease burden of their users remains unknown. The life-long consumption of drinking water from a contaminated source could, on the other hand, also lead to acquired immunity [23,24].

In our study, all *Giardia*-positive wells were located near wastewater treatment activities; either a wastewater treatment plant for municipal human sewage was located at a distance of 200–500 m or the septic tank of a household was located within 50–100 m. One of the *Giardia*-positive wells (14) also had increased levels of multiple indicator parameters (intestinal enterococci, TOC, electrical conductivity, and turbidity), indicating surface water access to the well. However, neither *E. coli* nor *C. perfringens*, suggested as suitable indicators for *Giardia* and *Cryptosporidium* [25,26], were detected in the 100-mL samples. This well was known to be located in the middle of a rural village and close to a road.

One *Giardia*-positive well (1) had no increased levels of indicator bacteria or chemical indicators of surface water contamination even though a wastewater treatment system was located at a distance of 200–500 m and surface water was known to have access to the well. In two of the *Giardia*-positive wells, *A. salmonicida* was also detected, but not coliform bacteria. In another study, protozoa and total coliform levels were clearly correlated [27]. High turbidity (>1.0 FTU), which indicated surface water access to the groundwater source, was observed in three autumn samples, two of which were *Giardia*-positive.

The wells studied were known to be located where contamination sources such as roads, sewage treatment/treatment plants, and habitations were known to be rather close to the aquifer. Contamination by surface water after snow thawing or rainfalls was possible in most of the wells. Most of the water supplies were opened decades ago, when habitation and human activities around the wells were most likely much less than today.

Ten of the wells were located close to a river or lake, a common location for small aquifers in Finland because this kind of location will guarantee a consistent supply of water. The location may allow bank filtration of river or lake water into the well during the dry season, when the groundwater table is low. After a heavy rain, floodwater may also contaminate the well. Studies of

past Finnish waterborne outbreaks have shown that some outbreaks were associated with groundwater wells located close to a river or lake [11]. All of the four plants with *Giardia* findings were located less than 50 m from a lake, river or ditch.

A. salmonicida was found in four samples in spring and in five samples in autumn. *A. salmonicida* is a common bacterium in natural waters as well as in well water, and has been previously isolated in Finnish groundwater wells [28,29] and elsewhere [30]. Its isolation in groundwater well may indicate surface water contamination. *A. salmonicida* was not connected to fecal contamination in a study by Hirotani *et al.* [31]. The pathogenicity of *Aeromonas* spp. as an enteric pathogen is not confirmed, and mesophilic *A. salmonicida* in particular has been regarded as an environmental organism with low pathogenic potential for humans. In addition to indicating surface water contamination, its presence could be associated with increased heterotrophic plate counts [32].

In 14 of the water supplies examined, coliform bacteria had been detected in previous samplings, and *E. coli* had occasionally been detected in five of the wells. These wells placed consumers at increased risk for acquiring waterborne illness, especially because only four of them had undergone disinfection treatment with either UV light or hypochlorite solution before distribution. Two of these wells tested positive for *E. coli*, indicating fecal contamination. *E. coli* was detected in the 1000-mL sample, but not in the 100-mL, suggesting that the use of volumes larger than 100 mL would be more accurate in monitoring fecal contamination. Larger volumes have proved useful in tracking contamination sources associated with waterborne epidemics [33]. Both *E. coli*-positive wells were located in either a pit or flat ground. The other was located near (under 50 m) the septic tank of a household, and both were near a cultivated field and ditch.

Intestinal enterococci were found in three water supplies, and all of these wells were located within 100 m of the septic tank of a household. They were found in samples of either 500 mL or 1000 mL, but not 100 mL. These results again suggest that using larger volumes of water may more often facilitate the detection of indicators of contamination than do the 100-mL samples used in the EU Directive [7].

Our study supports previous findings showing that the pH of Finnish groundwater is typically low (<6.5) [9]. In approximately half of the groundwater wells monitored, pH was lower than recommended (pH 6.7). Low pH may cause the corrosion of iron water pipes. In the project questionnaire, 11 of 19 water supplies reported low pH as their problem. In six of the water supplies, the water was alkalinized prior to distribution to consumers.

Another common problem in Finnish groundwater is its high content of iron and manganese [9]. Iron and manganese in excess decrease the usability of water as drinking water or for household use. In our survey, 20% of the water supplies contained excess iron (up to 780 µg/L, with a recommended maximum of 200 µg/L), and 25% of them contained excess manganese (up to 180 µg/L, with a recommended maximum of 50 µg/L). In the questionnaire, seven water supplies reported the problem. In only three of them, the iron and manganese were removed before distribution to consumers.

4. Experimental Section

4.1. Selection and Characterization of the Water Supplies

Water samples were collected from 20 small groundwater supplies around Finland in April and September–October 2005. The sampled supplies were selected based on a questionnaire answered for 248 small groundwater supplies owned mostly by cooperatives and operated by part-time working persons in the preceding year. Data on the water supply characteristics, microbiological quality and factors considered as potential fecal contamination threats of each water supply were obtained from the questionnaire and analyzed. The sites were selected according to these evaluations and the location of a water supply. The main selection criteria were the presence of an existing potential fecal contamination source in the neighborhood and the occasional detection of coliforms in the water quality compliance monitoring of the local health authorities.

4.2. Sampling and Analysis

Water samples were taken at a water supply from a tap or from a tap and well (if the tap was located after a collection tank), or only from a well with a submersible pump in the absence of a tap at the water plant. One sample was taken from the overflow of a well. The samples were taken prior to any potential treatments. For the microbiological analyses, all the equipment was disinfected before the sampling. The filters were removed from the taps, which were sterilized by flaming. The submersible pump was disinfected by submerging it in 10 mg/L hypochlorite solution for a minimum of 30 min. Each sample was taken with a new hose. Sterile containers were rinsed twice with sample water before sampling. For the *Giardia* and *Cryptosporidium* analyses, 100 L of water were filtered through an Envirochek® HV filter capsule (PALL Life Sciences, Port Washington, NY, USA). Other samples were taken with disinfected plastic containers and with a sterile glass bottle. Temperature, pH, and electrical conductivity were measured at the sampling site, and the evaluation of sensory qualities, such as odor, color, and turbidity, was performed repeatedly in a laboratory.

The water samples were refrigerated and transported to laboratories in Helsinki and Kuopio within 24 h and stored at refrigerated temperature prior to examination.

4.3. Detection of Enteric Pathogens

For the detection of *Giardia* spp. and *Cryptosporidium* spp., Envirochek® -concentrated samples were further treated according to the USEPA Method 1623 [34] as described by Rimhanen-Finne *et al.* [35]. In brief, for further concentration, the sample was first filtrated through a polycarbonate filter, which was then spooled with 10 mL of PBS-Tween20. The cysts and oocysts in the suspension were captured by using the immunomagnetic separation technique (Dynabeads® GC-Combo, Dynal Biotech ASA, Oslo, Norway). The final concentrate of 100 µL was divided into two portions, one of which was stored frozen at −20 °C for further molecular PCR and sequencing analyses. The other portion was immunostained using an Aqua-Glo G/C Direct Comprehensive Kit (Waterborne Inc., New Orleans, LA, USA). (Oo) cysts were counted under an epifluorescense microscope by

using positive controls, *i.e.*, the cysts of *Giardia intestinalis* (H3 isolate, Waterborne Inc. New Orleans, LA, USA) and the oocysts of *Cryptosporidium parvum* (Iowa isolate, Waterborne Inc. New Orleans, USA) as described by Rimhanen-Finne *et al.* [35]. The positive control cysts and oocysts were stored at 4 °C. The numbers of purified cysts and oocysts was enumerated from five stock solution aliquots in hemocytometer resulting in a mean concentration of 1.1×10^6 cysts mL^{-1} and 11.8×10^6 oocysts mL^{-1} [35]. DNA from frozen water concentrate that tested positive for *Giardia* in microscopy was isolated through five rounds of the frozen-thaw procedure following DNA isolation [35]. *Giardia*-specific PCR was performed with glutamate dehydrogenase gene-targeted PCR using the primers GDH1 and GDH4 [36].

Thermophilic campylobacters were identified in 4000-mL samples using the ISO 17995 method [37] with Bolton enrichment (LabM, Lancashire, UK) and modified Charcoal Cefoperazone Deoxycholate Agar (Oxoid, Cambridge, UK) incubated in a microaerobic atmosphere.

Noroviruses were analyzed from a 1000-mL water sample that was concentrated by filtering it through a positively charged nylon membrane [38]. Norovirus detection was carried out using the RT-PCR method, and the result was confirmed with microplate hybridization [39].

4.4. Analyses of Indicator Bacteria

CFUs of *Escherichia coli* and coliform bacteria were analyzed from both 100- and 1000-mL samples according to the SFS 3016 standard [40] using m-Endo LES (Merck KGaA, Darmstadt, Germany) agar plates and membrane filtration. The heterotrophic plate count was determined according to the ISO 6222 standard [41] on tryptone-yeast agar (Oxoid) incubated at (22 ± 1) °C for three days. The CFUs of intestinal enterococci were analyzed from 100-mL, 500-mL and 1000-ml samples according to the ISO 7899-2 standard [42] with membrane filtration and a Slanetz-Bartley medium (Oxoid).

Clostridium perfringens CFUs were counted in 100-mL and 1000-mL samples with the membrane filtration method on Tryptose-Sulphite-Cyclocerine agar (Difco) using the ISO/CD 6461-2 method.

The CFUs of *Aeromonas* spp. were counted in 100-mL and 1000-mL samples by using the membrane filtration technique on ADA (Ampicillin-Dextrin Agar) plates with ampicillin as a selective substance [43]. After 24 h of incubation at 30 °C, typical yellow colonies were subcultivated on blood agar for further identification. A total of 28 colonies from five *Aeromonas*-positive water supplies from autumn 2005 were further identified as *Aeromonas* spp. with API20 NE (bioMérieux, Marcy l'Etoile, France). For genospecies identification, the DNA of the colonies was isolated, and a fragment of the 16S rRNA gene was amplified with PCR according to the method described by Borrell *et al.* [16]. PCR products were digested with *AluI* and *Mbo1*. The pattern of fragments on agarose gels was compared with the results of Borrell *et al.* [16], and genospecies identification was performed on the basis of an RFLP pattern.

4.5. Chemical Analyses

Temperature, pH, and conductivity were measured on site using a YSI 556 MPS multiple parameter instrument or a pH/Cond 340i WTW-meter. Color was measured according to the ISO 7887-4 standard [44], and turbidity according to the ISO 7027 standard [45]. Iron and manganese concentrations were measured according to the SFS 5502 standard [46]. Nitrite nitrogen and nitrate nitrogen was measured using ISO 13395 standard method [47].

4.6. Statistical Analyses

Statistical analyses were performed using SPSS Statistics 22. For the results below the detection limit, half of the detection limit was used as a numerical value. The normality of microbiological and chemical parameter results from spring and autumn samples was tested using Shapiro-Wilk test and by visual evaluation of frequency distributions. Non-parametric methods were used, because normal distributions of the variables could not be obtained. Wilcoxon signed rank test was used to determine if there were statistically significant differences between results obtained from spring and autumn samples. The variation of the water quality results in the recognized environmental risk factor categories were tested with non-parametric Kruskal-Wallis one-way analysis of variance (ANOVA) test. Spearman's correlation coefficients were used to display the relationships between the water quality parameters. Differences and correlations were considered statistically significant when $p < 0.05$.

5. Conclusions

We detected *Giardia intestinalis* for the first time in the Finnish groundwater supplies. *E. coli* and coliform bacteria, as well as intestinal enterococci were detected in some wells, which together with *Aeromonas* findings indicate surface water access and possible contamination from the surroundings to the wells. These findings suggest an increased health risk associated with small drinking water supplies, even though among public they are usually considered safe. In addition, high iron and manganese concentrations, and low pH, which have also been detected previously in Finnish groundwater, degraded the quality of drinking water.

Acknowledgments

We would like to acknowledge the water supply operators for their responses to the questionnaire and participation in sampling.

Author Contributions

Ilkka T. Miettinen, Marja-Liisa Hänninen, Matti Valve, Anna-Liisa Kivimäki and Kirsti Lahti conceived and designed the experiments; Tarja Pitkänen, Tiina Juselius and Eija Isomäki performed the experiments; Tarja Pitkänen, Tiina Juselius and Anna-Liisa Kivimäki analyzed the data; Matti Valve produced the graphics; Tarja Pitkänen, Tiina Juselius, Anna-Liisa Kivimäki and Marja-Liisa Hänninen wrote the paper.

Conflicts of Interest

The authors declare no conflict of interest.

References

1. Richardson, H.Y.; Nichols, G.; Lane, C.; Lake, I.R.; Hunter, P.R. Microbiological surveillance of private water supplies in England—The impact of environmental and climate factors on water quality. *Water Res.* **2009**, *43*, 2159–2168.
2. Pitkänen, T.; Karinen, P.; Miettinen, I.T.; Lettojärvi, H.; Heikkilä, A.; Maunula, R.; Aula, V.; Kuronen, H.; Vepsäläinen, A.; Nousiainen, L.L.; *et al*. Microbial contamination of groundwater at small community water supplies in Finland. *Ambio* **2011**, *40*, 377–390.
3. Lapinlampi, T.; Raassina, S. *SY541 Vesihuoltolaitokset 1998–2000*; Finnish Environment Centre (SYKE): Helsinki, Finland, 2002. (In Finnish)
4. Isomäki, E. Pienet pohjavesilaitokset Suomessa. *Vesitalous* **2006**, *3*, 11–16. (In Finnish)
5. Decree of the Ministry of Social Affairs and Health Relating to the Quality and Monitoring of Water Produced by Small Water Supplies 401/2001, Finlex Data Bank; Edita Publishing Oy: Helsinki, Finland, 2001. Available online: http://www.finlex.fi/fi/laki/alkup/2001/20010401 (accessed on 20 August 2015). (In Finnish)
6. Decree of the Ministry of Social Affairs and Health Relating to the Quality Requirements and Monitoring of the Household Water 461/2000, Finlex Data Bank, Edita Publishing Oy: Helsinki, Finland, 2000. Available online: http://www.finlex.fi/fi/laki/alkup/2000/20000461 (accessed on 20 August 2015). (In Finnish)
7. European Union. Council directive 98/83/EC of 3 November 1998 on the quality of water intended for human consumption. *Off. J. Eur. Communities* **1998**, *L330*, 32–54.
8. Hulsmann, A. *Small Systems Large Problems—A European Inventory of Small Water Systems and Associated Problems*; Report of Web-based European Knowledge Network on Water WEKNOW/ENDWARE, European Commission; KWR Watercycle Research Institute: Nieuwegein, The Netherlands, 2005; p. 41.
9. Lahermo, P.; Tarvainen, T.; Hatakka, T.; Backman, B.; Juntunen, R.; Kortelainen, N.; Lakomaa, T.; Nikkarinen, M.; Vesterbacka, P.; Väisänen, U.; *et al*. *Tuhat kaivoa—Suomen kaivovesien fysikaalis-kemiallinen laatu vuonna 1999*; (*Summary: One thousand wells—The physical-chemical quality of Finnish well waters in 1999*). Report of Investigation 155; Geological Survey of Finland: Espoo, Finland, 2002, p. 92. Available online: http://tupa.gtk.fi/julkaisu/tutkimusraportti/tr_155.pdf (accessed on 20 August 2015).
10. Zacheus, O. *Talousveden valvonta ja laatu vuonna 2008. Yhteenveto viranomaisvalvonnan tuloksista*; Avauksia 18/2010; Terveyden ja hyvinvoinnin laitos (THL): Helsinki, Finland, 2010; p. 67. Available online: http://urn.fi/URN:NBN:fi-fe201205085417 (accessed on 20 August 2015). (In Finnish)
11. Zacheus, O.; Miettinen, I.T. Increased information on waterborne outbreaks through efficient notification system enforces actions towards safe drinking water. *J. Water Health* **2011**, *9*, 763–772.

12. Miettinen, I.T.; Zacheus, O.; von Bonsdorff, C.H.; Vartiainen, T. Waterborne epidemics in Finland in 1998–1999. *Water Sci. Technol.* **2001**, *43*, 67–71.
13. Pitkänen, T. Review of *Campylobacter* spp. in drinking and environmental waters. *J. Microbiol. Methods* **2013**, *95*, 39–47.
14. Rimhanen-Finne, R.; Hänninen, M.L.; Vuento, R.; Laine, J.; Jokiranta, T.S.; Snellman, M.; Pitkänen, T.; Miettinen, I.; Kuusi, M. Contaminated water caused the first outbreak of giardiasis in Finland, 2007: A descriptive study. *Scand. J. Infect. Dis.* **2010**, *42*, 613–619.
15. Simonen, A. *The Precambrian in Finland*; Bulletin 304; Geological Survey of Finland: Espoo, Finland, 1980; p. 58. Available online: http://tupa.gtk.fi/julkaisu/bulletin/bt_304.pdf (accessed on 20 August 2015).
16. Borrell, N.; Acinas, S.G.; Figueras, M.J.; Martinez-Murcia, A.J. Identification of *Aeromonas.* clinical isolates by restriction fragment length polymorphism of PCR-amplified 16S rRNA genes. *J. Clin. Microbiol.* **1997**, *35*, 1671–1674.
17. Corkal, D.; Schutzman, W.C.; Hilliard, C. Rural water safety from the source to the on-farm tap. *J. Toxicol. Environ. Health A* **2004**, *67*, 1619–1642.
18. Rutter, M.; Nichols, G.L.; Swan, A.; de Louvois, J. A survey of the microbiological quality of private water supplies in England. *Epidemiol. Infect.* **2000**, *124*, 417–425.
19. Hörman, A.; Korpela, H.; Sutinen, J.; Wedel, H.; Hänninen, M.L. Meta-analysis in assessment of the prevalence and annual incidence of *Giardia* spp. and *Cryptosporidium* spp. infections in humans in the Nordic countries. *Int. J. Parasitol.* **2004**, *34*, 1337–1346.
20. Hörman, A.; Rimhanen-Finne, R.; Maunula, L.; von Bonsdorff, C.H.; Torvela, N.; Heikinheimo, A.; Hänninen, M.L. *Campylobacter* spp., *Giardia* spp., *Cryptosporidium*, noroviruses and indicator organisms in surface water in southwestern Finland, 2000–2001. *Appl. Environ. Microbiol.* **2004**, *70*, 87–95.
21. Rimhanen-Finne, R.; Vuorinen, A.; Marmo, S.; Malmberg, S.; Hanninen, M.L. Comparative analysis of *Cryptosporidium*, *Giardia* and indicator bacteria during sewage sludge hygienization in various composting processes. *Lett. Appl. Microbiol.* **2004**, *38*, 301–305.
22. Said, B.; Wright, F.; Nichols, G.L.; Reacher, M.; Rutter, M. Outbreaks of infectious disease associated with private drinking water supplies in England and Wales 1970–2000. *Epidemiol. Infect.* **2003**, *130*, 469–479.
23. Von Hertzen, L.; Laatikainen, T.; Pitkänen, T.; Vlasoff, T.; Makela, M.J.; Vartiainen, E.; Haahtela, T. Microbial content of drinking water in Finnish and Russian Karelia—Implications for atopy prevalence. *Allergy* **2007**, *62*, 288–292.
24. Casemore, D. Towards a US national estimate of the risk of endemic waterborne disease—Sero-epidemiologic studies. *J. Water Health* **2006**, *4*, 121–163.
25. Ferguson, C.M.; Coote, B.G.; Ashbolt, N.J.; Stevenson, I.M. Relationships between indicators, pathogens and water quality in an estuarine system. *Water Res.* **1996**, *30*, 2045–2054.
26. Cizek, A.R.; Characklis, G.W.; Krometis, L.A.; Hayes, J.A.; Simmons, O.D., III.; di Lonardo, S.; Alderisio, K.A.; Sobsey, M.D. Comparing the partitioning behavior of *Giardia* and *Cryptosporidium* with that of indicator organisms in stormwater runoff. *Water Res.* **2008**, *42*, 4421–4438.

27. LeChevallier, M.W.; Norton, W.D.; Lee, R.G. Occurrence of *Giardia* and *Cryptosporidium* spp. in surface water supplies. *Appl. Environ. Microbiol.* **1991**, *57*, 2610–2616.
28. Hänninen, M.L.; Siitonen, A. Distribution of *Aeromonas.* phenospecies and genospecies among strains isolated from water, foods or from human clinical samples. *Epidemiol. Infect.* **1995**, *115*, 39–50.
29. Hänninen, M.L.; Oivanen, P.; Hirvelä-Koski, V. *Aeromonas.* speciesin fish, fish-eggs, shrimp and freshwater. *Int. J. Food Microbiol.* **1997**, *34*, 17–26.
30. Altwegg, M.; Steigerwalt, A.G.; Altwegg-Bissig, R.; Luthy-Hottenstein, J.; Brenner, D.J. Biochemical identification of *Aeromonas.* genospecies isolated from humans. *J. Clin. Microbiol.* **1990**, *28*, 258–264.
31. Hirotani, H.; Sese, C.; Kagawa, H. Correlations of *Aeromonas. hydrophila* with Indicator Bacteria of Water Qualityand Environmental Factorsin a Mountain Stream. *Water Environ. Res.* **1999**, *7*, 132–138.
32. Kersters, I.; van Vooren, L.; Huys, G.; Janssen, P.; Kersters, K.; Verstraet, W. Influence of temperature and process technology on the occurrence of *Aeromonas.* species and hygienic indicator organisms in drinking water production plants. *Microb. Ecol.* **1995**, *30*, 203–218.
33. Hänninen, M.L.; Haajanen, H.; Pummi, T.; Wermundsen, K.; Katila, M.L.; Sarkkinen, H.; Miettinen, I.; Rautelin, H. Detection and typing of *Campylobacter jejuni* and *Campylobacter coli* and analysis of indicator organisms in three waterborne outbreaks in Finland. *Appl. Environ. Microbiol.* **2003**, *69*, 1391–1396.
34. United States Environmental Protection Agency. *Method 1623: Cryptosporidium and Giardia in Water by Filtration/IMS/FA*; EPA-821-R-99–006; United States Environmental Protection Agency: North Chelmsford, MA, USA, 1999.
35. Rimhanen-Finne, R.; Hörman, A.; Ronkainen, P.; Hänninen, M.L. An IC-PCR method for detection of *Cryptosporidium* and *Giardia* in natural surface waters in Finland. *J. Microbiol. Methods* **2002**, *50*, 299–303.
36. Homan, W.L.; Gilsing, M.; Bentala, H.; Limper, L.; van Knapen, F. Characterization of *Giardia duodenalis* by polymerase-chain-reaction fingerprinting. *Parasitol. Res.* **1998**, *84*, 707–714.
37. International Organization for Stardardization. *Water Quality—Detection and Enumeration of Thermotolerant Campylobacter Species*; ISO 17995; International Organization for Stardardization: London, UK, 2005.
38. Gilgen, M.; Germann, D.; Luthy, J.; Hubner, P. Three-step isolation method for sensitive detection of enterovirus, rotavirus, hepatitis A virus, and small round structured viruses in water samples. *Int. J. Food Microbiol.* **1997**, *37*, 189–199.
39. Maunula, L.; Piiparinen, H.; von Bonsdorff, C.H. Confirmation of Norwalk-like virus amplicons after RT-PCR by microplate hybridization and direct sequencing. *J. Virol. Methods* **1999**, *83*, 125–134.
40. Finnish Standard Association. *Water Quality—Membrane Filter Technique for the Enumeration of Total Coliform Bacteria*, SFS 3016; Finnish Standard Association: Helsinki, Finland, 2001.

41. International Organization for Stardardization. *Water Quality—Enumeration of Culturable Micro-Organisms. Colony Count by the Inoculation in a Nutrient Agar Culture Medium*; ISO 6222; International Organization for Stardardization: London, UK, 1999.
42. International Organization for Stardardization. *Water Quality—Detection and Enumeration of Intestinal Enterococci. Part 2: Membrane Filtration Method*; ISO 7899-2; International Organization for Stardardization: London, UK, 2000.
43. Havelaar, A.H.; During, M.; Versteegh, J.F. Ampicillin-dextrin agar medium for the enumeration of *Aeromonas*. species in water by membrane filtration. *J. Appl. Bacteriol.* **1987**, *62*, 279–287.
44. International Organization for Standardization. *Water Quality—Examination and Determination of Colour*; ISO 7887-4; International Organization for Standardization: London, UK, 1994.
45. International Organization for Standardization. *Water Quality—Determination of Turbidity*; ISO 7027; International Organization for Standardization: London, UK, 1999.
46. Finnish Standards Association. *Metal Content of Water, Sludge and Sediment Determined by Flameless Atomic Absorption Spectrometry. Atomization in a Graphite Furnace. Special Guidelines for Aluminium, Cadmium, Cobolt, Chromium, Copper, Lead, Manganese, Nickel and Iron*; SFS Method 5502; Finnish Standards Association: Helsinki, Finland, 1990.
47. International Organization for Standardization. *Water Quality—Determination of Nitrite Nitrogen and Nitrate Nitrogen and the Sum of both by Flow Analysis (CFA and FIA) and Spectrometric Detection*; ISO 13395; International Organization for Standardization: London, UK, 1996.

Geochemical Characterization of Groundwater in a Volcanic System

Carmelo Bellia, Adrian H. Gallardo, Masaya Yasuhara and Kohei Kazahaya

Abstract: A geochemical investigation was undertaken at Mt. Etna Volcano to better define groundwater characteristics of its aquifers. Results indicate that the Na–Mg ± Ca–HCO_3^- ± (SO_4^{2-} or Cl^-) type accounts for more than 80% of the groundwater composition in the volcano. The remaining 20% is characterized by elevated Ca^{2+}. Waters along coastal areas are enriched in SO_4^{2-} or Cl^-, mainly due to mixing with seawater and anthropogenic effects. The majority of the samples showed values between −4‰ to −9‰ for $\delta^{18}O$ and −19‰ to −53‰ for δ^2H, suggesting that precipitation is the predominant source of recharge to the aquifers, especially in the west of the study area. The analysis of $\delta^{13}C$ and pCO_2 shows values 1 to 3 times higher than those expected for waters in equilibrium with the atmosphere, suggesting a partial gas contribution from deep sources. The diffusion of gasses is likely to be controlled by tectonic structures in the volcano. The ascent of deep brines is also reflected in the CO_2 enrichment (up to 2.2 bars) and enriched $\delta^2H/\delta^{18}O$ compositions observed in the salt mounts of Paternò.

Reprinted from *Resources*. Cite as: Bellia, C.; Gallardo, A.H.; Yasuhara, M.; Kazahaya, K. Geochemical Characterization of Groundwater in a Volcanic System. *Resources* **2015**, *4*, 358–377.

1. Introduction

Mt. Etna is located on the east coast of Sicily (Italy). It is the tallest active volcano in Europe and one of the most active volcanoes in the world [1]. The volcanic deposits are the most important groundwater reservoir for the entire Sicily, as it is the only drinking water resource for over one million people who live at distances of more than 100 km [2]. The volcano rises over an important regional tectonic system, which causes the crust to break up into an intricate system of fractures and faults that together with geology, paleotopography and geometry of the sedimentary basement are the major factors governing the groundwater flow in the area.

Furthermore, seismic events and volcanic eruptions frequently reshape the morphology of the terrain, potentially altering flow conditions and modifying the groundwater composition. Agriculture and the development of urban and industrial centers such as Catania are largely dependent on the neighboring volcano. In this context, population growth and new economic activities continue to mount pressure on the environment and hence call for a more sustainable use of the region's groundwater resources. Geochemistry and isotope investigations have been used commonly on Etnean aquifers to study the hydrological processes. For instance [3] determined that groundwater concentrations of minor and trace elements stood out with respect to other Italian aquifers due to the major contribution of volcanic gases and hydrothermal fluids. Later, [4] determined the origin and effects of fluid-rock interaction within Mt Etna by analyzing B, O, H, and Sr concentrations. Oxygen and Cl isotopes were used by [5] to determine groundwater recharge and flow paths along the flanks of Mt. Etna. Findings showed that groundwaters beneath

intensely cultivated areas were enriched in ^{18}O probably as a result of the evaporation of irrigation waters during summer. Finally, [6] investigated the isotopic signature of Etnean waters, and [7] used tritium activities to trace the age and movement of groundwater in the volcano in recent times.

The hydrology of Mt. Etna has been studied over a long period. This work further expands the current understanding by providing an updated snapshot in time of the geochemical and isotopic composition of Mt. Etna's groundwater.

2. Study Area

2.1. Geological Background

Mt. Etna is located on the eastern coast of Sicily, Italy. The morphology of the volcano is shaped by four summit craters, a caldera of about 18 km perimeter and maximum depth of 1000 m called "Valle del Bove", and numerous side cones scattered along its flanks (Figure 1). Slopes are gentle (7°–8°) up to an elevation of 1800–2000 m above sea level (A.S.L.), increasing to 20°–25° at higher elevations. The volcanic edifice consists of a lower shield unit overlain by a stratovolcano. The shield rests discordantly on Miocene flysch deposits to the NW, and argillaceous Pleistocene sediments to the SE [8,9] and consists of plateau terraces of submarine lavas derived from fissural emissions generated at an early stage, approximately 500 ka. The basal unit was followed by pyroclastic material and sub-aerial tholeiitic lavas outcropping rather discontinuously in the southern sectors of the volcano approximately 300 ka [10]. Products changed in composition about 200 ka to transitional and later Na-alkaline tholeiites [11].

Currently, Mt. Etna releases about 11.66 kTons/day of CO_2 from the summit and as diffuse soil emanations from the upper flanks [12]. This quantity is much larger than other active volcanoes and corresponds to about 10%–15% of the CO_2 produced by all the volcanoes on the planet [13].

The climate of the region follows the pattern of the Mediterranean region, with higher precipitations in autumn and winter. Most rainfall occurs to the east, reaching up to 1200 mm/year. To the south, the average precipitation decreases to about 440 mm/year, with a wide range of intermediate conditions in between. At heights above 2000 m precipitation tends to occur as snow.

2.2. Hydrogeological Setting

Mt. Etna hydrogeological settings are similar to other basaltic volcanoes: fissured and highly permeable lavas are interbedded with discontinuous layers of low permeability pyroclastics. According to [9,14], typical Etnean aquifers can be described as unconfined and hosted by highly permeable volcanites. On the basis of structural, geological and geophysical data, three main hydrogeological basins were defined (Figure 1): (1) the eastern basin, with flow towards the Ionian Sea; (2) the southern and western basins flowing towards the Simeto River; and (3) the northern basin with flow to the Alcantara River [14,15]. Groundwater recharge preferentially occurs at high elevations where rainfall infiltrates through the unsaturated sediments and then follows a radial pattern towards the peripheral sedimentary terrains. Groundwater flow originating at lower heights, where the volcanic cover is much thinner, is mainly controlled by the shape of the impermeable substrate. According to [16], Etna's volcanites generally have a high intrinsic permeability

(2.5×10^{-7} to 2.9×10^{-6} cm^2). In contrast, the permeability of the basement sediments would average 10^{-10} cm^2 [17].

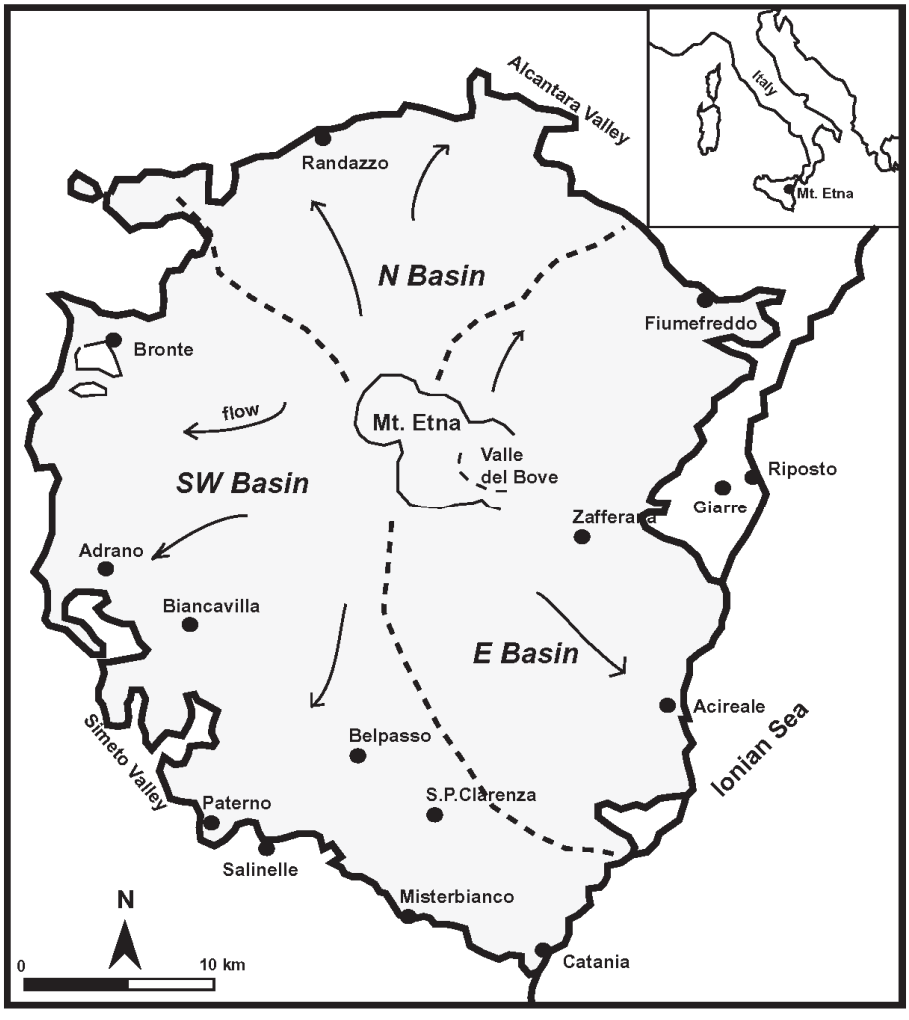

Figure 1. Outline of the investigation area and hydrogeological basins within Mt. Etna.

The absence of a developed hydrographic system on the surface suggests an important circulation of groundwater, highlighted by the presence of hundreds of springs and wells of significant flow rates. Yields over 80 L/s have been described by several authors since the 70s [16,18].

Recent hydrogeochemical studies (e.g., [19,20]) indicated that groundwater in Mt. Etna has a general composition of bicarbonate type, with a few samples of chloride-sulphate type. The relative abundance of major elements in solution is generally (Na, Mg) > Ca > K for cations, whilst HCO_3^- always prevails over other anions [20].

Findings from [21,22] using $\delta^{18}O$ and $\delta^{2}H$ data suggested that Etnean groundwaters are meteoric in origin. Nevertheless, more recent work from [5] showed that the isotopic imprint of groundwater in Mt. Etna might reflect several sources such as evaporation from the Mediterranean Sea to the east, moisture from the Atlantic Ocean on the lower northern flanks, and volcanic vapor affecting precipitation on the upper regions of the cone.

3. Sampling and Analytical Methods

An extensive sampling campaign was undertaken in early 2014 at Mt. Etna to determine the chemical characteristics of groundwaters in the volcano. Samples were collected during three stages from 46 boreholes, 14 springs, 2 surface water points, and 6 locations within the so-called "mud volcanoes" (Figure 2). The bores are all being used for water supply or are connected to storage tanks. As a first measure, piped water-supply and taps were disinfected with a 10% hypochlorite solution and water run for a few minutes before sampling commenced. Samples were then directly collected from the source, field-filtered at 0.45 µm, and stored in 500 mL plastic containers for the analysis of dissolved inorganic elements. Bottles were cooled to 4° and dispatched for analysis within 48 h. A number of field blanks and duplicates were also sent to the laboratory for quality control. Standard parameters (pH, EC, temperature) were measured *in situ* using a Hydrolab Qanta probe, while a colorimetric titration kit was employed to calculate the alkalinity (HCO_3^-) content in waters. Chemical concentrations were determined at the laboratories of the Geological Survey of Japan in Tsukuba. Major cations were analyzed by an inductively coupled argon plasma atomic spectrophometer (ICP-AES), and anion determinations were carried out by ion-chromatography. Additional samples were collected for the analysis of carbon-13 ($\delta^{13}C$), and treated in the field with $HgCl_2$ to prevent biological fractionation. These samples were stored in glass bottles and analyzed by a mass spectrometer. Results were reported as ‰ deviations (per mil) from the PeeDee Belemnite standard. Oxygen and hydrogen isotopes were also measured by an isotope ratio mass spectrometer. Measurements were referenced to the VSMOW international standard, and reported in the conventional delta notation.

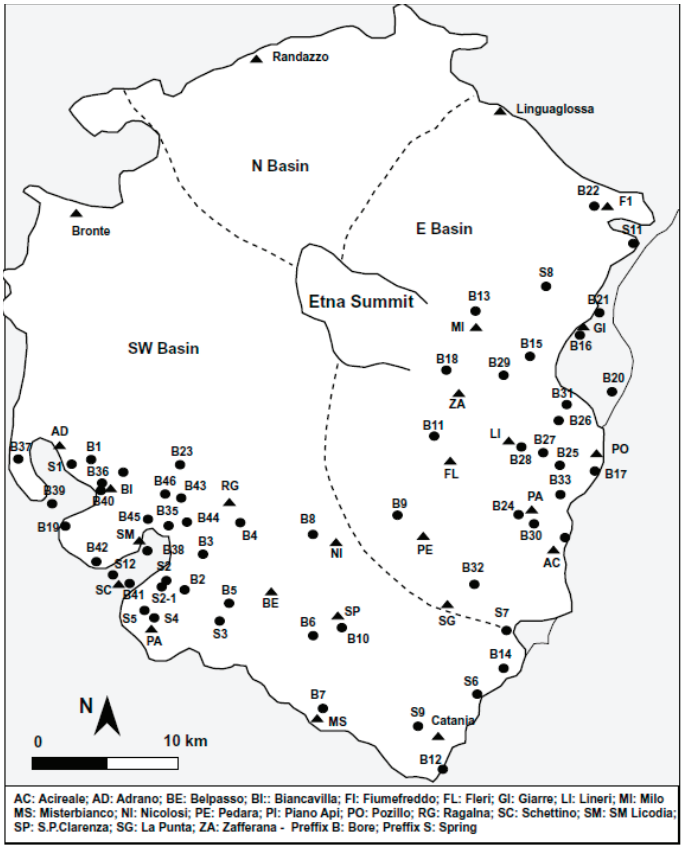

Figure 2. Location of the sampling sites in Mt. Etna.

4. Results and Discussion

4.1. Groundwater Composition

Table 1 summarizes the groundwater composition of Mt. Etna groundwaters found in this study.

With the exception of SO_4^{2-}, ion concentrations increase towards the west, where values are usually two to three times higher than neighboring regions (Figure 3).

There is a general inverse relationship between water mineralization and elevation. The lowest groundwater contents were recorded on the north, and towards the cone summit in the eastern basin. In contrast, maximum concentrations were measured on the southernmost flank of the volcano (western basin). Results also indicate that Etnean waters have low temperatures, with an average of 17 °C. The highest water temperatures were recorded in intense tectonically fractured areas such as Paternò, Biancavilla, and Adrano in the West, and between Pozzillo and Zafferana in the East. This is consistent with [23], who argued that in an active volcanic system such as Mt. Etna, the transfer of deep gases (and the associated heat) toward the surface occurs principally along zones of high permeability in the crust.

Table 1. Average major and trace elements composition of waters sampled in the Mt. Etna.

Sample	Basin	Temp.	EC	pH	HCO_3	F	Cl	NO_3	PO_4	SO_4	Na	K	Ca	Mg	TDS	Hardness	PCO_2 at 20°
		°C	µS/cm		meq/L	meq/L	meq/L	meq/L	meq/L	meq/L	meq/L	meq/L	meq/L	meq/L	mg/L	°fH	bars
B11	E	9.1	219	7.35	2.62	0.02	0.29	0.02	0.02	0.30	1.35	0.21	0.69	1.38	149	10.3	0.007
B12	E	18	1138	7.77	8.16	0.04	3.28	0.92	-	1.70	6.07	0.65	3.50	4.57	736.6	40.3	0.009
B13	E	11.4	289	7.92	1.26	0.01	1.49	0.30	-	0.57	1.33	0.25	0.64	1.87	252.3	12.6	0.001
B14	E	14.7	1123	8.29	3.84	0.03	6.15	1.48	-	2.99	7.73	0.52	1.91	5.95	997.9	39.2	0.001
B15	E	10.6	282	8.37	2.02	0.01	0.96	0.09	0.02	0.79	2.21	0.24	0.57	1.13	191.1	8.5	0.001
B16	E	-	300	0.03	3.00	-	-	1.43	2.75	-	0.34	0.33	1.1	-	-	-	-
B17	E	15.8	1329	6.85	8.86	0.03	4.25	0.73	-	3.76	8.69	0.77	3.73	5.53	912.9	46.2	0.079
B18	E	5.6	424	7.82	4.58	0.03	0.96	0.01	-	1.68	3.79	0.35	1.60	1.46	307.5	15.3	0.004
B20	E	14.1	298	8.39	2.70	0.01	0.51	0.24	0.05	0.52	1.12	0.33	1.92	0.61	203.7	12.6	0.001
B21	E	16.4	967	7.32	8.24	0.06	2.47	0.46	-	1.91	5.07	0.64	2.15	7.67	723.4	49.0	0.025
B22	E	13.9	373	7.87	3.66	0.02	0.70	0.08	-	0.65	2.46	0.28	1.20	1.30	224.7	12.5	0.003
B24	E	17.4	544	7.8	3.90	0.03	1.37	0.31	-	0.69	2.99	0.26	0.70	1.75	268.2	-	0.004
B25	E	16	1056	6.58	7.08	0.02	1.72	0.61	-	2.35	4.15	0.57	2.42	4.60	574.1	-	0.118
B26	E	17.5	1570	6.57	10.67	0.03	2.74	0.28	0.02	3.86	7.07	0.85	3.45	6.75	838.6	-	0.181
B27	E	17	718	6.58	5.03	0.02	1.03	0.85	-	1.42	2.62	0.40	1.78	3.10	410.7	-	0.084
B28	E	16	886	6.4	6.44	0.02	1.35	0.21	-	1.62	3.47	0.54	2.09	3.87	458.8	-	0.162
B29	E	26	944	7.33	8.52	0.01	1.14	0.16	-	0.95	5.15	0.46	1.88	3.59	449.4	-	0.025
B30	E	18.8	588	7.8	3.33	0.03	1.63	0.50	-	0.79	3.08	0.25	0.76	1.90	303.1	-	0.003
B31	E	29.8	1527	7	8.89	0.05	2.86	0.41	-	4.15	5.43	0.76	3.66	6.80	827	-	0.056
B32	E	17.8	996	7.25	6.93	0.03	2.39	0.19	-	1.57	4.82	0.47	1.45	4.64	522.7	-	0.025
B33	E	21.3	1180	6.8	8.54	0.03	1.77	0.61	0.02	2.52	4.35	0.52	2.78	5.71	647.5	-	0.085
S6	E	17.6	2300	7.95	4.37	0.00	17.3	0.77	-	3.59	18.62	0.82	3.74	4.65	1693.5	41.9	0.003
S7	E	16.8	-	7.64	1.52	0.03	2.97	1.77	-	2.78	3.25	0.81	1.44	5.03	638.1	32.3	0.002
S8	E	14.9	330	8.15	1.95	0.02	0.77	0.18	-	1.14	2.14	0.23	0.73	1.34	210.8	10.4	0.001
S9	E	15.5	981	8.44	6.14	0.04	2.88	1.25	0.05	2.52	5.49	0.50	2.68	5.29	729.9	39.8	0.001
S10	E	15.3	676	7.74	5.00	0.04	2.46	0.41	-	0.75	3.77	0.41	2.23	2.39	441.7	23.1	0.006

Table 1. *Cont.*

Sample	Basin	Temp.	EC	pH	HCO_3	F	Cl	NO_3	PO_4	SO_4	Na	K	Ca	Mg	TDS	Hardness	PCO_2 at 20°
		°C	µS/cm		meq/L	meq/L	meq/L	meq/L	meq/L	meq/L	meq/L	meq/L	meq/L	meq/L	mg/L	°fH	bars
S11	E	14.3	443	7.79	3.50	0.02	0.86	0.33	-	0.96	2.61	0.30	1.31	1.85	283.6	15.8	0.004
S12	E	19.7	1670	7.5	13.10	0.04	2.84	1.01	-	3.25	7.51	0.66	2.79	8.90	935.2	-	0.026
R1	River E	11.2	490	8.73	5.72	0.03	0.78	0.10	-	1.03	2.11	0.19	1.84	4.61	395.2	32.2	0.001
B1	W	7	1268	7.98	17.51	0.06	3.56	0.10	0.05	1.10	10.04	0.66	6.75	2.84	869.3	47.9	0.012
B2	W	15.9	1335	6.46	16.34	0.02	3.07	0.02	-	0.18	8.81	0.69	3.85	9.48	939.2	66.6	0.355
B3	W	15.1	1004	6.8	12.80	0.03	2.56	0.09	-	1.49	5.10	0.77	2.72	6.46	679.7	45.9	0.128
B4	W	8.8	832	6.2	12.18	0.03	0.91	0.08	-	0.87	4.12	0.48	0.64	6.82	486.9	37.3	0.502
B5	W	15.4	1441	6.71	17.71	0.04	2.17	0.21	-	0.56	6.82	0.78	6.09	6.07	852.2	60.8	0.218
B6	W	15	1153	7.11	12.36	0.04	2.86	0.29	-	0.93	5.65	0.57	5.09	4.83	746.7	49.5	0.061
B7	W	16.7	1013	7.49	7.94	0.03	2.90	0.75	-	1.46	4.89	0.54	3.28	3.58	624.3	34.3	0.016
B8	W	18.1	989	6.48	8.40	0.03	2.50	0.07	0.02	1.46	4.66	0.66	3.44	3.53	574.2	34.8	0.176
B9	W	13.9	384	8.24	2.68	0.04	0.66	0.08	-	0.68	2.26	0.23	0.81	0.94	182.3	8.8	0.001
B10	W	16.4	1951	6.84	23.85	0.06	4.65	0.17	0.02	0.72	6.83	0.59	1.21	18.04	1192	96.2	0.217
B19	W	17.1	1093.6	7.71	7.60	0.01	9.68	2.20	0.02	6.63	13.19	0.82	7.84	3.84	1488.4	58.3	0.009
B23	W	12.1	924	7.42	13.72	0.03	0.90	0.03	-	0.56	4.87	0.54	4.70	3.78	571.2	43.3	0.033
B34	W	18.7	1582	6.51	17.49	0.05	1.87	0.01	-	0.45	6.50	0.52	2.62	10.68	827.3	-	0.341
B35	W	14.9	1182	6.06	12.43	0.04	1.27	0.09	-	0.94	4.54	0.54	2.41	7.68	638.3	-	0.683
B36	W	23	2051	7.1	17.87	0.03	3.63	1.51	-	2.09	10.24	0.95	2.40	10.94	1114.8	-	0.090
B37	W	16.3	1800	7.41	13.33	0.04	4.40	0.93	-	3.09	9.94	0.56	2.02	8.87	995.6	-	0.033
B38	W	14.5	1194	6.51	11.84	0.03	1.44	0.19	0.03	1.15	4.40	0.53	2.41	7.62	648.3	-	0.231
B39	W	17.6	1766	6.98	14.72	0.04	3.16	0.97	-	2.62	8.30	0.68	2.55	9.65	976.8	-	0.097
B40	W	19	2560	7.3	21.90	0.09	5.32	4.80	-	4.42	11.72	0.91	5.83	14.72	1784.3	-	0.069
B41	W	18	1825	7.07	13.64	0.04	3.34	1.36	-	4.19	8.43	0.68	2.95	9.80	1060.1	-	0.073
B42	W	20	1860	6.8	14.57	0.04	3.51	0.97	-	3.15	8.64	0.61	3.17	9.42	1020.3	-	0.146
B43	W	16.4	1228	6.08	14.70	0.04	1.48	0.02	-	0.53	5.29	0.50	2.65	8.78	708.4	-	0.772
B44	W	20	1315	6.18	14.77	0.04	1.47	0.00	-	0.53	5.32	0.51	2.64	8.83	708.9	-	0.616
B45	W	16.2	1212	6.28	12.02	0.03	1.38	0.25	0.02	1.03	4.51	0.53	2.35	7.57	645.4	-	0.398

Table 1. *Cont.*

Sample	Basin	Temp.	EC	pH	HCO_3	F	Cl	NO_3	PO_4	SO_4	Na	K	Ca	Mg	TDS	Hardness	PCO_2 at 20°
		°C	µS/cm		meq/L	meq/L	meq/L	meq/L	meq/L	meq/L	meq/L	meq/L	meq/L	meq/L	mg/L	°fH	bars
B46	W	14.6	1250	5.93	13.72	0.04	1.22	-	-	0.63	4.73	0.55	2.51	8.33	662.3	-	1.017
S1	W	14.2	1264	8.48	10.82	0.04	3.05	0.61	0.06	2.70	8.46	0.66	5.13	3.50	822.8	43.1	0.002
S2	W	15	1169	6.85	15.47	0.03	1.75	0.07	-	0.33	7.24	0.62	1.82	9.82	778	58.2	0.138
S2-1	W	13.7	1215	7.08	16.73	0.05	2.23	-	-	0.20	8.64	0.67	3.24	10.22	902.5	67.3	0.086
S2-2	W	15	1240	7	15.85	0.04	2.06	0.02	-	0.25	6.81	0.53	5.30	4.64	717.4	49.7	0.100
S3	W	19.8	1734	6.96	22.34	0.05	1.98	0.06	-	1.09	7.83	0.37	0.86	12.64	866.8	67.5	0.158
S4	W	19.2	1851	6.15	22.56	0.03	2.15	0.04	-	0.69	8.49	0.49	0.48	13.91	917.4	71.9	1.039
S5	W	16	1505	8.33	15.61	0.04	3.85	0.32	-	1.74	9.19	0.66	5.22	4.53	881	48.7	0.005
SM1	Salinella	10.2	67,600	6.1	47.2	1.03	1343.4	-	-	-	1266.2	16.6	14.1	51.7	81,393.9	328.9	2.2
SM2	Salinella	36.5	110,600	6.1	26.0	-	1234.7	1.3	-	14.0	1158.1	19.0	17.0	96.1	75,158.2	565.5	1.3
SM2a	Salinella	12.6	71,700	6.1	28.4	2.03	1286.1	-	-	-	1186.9	19.6	16.3	88.9	77,382.8	525.6	1.4
SM2b	Salinella	11.8	71,600	6.3	35.4	2.36	1317.9	-	-	8.1	1215.7	19.5	17.6	88.5	80,007.4	530.4	1.2
SM2c	Salinella	16.4	72,100	6.3	28.2	1.39	1289.1	-	-	11.6	1186.4	16.5	19.3	76.7	77,444.8	479.6	0.9
SM3	Salinella	18.8	60,100	6.2	30.8	0.91	1138.8	-	-	10.2	1037.3	16.9	33.3	54.5	68,910.1	438.5	1.3
R	River W	9.5	1098	8.54	6.04	0.01	2.91	0.30	-	6.76	8.26	0.53	5.49	4.90	1198.8	51.9	0.001
M1	Seawater	10.0	39,800	7.8	3.3	1.07	626	-	-	58.6	546	12.9	69.8	45.7	40,308	577	0.003

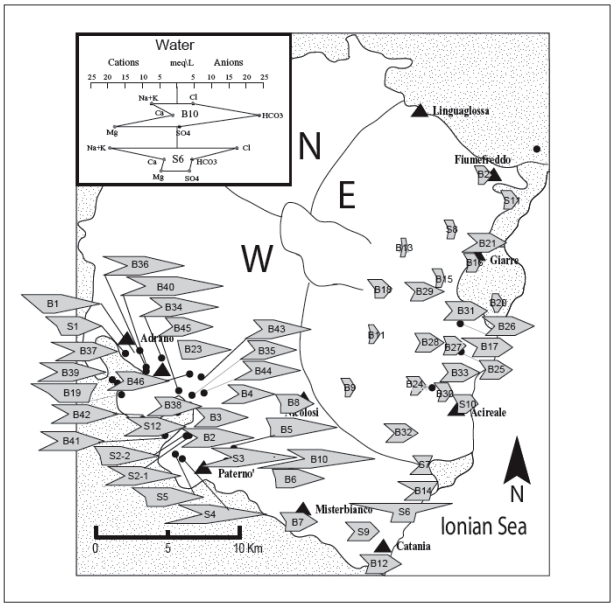

Figure 3. Stiff diagrams displaying average ion concentrations in the sampled waters.

Furthermore, high-temperature volatiles released from the magma could interact with descending meteoric waters causing a general increase of the temperature in the rest of the aquifer. This is in line with [24], who suggested a main magmatic signature linked to degassing of an enriched mantle beneath Mt. Etna. [25] characterized Etna's magma as CO_2-rich while [26], hypothesized that the asthenosphere beneath the volcano rises to a depth that permits the continuous escape of CO_2 from the mantle. Present findings of CO_2 partial pressure °pCO_2), also suggest that Etnean waters might interact with CO_2 of deep origin, arguably magmatic. Measured pCO_2 varies between 5×10^{-4} and 2.2 bars and more than 90% of the samples exhibit values 1 to 3 orders of magnitude higher than those expected for waters in equilibrium with the atmosphere ($pCO_2 = 10^{-3.6}$ bar). These positive emission anomalies could be attributed to the release of CO_2 by fresh magma that intruded into the volcano plumbing system [27,28]. In contrast, the anomalous high pCO_2 values (1.04 bars) in sample S4 could be ascribed to local waters rapidly charged with CO_2 and dissolved elements from the surrounding soil matrix. This would also explain the high conductance values among the sampled springs. Maximum pCO_2 values (up to 2.15 bars) were recorded at the "Salinella" mounts near Paternò, on the southern fringes of Etna. In here, the source of the fluids would be associated with a hydrothermal system enriched in CO_2 with temperatures between 100 °C to 150 °C that extends between Paternò and the central part of the Etna [29].

Direct inputs of deep CO_2 are a key factor in determining the chemistry of Etnean waters. In effect, the interaction between CO_2 and infiltrating rain water lowers the pH to values below 4 [30]. These low-pH waters become highly reactive resulting in chemical weathering of the host basaltic rocks. As a result of this process, HCO_3^- (along with H_2CO_3 and CO_3^{2-}) is gradually generated, whilst Mg, Ca, K, and Na are released into solution. The general positive relationship between

HCO_3^- and these cations (especially Na^+ and Mg^{2+}) supports the idea that dissolution from acidic waters is as a major mechanism for the mineralization of Etnean aquifers (Figure 4). Bicarbonate concentrations are normally higher in the western basin, with values up to 23.8 meq/L around the towns of Paternò, S.P. Clarenza, and Biancavilla. In contrast, groundwater in the eastern basin shows a more limited enrichment in HCO_3^-, with concentration values approximately 1/3 (~5 meq/L) of those observed in the west. This is in line with [31], who argued that chemical weathering in Etna is not spatially uniform since the presence of CO_2 in soils is more abundant in particular areas of the volcano, such as the south-western flank.

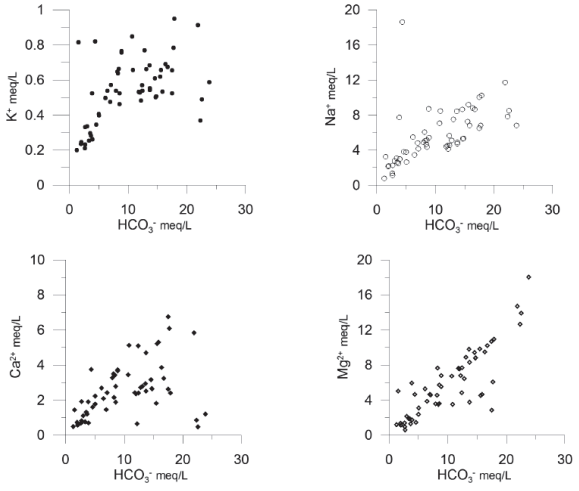

Figure 4. HCO_3^- against major cations in groundwater.

Furthermore, HCO_3^- concentrations appear to be influenced by the ground surface elevation. There is a negative trend between HCO_3^- and elevation, with the lowest concentrations towards the volcano's summit. As discussed, more restricted hydrological circuits mean that CO_2-enriched waters near the top of the edifice have fewer opportunities to react with the host basaltic rocks. Lower dissolution rates translate into lower HCO_3^- concentrations and a general decrease in the total dissolved solids content (TDS) of the waters.

Electrical conductivity (EC) from 1000 to 2000 µS/cm, and TDS values between 700 mg/L and 1400 mg/L were found to be representative for groundwater in the southernmost flank of Mt. Etna. Exceptional salinities detected at S6 near Catania (EC = 2300 µS/cm; TDS = 1694 mg/L) are attributed to partial mixing with seawater in proximities to the Ionian coast. Longer residence times favoring basalt leaching would be an additional factor explaining the higher salinity in the SW sector of Etna [32]. Conversely, the eastern flank is characterized by EC values between 500 and 1000 µS/cm, and TDS from 300 to 1100 mg/L. This lower TDS might be ascribed to water circulation in more transmissive sediments that facilitate the flow of meteoric recharge and reduce the transit time underground. Elevation would be another factor controlling the TDS distribution in groundwater. Dissolved solids in samples above 600m A.S.L. are usually below 500 mg/L, which

can be attributed to the limited water-rock interaction at high elevations. As expected, groundwater at higher elevations receives direct recharge from precipitation, which is unable to interact with the host rocks for long enough to produce major changes in its chemical composition.

Major cations (Ca^{2+}, Mg^{2+}, Na^{+}, K^{+}) show a similar distribution to TDS. Calcium concentrations average 2.7 meq/L. Higher values were recorded south of Adrano (7–7.8 meq/L), and between Belpasso and Camporotondo (5–7 meq/L) towards the western margin of the volcano. The lowest concentrations were measured south of Paternò and north of Ragalna, on the southwest (<1.5 meq/L). Again, groundwater in the western basin reflects more extensive water-rock interaction due to longer transit and residence times. This may be explained by the rainfall distribution, as maximum precipitation (*i.e.*, groundwater recharge) occurs on the eastern flank of the volcano, contrary to the western flank that receives lower rainfall and consequently shows prolonged interactions between groundwater and the host rock [33].

In particular, Ca^{2+} and K^{+} have a similar distribution, with sharp concentration variations around the region of Paternò. These changes occur over short distances and reflect different aquifers. Higher salinities can be related to contact with alkaline brines discharged by the Paternò mud volcanoes (Salinelle), although groundwater mineralization through permeable faults can still exert some influence.

Magnesium reaches maximum concentrations in the western basin at S.P Clarenza, and over a vast area up to Catania. There exists a close relationship between Mg^{2+} and HCO_3^{-}. This suggests that dissolution caused by CO_2-enriched waters on the host rocks is common to both species. In particular, the source of Mg^{2+} can be explained by the leaching of olivines and pyroxenes from the basaltic rocks in the substrate.

Chloride concentrations range from 0.3 to 17 meq/L. In principle, the abundance of Cl^{-} might be attributed to alteration of the volcanic rocks and to the interaction of groundwater with volcanic gases [3]. As in the case of Na^{+}, maximum Cl^{-} contents (~17.3 meq/L) were measured at S6, near Catania, likely due to mixing with seawater. Figure 5 shows that waters near the coast exhibit a Na/Cl ratio closer to the 1:1 line, unlike samples from the western basin that are partially depleted of Cl^{-}. Seawater intrusion and mixing between shallow groundwater and deep brines could be the reason for these patterns. This is also coincident with [9], who considered both mixing and water-rock interaction to be responsible for the increased salinity of groundwater in Mt. Etna. It is worthy to note that although evaporates do not crop out in the area, their presence beneath the volcanic cover has been hypothesized both from geological and hydrochemical data [21]. These deposits could thus be another contributing factor for Cl^{-} in groundwater.

Maximum concentrations of NO_3^{-} and SO_4^{2-} were observed in the valleys that exist at low elevations in the volcano (e.g., south of Adrano). High concentrations are also visible within the stretch of land south of Giarre to Fiumefreddo, suggesting the leakage of fertilizers into the aquifers. The availability of water resources and the quality of the soils in the lower flanks of the volcano have favored the agricultural exploitation of the region since ancient times. Under conditions of high oxygen, part of the ammonium—sulphate fertilizers applied on the ground would be rapidly converted to NO_3^{-}, which is not sorbed by the negatively charged soil colloids and moves readily to the water table [34]. At higher elevations (e.g., Valle del Bove), the SO_4^{2-}

inputs into groundwater could be controlled by the ascent of volatiles from vapor-dominated systems such as fumaroles rather than anthropogenic effects.

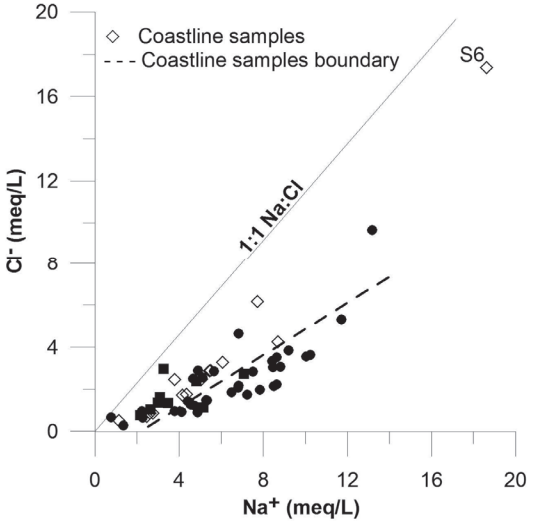

Figure 5. Relation of samples against the Na:Cl ratio.

In summary, groundwater in the area of study can be grouped into four main types: (1) Mg–Na ± Ca–HCO_3^- (with rare Cl^- or SO_4^{2-}) (54%); (2) Na–Mg ± Ca–HCO_3^- ± (SO_4^{2-} or Cl^-) (28%); (3) Na–Ca–Mg–HCO_3^- (12%); and (4) Na–Mg ± Ca–Cl (with HCO_3^- or SO_4^{2-}) (6%). The differences between the first and second group are minor and mainly associated with variations in the Na–Mg and SO_4^{2-}–Cl^- content (with relative concentrations normally higher for the second type). This implies that types "(1)" and "(2)" explain 82% of the waters in the region. Waters of the third group are associated with elevated Ca^{2+} concentrations, while the last type is characterized by high salinity. Samples enriched in Cl^- could be the result of mixing with seawater or solute diffusion from marine clay aquitards.

Additionally, carbonate waters are generally predominant in the western basin, probably due to the interaction with hydrothermal CO_2. In contrast, the Cl^-–SO_4^{2-} type is mainly found along the coast of the eastern basin due to saline influxes. Furthermore, the eastern coast is the area most densely inhabited and some anthropogenic effects are already reflected in the more elevated NO_3^- contents, likely derived from agricultural and urban wastewater (e.g., samples B14, S7, S9, S1).

4.2. Isotopic Signature

The isotopic signature of the sampled waters was also used to determine the recharge areas and circulation pathways in Mt. Etna (Table 2). Values for groundwater and spring samples fall between −4‰ to −9‰ for $\delta^{18}O$ and −19‰ to −53‰ for δ^2H. This is in close correlation with the Global Meteoric line ($\delta^2H = 8 \times \delta^{18}O$ +10‰, [35]) and the eastern Mediterranean local meteoric water line (EMMWL) defined by [36]: $\delta^2H = 8 \times \delta^{18}O + 22‰$, suggesting a predominant meteoric

origin for the collected samples (Figure 6). Similar trends had been reported by [4], who postulated that most waters in Mt. Etna originated as local precipitation infiltrated at an elevation between 1100 and 1900 m. Minor variations in the $\delta^{18}O$ of the samples also suggest limited effects of rock interaction on the original water composition.

Table 2. Typical isotopic composition of Etnean waters.

Sample No.	Sample Type	Basin	DIC $\delta^{13}C$ (PDB ‰)	$\delta^{18}O$ (‰ VSMOW)	$\delta^{2}H$ (‰ VSMOW)
B1	Bore	W	−0.1	−9.1	−51.1
B2	Bore	W	−1.6	−8.6	−45.3
B3	Bore	W	−2.4	−8.6	−47.0
B4	Bore	W	−1.3	−7.8	−41.2
B5	Bore	W	−1.6	−8.6	−45.3
B6	Bore	W	−2.4	−8.6	−47.0
B7	Bore	W	−1.3	−7.8	−41.2
B8	Bore	W	+0.2	−7.4	−38.8
B9	Bore	W	−1.0	−6.6	−38.9
B10	Bore	W	−1.2	−6.7	−28.6
B19	Bore	W	−10.3	−6.8	−36.7
B23	Bore	W	−7.9	−6.1	−29.0
S1	Spring	W	−1.8	−8.6	−50.2
S2	Spring	W	−1.8	−8.6	−50.2
S2-1	Spring	W	−1.2	−8.7	−46.3
S2-2	Spring	W	−0.6	−8.7	−46.6
S3	Spring	W	−0.1	−7.4	−40.1
S4	Spring	W	−0.7	−8.6	−46.6
S5	Spring	W	−0.1	−7.3	−40.1
R	River	W	−7.5	−8.2	−44.4
B11	Bore	E	−1.0	−7.5	−37.4
B12	Bore	E	−4.6	−6.7	−39.3
B13	Bore	E	−8.6	−7.2	−38.9
B14	Bore	E	−1.5	−7.1	−38.6
B15	Bore	E	−2.0	−7.4	−37.5
B16	Bore	E	-	−6.3	−33.0
B17	Bore	E	−1.8	−7.0	−39.1
B18	Bore	E	−4.6	−6.7	−37.7
B20	Bore	E	−9.4	−4.2	−19.2
B21	Bore	E	−14.5	−6.0	−34.3
B22	Bore	E	−6.9	−7.3	−46.7
B24	Bore	E	−7.7	−7.1	−31.5
B27	Bore	E	−1.8	−6.9	−39.1
B28	Bore	E	−5.0	−7.8	−42.2
B29	Bore	E	−5.8	−7.5	−41.2
B30	Bore	E	−9.4	−4.1	−19.2
B31	Bore	E	−14.5	−5.9	−34.3
B32	Bore	E	−6.9	−7.3	−46.7
B33	Bore	E	+0.8	−9.1	−53.3
S6	Spring	E	−11.2	−6.2	−33.7
S7	Spring	E	−11.2	−6.2	−33.7

Table 2. *Cont.*

Sample No.	Sample Type	Basin	DIC $\delta^{13}C$ (PDB ‰)	$\delta^{18}O$ (‰ VSMOW)	$\delta^{2}H$ (‰ VSMOW)
S8	Spring	E	−11.8	−6.7	−37.9
S9	Spring	E	−11.4	−6.7	−38.1
S10	Spring	E	−6.1	−6.9	−36.5
S11	Spring	E	−9.1	−7.1	−35.6
S12	Spring	E	−1.2	-	-
R1	River	E	−5.4	−8.0	−44.9
SM1	Salt mount	Paternò	-	+8.8	−14.5
SM2	Salt mount	Paternò	-	+10.4	−12.0
SM3	Salt mount	Paternò	-	+7.5	−13.6
Sm2a	Salt mount	Paternò	+5.3	+9.78	−18.2
Sm2b	Salt mount	Paternò	+3.0	+10.2	−21.5
Sm2c	Salt mount	Paternò	+1.4	+10.1	−19.8
M1	Seawater	-	-	+1.1	+1.3

A different trend is observed for waters collected in the salt mount brines. The "positive" isotopic ratio of the samples (*i.e.*, $\delta^{18}O$ up to about +10‰, and $\delta^{2}H$ ranging from −21.5‰ to a maximum of −12‰) suggests that these waters could be mixed with hydrothermal fluids of deep origin following a more prolonged interaction with the host rocks.

Figure 6 also evidences the contrast between the mainly meteoric groundwater against Cl-enriched fluids from the salt mounts. As postulated by [4], the anomalous enrichment of Cl^- might be related to the proximity of the sampled bodies to areas of intense magmatic outgassing, where Cl-rich gases are likely to interact with shallow aquifers. Considering that the ratio $Cl/\delta^{18}O$ in the salt mounts is higher than seawater (sample M1), the direct mixing between these two fluids would be improbable.

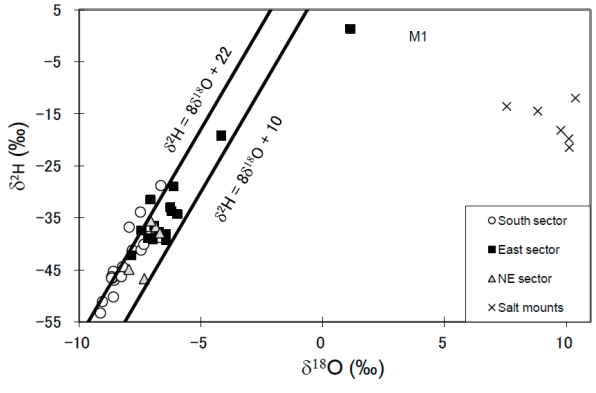

Figure 6. Relation between oxygen and hydrogen isotopic composition in Etnean groundwater.

Additional information may be inferred by assessing the geographical distribution of the stable isotope ratios in the volcano. Waters from the southern flanks of Mt. Etna are relatively homogeneous and generally fit with the EMMWL. In contrast, waters in the eastern sector deviate

from the meteoric line suggesting that more complex processes could take place there. These processes might be associated to heterogeneous recharge and irregular circulation patterns, especially on the alluvial lowlands of the eastern basin, where surface runoff and upward flows could also affect the chemical signature of the waters. These observations are consistent with [4,15]), who described considerably more diversity for waters in the eastern flanks of the volcano.

The isotopic composition of the waters might also be influenced by the terrain elevation, although the relationship is generally limited and not always distinguished (Figure 7). In effect, samples with a lighter isotope composition often coincide with higher elevations towards the cone summit, but the groundwater character still varies considerably, likely in response to additional underlying factors. As clouds rise up the volcano, the heavy isotopes are depleted and the residual precipitation gets isotopically lighter [37]. The most depleted samples would locate in the southern basin where the δ^2H composition approaches −55‰. These differences between the isotopic compositions in the south and other regions of the volcano could be another indication of variations in meteoric inputs and the heterogeneity of the hydrological circuits within Etna. A second trend suggests that waters become lighter from East to West, which is coincident with the main wind direction and the geographical distribution of precipitations. In effect, rainfall amounts peak on the eastern flanks of the Etna, mainly in relation to cooling sea breezes and clouds from the neighbor Mediterranean Sea [8]. The water vapor from the sea and the subsequent clouds and precipitation, are characterized by a high ^2H excess which in turn, is reflected in the composition of the waters [38]. In its migration across the volcano, falling precipitation undergoes fractionation and becomes increasingly lighter.

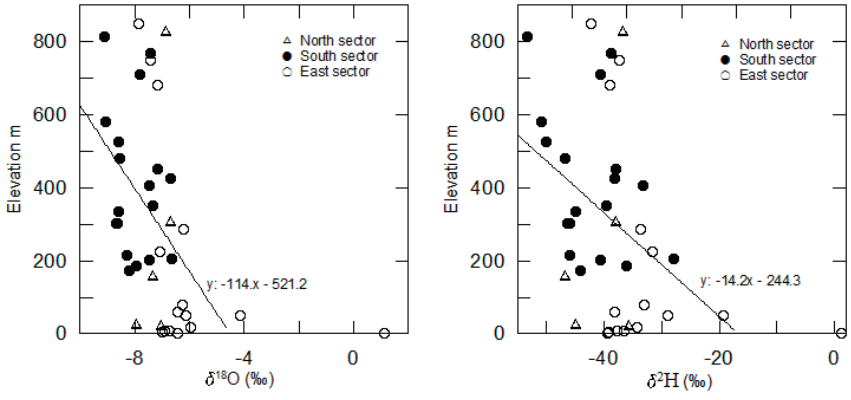

Figure 7. Stable isotopes in groundwater against elevation in the volcano.

Values for $\delta^{13}C$ vary from as low as −14‰ in proximities to the town of Giarre (B31), up to about 5‰ in waters nearby the mud volcanoes of Paternò. Measured values plot above the line of pCO_2 in the atmosphere and largely outside the typical range of groundwater suggesting a contribution of external CO_2 (Figure 8). Given that groundwater in Etna does not come in contact with outcrops or superficial carbonate rocks [14], the prevailing pCO_2 source would be at depth.

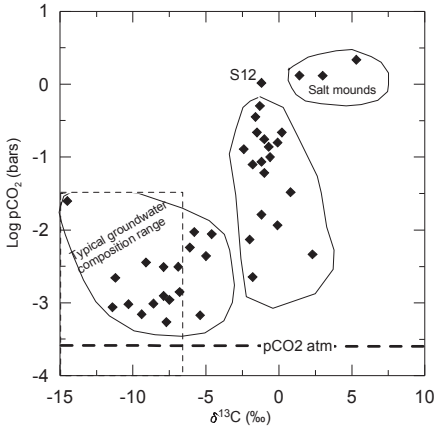

Figure 8. Partial pressure of CO_2 *vs.* $\delta^{13}C$ showing the possible contribution of magmatic gasses. Typical groundwater composition within the dashed area.

Under low HCO_3^- concentrations, $\delta^{13}C$ values range broadly from −2‰ to −15‰ (Figure 9). An increase in HCO_3^- (>10 meq/L) is coincident with $\delta^{13}C$ in the range of −2.4‰ and +2.3‰, with most samples clustering around −1.5‰. In such conditions, the equilibrium between HCO_3^- and CO_2 causes the isotopic composition of the latter species to become more positive. Therefore, the Etnean magmatic CO_2 becomes isotopically heavier [39]. This pattern suggests some additional inputs of CO_2, possibly related to hydrothermal fluids that stripped the gasses from a magmatic reservoir and transported them into the shallow aquifers. In such conditions, the rise of CO_2 would lower the pH of the circulating waters and result in higher concentration of dissolved HCO_3^- after weathering the host rocks. Thus, many waters in the studied area might be partially influenced by this secondary CO_2 despite their overall meteoric origin.

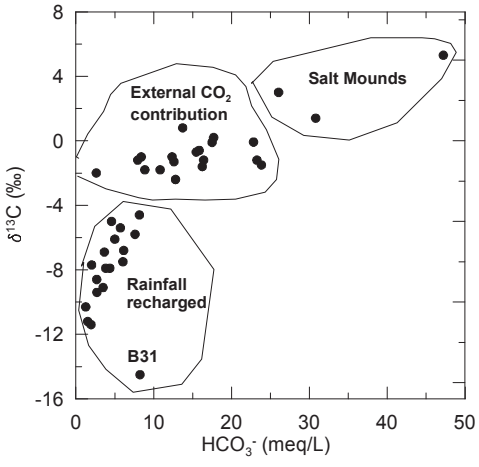

Figure 9. Change in groundwater composition in relation to the HCO_3^- and $\delta^{13}C$ concentrations.

In short, two major groundwater groups can be discriminated on the basis of $\delta^{13}C$: (1) waters with compositions below −4.6‰, mainly recharged by direct percolation of rainfall; (2) waters with $\delta^{13}C > -2.4$‰ in a stretch of land between Adrano and Misterbianco in the south, and around Pozillo to the east, that include a component of external dissolved gas. This trend suggests that the diffusion of CO_2 gasses in Mt. Etna is unevenly distributed, and essentially controlled by the main tectonic structures of the volcano. During their ascent to the surface, these gases interact in different ways with shallow water-bearing strata changing their concentrations as they cross the aquifers [23].

It is worthy to note that a more particular isotopic signature was recorded at the "Salinelle di Paternò". In these mud volcanoes, the $\delta^{13}C$ compositions ranged from 1.4‰ to 5.3‰ while the pCO_2 values varied from 1.3 to 2.2 bars. The enrichment in CO_2 and the high "positives" stable isotopic ratio observed ($\delta^{2}H \sim -12$‰ and $\delta^{18}O \sim 10.4$‰) seem to indicate a very deep origin of these fluids.

5. Summary and Conclusions

A new survey dataset of major ion concentrations and isotope ratios was used to update the knowledge of geochemical characteristics of groundwaters and to better understand the flow system around Mt. Etna. The Etnean groundwaters possess a marked bicarbonate-alkaline chemistry, which is consistent with an abundance of dissolved CO_2 gas and the composition of the volcanic host rocks. Chloride-sulphate and nitrate dominated waters can locally prevail along the Ionian Sea coast, largely due to urban contamination and the leakage of agricultural fertilizers. Other distinctive characteristics of the sampled waters include low temperatures, high conductance, and elevated hardness. The salinity of the waters decreases with elevation due to the proximity to recharge areas and shorter travel paths. Oxygen-deuterium isotopes showed that waters are essentially recharged by infiltrating rainfall. Especially to the south, most of the samples display a good correlation with the eastern Mediterranean meteoric water line. To the east, collected samples deviate from the meteoric line, suggesting more heterogeneous circulation paths, and variable degrees of interaction between meteoric waters and the aquifer rocks.

Furthermore, the isotope composition is influenced by the provenance of wet air masses from the Mediterranean Sea. In this regard, waters become isotopically lighter to the west, following the distribution of precipitation on the volcano. Similarly, the liquid-vapor fractionation of waters results in lighter waters along with an increase in elevation or in proximity to the cone summit.

The analysis of $\delta^{13}C$ indicates that at least a proportion of the waters, mainly in the southern region of the volcano, would be affected by external CO_2 contributions, possibly of hydrothermal origin. This is also supported by pCO_2 values 1 to 3 orders of magnitude higher than those expected for waters in equilibrium with the atmosphere. Furthermore, a high enrichment in CO_2 along with high positive values for $\delta^{2}H/\delta^{18}O$ suggest that waters in the salt mounts around Paternò would be influenced by brines originating at depth within the system.

Acknowledgments

The authors are deeply grateful to Gaetano Punzi, current Director of the Regional Geological Office for Land Reclamation, Sicily, for his help throughout the field work. This paper would never have been achieved without him. Many thanks also to Glenn Harrington, Adjunct Supervisor in the National Centre for Groundwater Research and Training, Flinders University, and Principal Hydrogeologist at Innovative Groundwater Solutions Pty Ltd, Australia, for his comments and assistance to improve the manuscript. The authors also wish to thank John Luczaj, and two anonymous reviewers for their suggestions and useful discussions. Special thanks to the AIST, Geological Survey of Japan for allowing us to use its facilities and equipment for the chemical analyses.

Author Contributions

Carmelo Bellia focused on the field work, laboratory analyses and interpretation of results. Adrian Gallardo collaborated with the interpretation of results and the manuscript preparation. Masaya Yasuhara and Kohei Kazahaya supervised the technical aspects of the program and worked on the data analysis and interpretation.

Conflicts of Interest

The authors declare no conflict of interest.

References

1. Gerlach, T.M. Etna's greenhouse pump. *Nature* **1991**, *315*, 352–353.
2. D'Alessandro, W.; Bellomo, S.; Bonfanti, P.; Brusca, L.; Longo, M. Salinity variations in the water resources fed by the Etnean volcanic aquifers (Sicily, Italy): Natural *vs.* anthropogenic causes. *Environ. Monit. Assess.* **2011**, *173*, 431–446.
3. Giammanco, S.; Ottaviani, M.; Valenza, M.; Veschetti, E.; Principio, E.; Giammanco, G.; Pignato, S. Major and trace elements geochemistry in the ground waters of a volcanic area: Mount Etna (Sicily, Italy). *Water Res.* **1998**, *32*, 19–30.
4. Pennisi. M; Leeman, W.P.; Tonarini, S.; Pennisi, A.; Nabelek, P. Boron, Sr, O, and H isotope geochemistry of groundwaters from Mt. Etna (Sicily)—Hydrologic implications. *GCA* **2000**, *64*, 961–974.
5. D'Alessandro, W.D.; Federico, C.; Longo, M.; Parello, F. Oxygen isotope composition of natural waters in the Mt Etna area. *J. Hydrol.* **2004**, *296*, 282–299.
6. Liotta, M.; Grassa, F.; D'Alessandro, W.; Favara, R.; Gagliano Candela, E.; Pisciotta, A.; Scaletta, C. Isotopic composition of precipitation and groundwater in Sicily, Italy. *Appl. Geochem.* **2013**, *34*, 199–206.
7. Catalano, R.; Imme, G.; Mangano, G.; Morelli, D.; Giammanco, S. Natural tritium determination in groundwater on Mt Etna (Sicily, Italy). *J. Radioanal. Nucl. Chem.* **2014**, *299*, 861–866.

8. Chester, D.K; Duncan, A.M.; Guest, J.E.; Kilbum, C.R.J. *Mount Etna: The Anatomy of a Volcano*; Stanford University Press: Stanford, CA, USA, 1985.
9. Aiuppa, A.; Bellomo, S.; Brusca, L.; D'Alessandro, W.; Federico, C. Natural and anthropogenic factors affecting groundwater quality of an active volcano (Mt. Etna, Italy). *Appl. Geochem.* **2003**, *18*, 863–882.
10. Clocchiatti, R.; Schiano, P.; Ottolini, L.; Bottazzi, P. Earlier alkaline and transitional magmatic pulsation of Mt. Etna volcano. *Earth Planet. Sci. Lett.* **1998**, *132*, 25–41.
11. Tanguy, J.C.; Condomines, M.; Kieffer, G. Evolution of Mount Etna magma: Constraints on the present feeding system and eruptive mechanism. *J. Volcanol. Geotherm. Res.* **1997**, *75*, 221–250.
12. Pering, T.D.; Tamburello, G.; Aiuppa, A.; McGonigle, A.J.S. The First Record of a High Time Resolution Carbon Dioxide Flux for the North-East Crater of Mount Etna. In Proceedings of the IAVCEI 2013 Scientific Assembly, Kagoshima, Japan, 20–24 July 2013.
13. McGee K.A.; Delgado H.; Cardenas Gonzales, L.; Venegas Mendoza, J.J.; Gerlach, T.M. High CO_2 emission rates at Popocatepetl volcano, Mexico. In Proceedings of the Abstracts AGU Fall Meeting, Baltimore, MD, USA, 29 May–2 June 1995.
14. Ogniben, L. Lineamenti idrogeologici dell'Etna. *Riv. Min. Sicil.* **1966**, *100–102*, 151–174. (In Italian)
15. Ferrara, V. Valutazione della vulnerabilità degli acquiferi. In *Carta della vulnerabilità all'inquinamento dell'acquifero vulcanico dell'Etna*; Civita M., Ed.; SELCA: Firenze, Italy, 1990. (In Italian)
16. Aureli, A. Idrogeologia del fianco occidentale etneo. In Proceedings of the 2nd International Congress on Underground Waters, Palermo, Italy, 28 April–1 May 1973; pp. 425–487. (In Italian)
17. Schilirò, F. Proposta metodologica per una zonazione geologicotecnica del centro abitato di Maletto. *Geol. Tec.* **1988**, *3*, 32–53. (In Italian)
18. Ferrara, V. Idrogeologia del versante orientale dell'Etna. In Proceedings of the 3rd international symptom on groundwaters, Palermo, Italy, 1–5 November 1975; pp. 91–134. (In Italian)
19. Aiuppa, A.; Allard, P.; D'Alessandro, W.; Giammanco, S.; Parello, F.; Valenza, M. Review of magmatic gas leakage at Mount Etna (Sicily, Italy): Relationships with the volcano-tectonic structures, the hydrological pattern and the eruptive activity. In *Etna Volcano Laboratory*; Calvary, S., Bonaccorso, A., Coltelli, M., Del Negro, C., Falsaperla, S., Eds.; Geophysical Monography Series AGU: Washington, DC, USA, 2004; Volume 143.
20. Kozlowska, B.; Morelli, D.; Walencik, A.; Dorda, J.; Altamore, I.; Chieffalo, V.; Giammanco, S.; Imme, G.; Zipper, W. Radioactivity in waters of Mt. Etna (Italy). *Radiat. Meas.* **2009**, *44*, 384–389.
21. Anza, S.; Dongarra, G.; Giammanco, S.; Gottini, V.; Hauser, S.; Valenza, M. Geochimica dei fluidi delI'Etna. *Miner. Petrogr. Acta* **1989**, *32*, 231–251. (In Italian)
22. Allard, P. Endogenous magma degassing and storage at Mount Etna. *Geophys. Res. Lett.* **1997**, *24*, 2219–2222.

23. D'Alessandro, W.D.; de Gregorio, S.; Dongarra, G.; Gurrieri, S.; Parello, F.; Parisi, B. Chemical and isotopic characterization of the gases of Mount Etna (Italy). *J. Volcanol. Geotherm. Res.* **1997**, *78*, 65–76.
24. Nakai, S.; Wakita, H.; Nuccio, P.M.; Italiano, F. MORB-type neon in an enriched mantle beneath Etna, Sicily. *Earth Planet. Sci. Lett.* **1997**, *153*, 57–66.
25. Spilliaert, N.; Allard, P.; Métrich, N.; Sobolev, A.V. Melt inclusion record of the conditions of ascent, degassing, and extrusion of volatile-rich alkali basalt during the powerful 2002 flank eruption of Mount Etna (Italy). *J. Geophys. Res.* **2006**, *111*, doi:10.1029/2005JB003934.
26. Hirn, A.; Nicolich, R.; Gallart, J.; Laigle, M.; Cernobori, L.; ETNASEIS Scientific Group Roots of Etna volcano in faults of great earthquakes. *Earth Planet. Sci. Lett.* **1997**, *148*, 171–191.
27. Giammanco, S.; Bonfanti, P. Cluster analysis of soil CO_2 data from Mt. Etna (Italy) reveals volcanic influences on temporal and spatial patterns of degassing. *Bull. Volcanol.* **2009**, *71*, 201–218
28. Camarda, M.; de Gregorio, S.; Gurrieri, S. Magma-ascent processes during 2005–2009 at Mt. Etna inferred by soil CO_2 emissions in peripheral areas of the volcano. *Chem. Geol.* **2012**, *330–331*, 218–227.
29. Giammanco, S.; Neri, M. Rapporto sull'attività parossistica della Salinella dello Stadio di Paternò. In *UF Vulcanologia e Geochimica*; INGV Sezione de Catania: Sicily, Italy, 2005. (In Italian)
30. Anza, S.; Badalamenti, B.; Giammanco, S.; Gurrieri, S.; Nuccio, P.M.; Valenza, M. Preliminary study on emanation of CO_2 from soils in some areas of Mount Etna (Sicily). *Acta Vulcanol.* **1993**, *3*, 189–193.
31. Giammanco, S.; Gurrieri, S.; Valenza, M. Soil CO_2 degassing on Mt. Etna (Sicily) during the period 1989–1993: Discrimination between climatic and volcanic influences. *Bull. Volcanol.* **1995**, *57*, 52–60.
32. Brusca, L.; Aiuppa, A.; D'Alessandro, W.; Parello, F.; Allard, P.; Michel, A. Geochemical mapping of magmatic gas-water-rock interactions in the aquifer of Mount Etna volcano. *J. Volcanol. Geotherm. Res.* **2001**, *108*, 199–218.
33. D'Alessandro, W.; Federico, C.; Aiuppa, A.; Longo, M.; Parello, F.; Allard, P.; Jean-Baptiste, P. Groundwater circulation at Mt Etna: Evidenses from ^{18}O, ^{2}H and ^{3}H contents. In Proceedings of the 10th International Symposium on Water-Rock Interaction, Villasimius, Italy, 10–15 June 2001.
34. Follet, R.F. Fate and Transport of Nutrients: Nitrogen. In *Agricultural Research Service, Soil-Plant-Nutrient Research Unit*; Working Paper No. 7; United States Department of Agriculture: Fort Collins, CO, USA, 1995; p. 33.
35. Craig, H. Isotopic variations in meteoric waters. *Science* **1961**, *133*, 1702–1703.
36. Gat, J.R.; Carmi, H. Evolution of the isotopic composition of atmospheric waters in the Mediterranean Sea area. *J. Geophys. Res.* **1970**, *75*, 3039–3040.
37. Mazor, M. *Chemical and Isotopic Groundwater Hydrology*; Marcel Dekker Publisher: New York, NY, USA, 1991.

38. Gat, J.R.; Klein, B.; Kushnir, Y.; Roether, W.; Wernli, H.; Yam, R.; Shemesh, A. Isotope composition of air moisture over the Mediterranean sea: An index of the air—Sea interaction pattern. *Tellus. Ser.* **2003**, *B55*, 953–965.
39. Caracausi, A.; Italiano, F.; Paonita, A.; Rizzo, A.; Nuccio, P.M. Evidence of deep magma degassing and ascent by geochemistry of peripheral gas emissions at Mount Etna (Italy): Assessment of the magmatic reservoir pressure. *J. Geophys. Res.* **2003**, *108*, doi:10.1029/2002JB002095.

The Energy-Water Nexus: Spatially-Resolved Analysis of the Potential for Desalinating Brackish Groundwater by Use of Solar Energy

Jill B. Kjellsson and Michael E. Webber

Abstract: This research looks at coupling desalination with renewable energy sources to create a high-value product (treated water) from two low value resources (brackish groundwater and intermittent solar energy). Desalination of brackish groundwater is already being considered as a potential new water supply in Texas. This research uses Texas as a testbed for spatially-resolved analysis techniques while considering depth to brackish groundwater, water quality, and solar radiation across Texas to determine the locations with the best potential for integrating solar energy with brackish groundwater desalination. The framework presented herein can be useful for policymakers, regional planners, and project developers as they consider where to site desalination facilities coupled with solar photovoltaics. Results suggest that the northwestern region of Texas—with abundant sunshine and groundwater at relatively shallow depths and low salinity in areas with freshwater scarcity—has the highest potential for solar powered desalination. The range in capacity for solar photovoltaic powered reverse osmosis desalination was found to be 1.56×10^{-6} to 2.93×10^{-5} cubic meters of water per second per square meter of solar panel ($m^3/s/m^2$).

Reprinted from *Resources*. Cite as: Kjellsson, J.B.; Webber, M.E. The Energy-Water Nexus: Spatially-Resolved Analysis of the Potential for Desalinating Brackish Groundwater by Use of Solar Energy. *Resources* **2015**, *4*, 476–489.

1. Introduction

The relationship between the water and energy sectors—for example the energy required to distribute, collect, and treat water and wastewater and the water required to extract and process fossil fuels and to generate electricity—is of increasing interest to policymakers and planners. A growing population has placed a stress on water resources, which is exacerbated by an increased demand for water for energy production. The decreasing water quality and increasing depth and distance to raw water sources increases the strain that is already on the available water supply. As regions look at more energy intensive options such as conveying water greater distances and treating lower quality water with technologies such as desalination, the energy required to treat and transport raw water increases. Since constraints on one of these two resources exacerbate the strains on the other, solutions to the problem of limited resources often address both constraints simultaneously.

As population and water demand increase, there is a need for new freshwater sources. Because brackish water is abundant, desalination of brackish water represents one possible alternative supply. However, desalination is an energy intensive treatment method which remains an inhibitor to its broader adoption. At the same time, concerns about carbon emissions and their effects on the climate favor the use of renewable energy over conventional fossil fuels. However, renewable energy

technologies such as wind and solar are intermittent, which can present a challenge to grid operation if large-scale storage (such as batteries, pumped hydroelectric, or compressed air energy storage) is not available [1]. One possible solution is to couple solar photovoltaic (PV) with desalination that can be operated intermittently, such that stored, treated water is a proxy for energy storage. At the same time, using the water facility only when solar power is available reduces fluctuations in power supply to the electric grid, adding value to the integrated facility.

This research evaluates the potential of co-locating desalination plants for inland brackish groundwater treatment and solar PV generation. This project explores the spatial component using Geographic Information Systems (GIS) to assess the co-location of solar and brackish groundwater resources to estimate the potential for an integrated facility to solve several problems simultaneously. Because Texas has an isolated electric system, growing population, water scarcity, and an abundance of solar energy and brackish groundwater, it is used as a testbed for this analysis. However, the approach developed here is applicable outside Texas. Using temporally and spatially resolved solar irradiance and brackish groundwater depth and quality data, a framework was developed to evaluate these resources. This framework is intended to be useful for policy makers, regional planners and project developers as they look towards alternative water supply in water stressed areas.

Literature surrounding the technical and economical aspects of coupling desalination and solar PV exist, as does research on the availability of these resources. The coupling of desalination with renewable energy is also a growing field of research [2,3]. Similar research has also been conducted on the sustainable siting of co-located seawater desalination facilities with solar PV factoring in technical, social and economical impacts such as solar insolation, ocean salinity, water temperature, water stress, population and ability to pay [4], as has research on resource optimization of wind-powered brackish groundwater RO desalination [5]. What is lacking from the literature is methodologies for determining the optimal locations of co-located facilities for brackish groundwater reverse osmosis (RO) and PV based on resource characteristics at a given location. This research aims to fill that knowledge gap. While the authors are aware of the environmental concerns associated with greenhouse gas emissions and disposal of the brine waste stream, the aim of this paper is not to address these issues but rather to deliver a framework for the geographic analysis of the solar and water resources impacting a coupled PV-RO facility.

2. Background on Solar-Powered Desalination and Brackish Groundwater

While the population in Texas is expected to grow 82% from 2010 to 2060, water use is estimated to grow only 22% due to decreases in agricultural water use from efficiency improvements and municipal water use from conservation measures [6]. Municipal water demand is expected to increase from 4.9 million acre-feet in 2010 to 8.4 million acre-feet in 2060 while natural fresh water supplies are estimated to decrease 10% over this period [6]. Therefore, at the current rate of production and consumption, future supplies of water will not meet future demand unless alternative sources are tapped. Given the existing strain on freshwater along with a wealth of solar and brackish water resources, this research will focus on Texas as a testbed; however, the research methodology and results will be broadly applicable to areas with similar resources and prevailing conditions.

Texas has an abundance of brackish groundwater, thought to be more than 2.7 billion acre-feet [7], which can possibly be desalinated and used to meet public needs. Brackish groundwater is defined as water with a total dissolved solids (TDS) concentration of 1000 to 10,000 mg/L. For comparison, seawater has a TDS concentration of 35,000 mg/L. The Texas Commission on Environmental Quality (TCEQ) has set a primary standard concentration for TDS of 500 mg/L and a secondary standard of 1000 mg/L for public use [7].

RO is the most common type of desalination technology worldwide, accounting for 60% of desalination capacity in 2010 [8]. In Texas, RO accounts for 80% of desalination systems in operation [9]. RO applies pressure to a solution on one side of a selective membrane to reverse the natural flow of solvent to the side with higher solute concentration. The solute remains, while the pure solvent passes to the other side, thereby producing freshwater. Electrodialysis, a less common desalination method accounting for 3.6% of desalination capacity worldwide in 2010 [8], uses electromotive forces applied to electrodes that are adjacent to both sides of a membrane to purposely move salt ions through the membrane leaving behind freshwater. ED is best applied to treatment of brackish-water with TDS up to 5000 mg/L and is not economical for higher concentrations [10], except in cases where ED is used for partial treatment [11]. Both methods are used coupled with PV systems [10]. RO and ED are the most common forms of desalination to be coupled with PV [10]. Thermal methods of desalination, accounting for 34.8% of desalination worldwide in 2010 [8], are not well-suited for coupling with PV because they are heat-based as opposed to electricity-driven.

PV cells are a rapidly growing technology with costs decreasing over time. The price of solar PV modules in 1987 was roughly $9/W [12]. From 1998 to 2011 the price fell from $4.90/W to $1.28/W [13]. Typical PV levelized cost of energy (LCOE) are in the range of $0.20–$0.40/kWh for low latitudes with high insolation of 2500 kWh/m^2/year, $0.30–$0.50/kWh for 1500 kWh/m^2/year (which is typical of Southern Europe), and $0.50–$0.80 per kWh for high latitudes with 1000 kWh/m^2/year [12].

In Texas, the solar energy potential, or the amount of solar radiation available to a solar PV cell, ranges from 872 to 1310 kWh/m^2/year during the winter and from 2150 to 2884 kWh/m^2/year during the summer [14]. The high end of the range corresponds to the western portion of the state while the low end corresponds to the eastern portion of the state. Annual average global tilt solar radiation across Texas is shown in Figure 1. There is a range from 4.76 kWh/m^2/day to 6.58 kWh/m^2/day from east to west.

The most common combination of renewable energy and desalination employed worldwide is PVRO, and accounts for 31% of renewable energy-powered desalination installation [16]. If solar energy can be located near the desalination plant, using solar panels directly for desalination eliminates the need to incorporate solar energy into the grid, although grid interconnectedness provides support for the system and could allow for continuous operation of the desalination plant.

The energy intensity of desalinating brackish groundwater has been estimated to be 0.5–3 kWh/m^3 of product (or treated) water [17] while other sources estimate this value to be 1–2.5 kWh/m^3 of product water [18]. The energy requirement is proportional to the TDS concentration as well as the depth to the groundwater source. There are currently 46 brackish water desalination plants in Texas [19]. Twelve of these facilities treat brackish surface water and account

for a design capacity of 50 million gallons per day (56,000 acre-feet per year) [19]. Thirty-four of these facilities use brackish groundwater as their raw water source, which acounts for a design capacity of 73 million gallons per day (81,760 acre-feet per year) [19]. In the 2012 State Water Plan, 5 out of 16 regional water planning groups recommended brackish groundwater desalination as a water management strategy, accounting for 181,568 acre-feet by the year 2060 [19]. Desalination plants currently in operation in Texas are spread throughout the state, as shown in Figure 2. Only the northern portion of the state, known as the panhandle, does not have desalination facilities.

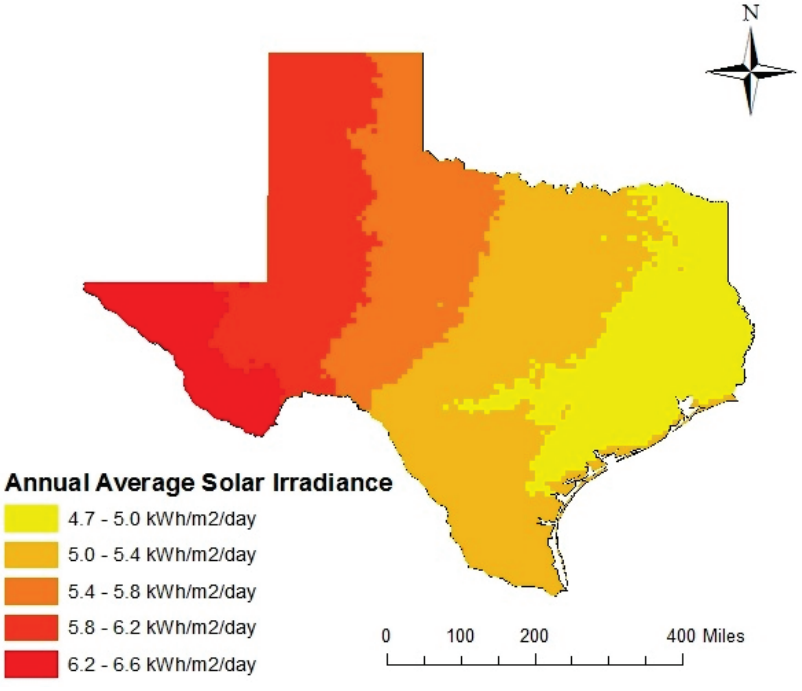

Figure 1. Global tilt solar radiation across Texas from the National Renewable Energy Laboratory (NREL)'s National Solar Radiation Database dataset [15].

This research focuses on RO desalination since the majority of desalination facilities in Texas already utilize this technology. PV cells will be the primary focus of solar power generation because PV technology can produce energy from both direct and diffuse radiation as opposed to other concentrating solar power (CSP) technologies, which can only make use of the direct radiation. Diffuse radiation is the radiation that is scattered from the direct beam by the atmosphere. Integrating PV with desalination and using water storage as a proxy for energy storage can advance the implementation of these two technologies by each one solving the problems of the other.

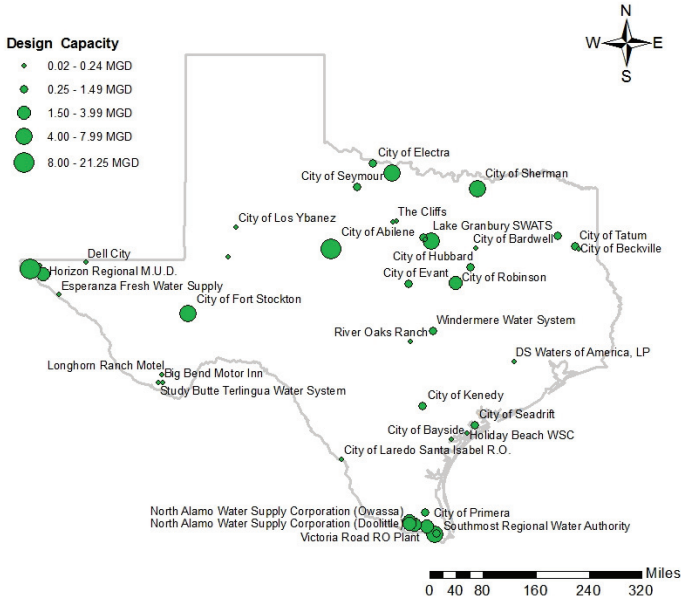

Figure 2. Existing desalination plants and their design capacities in Texas.

3. Data and Methodolgy

3.1. Data

Data for this research was obtained from the following two sources: The Texas Water Development Board's (TWDB) Groundwater Database [20] and the National Renewable Energy Laboratory's (NREL) National Solar Radiation Database (NSRD) [15]. The TWDB database was used to acquire well location coordinates, well depth, and well total dissolved solids (TDS) concentrations for wells with well depths in the range of 100–12,000 feet and TDS concentrations in the range of 1000–30,000 mg/L. TDS range was selected to correspond to brackish water. Available for download online, NREL data provides monthly and average daily total solar resource averaged over cells of 0.1 degrees in both latitude and longitude, or nearly 10-km in size, using 1998–2005 data and projected using 1983 North American geographic coordinate system. For this research, the global tilt radiation was used, which is the total (direct and diffuse) radiation on a tilted surface.

3.2. Methodology

This research was carried out by first determining the spatial variability of brackish water resources and of well characteristic data. Next, an integrated analysis was conducted to estimate the solar-powered desalination capacity across Texas as a function of different factors which included solar radiation, well depth and TDS concentration.

3.2.1. Model Assumptions

The following assumptions were made in carrying out this research: the efficiency of solar PV panels was assumed to be 15% for calculating the power generation from solar PV panels as reported by industry as a typical efficiency [13], a pump efficiency of 65% was assumed based on literature [5], and a specific gravity of 9.81×10^3 N/m^3 was assumed for calculating the power requirements of desalination [5].

3.2.2. Spatial Variability of Brackish Groundwater Well Characteristics and Solar Resources

Brackish water wells with depths in the range of 100–12,000 feet across Texas were analyzed using the software program ArcGIS [21]. Locations were provided in decimal degree units and were projected using North American 1983 geographic coordinate system. Using the "Spherical Kriging Interpolation" tool in ArcGIS, the well depth and TDS concentration was estimated for locations across Texas and projected to two different rasters. Using "Extract by Mask" tool and an outline of Texas layer imported from ArcGIS online, the output was fit to Texas. Using the "Project Raster" tool, the rasters were projected to USA Contiguous Albers Equal Area Conic spatial reference in order to preserve the area. This spatial reference will be important in later use of the rasters with the "Raster Calculator" tool. In order to prepare the solar data for raster calculation, the data from NREL was converted to a raster using the "Polygon to Raster" tool.

3.2.3. Potential Capacity of Solar-Powered Desalination

The power requirements of desalination by RO depends on the RO and pumping power requirements. It is assumed that the desalination facility is located at the well so that power required for the transportation of brackish groundwater is negligible. Thus, the power for desalination can be expressed by Equation (1) [5]:

$$W_{\text{desalination}} = W_{\text{RO}} + W_{\text{pumping}} \tag{1}$$

where

$W_{\text{desalination}}$ = Power needed for desalination, W

W_{RO} = Power needed for RO treatment, W

W_{pumping} = Power needed to pump brackish groundwater to the surface, W

The following Equation (2) is an extended version of Equation (1) with the equations for RO and pumping energy substituted into the Equation [5]:

$$W_{\text{desalination}} = \left(\frac{v \times \gamma \times WD}{\eta_{\text{pump}}}\right) + \left(\frac{1{,}000\ N\ L}{m^2\ mg} \times v \times (TDS_{\text{in}} - TDS_{\text{out}})\right) \tag{2}$$

where

γ = specific weight of water, N/m^3

WD = well depth, m

η_{pump} = net efficiency of pump and motor system

TDS_{in} = TDS of feed water, mg/L
TDS_{out} = TDS of treated water, mg/L (desired water quality, 500 mg/L)
v = volumetric flow rate of feed water, m^3/s

The coefficient of the second part of the equation, 1000 N L/m^2 mg , was changed from the cited authors' work to reflect the empirical data for the energy intensity of brackish groundwater desalination in Texas [22]. The authors appear to have used a theoretical minimum value in the equation based on the theoretical power requirements to overcome osmotic pressure. For this research, the authors have chosen to modify the equation to reflect the empirical data from the Kay Bailey Hutchison brackish groundwater desalination plant in El Paso, Texas to more accurately predict the energy requirements. The coefficient was interpreted from the enegy intensity and TDS data.

Equation (3) is used for the calculation of power generation from PV [23]:

$$W_{PV} = \eta_{PV} \times GTR \times A_{PV} \times \frac{day}{24\ h} \tag{3}$$

where

W_{PV} = operating electrical power, W
η_{PV} = Efficiency of electrical power operating subsystem
GTR = Global tilt radiation, $Wh/m^2/day$
A_{PV} = Surface area of PV cell, m^2

Setting the operating electrical power generated by PV cells (Equation (3)) equal to the power requirements of desalination (Equation (2)) and solving for the flow rate, v (assuming there is no battery included in the PV system) yields the following Equation (4):

$$v = \frac{\eta_{PV} \times GTR \times A_{PV} \times \frac{day}{24\ h}}{\left(\frac{\gamma \times WD}{\eta_{pump}}\right) + \left(\frac{1{,}000\ N\ L}{m^2\ mg} \times (TDS_{in} - TDS_{out})\right)} \tag{4}$$

Equation (4) suggests that if well depth is small, incoming total dissolved solids concentration is small, and the solar radiation is high then the amount of water that can be treated is higher than in places where sunshine is less prevalent, wells are deeper, and water is more saline.

Using the "Raster Calculator" tool in GIS, the well depth, TDS concentration, and solar radiation rasters from the previous two steps in this analysis could be used in the equation to solve for the potential treatment (as a flow rate, v) for different locations based on their local water and solar conditions. The output is also in raster form. Having the rasters projected to the same spatial reference in the previous steps allowed for the mathematical operations used in raster calculator to be performed on a cell by cell basis, *i.e.*, for every location across Texas.

While the raster shows the variance across Texas, it can be desirable to know a more precise location of the optimal events as well as the values of the variables that resulted in that output. In order to determine these values, the output raster was converted back to points using the "Raster to Point" tool and X, Y coordinates were added using the "Add XY Coordinates" tool.

4. Results and Analysis

Brackish water wells with depths in the range of 100–12,000 feet and TDS in the range of 1000–30,000 mg/L across Texas are depicted on the maps in Figures 3 and 4. Figure 3 shows the wells with greater well depths with larger blue circles and Figure 4 shows the same wells with the larger red circles representing higher TDS concentrations.

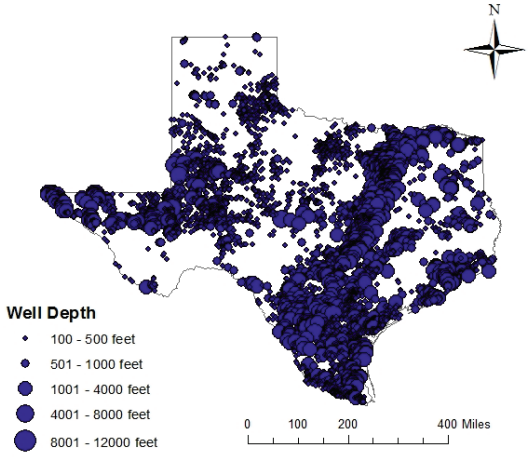

Figure 3. Each dot represents a well from the Texas Water Development Board (TWDB) database. The larger dots represent greater distances to brackish water level.

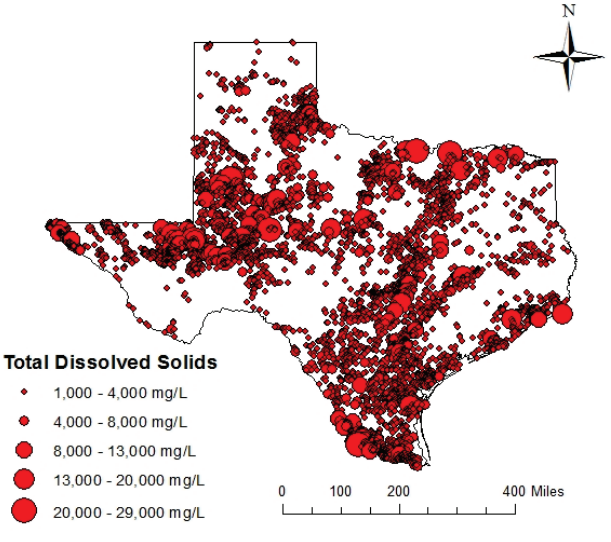

Figure 4. Each dot represents a well from the TWDB database. The larger dots represent higher total dissolved solids concentration for that well.

Wells appear to be concentrated in the southern tip of Texas and along the coast as well as in the northwestern portion of the state. Well depth and TDS concentrations seem to be uniformly spread in these regions. The depth and TDS concentrations of the wells was also depicted after interpolation across the state was performed as a way to predict the depth and TDS concentration at any location across Texas based on the known values for existing wells, as shown in Figures 5 and 6.

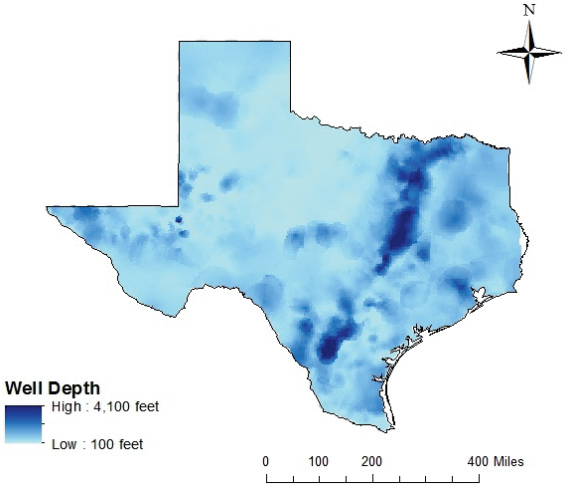

Figure 5. The depth of wells across Texas after interpolation was used to estimate well depth for areas without data.

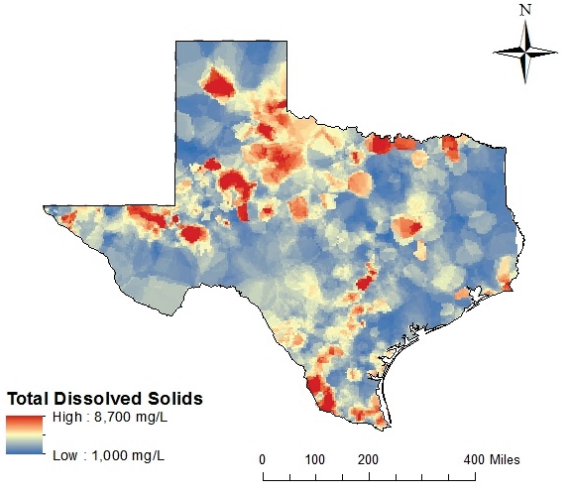

Figure 6. The total dissolved solids concentration of the brackish groundwater across Texas after interpolation was performed to estimate total dissolved solids (TDS) concentrations for areas without data.

Figure 7 shows the capacity (as a volumetric flow rate, v) that one square meter of PV array could produce and the location of the six highest calculated capacities. Table 1 shows the values of the variables that resulted in these highest capacities.

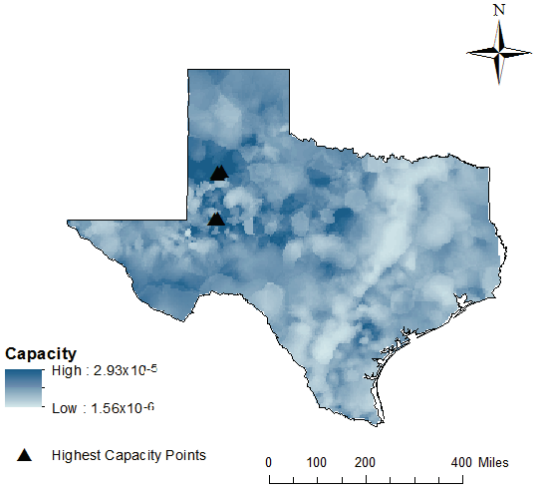

Figure 7. Desalination capacity across Texas calculated using well characteristic and solar radiation data.

Table 1. Variable Values for Six Points with the Highest Capacities.

Longitude (Decimal Degrees)	Latitude (Decimal Degrees)	Capacity (m^3/s)	TDS (mg/L)	Well Depth (m)	GTR ($Wh/m^2/day$)
–102.1313625	33.42166	2.927×10^{-5}	1142	42.4	6008
–102.1313625	33.3767	2.923×10^{-5}	1141	42.5	5998
–102.1313625	32.02784	2.889×10^{-5}	1142	43.4	5992
–102.1313625	32.0728	2.888×10^{-5}	1142	43.4	5992
–101.9964763	33.46663	2.886×10^{-5}	1173	41.0	5968
–102.2212867	32.02784	2.850×10^{-5}	1157	44.0	6024

The framework for the optimization performed is important because it helps tease out the non-obvious tradeoffs. While it might appear obvious that low salinity, shallow depths to brackish groundwater and high solar insolation would be ideal, they might not be available at the same location. In instances when they are not, it can be difficult to know which variable plays a less important role and to what degree. Optimization helps to answer these questions.

5. Discussion and Conclusions

Using the methodology presented herein, a PV system covering an area of 1 m^2 is capable of producing roughly 2.93×10^{-5} m^3/s in some regions of Texas if located where optimal conditions are present. These optimal conditions include low well depth, low TDS and high solar radiation. By using PV to power the pumping and RO processes that are a part of desalination, the negative impacts of carbon emissions from such an energy-intensive process are reduced compared to if conventional fossil fuel sources are used.

Interestingly, locations with deeper wells also have higher TDS concentrations. However, this is not always the case, as is evident in the northern region. The area with deeper wells across Texas going from the southwest to the northeast part of the state follows along Interstate 35. While it is not certain, this could be because there is a lot of development along Interstate 35, including some of Texas' largest cities such as Dallas, Fort Worth, Austin and San Antonio. The Trinity and Carrizo-Wilcox aquifers, two of Texas' major aquifers, also run a similar path across Texas. The Balcones Escarpment, or Balcones Fault, runs from the southwest of Texas and up, also following a similar path through Texas. While there might be a correlation between the area of deeper wells across Texas, the natural land and water systems, and the development along it, the authors merely wish to point out these patterns but did not evaluate their relationship.

More than providing information for Texas, this research presents a framework for analyzing the optimal locations of a co-located desalination facility and PV array by optimizing the utilization of the combination of resources available. This method could be applied to other locations where the input conditions are very different to help planners and others who must contemplate options for where to site water treatment facilities. This analysis, being performed on a statewide level, crosses many aquifers. This approach used a kriging interpolation which uses a distance-weighted averaging approach to estimate the value at an unknown point based on neighboring points. The appropriateness of this approach should be tested and other alternative interpolation methods could be analyzed to determine which most accurately predicts well characteristics at locations where measuerments have not been taken in order to improve the results of this analysis. The study could be scaled down to an individual aquifer level, thereby improving our understanding of individual aquifer characteristics and potential for desalination of brackish water from them. Another consideration that needs to be addressed before implementing new solar-powered desalination facilities is whether there is a sufficient supply of water available to protect aquifers from the harmful effects of overuse, such as land subsidence. The disposal of the brine waste stream is also of environmental concern and methods for disposal should also be evaluated.

For this research, a sensitivity analysis would help quantify the trade-offs associated with siting a co-located facility based on the solar resources or water resources available. Considering the large spread of desalination plants currently in Texas, an economic analysis could be performed to determine the cost of installing PV at desalination facilities currently in operation that meet the optimal conditions set forth in this report. Future research might also include analyzing different solar technologies, such as concentrating solar power or solar thermal power, and other renewable energy sources such as wind and geothermal as well as different desalination technologies, *i.e.*, thermal

treatment methods. By coupling wind and solar power with RO desalination, the co-located facility could operate for longer hours during the day, since wind is stronger at night [24].

Acknowledgments

The authors would like to thank the Texas State Energy Conservation Office (SECO) and the Tarrant Regional Water District (TRWD) for their support of this research.

Author Contributions

Both authors contributed to the writing of this article and have approved the final manuscript.

Conflicts of Interest

The authors declare no conflict of interest.

References

1. Mbarga, A.A.; Song, L.; Williams, W.R.; Rainwater, K. Integration of Renewable Energy Technologies With Desalination. *Curr. Sustain. Renew. Energy Rep.* **2014**, *1*, 11–18.
2. Clayton, M.E.; Stillwell, A.S.; Webber, M.E. Implementation of Brackish Groundwater Desalination Using Wind-Generated Electricity: A Case Study of the Energy-Water Nexus in Texas. *Sustainability* **2014**, *6*, 758–778.
3. Rainwater, K.; Nash, P.; Song, L.; Schroeder, J. The Seminole Project: Renewable Energy for Municipal Water Desalination. *J. Contemp. Water Res. Educ.* **2013**, *151*, 50–60.
4. Grubert, E.A.; Stillwell, A.S.; Webber, M.E. Where does solar-aided seawater desalination make sense? A method for identifying sustainable sites. *Desalination* **2014**, *339*, 10–17.
5. Venkataraman, K.; Ortegon, J.; Uddameri, V.; Dyke, R. Mapping of Wind-Powered Desalination Potential in South Texas. In Proceedings of the AWRA 2012 Spring Specialty Conference, New Orleans, LA, USA, 26–28 March 2012.
6. Bennett, J.; Dascaliuc, S.; Grossman, N. *Water for Texas 2012 State Water Plan*; Technical Report; Texas Water Development Board: Austin, TX, USA, 2012.
7. *Desalination: Brackish Groundwater*; Technical Report; Texas Water Development Board: Austin, TX, USA, 2004.
8. What Technologies Are Used? Available online: http://www.desalination.com/market/technologies (accessed on 11 March 2015).
9. Arroyo, J.; Shirazi, S. *Cost of Water Desalination in Texas*; Texas Water Development Board: Austin, TX, USA, 2009; pp. 1–7.
10. Al-Karaghouli, A.; Renne, D.; Kazmerski, L. Technical and economic assessment of photovoltaic-driven desalination systems. *Renew. Energy* **2010**, *35*, 323–328.
11. McGovern, R.K.; Zubair, S.M.; Lienhard V, J.H. The cost effectiveness of electrodialysis for diverse salinity applications. *Desalination* **2014**, *348*, 57–65.

12. Price, S.; Margolis, R. *2008 Solar Technologies Market Report*; Technical Report January; National Renewable Energy Laboratory: Golden, CO, USA, 2010.
13. SunShot. *Photovoltaic System Pricing Trends Historical, Recent, and Near-Term Projections*; Technical Report; U.S. Department of Energy: Washington, DC, USA, 2012.
14. Wogan, D.M.; Webber, M.; da Silva, A.K. A framework and methodology for reporting geographically and temporally resolved solar data: A case study of Texas. *J. Renew. Sustain. Energy* **2010**, *2*, doi:10.1063/1.3496493.
15. Dynamic Maps, GIS Data, and Analysis Tools. Available online: http://www.nrel.gov/gis/solar.html (accessed on 15 May 2015).
16. Papapetrou, M.; Wieghaus, M.; Biercamp, C. *Roadmap for the Development of Desalination Powered by Renewable Energy*; Technical Report; ProDes: Stuttgart, Germany, 2010.
17. Carter, N. *Desalination and Membrane Technologies: Federal Research And Adoption Issues*; Technical Report; Congressional Research Service: Washington, DC, USA, 2013.
18. Papadakis, G. *ADIRA Handbook: A Guide to Autonomous Desalination System Concepts*; Technical Report; European Union: Istanbul, Turkey, 2008.
19. *Desalination: Brackish Groundwater*; Technical Report; Texas Water Development Board: Austin, TX, USA, 2013.
20. Groundwater Database Reports. Available online: http://www.twdb.texas.gov/groundwater/data/gwdbrpt.asp (accessed on 28 November 2012).
21. Environmental Systems Research Institute. *ArcGIS Desktop: Release 10.2.2*; Environmental Systems Research Institute: Redlands, CA, USA, 2014.
22. MacHarg, J.P. *Energy Optimization of Brackish Groundwater Reverse Osmosis Desalination*; Technical Report; Texas Water Development Board: Austin, TX, USA, 2011.
23. Aybar, H.S.; Akhatov, J.S.; Avezova, N.R.; Halimov, A.S. Solar powered RO desalination: Investigations on pilot project of PV powered RO desalination system. *Appl. Sol. Energy* **2011**, *46*, 275–284.
24. Clayton, M.E.; Kjellsson, J.B.; Webber, M.E. Can renewable energy and desalination tackle two problems at once? *Earth*, 26 October 2014.

The Energy-Water Nexus: An Analysis and Comparison of Various Configurations Integrating Desalination with Renewable Power

Gary M. Gold, Michael E. Webber

Abstract: This investigation studies desalination powered by wind and solar energy, including a study of a configuration using PVT solar panels. First, a water treatment was developed to estimate the power requirement for brackish groundwater reverse-osmosis (BWRO) desalination. Next, an energy model was designed to (1) size a wind farm based on this power requirement and (2) size a solar farm to preheat water before reverse osmosis treatment. Finally, an integrated model was developed that combines results from the water treatment and energy models. The integrated model optimizes performances of the proposed facility to maximize daily operational profits. Results indicate that integrated facility can reduce grid-purchased electricity costs by 88% during summer months and 89% during winter when compared to a stand-alone desalination plant. Additionally, the model suggests that the integrated configuration can generate $574 during summer and $252 during winter from sales of wind- and solar-generated electricity to supplement revenue from water production. These results indicate that an integrated facility combining desalination, wind power, and solar power can potentially reduce reliance on grid-purchased electricity and advance the use of renewable power.

Reprinted from *Resources*. Cite as: Gold, G.M.; Webber, M.E. The Energy-Water Nexus: An Analysis and Comparison of Various Configurations Integrating Desalination with Renewable Power. *Resources* **2015**, *2*, 227–276.

1. Introduction

Energy and water are inseparable: energy is used to collect, treat, and distribute water while water is used to cool reactors, run turbines, and act as a working fluid for power plants. Management strategies for water and energy should be aligned due to the strong interdependence between vital water and energy resources.

Both water and energy face current and future challenges caused by societal demands. In the water sector, rising population, overconsumption of freshwater resources, and a changing climate have and will continue to create challenges to meet water demand around the world. Specifically, areas such as the southwest United States are experiencing rapid population growth, more than double the national average in recent years [1]. At the same time, many regions including the southwest United States are facing alarming drought conditions. These droughts are expected to increase in duration and intensity in years to come [2] due to natural weather variability and factors associated with a changing climate. As the availability of current water resources diminishes, municipalities and water planners are looking towards new and innovative solutions to keep up with rising water

demand. However, alternative water resources are often times located further away from demand centers or are of lower quality and therefore require more energy for transportation and treatment.

A promising alternative to relying more on freshwater supplies is desalination of brackish and saline water. Desalination of seawater is gaining support in coastal areas while desalination of brackish groundwater is seen as a potential solution for inland regions. While desalination offers the advantage of diversifying water supplies, the energetic impacts can be significant. Desalination requires significantly more energy than typical surface water treatment. This energy investment can incur high financial costs on desalination operations and also result in significant carbon dioxide emissions.

Renewable energy technologies offer a solution to meet the energy demands of desalination. By using renewably generated electricity, it is possible to meet the energy demand of desalination in a sustainable way. Coupling renewable power such as wind and solar with desalination offers a means to meet the energetic needs of desalination without increasing reliance on fossil fuels. Such an integration of technologies would limit carbon dioxide emissions.

At the same time, desalination provides a solution to inherent difficulties associated with renewable energy. Wind and solar power are limited by both diurnal and seasonal variability. Wind power faces predictable daily and seasonal variability and less predictable weather-induced fluctuations. These fluctuations are challenging because inland wind availability does not typically match energy demand. In many regions, wind speeds are strongest during nighttime hours, when energy demand is low, and are weakest in the afternoons, when energy demand peaks. Seasonally, wind speeds are strongest during winter months, the time when energy demand drops in warm regions, while weaker during summer months, when energy demand peaks. The fact that wind power availability is out of phase with energy demand creates challenges implementing wind power. It's difficult for operators to incorporate grid-scale wind farms due to the variable nature of power from these facilities. The daily and seasonal fluctuations do not allow operators to meet energy demand on the same dispatchable basis as conventional power plants. The inherent variability of wind power can be a major setback in the advancement of renewable power technologies.

Desalination offers a solution to the variability of wind power because water treatment is a time-flexible process that can be operated during off-peak hours. Integrating a desalination plant with wind power provides an opportunity to utilize electricity generated from renewables in a way that is not negatively impacted by its inherent variability. A grid-connected integrated facility can provide energy for desalination when energy demand is low while generating electricity for the grid during times when demand rises. By supplying energy for desalination during off-peak hours, grid-scale wind power can be used to produce freshwater while also providing municipal electricity in a way that is not negatively impacted by daily and seasonal fluctuations.

Collocating a desalination facility with a solar farm offers multiple benefits. The exchange of heat between relatively cool water and warm solar panels is an opportunity to improve solar power production. Typically, photovoltaic (PV) solar panels suffer a loss in efficiency when the PV cells heat up. Solar energy is lost as "waste heat" that is not converted into electricity when these panels increase in temperature. However, efficiency losses can be mitigated if solar panels are cooled. Brackish groundwater is typically at a relatively cool temperature and can therefore be used to

decrease the temperature of solar panels for a solar-power facility co-located with a desalination plant. In cooling solar panels with brackish groundwater water, coupling desalination with a solar power plant can increase the efficiency of solar power production.

Furthermore, there are water-treatment benefits of providing on-site solar power at a desalination facility. Using slightly warm feed water for desalination reduces the energetic requirement of the water treatment process. Therefore, preheating feed water using onsite solar panels prior to desalination is an opportunity to reduce the energy consumption and costs. Coupling desalination with solar power can be mutually beneficial to both technologies as water is used to improve the efficiency of solar-power production, while solar panels are used to reduce the energy required for desalination.

Additionally, a joined facility that produces water and electricity can mitigate risks associated with potential fluctuations in the water or energy markets. By providing two sources of revenue, water and electricity, an integrated facility can protect itself from the risk of declining water or electricity sales. If water sales dip for a period of time, the facility can still bring in money by selling electricity to the grid. Likewise, if wind and solar resources are weak on certain days, the facility will still be able to have revenue from producing water. Providing two sources of revenue at an integrated facility provides diversity to reduce the risk of fluctuations in the water or energy sectors.

The three technologies studied in this investigation, desalination, wind, and solar power, are rapidly developing. However, all three face inherent challenges. Integrating these technologies can advance their development and implementation. Additionally, coupling desalination with wind and solar power solves challenges faced by both the energy and water sectors. A desalination facility integrated with wind and solar power can meet water-supply challenges while simultaneously providing sustainable renewable power. Coupling desalination with renewable power allows the water and energy sectors to work together to meet current and future needs for strained resources.

This analysis focuses on brackish groundwater desalination in the region of Central Texas. Previous geographic studies have indicated that Central Texas offers a viable location to integrate desalination with renewable power due to the availability of brackish groundwater, wind, and solar resources in this region [3]. The methodology outlined in this report is widely applicable to regions beyond Texas where these resources are similarly available.

2. Background

2.1. Reverse Osmosis Desalination of Brackish Groundwater

Desalination of brackish and saline water is becoming an increasingly popular means for municipalities to meet water demand. Water with total dissolved solids (TDS) between 1000 and 10,000 mg/L is considered “brackish”, while water with TDS greater than 10,000 mg/L is considered “saline” [4]. In these TDS ranges, water is not useful for most purposes without treatment. However, desalination provides a means to reduce the salt content so that the water may be used for municipal, agricultural, or industrial purposes. There are a multitude of desalination technologies and

methodologies including multistage flash distillation, multi effect distillation, vapor compression, electrodialysis, and reverse osmosis (RO).

The investigation discussed in this paper focuses on reverse osmosis. RO desalination is a process in which high pressure feed-water is forced through a semi-permeable membrane. The membrane filters out bluedissolved salt ions, resulting in two separate products: low TDS product water and high concentrate brine [5]. Recovery of low TDS product water ranges from 50% to 90% depending on water quality and operating conditions [6]. Reverse osmosis is currently the world's leading technology for new desalination installations and has developed an 80% share of current desalination plants worldwide [7]. Additionally, RO desalination is an electricity-driven process and therefore can be viably integrated with wind- or solar-generated electricity.

Brackish groundwater is an abundant resource in Texas and one for which there is less competition than there is for fresh water because treatment is required before municipal, agricultural, or industrial use. The Texas Commission on Environmental Quality has established a primary standard for TDS at 500 mg/L and a secondary standard at 1000 mg/L for municipal use while groundwater containing TDS up to 3000 mg/L can be used for irrigation [4]. There are currently 46 municipal brackish water desalination plants in operation throughout Texas, 12 of which treat surface water while the remaining 34 use brackish groundwater as a feed source. Reverse osmosis is the primary desalination technology, used in 44 of the 46 desalination plants in the state of Texas [4]. Desalination of brackish groundwater is a growing water-supply option in the state, with a design capacity that has increased from 104 million cubic meters per year in 2005 to 166 million cubic meters per year in 2010 [8].

Strong recommendations to expand desalination practices in Texas have been indicated by the Texas Water Development Board (TWDB). By the year 2060, the Board projects a 22% increase in water demand and 10% decrease in water supply [9]. To meet this growing water demand, TWDB has suggested increasing brackish groundwater desalination capacities to 224 million cubic meters per year by 2060, accounting for approximately 2% of all recommended water management strategies [4].

There are a number of challenges associated with desalination that can limit implementation. For inland desalination plants, brine disposal is an environmental and economic concern. Current options include wastewater or surface water discharge following treatment, land application, deep well injection, evaporation ponds, and zero point discharge [10]. The major challenge, however, is the high energetic requirement of desalination. Desalination consumes approximately ten times as much energy as typical surface water treatment [6]. This significant energy requirement can be environmentally detrimental by driving up reliance on fossil fuels and increasing carbon dioxide emissions. Additionally, meeting energetic requirements can be costly to plant operators and are typically the single largest expense of desalination facility operations. Electricity costs of RO desalination typically comprise of 30% to 50% of total desalination operational expenses [11]. While desalination of brackish groundwater offers a promising means to meet increasing water demand, challenges associated with the high energy requirement of this process must be considered.

2.2. Wind-Powered Desalination

The United States wind power industry is growing rapidly. Adding 13.1 gigawatts (GW) of new capacity and bringing in an investment of 25 billion dollars in 2012, the installed wind power capacity in the U.S. rose to 60 GW [12]. These additions made wind power the largest source of electrical-generating capacity additions in the country. Wind power constituted 43% of new power additions in 2012 to overtake natural gas as the leading source of new capacity for that year [12]. Figure 1 indicates that the the growth in wind power has been a long-term trend over the past decade, as energy planners hope to diversify power sources, limit reliance on fossil fuels, and curb carbon emissions.

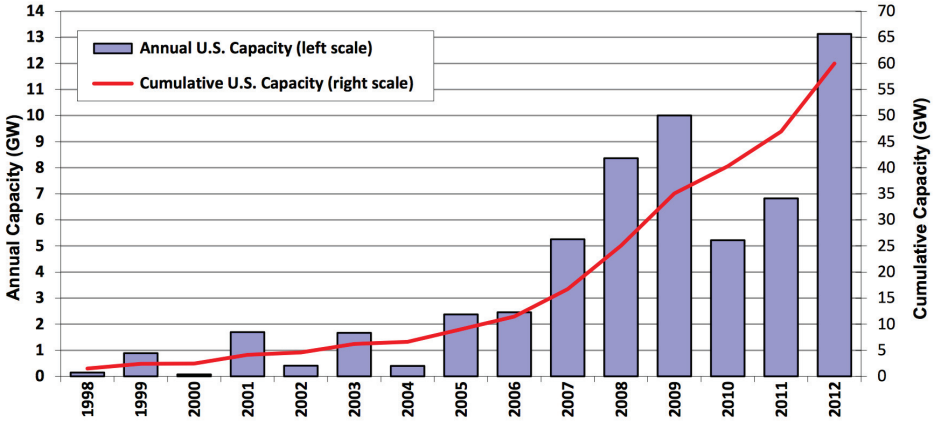

Figure 1. Annual and cumulative wind power added in the United States [13].

Despite the rapid growth of wind power in recent years, the inherent variability of wind limits this technology. Daily and seasonal fluctuations in the availability of wind power prohibits plant operators from using wind power on a dispatchable basis to meet demand as they do with conventional power plants. An additional complication is that the diurnal and seasonal variability of inland continental wind mismatches demand [14]. When electricity demand peaks during the afternoon, inland continental wind speeds are typically weak. When electricity demand decreases at night and in the early morning, inland continental wind speeds peak. Similarly, inland continental wind speeds are weakest during the summer, when electricity demand is highest, and strongest during the winter and shoulder months, when electricity demands are typically lower [14]. Fluctuations in wind power availability that mismatches demand creates challenges in integrating wind power to the grid for policy makers in the energy sector, who have indicated a pressing need for the development of storage technologies [15]. A possible solution to these challenges is to dedicate wind power to a time-flexible process, such as water treatment. Desalination is a process that can be operated intermittently, a characteristic that makes it conducive to integration with wind power. In essence, desalinated water could act as a proxy for storing wind energy. Additionally, when wind power generation is above the requirement for desalination, wind-generated electricity can be sold to the grid. When wind power is

below the requirement for desalination, electricity can be purchased from the grid to power the water treatment process. This idea provides a solution to the intermittency of wind-power availability and to problems associated with the high energy intensity of desalination.

Wind-driven desalination has been investigated since the 1980s when installation projects began in Europe. Development began in Ile du Planier, France starting in 1982, comprising of a 4 kW turbine used to desalinate seawater [16]. While the majority of wind-driven RO desalination systems treat seawater, there have been a few investigations into wind-powered brackish groundwater desalination. A current demonstration project in Seminole, Texas is investigating wind-powered RO desalination of brackish groundwater from the Ogallala aquifer. The required power in this project is supplied by a combination of grid-electricity and electricity generated by a 50 kW wind turbine [11]. The operational analysis of this demonstration project is still to come at the time of writing this paper, however, the project indicates the technical feasibility of wind-powered RO desalination of brackish groundwater. Additionally, research into the economic feasibility of these systems has indicated that wind-powered desalination can be cost competitive with stand-alone desalination facilities in regions with strong wind resources high electricity costs [17].

Due to the inherent variability of wind-power production, the majority of wind-driven desalination projects and operations include battery storage or backup power by alternative sources such as a diesel generator. Studies exist that have investigated the possibility of combining wind-power with grid-electricity to drive the desalination process [18,19]. This possibility offers a potential solution to the intermittent nature of wind power. Recently, studies have investigated a configuration in which a desalination facility and wind farm are grid connected. Electricity purchased from the grid can potentially drive desalination during hours when wind-power is not available. Additionally, including an on-grid wind farm enables the facility to sell electricity to the grid during times when it is economically attractive to sell wind-generated electricity rather than use it for desalination. Grid-connected wind desalination was determined to be economically feasible in a study by Clayton, Stillwell, and Webber that investigated integration of desalination with wind-power in a grid-connected configuration [3]. One of the goals of this investigation is to expand on work conducted in that analysis by adding an investigation of integrating both wind and solar power with RO desalination.

2.3. Solar-Powered Desalination

Similar to the wind power industry, the solar power sector is experiencing rapid growth as indicated by Figure 2.

Like wind power, solar power faces challenges associated with variability. Although solar-power production more closely matches demand than wind, operators nonetheless experience challenges with integrating solar power with the electricity grid due to daily and seasonal fluctuations. Specifically, solar insolation captured during off-peak morning hours is often of low value due to limited energy demands in the early morning [15]. A possible solution to this challenge is to use low-valued solar power for a time-flexible process such as water treatment by integrating solar power with desalination. During off-peak hours, solar-generated electricity can power the desalination

process, enabling the treated water to act as a storage proxy for solar energy. When energy demand and electricity prices rise, the higher-valued electricity generated from the solar farm can be sold to the grid. Coupling solar power with desalination can advance the implementation of solar-power technology by providing a use for electricity generated during off-peak hours.

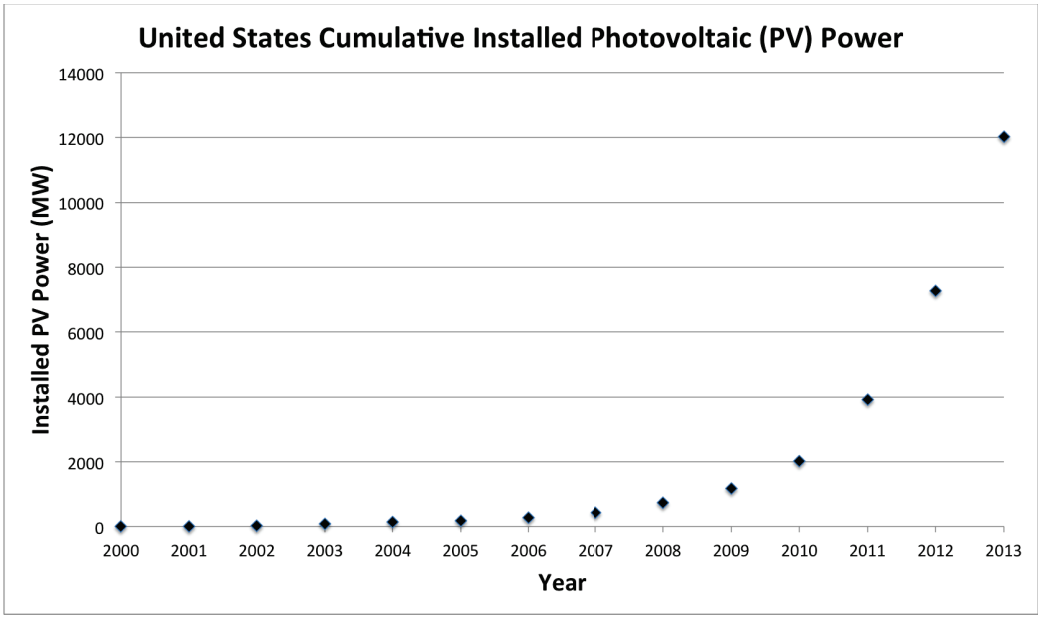

Figure 2. United States cumulative installed photovoltaic (PV) solar capacity [21].

For desalination applications, electricity generated from a solar farm can be used to power pumps that develop the high pressure needed to force feedwater through the semi-permeable membrane used in the desalination process. Investigation into solar-powered desalination has been conducted since the 1970s and demonstration projects were developed as early at 1978 [22]. Since this time, there have been a number of demonstration units and small-scale plants implemented. However, projects have been limited to supplying relatively modest amounts of product water, with the largest plant producing approximately 75.7 cubic meters per day [23], a small fraction of the product water supplied by municipal desalination plants in the United States.

Despite a general decreasing trend in the cost to produce desalinated water using solar energy, PV-powered RO desalination is not yet cost-competitive with conventional desalination plants that use energy from the grid [24]. The majority of solar-powered desalination projects are designated to remote regions where grid electricity is not available. Additionally, most current PV-powered RO operations require battery storage of electricity in order to provide energy during hours when solar power cannot be produced.

An integrated solar power/desalination facility that is connected to the grid could potentially supply fresh water and renewable power without the need for battery storage. A grid-connected system provides the opportunity to use either solar-generated electricity or electricity purchased from

the grid to power desalination depending on times of day when each option is economically attractive. An on-grid PV system additionally allows the integrated facility to sell electricity to the grid during hours of peak electricity demand, when electricity prices are high. Grid-connected solar-powered desalination can potentially offer an economically attractive opportunity for an integrated facility to generate revenue from both water production and electricity generation.

2.4. Wind/Solar-Powered RO Desalination

Hybrid systems in which wind and PV solar energy are used to power desalination have been investigated for quite some time. Providing a combination of wind and solar energy can be advantageous because power availability from these sources often occurs during different times of day. As discussed previously, solar power typically peaks in the afternoon while the highest wind speeds occur during the night in many regions. Additionally, solar insolation is strongest during summer months, while more wind power is typically generated during the winter than during summer. Hence, power generated from wind and solar technologies do not match one another on a daily or seasonal basis. Power from wind can be used during certain times when solar power is not available and vice versa. The diurnal and seasonal variability of wind and solar power is conducive to combining these renewable energy technologies.

Successful operation of a hybrid wind/PV solar RO desalination unit has been reported in some arid and isolated regions. Daily production of 3 cubic meters has been maintained in an Israeli demonstration project that desalinates brackish groundwater using a combination of PV solar and wind power [25]. This unit included two-day battery storage by a backup diesel generator for times when wind and solar power could not generate sufficient electricity for desalination. From this investigation and similar ones, it is clear that backup power would be necessary due to the intermittent nature of wind and solar power.

Additional considerations regarding wind and solar powered desalination include capital and operational costs as well as the potential for energy recovery. These considerations were analyzed by Zhu *et al*., (2010) is a an analysis focusing on optimizing specific energy consumption [26]. Results from this analysis provide context and important considerations for the study of desalination powered by renewable energy. However, capital and operational costs as well as the potential for energy recovery are beyond the scope of this work. The analysis discussed here focuses on operational profiles and potential revenue.

Possible extensions not included in this analysis are the potential for energy storage through battery technology and different energy systems such as biofuels for off-grid cases. There are advantages and limitations to energy storage for desalination that have been recently analyzed [27]. Likewise, additional energy sources such as biofuels and biogas have been studies for off-grid membrane desalination in a number of applications [28]. While these considerations are important to the field of renewable power and desalination, the focus of the analysis discussed here is limited to wind and solar-powered desalination without energy storage. Future work may incorporate additional energy sources and storage potential.

2.5. Photovoltaic Thermal System Used for Reverse Osmosis Desalination

2.5.1. Photovoltaic Thermal Solar Technology

In recent years, there have been substantial research developments regarding photovoltaic thermal (PVT) solar technologies as a way to improve the efficiency of harnessing solar energy. These systems are a combination of photovoltaic and thermal solar components that can produce both electricity and heat for useful purposes. Though many collector types have been investigated, air or water is often used a heat collector in these panels [29]. Figure 3 displays a typical configuration of a flat-plate PVT solar panel. These systems include an enclosed PV model that is cooled by a working fluid entering one end of the panel and leaving through the opposite end. For the analysis discussed in this investigation, brackish groundwater is considered as the PVT module coolant.

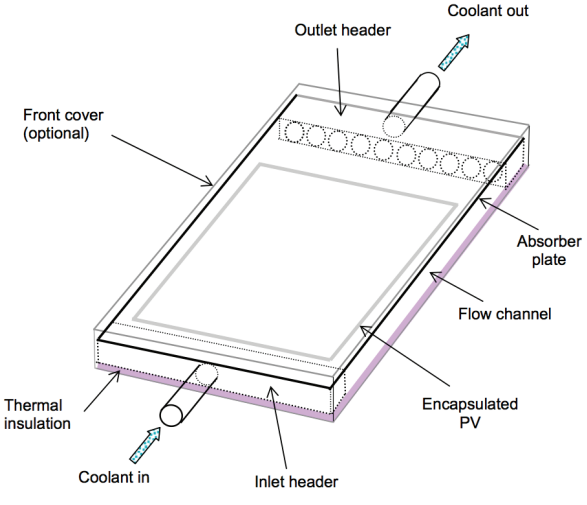

Figure 3. Configuration of a flat-plat photovoltaic thermal (PVT) panel [29].

Traditional PV panels convert only 5% to 18% of incoming solar insolation into electricity [30]. A majority of solar energy is converted to heat, raising the temperature of the solar cells. Studies have indicated a significant correlation between the PV module temperature and the efficiency of solar energy conversion into electricity. As the temperature of the PV panel increases, efficiency of energy conversion to electricity declines [30,31]. By cooling the solar panels, the efficiency of electricity production can be improved. A PVT solar system, compared to a traditional PV system, can significantly enhance solar power production by limiting the temperature increase of the panels.

Additionally, heat extracted from the solar panels by the coolant can be resourcefully reused. For instance, a European company, Solimpeks, has developed PVT panels cooled by water, in which the hot water leaving the solar panels is used for domestic purposes. The company suggests that its PVT panels are significantly more efficient than typical PV solar systems due to the cooling mechanism. The advertised efficiency of solar energy conversion to electrical power is 25%, more than 50%

greater than that of non-cooled PV solar panels [32]. Although there has been extensive research regarding PVT solar panels over the past decade, applications for heated water using this technology are still very limited [29].

Studies have been conducted regarding PVT solar modules for desalination using processes other than reverse osmosis. For instance, the use of "waste heat" for Multiple Effect Evaporation (MEE) has been investigated and simulated by researchers in Israel [33]. MEE systems utilize heat for an evaporation process in which water is separated from solids in a multi-stage system. The process allows for relatively high operating flexibility and short start up time, making it conducive to meeting water demand efficiently [34]. Researchers suggest that power generation from the combined PVT-desalination process can outperform that of conventional solar farms [35]. Additionally, under specific circumstances, these studies suggest that PVT-MEE desalination can be cost competitive with conventional desalination [33].

The investigation discussed in this paper considers a design in which brackish groundwater is used to cool the panels of the modeled solar farm. Research over the past couple of decades has accelerated improvements in PVT systems that have drastically increased the thermal and electrical efficiencies of these modules [36]. Integrating desalination with solar power offers a potential application for new and exciting PVT technologies. Brackish groundwater can be used in a PVT system to cool solar panels and collect PVT "waste heat". This configuration is possible because brackish groundwater is typically at a relatively cool temperature compared to the solar panels. By incorporating a design that includes PVT solar modules, the temperature difference between the cool brackish groundwater and the hot solar panels can be used to an engineering advantage to improve the efficiency of solar power production. Using brackish groundwater as a coolant in the PVT system prior to treatment can increase the percent of incoming solar insolation that is converted into electricity. As discussed in the following section, exchanging thermal energy between the brackish groundwater and the solar panels is also advantageous in the water treatment process. Additional implications of heating brackish groundwater prior to desalination should be considered in experimental studies of this technology. However, these additional considerations are beyond the scope of the systems analysis discussed in this paper.

2.5.2. Reverse Osmosis Feed Water Temperature

Recent studies indicate that raising the temperature of feed water in the RO process can reduce energetic requirements for treatment. As discussed previously, RO is a pressure-driven process in which a significant amount of energy is required to provide a high pressure to force feed water through a semi-permeable membrane. A feed pressure of up to 300 to 400 pounds per square inch (PSI) is required for brackish groundwater desalination [6]. However, research at the University of Texas at El Paso (UTEP) Center for Inland Desalination has indicated that the required pressure can be reduced if the water temperature is increased. These studies indicate that the specific energy required to drive the desalination process is reduced by 3.4% when feed water temperature increases from 25 degrees Celsius to 30 degrees Celsius [37]. By preheating brackish groundwater before RO

treatment, it is possible to reduce the energy intensity of the process by limiting the pressure required to force water through the RO membranes.

2.5.3. Texas as a Testbed

This study focuses on Texas, although the methodology is applicable to other regions with available resources. As indicated previously, Texas is facing tough circumstances with respect to population growth and depletion of water resources. The 2012 State Water Plan has recommended increasing brackish groundwater desalination as a water management strategy and outlined a number of projects that can provide new water supplies through this process. While desalination may provide a means to meet water supply challenges, the potential increase in energetic requirements to collect and treat brackish groundwater are incongruent with goals to limit the reliance on fossil fuels and reduce carbon emissions. Additionally, municipalities are likely to experience undesirable increases in the cost of water treatment as a result of advancement in desalination activities. Given the State's plan to install brackish groundwater desalination facilities, it will be prudent for Texas water planners to consider integrating these facilities with renewable power to mitigate unwanted increases in carbon emissions and electricity costs from the grid. Based on plans indicated by water managers across the state, Texas is a time-relevant location to choose for this investigation.

Additionally, the geographic availability of water, wind, and solar resources in Texas, make the state a feasible location for this analysis. Wind speeds adequate for generating power are prevalent in Texas and the state is the nationwide leader in wind power. Over 20% of installed wind capacity in the United States is in Texas, with 12,355 megawatts (MW) of the total 61,108 MW [38]. The wind power sector in Texas is growing rapidly, and the state installed more wind power capacity (1826 MW) than any other state in the year 2012 [12]. Additionally, Texas is the lowest cost region for installing wind power projects [12]. Generally, a wind power classification greater than three is considered to be profitable for generating power from a utility scale wind turbine. As shown in Figure 4, regions of central Texas and the panhandle have wind classifications above this required threshold [3]. The availability of wind and the relatively low cost of installation compared to other states make Texas a conducive environment for the development of wind farms as means to meet the growing energy demand.

Texas is also an attractive region for the development of solar power. In a recent assessment of technical potential for PV solar power accounting for the prospective market, economic and technical considerations, and available resources, Texas was rated as the state having the greatest potential for utility-scale solar power [40]. While solar insolation is strongest in the west and central region of the state, there is technical potential for utility scale solar power throughout much of Texas as a result of available solar resources as well as large and growing populations [41]. Texas currently ranks seventh in the United States in total installed solar capacity with 134 MW and ninth lowest in the Nation for installed cost at $5.83 per Watt [42]. Solar energy potential increases from east to west across the state, as shown in Figure 5, which displays the annual average solar insolation. Across the state, solar insolation ranges from 2 to 7.2 kilowatt hours (kWh) per square meter per day [43]. This

range of solar insolation, in addition to growing energy demand in the state, makes Texas an ideal region for utility-scale PV solar installations.

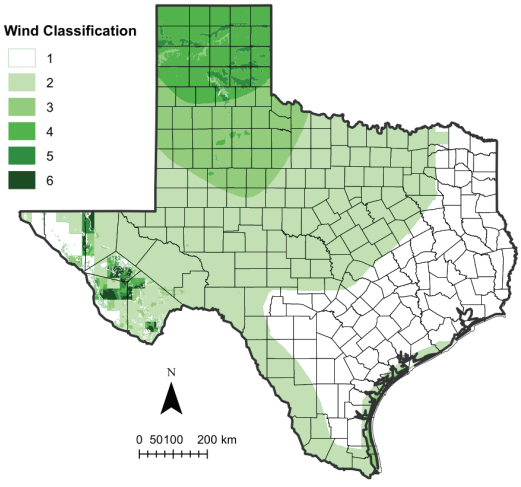

Figure 4. Geographic variability of wind classification across Texas [39].

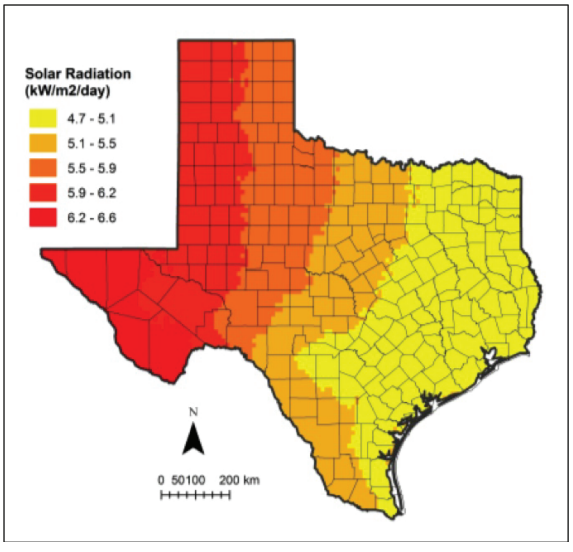

Figure 5. Annual average solar insolation in Texas [43,44].

The abundance of brackish groundwater throughout the State is another key reason Texas is a conducive location for this analysis. As shown in Figure 6, there are over 10,000 current wells reaching groundwater considered "brackish" (TDS between 1000 and 10,000 mg/L) [45]. There is an estimated 2.7 billion acre-feet of brackish groundwater in the Texas [4]. The strategies outlined

by water planners and availability of brackish groundwater make Texas a suitable region to study in this analysis.

Given the availability of these resources around the state, Texas offers an appropriate location to study the integration of brackish groundwater desalination with wind and solar power. Developing a model with Texas as a testbed enables this analysis to provide a methodology that will also be applicable to other regions with similar solar, wind, and water resources.

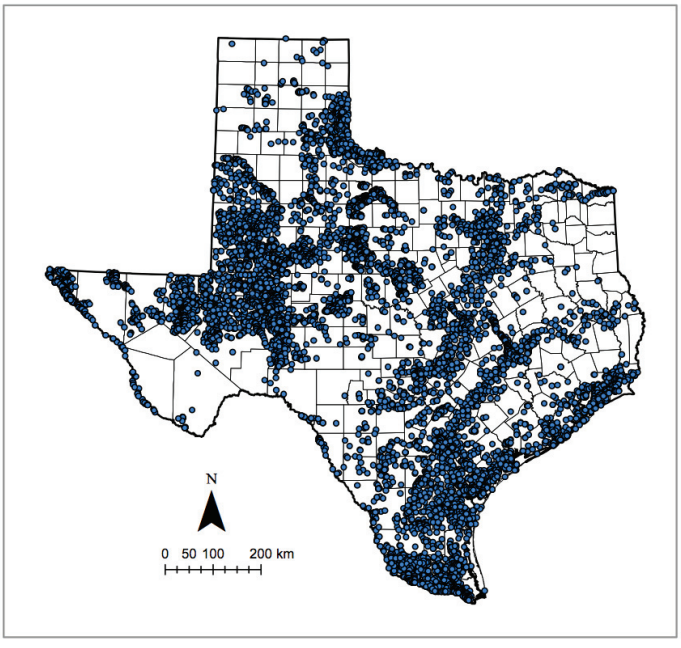

Figure 6. Brackish groundwater wells in Texas [45].

This investigation offers an analysis of desalination powered by renewable energy sources. By developing a water treatment model based on fluid dynamics, an energy model based on thermodynamics, and an optimization model that integrates the water treatment and energy models, this investigation provides insight into the potential for powering desalination with renewable energy. Consideration is given toward the economics of wind and solar powered desalination in the optimization model. This model develops a daily schedule for desalination based on electricity prices and availability of renewable power. Additionally, the optimization model develops results and a methodology to determine expected revenue from water production, electricity sales to the grid, as well as the cost of electricity purchased from the grid for a desalination facility integrated with wind and solar power. By modeling a desalination plant coupled with wind and solar power and considering the economics of this idea, the hope of this analysis is to gain a practical understanding of the benefits and tradeoffs involved in water treatment powered by renewable energy.

Additionally, the analysis performed here offers a novel approach to blueinvestigate the energy-water nexus in the realm of water treatment and renewable power. As discussed in the previous sections, earlier models have analyzed solar-powered desalination, wind-powered desalination, and solar/wind-powered desalination. However, few models have analyzed the possibility of solar and/or wind powered desalination in which the facility is also integrated with an electricity grid, in this case with the Electric Reliability Council of Texas (ERCOT) grid. Moreover, with the exception Clayton's analysis of wind-powered desalination [3], there have not been investigations to model an integrated facility in which power can not only be bought from the grid, but also sold to the grid from the modeled wind or solar farm. There are potentially times of day when electricity prices are high enough that an integrated facility would prefer to sell wind or solar-generated electricity to the grid rather than use the electricity for desalination. An economic analysis of a modeled wind/solar powered desalination facility can provide insight into the expected operational schedule of such a facility. The analysis in this investigation builds and uses an optimization model to determine times of day when it is economically beneficial to make one of three decisions: use wind or solar power for desalination, sell wind or solar power to the grid and buy electricity from the grid to power desalination, or halt the desalination process. In addition, the analysis develops a model to estimate daily revenues from desalinated water sales and wind/solar power production as well as the expected cost of electricity from the grid. By analyzing grid-connect wind and solar-powered desalination, this investigation fills a knowledge gap regarding how an integrated wind/solar-powered desalination facility can interact with the electricity grid to provide both desalinated water and renewable power.

Furthermore, this investigation includes analysis of a PVT solar configuration in which water is used to cool solar panels while thermal energy from solar panels is used to preheat feed water. As discussed in previously, a PVT solar module can be used as a sort of heat exchanger between the solar panels and brackish groundwater. Transferring heat from the solar panels to the water is mutually beneficial for solar power production and water treatment: cooler solar panels are more efficient at converting solar insolation into electricity while preheated water requires less energy in the desalination process. By considering the possibility of using PVT solar panels as part of a desalination plant, this investigation attempts to fill the void in offering a new and potentially beneficial use for PVT panels. This investigation hopes to answer questions regarding how a PVT solar configuration may perform compared to other configurations in a modeled desalination plant and offer insight into the potential for use of PVT solar panels at a desalination facility.

Another novel aspect of this this investigation is to investigate the potential to diversify revenue in a desalination facility combined with renewable power. It is possible that providing wind and solar power at a desalination facility can mitigate risks associated with declining water sales by providing revenue from electricity. Similarly, the facility may also reduce the risk of declining electricity sales by selling water. A desalination facility integrated with renewable power brings in revenue from two different markets, water and energy, incorporating diversity in revenue.

3. Modeling Methods

3.1. Overview

The methodology in this investigation is divided into three sections to develop the tools necessary to conduct an investigation of a brackish groundwater reverse osmosis desalination plant powered by wind- and/or solar-generated electricity. The three models used as the basis for this analysis are as follows: (1) water treatment model; (2) energetic model; (3) integrated optimization model.

Using these models, four different scenarios are analyzed in this investigation to compare desalination powered by different energy sources and a combination of these sources. Scenario A analyzes a desalination plant that can be powered by electricity generated at an integrated solar farm or by grid-purchased electricity. Correspondingly, power from the modeled solar farm can be either used for desalination or sold to the electricity grid, as shown in Figure 7.

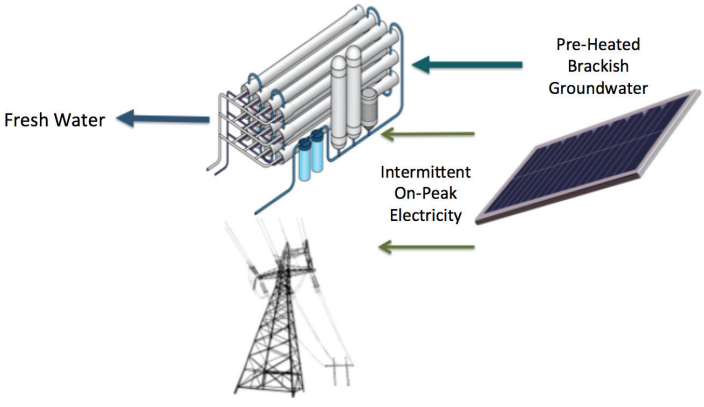

Figure 7. Scenario A models a desalination facility integrated with solar power that can either use solar-generated electricity for water treatment or sell solar-generated electricity to the grid.

Scenario B assumes the same circumstances, except incorporating a modeled wind farm rather than a solar farm, similar to work by Clayton, Stillwell, and Webber [3]. Desalination in this scenario can either be powered by the wind turbines or by electricity purchased from the grid; similarly, wind power can be either used for desalination or sold to the grid, as shown in Figure 8.

Scenario C analyzes a desalination facility integrated with a wind farm and co-located with a solar farm. In Scenario C, wind-generated energy can be sold to the grid or used for desalination; similarly, desalination can be powered by either wind-generated electricity or by electricity purchased from the grid. Solar-generated electricity from the co-located solar farm is assumed to be sold to grid. In addition to the opportunity to sell solar power, the purpose of the co-located solar farm is to provide heat exchange between the solar panels and the pretreated brackish groundwater using PVT modules. The brackish groundwater is assumed to be preheated before water treatment to reduce the energy

intensity of desalination while the solar panels are assumed to be cooled using brackish groundwater to improve the efficiency of solar power production. In Scenario C, the solar farm and desalination facility are co-located for the purpose of yielding these mutual benefits and it is therefore assumed that all solar-generated electricity is sold to the grid. Revenue generated from the co-located solar farm can also be an important source of revenue from this facility to make desalination integrated with renewable power more attractive. This scenario is shown in Figure 9.

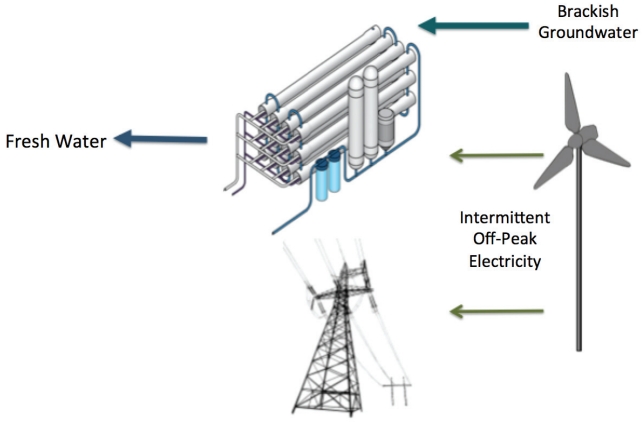

Figure 8. Scenario B models a desalination facility integrated with wind power that can either use wind-generated electricity for water treatment or sell wind-generated electricity to the grid.

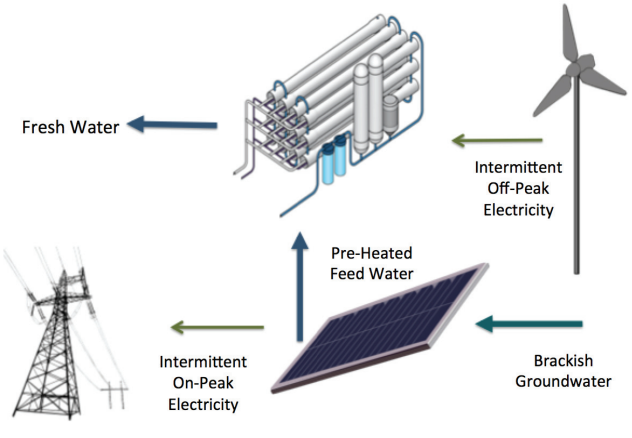

Figure 9. Scenario C models a desalination facility integrated with a wind farm and co-located with a solar farm. Wind-generated electricity is used to power the water treatment process while the solar panels are used to reduce the energetic intensity of desalination.

Finally, Scenarios A, B, and C are compared to Scenario D in which desalination is powered solely by electricity purchased from the grid. Electricity from the grid is assumed to be purchased at an industrial price, as discussed in the section regarding the integrated this model. This final scenario is shown in Figure 10.

The following sections describe the models used to analyze Scenarios A, B, and C of desalination powered by renewable energy, and Scenario D of desalination powered by the electricity grid.

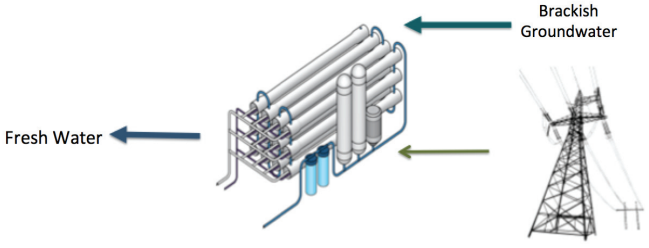

Figure 10. Scenario D models the traditional approach of a desalination facility that is powered by electricity purchased from the grid.

3.2. Water Treatment Model

The power requirement for brackish groundwater desalination is estimated to determine the energetic needs of the proposed integrated facility and to size the modeled wind and solar farms. Using a modified version of the approach developed by Clayton, Stillwell, and Webber [3], the total power needed by the desalination facility (P) is estimated by combing the power required for pumping water from the aquifer and through pipelines (P_P) and the power required to push water through the desalinating membranes (P_D), as shown in Equation (1).

$$P = P_P + P_D \tag{1}$$

The power required for pumping, shown in Equation (2), utilizes the Darcey-Weisbach for head loss in a pipe due to frictional and gravitational forces. The calculated pumping power requirement is a function of the density of water (ρ), the pump efficiency (η_P), the acceleration due to gravity (g), the desalination capacity factor (CF_D), the depth to the aquifer (z), the pipe length (l), the pipe diameter (D), and the friction factor (f), as shown in Equation (2).

$$P_P[kW] = \left(\frac{\rho[\frac{kg}{m^3}]g[\frac{m}{s^2}]q[\frac{m^3}{s}]}{1000\eta_P CF_D}\right) \times \left(z[m] + \frac{\left(\frac{4q[\frac{m^3}{s}]}{\pi(d[m])^2}\right)^2}{2g[\frac{m}{s^2}]} \times \frac{f}{d[m]} \times (z[m] + l[m])\right) \tag{2}$$

The flow rate of water (q) is calculated from the desired daily treated water generation (G_D) divided by the reverse osmosis recovery factor (R_D), which is the ratio of product water to incoming groundwater, assumed to be 0.8 in this analysis. The calculation used to determine the assumed flow rate is given in Equation (3).

$$q[\frac{m^3}{s}] = \frac{G_D[\frac{m^3}{d}]}{R_D} \times \frac{1}{86400}[\frac{d}{s}] \tag{3}$$

The power required for the reverse osmosis desalination process (P_D) is a function of the energy intensity of desalination (E_D), the desalination capacity factor (CF_D), and the flow rate (q), as shown in Equation (4).

$$P_D[kW] = \frac{E_D[\frac{kWh}{m^3}]q[\frac{m^3}{s}]}{CF_D} \times 3600\frac{[s]}{[hour]} \quad (4)$$

The energy intensity of desalination used in this analysis is 1.5 $\frac{kWh}{m^3}$ based on values reported in literature for reverse osmosis desalination of brackish groundwater [46–48]. The 1.5 $\frac{kWh}{m^3}$ value is used for models in this investigation that do not assume brackish groundwater is preheated before treatment.

As indicated previously, research has shown that preheating brackish groundwater before treatment can alleviate the energy intensity of the desalination process by decreasing the pressure required to force water through the semi-permeable membrane. Research at the Center for Inland Desalination at the University of Texas at El Paso (UTEP) suggests that the specific energy required to operate desalination units decreases by 3.4% if water is heated just 5 degrees Celsius [37]. Using results from this research, it is assumed that the energetic intensity of desalination (E_D) is reduced by 3.4% for the scenarios involving PVT solar panels that enable the water to be preheated prior to the desalination process. Hence, for Scenarios A and C, which assume brackish groundwater is preheated before treatment, the energy intensity of desalination used is 1.4 kWh/ m^3

The desalination capacity factor (CF_D) is the ratio of the actual output of treated water to the potential output of treated water for the plant operating in an ideal situation. This factor is included to account for maintenance interruptions and is assumed to be 0.95 (the actual output is 95% of potential output).

For this analysis, a daily product water generation of 3000 m^3/day is used, which is just over 790,000 gallons per day. This daily water generation would be capable of supplying the municipal demand serving a population of 4000 assuming a per capita demand of 195 gallons per person per day, the average daily use in Texas's 40 largest cities in 2000 [49]. However water conservation efforts recommended by the Texas Water Development Board encourage 1% annual reduction in water demand until the goal of 140 gallons per person per day is reached [50]. Assuming a daily use meeting this goal, the modeled desalination plant would meet the daily municipal demand for a population of approximately 5600.

Equation (1) through Equation (4) represent the water treatment model used in this investigation. These equations are used in order to determine the energetic requirement of the desalination plant modeled in this analysis. Parameter assumptions used in the water treatment model are shown in Table 1.

Utilizing this water treatment model, Scenarios A, B, C, and D were analyzed in order to estimate the energetic requirement of brackish groundwater desalination. This estimation was incorporated into the energy model discussed in the following section.

Table 1. Water treatment model parameter values.

Parameter	Symbol	Value
Depth to aquifer	z	275 m
Pipe length	l	5250 m
Density of water	ρ	1000 kg/m^3
Pump efficiency	η_P	0.65
Acceleration due to gravity	g	9.81 m/s^2
Pipe diameter	D	0.3 m
Friction factor	f	0.0162
Reverse osmosis recovery factor	R_D	0.8
Energy intensity of reverse osmosis for Scenarios B and D	E_D	1.5 kWh/m^3
Energy intensity of reverse osmosis for Scenarios A and C	E_D	1.4 kWh/m^3
Desalination capacity factor	CF_D	0.95
Desired daily product water	G_D	3000 m^3/day

3.3. Energy Model

The energetic model was developed to estimate the appropriate size for the required wind and/or solar farm to integrate or collocate with desalination in Scenarios A, B, and C. Using historical wind and solar farm output data as well as basic principles of thermodynamics, the energetic model is used to estimate sizing and power output that can be used alongside the water treatment model for this analysis of desalination powered by renewable energy.

3.3.1. Solar Farm Sized for Preheating Water in Scenario C

A thermodynamic analysis of the heat required to raise brackish groundwater temperature sufficiently to reduce the energetic intensity of desalination was performed following basic thermodynamic principles [51]. For Scenario C, it is assumed that brackish groundwater is preheated before treatment to lower the energetic requirement of desalination and that the solar panels are cooled with pretreated water to improve the efficiency of solar-power production. In this scenario, the solar farm is assumed to be co-located with a desalination plant to yield these mutual benefits. Accordingly, the solar farm is sized to provide sufficient thermal energy to enable water to be heated before treatment. Based on results from the UTEP Center for Inland Desalination [37] discussed previously, the energy intensity of desalination can be reduced by approximately 3.4% if brackish groundwater is heated 5 degrees Celsius. In accordance with this research, the solar farm is sized to provide sufficient thermal energy to heat brackish groundwater by 5 degrees Celsius, from 25 to 30 degrees.

The "Zeroth" Law states that all mass is conserved within the boundaries of a closed system and all mass that enters an open system must exit or be stored in the system. Here, an open system of the PVT modules is assumed to be operating at steady state, such that the mass entering equals the mass exiting. The working fluid and mass of interest in this scenario is water, which is assumed to absorb

thermal energy from the solar panels. The PVT solar panels in Scenario C act as a heat exchanger in which “waste heat" from the relatively hot panels is transferred to the relatively cool water. As previously discussed and shown in Figure 3, a working fluid, water in this case, enters one end of the PVT panel and exits the other end at a higher temperature. The mass of water entering the PVT exchanger ($\dot{m}_{in}$) equals the mass of water exiting ($\dot{m}_{out}$), as shown in Equation (5).

$$\dot{m}_{in} = \dot{m}_{out} = constant \tag{5}$$

The mass flow rate of water ($\dot{m}$) is calculated based on the desired daily product water (G_D). This value must be divided by the desalination recovery rate (R_D) to account for the fact that not all pumped water is treated to drinking-water quality in the desalination process. Additionally, the desired daily product water (G_D) must be divided by the inverse of density for water ($\frac{1}{\rho}$) to convert a volume flow rate to a mass flow rate. The calculation of this mass flow rate ($\dot{m}$) is shown in Equation (6).

$$\dot{m}[\frac{kg}{s}] = \frac{G_D[\frac{m^3}{day}]}{\frac{1}{\rho}[\frac{m^3}{kg}]R_D} \times \frac{1}{86400}[\frac{day}{sec}] \tag{6}$$

The “system” in this thermodynamic analysis is defined as a control volume consisting of the brackish groundwater passing through the PVT panels. Heat ($\dot{Q}$) is transferred from the hot solar panels to the relatively cool brackish groundwater. The specific enthalpy of the brackish groundwater entering the PVT panels ($\dot{h}_{in}$) is increased and the water leaves with a higher specific enthalpy ($\dot{h}_{out}$) due to the heat transfer from the warm panels to the cool water. This concept is the conservation of energy, known as the First Law of Thermodynamics, and presented in Equation (7).

$$\dot{Q}[kW] = \dot{m} \times (h_{out}[\frac{kJ}{kg}] - h_{in}[\frac{kJ}{kg}]) \tag{7}$$

The specific enthalpy of water is a function of water temperature and can be found using thermodynamic property tables [51]. The energetic model assumes water temperature is increased five degrees Celsius, from 25 to 30 degrees Celsius based on research of preheating reverse osmosis feed water [37] and the temperature of naturally occurring groundwater in central Texas [52]. Hence, specific enthalpies of entering and exiting water in Equation (7) are taken at 25 and 30 degrees Celsius, respectively. While density is also a temperature dependent property, this value varies negligibly for water between 25 and 30 degrees Celsius. Parameter value for Equations (6) and (7) are listed in Table 2.

Table 2. Heat exchange parameters.

Parameter	Symbol	Value
Inverse of density of water	$\frac{1}{\rho}$	0.001003 $\frac{m^3}{kg}$
Specific enthalpy of water entering PVT panel	h_{in}	104.89 $\frac{kJ}{kg}$
Specific enthalpy of water exiting PVT panel	h_{out}	125.79 $\frac{kJ}{kg}$

Finally, the required solar farm capacity in Scenario C ($C_{SOLAR,C}$) is estimated by dividing the heat ($\dot{Q}$) found in Equation (7) by the thermal efficiency of the PVT solar modules (η_{PVT}). In this analysis, a thermal efficiency of 0.55 is assumed based on average values reported from studies regarding experimental performance of PVT solar panels [35,53]. This final calculation of the solar farm sizing in Scenario C is shown in Equation (8).

$$C_{SOLAR,C}[kW] = \frac{\dot{Q}[kW]}{CF_{SOLAR}\eta_{PVT}} \tag{8}$$

These calculations were performed to estimate the solar power capacity for a modeled solar farm that is sized to preheat brackish groundwater. The next section uses similar methodology, but is used to estimate the required size for a solar farm used to power desalination.

3.3.2. Solar Farm Sized for BWRO Desalination in Scenario A

In the energetic model for Scenario A, the solar farm is integrated with the BWRO desalination facility for the primary purpose of supplying power for the water treatment process. Hence, the modeled solar farm is sized to meet the power requirement of BWRO desalination. The required power in this process (P) is calculated using Equation (1) and divided by the solar power capacity factor (CF_{SOLAR}) to account for the intermittent nature of available solar power. Using the estimated power for desalination and the capacity factor, Equation (9) is developed to calculate the required solar farm size for Scenario A ($C_{SOLAR,A}$).

$$C_{SOLAR,A}[kW] = \frac{P[kW]}{CF_{SOLAR}} \tag{9}$$

The solar energy supplied to BWRO desalination plant will not be constant because of the inherent daily and hourly variability of solar resources. Therefore, the modeled solar farm utilizes the capacity factor (CF_{SOLAR}) to size the facility to meet the heating requirement of the BWRO desalination facility based on the average generation from the solar farm. Data of hourly solar insolation measured in Abilene, a city in Central Texas, was used to determine average solar insolation and calculate the solar farm capacity factor (CF_{SOLAR}) [44,54]. Based on these data, on a typical day, it is determined that average incoming solar insolation is 21% of peak incoming solar insolation at the location and therefore average output for the modeled solar farm is 21% of peak installed solar capacity. The capacity factor for solar power (CF_{SOLAR}) of 0.21 is used in Equation (9) to estimate the required solar farm capacity ($C_{SOLAR,C}$) based on the power required for desalination (P) in Scenario A.

Using data solar insolation data recorded in Abilene [54], the modeled solar farm is sized in Scenario A assuming that typical output is 21% of peak solar farm capacity. On some days, it is therefore possible that power generation from the solar farm may be above or below the required power for desalination. Solar-generated electricity can be sold to the grid on days when power is above typical output while electricity can be purchased from the grid on days when output is below the requirement for water treatment. This idea is incorporated in the integrated model and is an essential concept of the grid-connected integrated facility discussed in this investigation.

3.3.3. Wind Farm Sizing for Scenarios B and C

Another primary purpose of this investigation is to compare the benefits and tradeoffs of integrating desalination with different sources of renewable power, namely wind versus solar. An integrated facility consisting of a solar farm (Scenario A), a wind farm (Scenario B), and a combination of a wind and a solar farm (Scenario C) are investigated in this analysis. The methodology for the energetic module in Scenario B is based on the wind-powered desalination investigation performed by Clayton, Stillwell, and Webber [3].

The wind farm modeled in Scenario B is sized to meet the power requirement of BWRO desalination. Similar to the solar farm modeled in Scenario A, the wind farm modeled in Scenario B will not be constant due to the inherent variability of wind resources. Therefore, the modeled wind farm is sized to meet the power requirement of the BWRO desalination facility based on average generation from the wind farm. Data of wind-power generation from the Sweetwater 1 Wind Farm in Central Texas were used in this analysis to determine the average output and calculate the wind farm capacity factor (CF_{WIND}) [55]. Based on these data, it is determined that average output is approximately 35% of installed capacity. Therefore, the modeled wind farm will be sized to provide power for the BWRO facility accounting for a wind farm capacity factor (CF_{WIND}) of 0.35. The required wind farm size for Scenario B ($C_{WIND,B}$) is a function of this capacity factor and the estimated power requirement of BWRO desalination (P), as shown in Equation (10).

$$C_{WIND,B}[kW] = \frac{P[kW]}{CF_{WIND}} \tag{10}$$

Similar to the solar farm in Scenario A, the wind farm in Scenario B is sized based on the energetic requirement of BWRO desalination assuming average of the peak output from the wind turbines. Power generation from the wind farm can vary above or below the required power for desalination due to fluctuations in wind power availability. Hence, when wind power generation is above the requirement for desalination, wind-generated electricity can be sold to the grid. When wind power is below the requirement for desalination, electricity can be purchased from the grid to power the water treatment process. The integrated model incorporates this idea for the grid-connected wind farm in Scenario B.

Results from the water treatment and energy models are used in the integrated model to investigate the potential daily operational schedule for desalination powered by renewable energy, as discussed in the following section.

3.4. Integrated Model

A grid-connected BWRO desalination facility integrated with renewable power offers an opportunity to provide both treated water and electricity. One of the goals of this analysis is to develop a daily operational schedule to understand when wind and solar-generated electricity would be used for desalination versus when this electricity would be sold to the grid. A related assessment is investigating the times electricity must be purchased from the grid in order to meet the energetic requirement for desalination when renewable power is unavailable or sold for other uses.

The integrated model discussed in this section provides these assessments. Using results from the water treatment and energy models, the integrated model provides an analysis of the potential daily operational schedule of a desalination facility integrated with wind or solar power. Additionally, the integrated model estimates potential daily revenue from desalination, daily revenue from power production, and the daily cost of electricity purchased from the grid.

The integrated model is programmed to develop a daily operational schedule that would maximize overall daily revenue from a modeled desalination facility integrated with renewable power. Capital and operational costs are an important consideration, however, are beyond the scope of this work, which focuses on daily revenue. To perform this optimization, a General Algebraic Modeling System (GAMS) [56] was developed for each of the three Scenarios (A, B, and C) and compared to a baseline case of desalination powered by grid-purchased electricity (Scenario D). The model is based on 15 min time intervals, the given interval for electricity pricing in Texas as determined by the Electric Reliability Council of Texas (ERCOT). At each 15 min time interval, the model optimizes operations by determining if the facility should produce water using wind/solar-generated electricity, produce water using electricity purchased from the ERCOT grid, or pause desalination in order save money on electricity and brine disposal. For Scenarios A, B, and C, the model determines if wind- or solar-generated electricity should be used for water production or sold to the ERCOT grid, depending on which option is more profitable at the given 15 min interval. By developing optimal operational schedules for wind/solar powered desalination, the integrated model offers insight into how an integrated facility may interact with the electric grid.

Wind and solar resources as well as electricity prices vary seasonally. Therefore, the operational analyses in this investigation develops optimal daily profiles for a typical summer day and a typical winter day. Electricity and output data from July, August, and September were used for summer months while data from December, January, and February were used for winter months. The following section discuss this seasonal analysis of optimal daily profiles and provide details regarding modeling differences between Scenarios A, B, C, and D.

3.4.1. Water Production Revenue and Cost for Scenarios A, B, C and D

For all scenarios analyzed in this investigation, the revenue generated from desalination (R_{DESAL}) is calculated by multiplying the price of water (Pr_{WATER}) by the quantity of water generated in each of the 15-minute interval ($G_{D,t}$), as shown in Equation (11).

$$R_{DESAL}[\frac{\$}{day}] = Pr_{WATER}[\frac{\$}{m^3}] \times \sum_{t=1}^{96} G_{D,t}[\frac{m^3}{t}] \tag{11}$$

Additionally for all scenarios, the analysis of desalination must account for the cost of disposing of the high salinity brine (C_{BRINE}) that is generated in the reverse osmosis process. This cost is a function of the unit cost of brine disposal (Pr_{BRINE}) and the quantity of water generated in the each 15 min interval, demonstrated in Equation (12).

$$C_{BRINE}[\frac{\$}{day}] = Pr_{BRINE}[\frac{\$}{m^3}] \times \sum_{t=1}^{96} G_{D,t}[\frac{m^3}{t}] \tag{12}$$

Municipal water prices in Texas range from \$0.20 to \$2.80 per m^3 [57]. This investigation was therefore performed to compare low, moderate, and high water prices of \$0.20, \$1.60, and \$2.80 per m^3. The unit cost of brine disposal is assumed to be \$0.04 per m^3 based on the assumption of deep-well injection as the brine disposal method at the modeled desalination facility [58,59].

To estimate the electricity that must be provided by either the grid or the renewable energy sources, the power used for water production (E_{DESAL}) must be calculated in each 15 min interval based on the desired daily product (G_D), power required per unit of water production (P), and quantity of water produced in each interval ($G_{D,t}$), as shown in Equation (13).

$$E_{DESAL}[\frac{kWh}{t}] = \frac{P[kW]}{G_D[\frac{m^3}{day}]} \times *G_{D,t}[\frac{m^3}{t}] \times 24\frac{[hour]}{[day]} \quad (13)$$

An additional cost that Scenarios A, B, C and D all incorporate is the cost of electricity purchased from the grid. Recall that in Scenarios A, B, and C, electricity can be purchased from the grid if wind- or solar-generated electricity is unavailable or if wind- or solar-generated electricity is sold to the grid rather than used for desalination. For this analysis, the price of electricity purchased from the grid ($P_{ELECTRICITY}$) is assumed to be \$0.068 per kilowatt hour (kWh), the average price of electricity for industrial consumers in 2011 [60]. The total cost of grid-purchased ($C_{ELECTRICITY}$) electricity is a function of this price and the quantity of electricity purchased from the grid (E_{GRID}) during each 15 min interval, as shown in Equation (14).

$$C_{ELECTRICITY}[\frac{\$}{day}] = P_{ELECTRICITY}[\frac{\$}{kWh}] \times \sum_{t=1}^{96} E_{GRID}[\frac{kWh}{t}] \quad (14)$$

For all scenarios analyzed in this investigation, the price of electricity used is the average wholesale electricity price for each 15 min interval during the given season (summer or winter). ERCOT data from 2012 was used for grid electricity prices ($P_{ELECTRICITY}$) [61].

A constraint included in the models for Scenarios A, B, C and D is that for the daily water production must be at least 1000 m^3 per day. This constraint is included to model a practical scenario in which a minimum daily requirement of water must be met regardless of the economic favorability of the operations to meet water demand of a municipality. The facility is designed to produce 3000 m^3 per day, but may generate less water if economic circumstances indicate it is more profitable to halt desalination during certain times of day.

Equations (11)–(14) are used in the integrated GAMS model for all scenarios, A, B, C, and D. The following sections discuss additional equations used respectively by each unique scenario.

3.4.2. Integrated GAMS Model for Scenario A

The integrated GAMS model for Scenario A calculates the solar-generated electricity sold to the grid and the solar-generated electricity used for desalination. Data from Abilene discussed previously were used to estimate the expected availability of solar energy at each 15 min interval throughout the day. The electricity provided by the modeled solar farm ($E_{SOLAR_A,t}$) is assumed to be proportional to the direct solar insolation (SR) at the given 15-minute interval, as shown in Equation (15). Note

that the factor of 1/4 is included in the following equation to account for the fact that there are four fifteen-minute intervals, the time step of this analysis, in each hour.

$$E_{SOLAR_A,t}[\frac{kWh}{t}] = \frac{SR_t[\frac{W}{m^2}]}{SR_{MAX}[\frac{W}{m^2}]} \times C_{SOLAR,A}[kW] \times \frac{1}{4}\frac{hour}{t} \tag{15}$$

The electricity generated at the solar farm sold the the grid in Scenario A ($E_{SOLAR-GRID_A,t}$) is calculated by taking the solar energy produced ($E_{SOLAR_A,t}$) minus the energy used for desalination ($E_{DESAL_A,t}$) in each 15 min time interval, represented in Equation (16).

$$E_{SOLAR-GRID_A,t}[\frac{kWh}{t}] = E_{SOLAR_A,t}[\frac{kWh}{t}] - E_{DESAL_A,t}[\frac{kWh}{t}] \tag{16}$$

The revenue from solar energy sold to the grid in each 15-minute interval ($R_{SOLAR_A,t}$) is calculated by multiplying the amount of solar energy sold to the grid ($E_{SOLAR-GRID_A,t}$) by the electricity price ($Pr_{ELECTRICITY}$) at each time period. Total revenue from solar energy (R_{SOLAR_A}) is then taken as the sum of the revenue in each 15-minute interval. These relationships are shown in Equations (29) and (30).

$$R_{SOLAR_A,t}[\frac{\$}{t}] = E_{SOLAR-GRID_A,t}[\frac{kWh}{t}] \times Pr_{ELECTRICITY}[\frac{\$}{kWh}] \tag{17}$$

$$R_{SOLAR_A}[\$] = \sum_{t=1}^{96} R_{SOLAR_A,t}[\frac{\$}{t}] \tag{18}$$

For the price of electricity in each 15 min interval ($Pr_{ELECTRICITY}$), ERCOT West Zone Real Time electricity prices from 2012 were used [61]. The wind and solar farms from which the data were collected are located in this electricity pricing zone.

Finally, the total revenue for Scenario A (R_A) can be calculated based on the revenue from desalination (R_{DESAL}), revenue from solar power (R_{SOLAR}), cost of electricity from the grid ($C_{ELECTRICITY}$), and cost of brine disposal (C_{BRINE}), as shown by Equation (19).

$$R_A[\$] = R_{DESAL_A}[\$] + R_{SOLAR_A}[\$] - C_{ELECTRICITY_A}[\$] - C_{BRINE_A}[\$] \tag{19}$$

By maximizing the objective function defined in Equation (19), the GAMS model computes a daily schedule for Scenario A to maximize daily revenue.

3.4.3. Integrated GAMS Model for Scenario B

The integrated GAMS model for Scenario B is developed in a similar fashion to that for Scenario A, except using a modeled wind farm rather than a modeled solar farm. For input data to estimate the availability of wind resources, daily profiles from the Sweetwater 1 Wind Farm were used. The electrical energy provided by the modeled wind farm is assumed to be proportional to the average capacity factor from the Sweetwater 1 Wind Farm dataset at each 15 min interval for the given season (summer or winter), as shown in Equation (20). Note that the factor of 1/4 is included in the following equation to account for the fact that there are four fifteen-minute intervals, the time step of this analysis, in each hour.

$$E_{WIND,t}[\frac{kWh}{t}] = CF_{AVG,t} \times C_{WIND,B}[kW] \times \frac{1}{4}\frac{hour}{t} \tag{20}$$

Similar to the solar farm in Scenario A, the electricity generated from the wind farm in Scenario B that is sold to the grid ($E_{WIND-GRID_B,t}$) is calculated by taking the difference of wind energy produced ($E_{WIND_B,t}$) the energy used for desalination ($E_{DESAL_B,t}$) in each 15 min time interval, represented in Equation (25).

$$E_{WIND-GRID_B,t}[\frac{kWh}{t}] = E_{WIND_B,t}[\frac{kWh}{t}] - E_{DESAL_B,t}[\frac{kWh}{t}] \tag{21}$$

The revenue from wind energy sold to the grid in each 15-minute interval ($R_{WIND_B,t}$) is calculated by multiplying the amount of wind energy sold to the grid ($E_{WIND-GRID_B,t}$) by the electricity price ($Pr_{ELECTRICITY}$) at each time period. Total revenue from wind energy (R_{WIND_B}) is then taken as the sum of the revenue in each 15 min interval. These relationships are shown in Equations (26) and (27).

$$R_{WIND_B,t}[\frac{\$}{t}] = E_{WIND-GRID_B,t}[\frac{kWh}{t}] \times Pr_{ELECTRICITY}[\frac{\$}{kWh}] \tag{22}$$

$$R_{WIND_B}[\$] = \sum_{t=1}^{96} R_{WIND_B,t}[\frac{\$}{t}] \tag{23}$$

Similar to Scenario A, the total revenue for Scenario B (R_B) can be calculated using the revenue from desalination (R_{DESAL_B}), revenue from wind power (R_{WIND_B}), cost of electricity from the grid ($C_{ELECTRICITY_B}$), and cost of brine disposal (C_{BRINE_B}), as shown by Equation (24).

$$R_B[\$] = R_{DESAL_B}[\$] + R_{WIND_B}[\$] - C_{ELECTRICITY_B}[\$] - C_{BRINE_B}[\$] \tag{24}$$

Equation (24) is used as the objective equation in the GAMS model to determine the daily schedule that maximizes total revenue for Scenario B.

3.4.4. Integrated GAMS Model for Scenario C

Scenario C models a desalination facility integrated with a wind farm to power water production and co-located with a solar farm to provide preheating of brackish groundwater. Wind energy can be used for water treatment or sold to the grid depending on temporally varying electricity prices. Correspondingly, desalination can be powered by either wind-generated electricity or by electricity purchased from the grid. The desalination plant coupled with wind power utilizes the same governing Equations (25)–(27) in Scenario C as in Scenario B, shown below.

$$E_{WIND-GRID_C,t}[\frac{kWh}{t}] = E_{WIND_C,t}[\frac{kWh}{t}] - E_{DESAL_C,t}[\frac{kWh}{t}] \tag{25}$$

$$R_{WIND_C,t}[\frac{\$}{t}] = E_{WIND-GRID_C,t}[\frac{kWh}{t}] \times Pr_{ELECTRICITY}[\frac{\$}{kWh}] \tag{26}$$

$$R_{WIND_C}[\$] = \sum_{t=1}^{96} R_{WIND_C,t}[\frac{\$}{t}] \tag{27}$$

In Scenario C, the purpose of collocating the desalination plant with a solar farm is to provide preheating of brackish groundwater and cooling of solar panels. As discussed previously, all solar power is assumed to be sold to the grid in this scenario. Hence, the solar electricity sold to the

grid ($E_{SOLAR-GRID_C,t}$) in this case is the summation of the solar electricity generated, as shown in Equation (28).

$$E_{SOLAR-GRID_C,t}[\frac{kWh}{t}] = E_{SOLAR_C,t}[\frac{kWh}{t}] \tag{28}$$

Once this modification is made, the governing equations to calculate the revenue from solar energy (R_{SOLAR}) in Scenario C are the same as those for Scenario A, shown below.

$$R_{SOLAR_C,t}[\frac{\$}{t}] = E_{SOLAR-GRID_C,t}[\frac{kWh}{t}] \times Pr_{ELECTRICITY}[\frac{\$}{kWh}] \tag{29}$$

$$R_{SOLAR_C}[\$] = \sum_{t=1}^{96} R_{SOLAR_C,t}[\frac{\$}{t}] \tag{30}$$

Total revenue in Scenario C accounts for revenue from desalination (R_{DESAL_C}), revenue from solar-generated electricity (R_{SOLAR_C}), revenue from wind-generated electricity (R_{WIND_C}) as well as the cost of electricity from the grid ($C_{ELECTRICITY_C}$) and the cost brine disposal (C_{BRINE_C}), as shown in Equation (31). The potential efficiency increase associated with cooler solar panels is not considered in this analysis.

$$R_C[\$] = R_{DESAL_C}[\$] + R_{SOLAR_C}[\$] + R_{WIND_C}[\$] - C_{ELECTRICITY_C}[\$] - C_{BRINE_C}[\$] \tag{31}$$

The objective function shown in Equation (31) is maximized for each 15-minute interval to develop an optimal daily schedule for the desalination facility integrated with wind power and co-located with a solar farm.

3.4.5. Integrated GAMS Model for Scenario D

Scenarios A, B, and C are compared to a situation in which all energy required for desalination is purchased from the ERCOT electric grid. For this case, the electricity purchased from the grid in each 15-minute interval ($E_{GRID_D,t}$) is equal to the energy required for desalination ($E_{DESAL_D,t}$) in that time period, indicated in Equation (32).

$$E_{GRID_D,t}[\frac{kWh}{t}] = E_{DESAL_D,t}[\frac{kWh}{t}] \tag{32}$$

The total cost of grid-purchased electricity is the summation of the electricity purchased in each of these intervals ($E_{GRID_D,t}$) multiplied by the industrial electricity price ($Pr_{ELECTRICITY}$), as shown in Equation (33).

$$C_{ELECTRICITY_D}[\$] = Pr_{ELECTRICITY}[\frac{\$}{kWh}] \times \sum_{t=1}^{96} E_{GRID_D,t}[\frac{kWh}{t}] \tag{33}$$

The total project revenue for Scenario D is the revenue from desalination minus the costs of electricity and brine disposal, shown in Equation (34).

$$R_D[\$] = R_{DESAL_D}[\$] - C_{ELECTRICITY_D}[\$] - C_{BRINE_D}[\$] \tag{34}$$

Equation (34) represents the objective function for a typical scenario is which desalination is powered by electricity purchased from grid.

The equations developed in the optimal operation analysis for Scenarios A, B, C, and D were run in a GAMS optimization model. Using the revenue equation as the criterion value in each case, the model maximizes total profits by determining when desalination should be powered by wind/solar-generated electricity or when wind/solar-generated electricity should be sold to the grid and desalination should be powered by grid-purchased electricity. If electricity and brine-disposal costs are greater than revenue from desalination at any given time, the model can also discontinue desalination to maximize total project revenue. By running this optimization model, daily schedules for desalination were developed for a typical summer and a typical winter day. Additionally, revenues from desalination, wind power, and solar power were calculated, as well as electricity cost from the grid. Using results from the water treatment and energy models, this integrated model offers insight into potential operations of a grid-connected desalination facility powered by renewable energy. Results from these models are discussed in the following sections.

The design variables in this analysis vary in each scenario. In Scenario A, the model determines if solar generated electricity is sold to the grid or used for water treatment. Likewise, for Scenario B, the model determines if wind-generated electricity is sold to the grid or used for desalination. Scenario C considers the same decision as Scenario B, but with the addition of pre heating feed water. For Scenario D, the model determines if electricity should be purchased from the grid or if desalination should be halted in each time interval. In all the scenarios described above, the determination is made with the goal of maximizing daily operational revenue. In essence, the design variable is what the model chooses to do with electricity at any given time interval to maximize the criterion function of daily revenue.

4. Results and Discussion

4.1. Overview

Four Scenarios (A, B, C, and D) were analyzed each at three different water prices ($0.2, $1.6, and $2.8 per cubic meter) to generate optimal daily profiles for two different seasons (summer and winter). Results from the water treatment and energy models were utilized in an integrated model to investigate the potential operational schedule of a desalination facility integrated with renewable power. Optimal operational schedules developed by the integrated model offer insight into the potential benefits and tradeoffs associated with combining desalination with wind and solar power.

4.2. Water Treatment Model Results

The primary purpose of the water treatment model is to provide an estimate of the energy intensity of BWRO desalination for a specified location, in this case, Central Texas. Recall that Scenarios A and C involved the assumption of preheating water before treatment, while Scenarios B and D assume water is fed to the treatment facility at its underground temperature. Hence, the power requirement for water treatment will be reduced for Scenarios A and C compared to Scenarios B and D based

on the assumption that preheating feed water lowers the energetic intensity of reverse-osmosis desalination [37].

For Scenarios B and D, using the parameters summarized in Table 1, an estimated 440 kW of power is required by the BWRO desalination plant. Of this 440 kW, approximately 194 kW is required for pumping water from the ground and through facility pipelines, while 246 kW is needed for the reverse osmosis treatment process. For the cases that assume preheating of brackish groundwater, Scenarios A and C, the power requirement is estimated to be approximately 432 kW (194 kW for pumping and 238 kW for reverse osmosis treatment). The reduction in the energy consumed by desalination for the cases assuming preheating in this modeled situation is quite small. Because the water treatment model assumes a conservative estimate for the reduction in specific energy due to preheating of approximately 3.4% [37], the overall energy requirement in the preheating case remains very similar to the non-preheating case. However, a more significant reduction in the energy requirement of BWRO desalination could be achieved for models assuming larger quantities of daily product water or assuming water is heated to a higher temperature.

The results shown in Table 3 indicate that while the specific energy intensity of desalination can be reduced by preheating water before treatment, the reduction in the energetic requirement of the desalination plant may be minimal. However, a configuration of desalination coupled with solar power offers the additional benefit of improving solar panel efficiency. While improvements in the energetic performance of these systems may be small, benefits to solar power production must also be considered and could make a desalination facility integrated with solar power a favorable configuration.

Table 3. Water treatment power requirement.

	Scenarios A and C	**Scenarios B and D**
Total power requirement by desalination plant	432 kW	440 kW
Power required for pumping	194 kW	194 kW
Power required for RO treatment	238 kW	246 kW

4.3. Energy Model Results

The energy model was developed to estimate the size of the modeled solar and/or wind farm to be integrated with BRWO desalination. This section discusses the results the energetic analysis.

For Scenario A, the solar farm was sized to provide adequate power for water treatment when solar resources are available. In this scenario, the BWRO facility power requirement makes use of the reduced energy intensity due to the assumption of preheating water before treatment. Using this power requirement and a capacity factor 0.21 taken from solar data in Abilene [54], the model estimates a 2057 kW solar farm to be coupled with desalination for this application.

The other configuration involving solar power, Scenario C, sizes the solar farm in order to provide adequate thermal energy to preheat water before treatment. Based on principles of thermodynamics discussed in Chapter 3 [51], the energy model estimates a 1644 kW solar farm would provide

adequate thermal energy for preheating of feed water to reduce the energetic intensity of desalination by the assumed value of 3.4%.

Finally, the energetic model is used to estimate the required wind farm size to provide adequate power for BWRO desalination. Scenario C assumes water is preheated before treatment while Scenario B does not include a solar farm so this assumption is omitted. The estimated wind farm size of Scenario B (1257 kW) is therefore higher than that of Scenario C (1233 kW). These results, as well as the results solar farm sizing in the energy model are summarized in Table 4.

Table 4. Solar and wind farm sizes.

	Solar Farm	**Wind Farm**
Scenario A	2057 kW	N/A
Scenario B	N/A	1257 kW
Scenario C	1644 kW	1233 kW

The solar farm capacity to provide power for water production is greater than the required size to provide preheating of groundwater. Accordingly, feed water in Scenario A can be assumed to be preheated, because the solar farm size is greater than the necessary capacity for preheating that is estimated for Scenario C.

The results in Table 4 indicate that the capacity of the required solar and wind farms for a BWRO facility integrated with renewable power is significantly greater than the nominal power required for water production at the desalination facility. This result is expected because of the intermittent nature of wind and solar power, accounted for by the sizing capacity factors. To generate the desired daily product of 3000 m^3 per day, the solar and wind farms must have a capacity significantly larger than the power required for desalination in order to accommodate for days and hours when wind speeds and solar insolation may be weaker than the farm's capacity and therefore the wind and solar farm output is less than the facility's maximum power output. A key benefit of coupling renewable power with desalination is that water treatment is a time-flexible process that can be operated when wind and solar resources are available to drive water production. Water is easily stored and therefore water treatment offers an ideal opportunity to utilize renewable energy, which is often produced at non-ideal times. The fact that water treatment process can be operated on a schedule determined by power availability rather than power demand makes combining wind and solar with desalination a plausible option. The energy model and associated wind and solar farm sizings estimated here indicate that it is possible to supply the desired daily product at a water treatment facility coupled with renewable power as long as the wind and solar farms are sized adequately above the nominal power requirement for desalination.

4.4. Operational Profiles from the Integrated Model

Results from the water treatment model and the energy model were used in an integrated model to develop daily schedules for a BWRO facility integrated with renewable power. By developing

an optimization program to maximize revenue, the integrated model offers insight onto how a desalination plant may perform if coupled with wind and solar power. Additionally, the optimization model gives indications regarding how the desalination facility may balance the use of grid-purchased electricity versus using renewably-generated electricity.

4.4.1. Operational Profiles for Scenario A

Scenario A models a BWRO desalination plant integrated with solar power in which the solar farm is sized to provide power for water production. To gain understanding into the operations of a grid-connected solar farm, the optimization model allows for the plant to sell solar power to the ERCOT grid and buy electricity for desalination during times when it is economically favorable to do so. This situation was analyzed for a typical summer and winter day, as well for water prices of \$0.20, \$1.60, and \$2.80 per m^3. Figure 11 shows the potential daily operations for Scenario A on a typical summer day.

In Figure 11, it is interesting to note that there exist significantly long times of day when solar-generated electricity is sold to the grid rather than used for water treatment. During times when electricity prices are high, specifically during late afternoon and early evening, it is more profitable for the integrated BWRO/solar facility to sell solar-generated electricity to the grid, rather than use it for desalination. For water prices of \$1.60 and \$2.80 per m^3, the facility elects to purchase additional electricity because producing water is economically attractive in the cases modeling moderate and relatively high water prices. For a water price of \$0.20 per m^3, the facility chooses to halt desalination and only produce the minimum desired daily product when solar power is unavailable or being sold to the grid.

Similarly, for Scenario A during winter, there are times of day when electricity prices are high enough that it is economically attractive to sell solar-generated electricity to the grid rather than use it for water production. Additional electricity is purchased from the grid to power desalination for water prices of \$1.60 and \$2.80 per m^3, while desalination is temporarily discontinued when the modeled water price is \$0.20 per m^3.

The optimal operational profiles for Scenario A indicate that coupling desalination with solar power offers a potential benefit in providing flexibility to the integrated facility; revenue can be generated from water production or from solar power production depending on the season and time of day. However, the daily profiles also indicate that coupling solar power with desalination may not be appropriate for regions with high electricity prices and low water prices. Figures 11 and 12 suggest that there are a number of times of day when the facility would prefer to sell solar-generated electricity to the grid and purchase additional electricity for desalination. The fact that solar power availability typically matches demand means that it is often economically attractive to use solar-generated electricity to meet demand from the grid, rather than use it for a time-flexible process such as desalination. The operational profiles shown in Figures 11 and 12 suggest that there are a number of times of day during both winter and summer that the integrated facility may choose to sell solar-generated electricity rather than use this on-peak energy source for desalination.

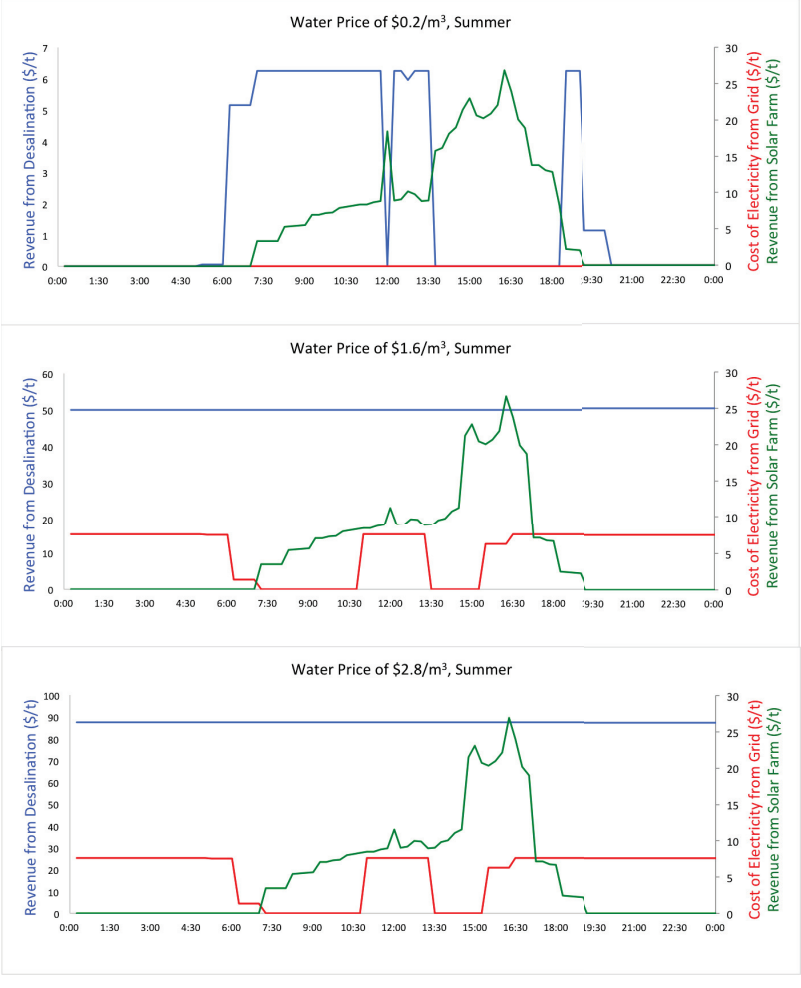

Figure 11. Optimal operational profiles for Scenario A during summer.

4.4.2. Operational Profiles for Scenario B

Results from Scenario B indicate that coupling desalination with an off-peak energy source such as wind power may be a better fit configuration to integrate with water production than solar power. In Scenario B, there are very limited periods of time when the facility elects to sell wind power to the grid, rather than use it for desalination. Throughout most of the day, wind is dedicated to the water treatment process. These results are in sharp contrast with results for Scenario A, when the facility elects to sell power to the grid on multiple instances. As indicated in the following results from Scenario B, coupling wind power with desalination is preferable to integrating solar power with desalination.

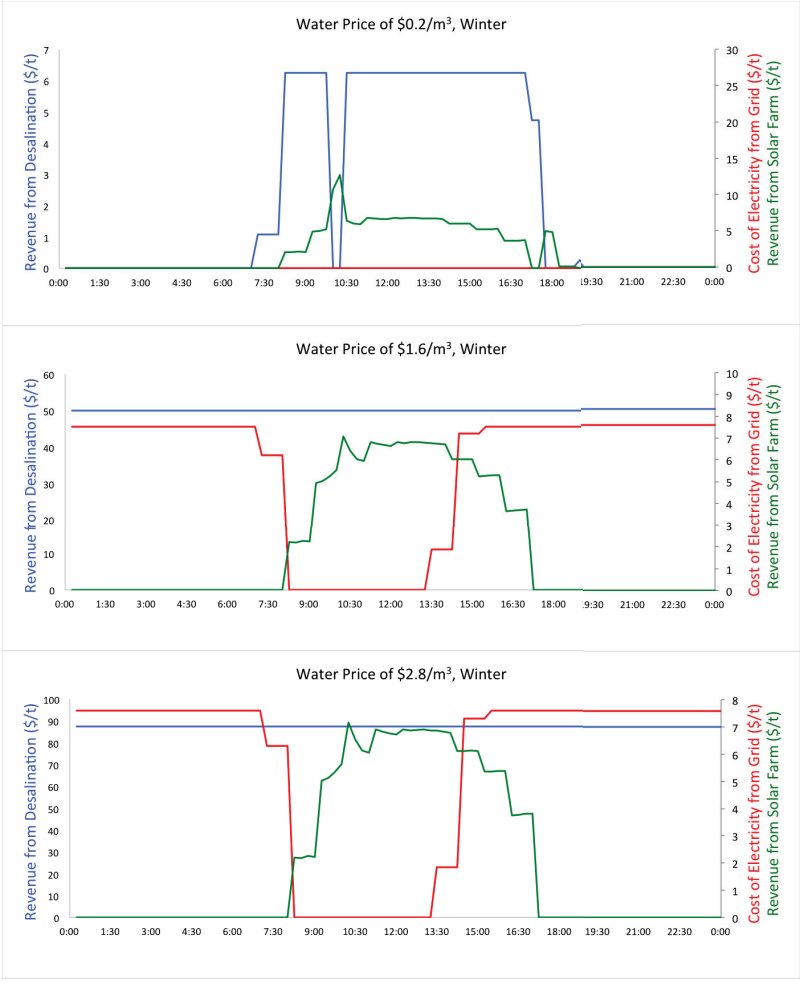

Figure 12. Optimal operational profiles for Scenario A during winter.

In the summer profile for Scenario B, there is a brief period in the afternoon when wind-generated electricity is sold to the grid rather than used for water production. Additional electricity was purchased during this time at a modeled water prices of $1.60 and $2.80 per m^3 so that the BWRO facility may continue to operate at full capacity. At the water price of $0.20 per m^3, desalination was discontinued in the afternoon when electricity prices rise and the facility chooses to sell wind-generated electricity to the grid. These results are shown in Figure 13.

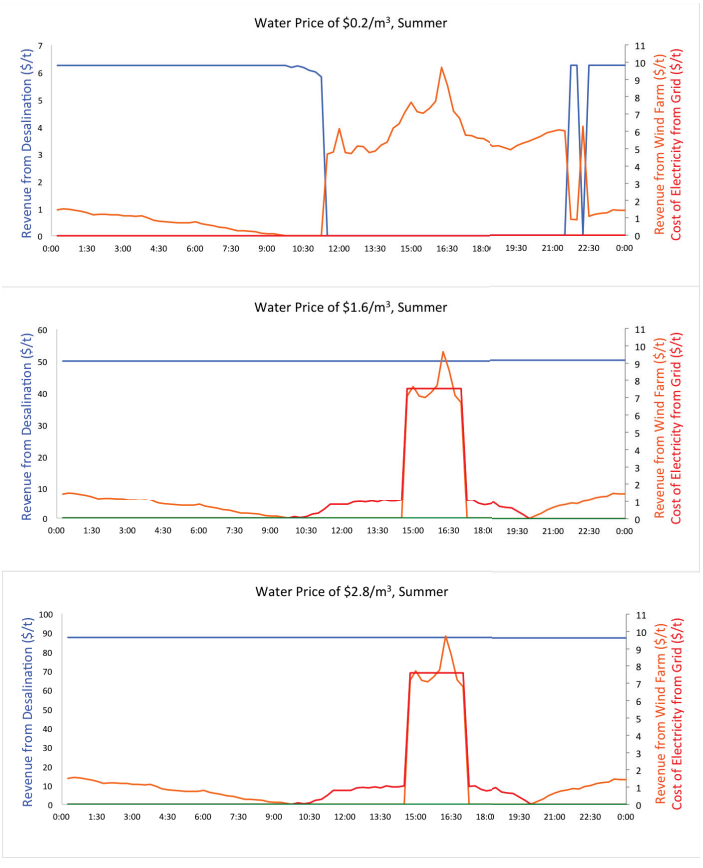

Figure 13. Optimal operational profiles for Scenario B during summer.

For the winter day in Scenario B shown in Figure 14, wind power is dedicated to desalination rather than sold to the grid. For the cases modeling moderate and high water prices, wind-generated electricity is used exclusively for desalination whenever available and only excess wind power is sold to the grid once the energetic requirement for water production is met. This result occurs because wind power mismatches energy demand, meaning peak output from the farm occurs during the off-peak hours of energy demand. Accordingly, electricity prices are not high enough when wind speeds are strong to warrant selling wind-generated electricity to the grid. Figure 14 showing Scenario B during a typical winter day indicates that wind power is used for water production throughout the entirety of the day in the situations modeling moderate and high water prices. In these cases, it makes sense for the facility to use wind power exclusively for water production and only sell wind-generated electricity to the grid once the demand from desalination is met. The fact that the plant elects to use wind-generated electricity for desalination rather than sell wind power to the grid indicates that using wind power for a time-flexible process such as desalination may be an appropriate application for this intermittent energy source.

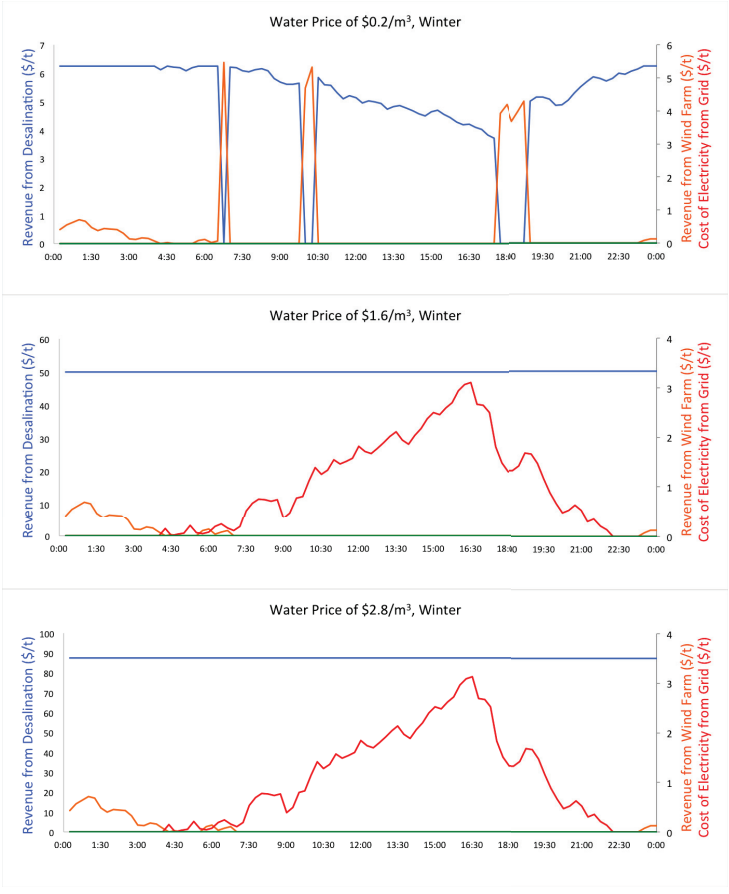

Figure 14. Optimal operational profiles for Scenario B during winter.

A comparison of Scenario A and Scenario B shows that electricity is sold to the grid more frequently when the desalination plant is coupled with solar power than when desalination is integrated with wind power. This result occurs because solar power production matches energy demand while wind power production typically mismatches demand. A comparison of the operational profiles for Scenarios A and B indicate that wind power is better suited than solar power for a time flexible process such as water production than solar power. The following section compares these operational profiles.

4.4.3. Operational Profiles for Scenario C

Results from Scenario C indicate that using a co-located solar farm to preheat brackish groundwater water (while simultaneously cooling solar panels with water) and dedicating wind-generated electricity to water production may be a prudent appropriation of resources for

a desalination facility integrated with renewable power. As shown in the following section, this configuration appears to offer beneficial timing of available wind and solar power. Solar panels can be used to reduce the energy required to treat water while generating electricity to meet demand from the grid. Wind power, which mismatches energy demand, can be used for time-flexible process such as desalination. The results from Scenario C demonstrate this idea.

During a typical summer day, shown in Figure 15, wind-generated electricity is able to provide adequate power for desalination for a majority of the day, while solar-generated electricity is sold to the grid during times of high energy demand. For the modeled water price of \$0.20 per m^3, water treatment is operated throughout the night and early morning. Wind-generated electricity is sufficient to power this process, as indicated by the fact that electricity is not purchased from the grid while desalination is operated. When electricity prices rise in the afternoon, desalination is discontinued because it is economically favorable to sell wind-generated electricity to the grid rather use wind power for desalination in the model when the water price is low. For the case with this low modeled water price, the BWRO desalination plant is not operating at capacity, but rather provides the minimum daily requirement, 1000 m^3 of treated water.

At the modeled moderate and high water prices, desalination is economically attractive and facility operates at capacity all day. Throughout the night and during a majority of the day, the facility uses exclusively wind-generated electricity to produce water. There is a short period of time in the afternoon when electricity is purchased from the grid to power the desalination process and wind resources are sold to the grid. However, for water prices of \$1.60 and \$2.80 per m^3, the BWRO facility is able to produce water using wind-generated electricity throughout most of the day. During the night, morning, and part of the afternoon, wind resources are sufficient to power desalination and no electricity is purchased by the BWRO plant. Electricity prices are high enough in late afternoon (approximately 15:00 to 17:00) such that wind-generated electricity is sold to the grid and additional electricity is purchased to power desalination. For the remainder of the day, water treatment is powered solely by wind-generated electricity and only excess wind power is sold to the grid at times when wind speeds are strong enough to power water production and produce excess electricity to sell to the grid. The fact that the facility would be reliant on wind rather than grid-purchased electricity for most of the day indicates that wind power is ideal for coupling with desalination; wind power is typically available during time periods when energy demand from the grid is low and therefore can be paired with a time-flexible process such as desalination. Figure 15 demonstrates this idea with the indication that wind-generated electricity is dedicated to desalination during a majority of the day and there is only a short period of time when electricity is purchased from the grid.

Additionally, Figure 15 indicates that solar-generated electricity is well suited to meet energy demand from the grid. As expected, revenue is generated from solar power during daytime hours and peaks during the late afternoon when energy demand rises and solar insolation is strong. The times when the facility is able to sell solar power to the grid match times of highest demand, in the morning and afternoon. Accordingly, the facility is able to sell electricity at peak prices. Revenue from selling solar electricity is an important component in the analysis of revenue sources for Scenario C, discussed later in this report. The results in Figure 15 demonstrate that wind power can adequately

supply the energetic requirement for desalination while solar-generated electricity can bring in an additional revenue stream during peak times of day.

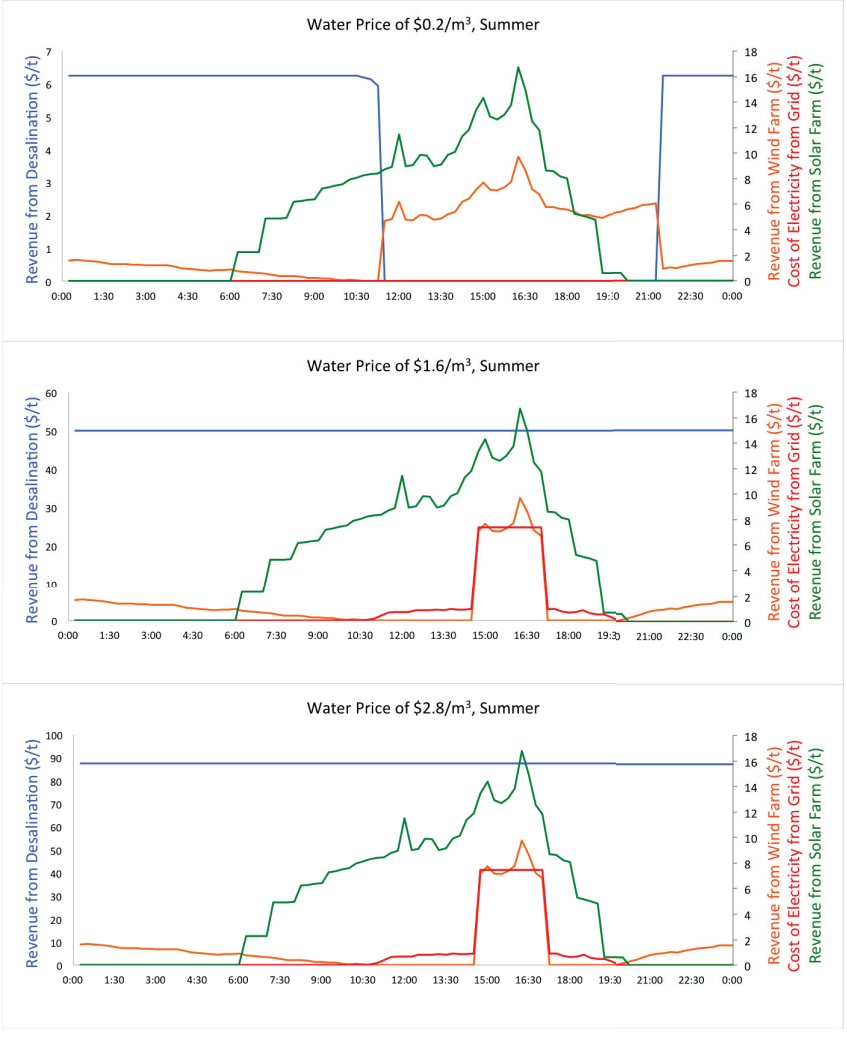

Figure 15. Optimal operational profiles for Scenario C during summer.

The winter profiles for Scenario C also demonstrate a situation in which wind-generated electricity is dedicated to desalination while solar power is produced during times with relatively high electricity demand. Figure 16 suggests that wind resources are used only for desalination when the modeled water price $0.20 per m^3, with the exception of three very short time periods where wind-generated electricity is sold to the grid and water treatment is temporarily discontinued. For the majority of the day, wind power is dedicated to desalination and provides adequate power for the treatment process.

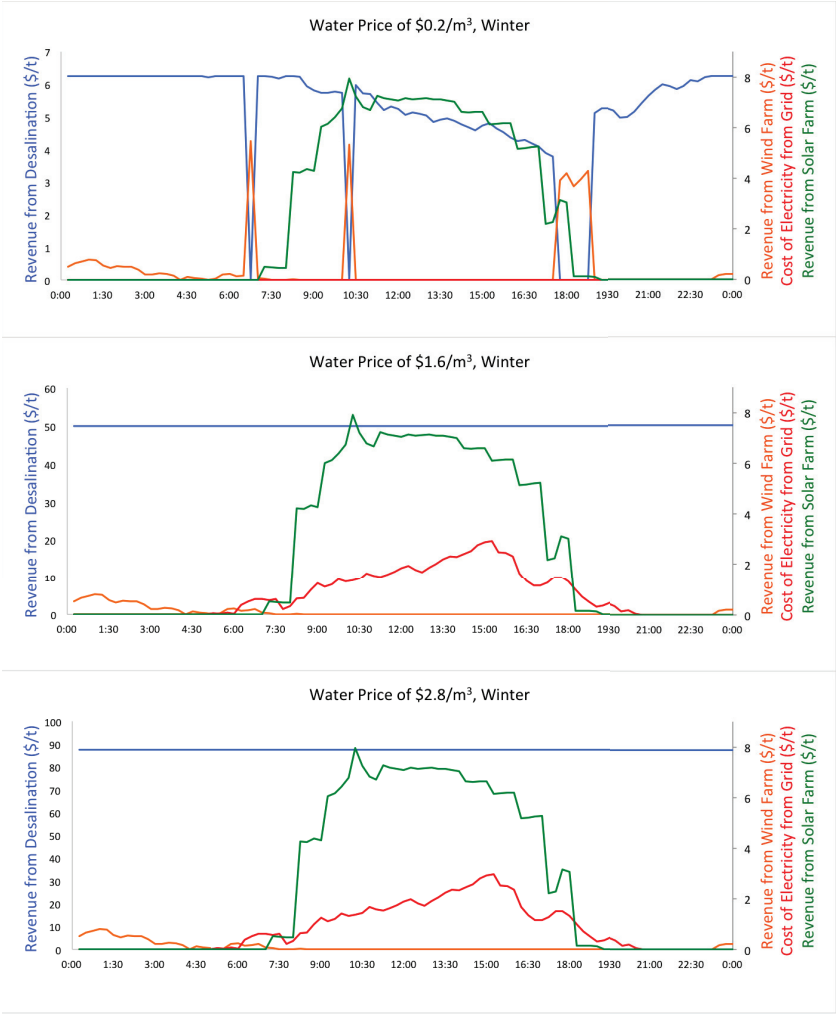

Figure 16. Optimal operational profiles for Scenario C during winter.

For the relatively moderate and high modeled water prices of $1.60 and $2.80 per m^3, wind-generated electricity is used exclusively for water production. Only excess wind-power, beyond that required for desalination, is sold to the grid during nighttime hours and in the very early morning. There exists no times in the day when it is economically favorable to sell wind power to the grid and purchase electricity for desalination, indicating that integrating desalination with wind power is a suitable combination based on the time-availability of wind resources. Because wind-generated electricity is typically available during times of low energy demand, the integrated model suggests that wind energy should be dedicated to desalination rather than sold to the grid at the modeled facility in order to limit cost and maximize total project revenue. Figure 16 indicates that dedicating

wind power to water production is an economically attractive approach, as there exist limited times in the day when wind power is sold to the grid rather than used for desalination.

Similar to the summer profile, solar power in the profile for the typical winter day shows that using solar power to meet energy demand from the grid and to preheat water at the BWRO plant is an appropriate use of resources. Figure 16 indicates that revenue from solar power is generated during a majority of the day (from about 7:00 to 19:00) when energy demand from the grid is relatively high. The modeled facility therefore generates revenue from the sale of solar-generated electricity, while using wind power to meet the energy demands of the water treatment process.

Results from Scenario C shown in Figures 15 and 16 indicate that this configuration fits aptly with the intermittent nature of wind and solar resources: wind power is typically available during times of low energy demand and can therefore be used for desalination while solar power is typically available during times of peak energy demand and can therefore be sold to the grid. The relatively low frequency of purchasing grid electricity for the operational profile of Scenario C indicates that wind provides adequate power for water production. Additionally, the solar farm is an important aspect of this configuration for its role in reducing the energy intensity of the BWRO treatment process. The operational analysis shown here provides insight into the potential performance of a desalination facility integrated with both wind and solar power.

4.4.4. Operational Profiles for Scenario D

Finally, the integrated model was run for Scenario D, assuming electricity is supplied solely by the ERCOT grid at the average retail price of electricity for industrial consumers from 2012, which was \$0.068 per kilowatt hour [60]. Scenario D can be used as a reference point to compare desalination power by renewable energy in Scenarios A, B, and C to a standard case in which desalination is powered by grid-purchased electricity.

Results for Scenario D indicate that the model is highly sensitive the chosen price of water. At a water price of \$0.20 per m^3, the plant elects to not operate at capacity, but rather provide only the minimum daily product of 1000 m^3 per day indicating that it is not economically desirable to produce water at this price. Intermittent times of day for desalination are chosen to produce the minimum daily product. For the remainder of the day, the plant discontinues desalination to maximize project revenue because the cost of electricity and brine disposal are greater than the revenue from water sales. These findings suggest that a desalination facility without integrated renewable power may not be an economically attractive option for water production in regions with low water prices. As indicated by Figure 17, it is prudent for plant to discontinue desalination and only provide the minimum daily product for Scenario D at a water price of \$0.20 per m^3. As shown in Figure 17, the operation of water production is intermittent. The intermittent operation is a result of the optimization setup. The model selects random times to produce water to meet the minimum requirement.

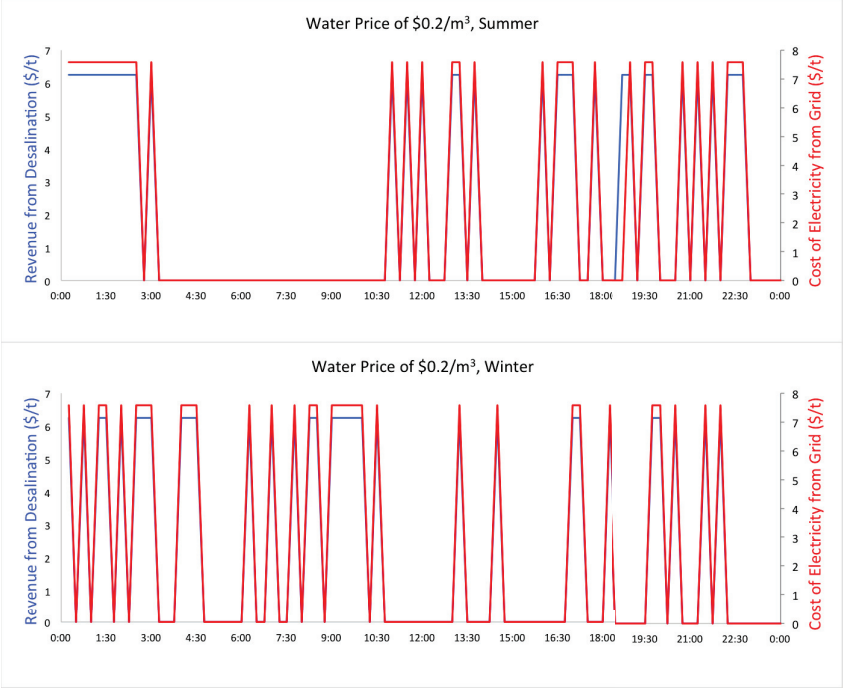

Figure 17. Operational profiles for Scenario D assuming a low modeled water price.

The analysis of Scenario D indicates that when the modeled water price is moderate to high, water production is profitable for the BWRO plant and therefore the facility chooses to operate at capacity at all times. At any chosen water price above $1.60 per m^3, the facility elects to produce the daily maximum of water because the cost of selling water outweighs the costs of purchasing electricity from the grid and of brine disposal. For any modeled water price greater than $1.60 per m^3, the facility will produce water throughout the entirety of the day using electricity purchased from the grid at an industrial electricity price. This result indicates that desalination may be economically attractive for regions with moderate to high electricity prices in Texas, even when no renewable power is provided and the facility purchases electricity from the grid. However, this determination cannot be fully concluded without an analysis of capital and operational costs. An analysis of capital and operational costs is beyond the scope of this work, but may be included in future work.

It is economically desirable for the plant to produce water for the moderate and high water prices of $1.60 and $2.80 per m^3. Electricity is purchased from the grid to supply the energetic requirement of desalination for the entirety of the day, as shown in the figure below.

Results from Scenario D provide insight into the findings from Scenarios A, B, and C and demonstrate the sensitivity of this model to the chosen price of water. For the low modeled water price in Scenario D, it is not economically desirable to produce water and therefore the plant elects to only provide the minimum daily product. These results correspond to cases where the model chooses

to halt desalination in Scenarios A, B, and C. For the renewable power configurations (solar power in Scenario A and wind power in Scenarios B and C) electricity resources are used for desalination to produce only the minimum daily product at selected times. Once the minimum desired daily product is met, wind- and solar-generated electricity are sold to the grid to maximize profits because it is more profitable to sell electricity than to produce water at a low modeled price of water. In these cases, the maximum allowable wind and solar power are sold to the grid and the minimum allowable amount of water is produced to maximize revenue. The model only desalinates water using renewable power when electricity prices are low.

Conversely, for the moderate and high water prices in Scenario D, it is economically desirable to produce water and therefore the plant elects to operate at capacity at all times. This result corresponds to findings in the operational profiles of Scenarios A, B, and C with respect to purchasing electricity from the grid. In these scenarios, there are certain times of day when it is more profitable to sell solar- or wind-generated electricity to the grid rather than use it for desalination. However, producing water is still economically profitable, and therefore additional electricity is purchased to enable the plant to operate at capacity at all times of day. Scenario D indicates that desalination is economically attractive for moderate and high modeled water prices, even when the plant must spend additional money to purchase electricity. Results from Scenario D correspond to findings in Scenarios A, B, and C indicating electricity is purchased from the grid during times when renewable power is sold to the grid to continue desalinating water at all times.

Results from Scenario D are valuable in assessing the sensitivity of the model to the chosen water price. When a low modeled water price is selected, desalination is not profitable because the cost of electricity and brine disposal outweigh revenue from water production. The facility therefore elects to only produce the minimum daily product. When a moderate to high water price is chosen, desalination is economically attractive and the facility elects to produce water at capacity throughout the entirety of the day. These findings indicate that desalination can be profitable for regions in Texas with moderate to high water prices, even if renewable power is not provided and the facility purchases electricity from the grid.

4.5. Comparison of Electricity Costs

A comparison of electricity costs indicates that integrating desalination with renewable power can significantly reduce operational costs of water treatment. Tables 5 and 6 list electricity costs for each scenario for a typical summer and winter day, respectively.

Scenario C provides the configuration with the lowest daily cost of electricity due to the capability of this modeled facility to power the treatment process with wind energy while using solar panels to reduce the energetic intensity of desalination. Having wind power on site significantly reduces electricity costs because the facility chooses to use wind power for desalination throughout most of the day in this scenario. Compared to Scenario D, in which all electricity for water production is purchased from the grid, daily electricity costs in Scenario C are significantly lower. Offering such a configuration can significantly reduce operational expenses at a desalination plant because the

electricity costs often comprise the greatest expense of a desalination plant [11]. Scenario C provides the most cost-effective configuration for reducing electricity costs.

Table 5. Daily electricity cost for a typical summer day.

Water Price	\$0.20 per m^3	\$1.60 per m^3	\$2.80 per m^3
Daily cost of electricity for Scenario A	\$0	\$409	\$409
Daily cost of electricity for Scenario B	\$0	\$97	\$97
Daily cost of electricity for Scenario C	\$0	\$91	\$91
Daily cost of electricity for Scenario D	\$243	\$729	\$729

Table 6. Daily electricity cost for a typical winter day.

Water Price	\$0.20 per m^3	\$1.60 per m^3	\$2.80 per m^3
Daily cost of electricity for Scenario A	\$0	\$426	\$426
Daily cost of electricity for Scenario B	\$0	\$89	\$89
Daily cost of electricity for Scenario C	\$0	\$78	\$78
Daily cost of electricity for Scenario D	\$243	\$729	\$729

Scenario B, the modeled desalination facility integrated with wind power, offers another economical solution to limiting energy costs. The daily cost of electricity in Scenario B is a fraction of that in Scenario A. This result indicates that integrating desalination with wind power is an intelligent paring while desalination integrated with solar power may not be a good fit. In Scenario B, the times when wind is available coincide with times of low energy demand and therefore low electricity prices on the grid. Therefore, the facility chooses to use wind to power water treatment rather than selling wind-generated electricity. Because wind is used for desalination, electricity costs from the grid are low in Scenario B. Conversely, the times when solar power is available coincide with times of high electricity prices and the facility therefore chooses to sell solar power to the grid rather than use it for desalination. The configuration in Scenario A is required to purchase energy to power water treatment from the grid which results in relatively high electricity costs. As indicated by the comparison shown in Tables 5 and 6, electricity costs for the desalination facility integrated with wind power are significantly lower than the modeled desalination facility integrated with solar power. Pairing wind with water treatment offers an economically attractive configuration that can significantly reduce electricity purchases from the grid and operational expenses.

Scenario C, the configuration of desalination integrated with a wind farm and co-located with a solar farm, is a prudent option for reducing electricity costs. This facility is able to power desalination with an on-site resource (wind) while using an onsite technology (solar panels) to reduce the electricity requirement of desalination. The modeled scenarios shown here suggest that paring desalination with renewable power can significantly limit operational expenses.

4.6. Comparison of Revenues from Water and Electricity in Scenario C

The analysis of Scenario C indicates this configuration is also economically preferable because it allows the facility to generate significant revenue from two different and unrelated sources: water and electricity. By selling water from the integrated desalination facility and on-peak electricity from the co-located solar farm (and a small amount of electricity from the wind farm), the configuration offered in Scenario C can reduce risks associated with a decline of either water or electricity sales. For periods of time where water sales drop, the facility can potentially profit from electricity generation. When solar resources are weak, the facility can still bring in money from water sales. The revenue breakdown discussed in this section indicates that electricity sales from the co-located solar farm and integrated wind farm make a significant portion of overall revenue from the facility modeled in Scenario C.

Figure 18 shows the revenue breakdown for a low modeled water price of \$0.20 per m^3.

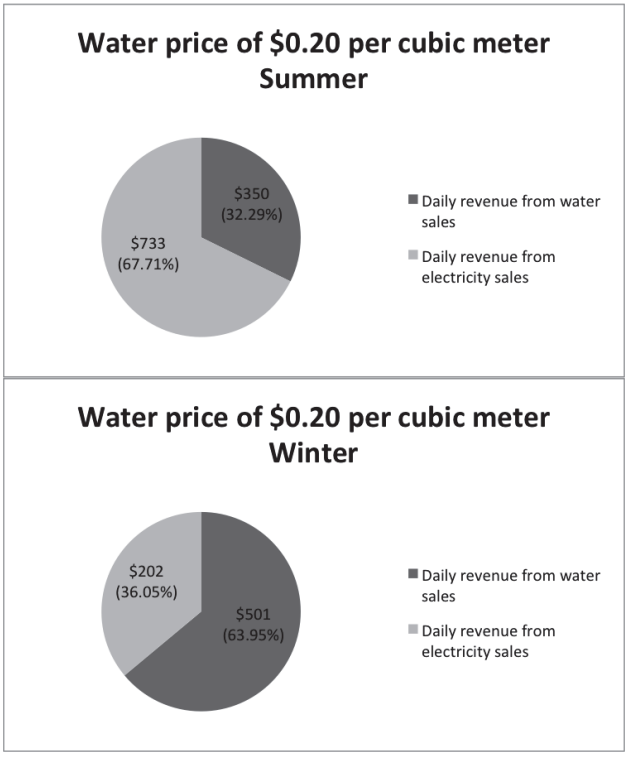

Figure 18. Relative revenue from water and electricity sales for cases with a low modeled water price.

As indicated in Figure 18, daily revenue from electricity sales comprise a significant portion of overall revenue at a low water price. For the modeled summer day, revenue from solar and wind power production are actually greater than revenue from water sales. Revenue from water sales outweighs that from electricity sales for the winter day, however, electricity sales nonetheless provide

over 35% of overall revenue. The fact that revenue expected from electricity sales and water sales are comparable indicates that the facility will not be at risk of major losses on a day where either electricity or water sales are low. If the facility is not able to sell water on a particular day, the plant can still generate significant revenue from electricity generation. On days when solar and wind power production are weaker than usual, the facility will still be able to generate revenue from water production. By providing these two revenue streams, the configuration offered in Scenario C can potentially reduce risks associated with dips in either water or electricity sales. Diversity in revenue streams could me a prudent approach.

For modeled cases with moderate and high electricity prices, revenue from water sales outweighs that from electricity, as shown in Figures 19 and 20. However, revenue from electricity is nonetheless significant in these cases.

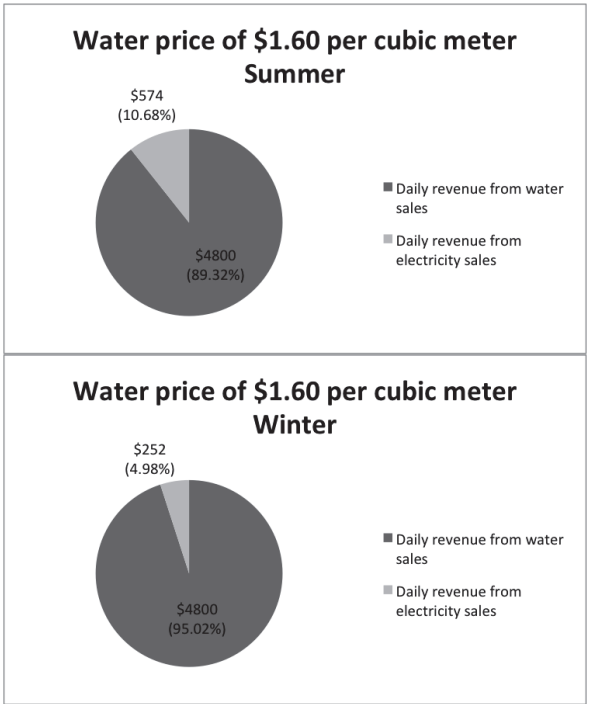

Figure 19. Relative revenue from water and electricity sales for cases with a moderate modeled water price.

Figures 19 and 20 indicate for regions with moderate or high water prices, revenue from water sales will control the overall potential profitability of the facility. However, although electricity sales are a much smaller portion of overall plant revenue, solar and wind power production can still improve the economic attractiveness of the desalination facility in these cases. The model indicates that the percentage of revenue from electricity ranges from approximately 3% to 11% when the modeled water price is moderate to high. These numbers suggest that revenue from electricity could still be significant to overall plant revenue, even though revenue from water sales are much greater

than that of electricity sales. The facility is able to generate more of its profit from water because of the increased water rate, however, revenue from electricity sales makes up a noticeable portion of overall operating revenue in these cases.

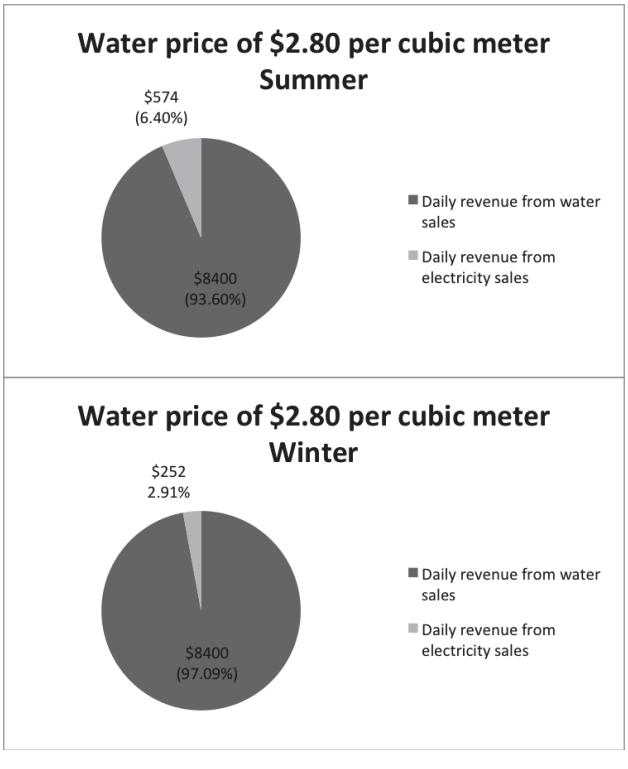

Figure 20. Relative revenue from water and electricity sales for cases with a high modeled water price.

Risk from reduced water production can be mitigated by altering the sizing methodology of the integrated wind farm or co-located solar farm. Recall that in Scenario C, the wind farm is sized to provide adequate power for water production while the solar farm is sized to provide preheating of brackish groundwater. However, the size of the wind and/or solar farm can be increased if the investor would like to further reduce the risk of a decline in water sales. Likely, the solar farm capacity will be increased, which would allow the facility to sell more solar power and generate a greater portion of overall profit from electricity. Sizing the solar farm for economic purposes rather than to preheat feed water for the desalination facility can make Scenario C a less risky investment by ensuring a significant portion of revenue is generated from electricity generation.

The revenue breakdown between water and electricity in Scenario C indicates that this configuration offers an investment that is potentially protected from changes in the water or electricity markets. The facility can generate significant revenue from electricity if water sales decline. Likewise, the facility can make money from water production on days when solar or wind resources

are weak. Diversity in revenue streams is an important consideration of a desalination plant integrated with renewable power.

The analysis performed in this investigation contributes insight into the water-energy nexus involved with desalination. Results indicate that wind and solar power have advantages for pairing with brackish groundwater desalination. Additionally, this investigation provides a modeling methodology to study desalination integrated with wind and solar power. The following section highlights some of the key results, discusses ideas for future work, and offers policy recommendations.

5. Conclusions

As demonstrated in the integrated model for Scenario C, wind-generated electricity is sufficient to meet the energetic requirement of desalination for a majority of the day while solar-generated can be sold to the grid at times of relatively high energy demand. The operational profile for this configuration indicates that electricity purchased from the grid is limited. Having power from the wind farm available during night and early morning limits the amount of electricity purchased from the grid by the integrated facility. The configuration is therefore not heavily reliant on carbon-emitting fossil fuels and offers a suitable use for intermittent wind resources. Additionally, the analysis indicates that the facility can generate significant revenue from solar power, which is produced at on-peak hours when electricity prices are high. The times when solar-generated electricity is sold to the grid in Scenario C match times of relatively high energy demand. Hence this configuration offers an advantage of providing an additional revenue stream from solar power production that could be important to diversifying the revenue streams at the facility. By selling electricity to the grid during times of peak demand and preheating feed water to reduce the energetic intensity of water production, the solar farm is a key aspect of Scenario C. The BWRO facility integrated with wind power and co-located with a solar farm offers advantages inherent to both wind and solar power.

The breakdown of daily revenue in Scenario C indicates that this configuration may provide an opportunity to mitigate risks associated with fluctuations in the water or electricity markets. In Scenario C, the facility is able to generate revenue from both water and electricity sales, diversifying potential profit sources. The analysis demonstrates that revenue from electricity and water sales are comparable in size for cases with low modeled water prices, meaning the facility will not be dependent on one revenue source, but rather will have diversity. For cases with moderate to high water prices, revenue from water sales is greater than that from power production, however, revenue from electricity is still significant in these cases. In finding that revenue from electricity sales are significant in all cases, it can be concluded that providing a co-located solar farm is an opportunity to incorporate diversity in the revenue streams of the facility. The model of Scenario C suggests that the facility will be protected from suffering big losses if either water or electricity sales decline. If the facility is unable to sell water for a particular period of time, electricity sales can still bring in revenue. Likewise, on days when solar or wind resources are weak and electricity is not being generated, the facility can still profit from water production. By providing two sources of revenue, a

desalination facility integrated with wind power and co-located with a solar farm can reduce the risk of investing in stand-alone desalination or renewable energy.

5.1. Future Work

There are many extensions on this analysis of the water-energy nexus that are possible. While this analysis investigated potential daily revenue from solar power, wind power, and water production, future work estimating the cost of the required technologies would be a useful addition. In particular, an investigation of the capital and operational costs of a desalination facility powered by a wind farm and co-located with a solar farm with PVT modules would offer insight into benefits and tradeoffs associated with such as system. The cost of providing both wind and solar power are likely significant considerations that must be accounted for and therefore a cost-benefit analysis of such a system would be useful. The breakdown of daily revenue water and electricity sales estimated in this investigation would offer useful methodology if such a cost-benefit analysis is performed. Additionally, the potential for the integrated facility to participate in an ancillary services market should be considered in the cost-benefit analysis. Power providers can often benefit from selling ancillary services in addition to directly participating in the real-time electricity market. It is possible that the wind and solar farm modeled in this analysis can improve their profitability by being part of the ancillary services market. A cost-benefit analysis of capital and operational costs that includes potential to sell ancillary services would be a useful extension of the work discussed in this investigation.

5.2. Recommendations

A key recommendation concluded by the investigation is that the energy and water sectors have a chance to collaborate for the benefit of both parties. Meeting water needs can have adverse consequences on the energy sector's goal of reducing reliance on carbon-emitting fuels. At the same time, however, supplying drinking water offers an opportunity to advance renewable power technologies, taking positive steps on the energy front. Integrating desalination with renewable power is a unique opportunity to advance the implementation and uses of wind and solar power. Results from this investigation indicate that collaboration can unite the water and energy sectors for the benefit of both parties. Particularly, combining desalination, wind power, and solar power can overcome challenges associated with each of these technologies and may be preferable to stand-alone water or power producing facilities.

Acknowledgments

Gary M. Gold would like to acknowledge the National Science Foundation for the Graduate Research Fellowship funding opportunity.

Additional support was also provided by the Texas State Energy Conservation Office.

Author Contributions

Gary Gold synthesized the maps, text, analysis, and figures in this paper. Michael E. Webber was a principal investigator and provided text, guidance, and editing to this paper.

Conflicts of Interest

The authors declare no conflict of interest.

References

1. United State Census Bureau. *State and County Quick Facts*; United State Census Bureau: Washington, DC, USA, 2010.
2. United States Global Change Research Program, National Climate Assessment. *Climate Change Impacts in the United States*; United States Global Change Research Program: Washington, DC, USA, 2014.
3. Clayton, M.; Stillwell, A.; Webber, M. Implementation of Brackish Groundwater Desalination Using Wind-Generated Electricity: A Case Study of the Energy-Water Nexus in Texas. *Sustainability* **2014**, *6*, 758–778.
4. *Desalination : Brackish Groundwater*; Texas Water Development Board: Austin, TX, USA, 2013.
5. Miller, J.E. *Review of Water Resources and Desalination Technologies*; Sandia National Laboratories: Albuquerque, NM; Livermore, CA, USA, 2003.
6. Committee on Advancing Desalination Technology. *Desalination: A national perspective*; The National Academies Press: Washington, DC, USA, 2008.
7. Greenlee, L.F.; Lawler, D.F.; Freeman, B.D.; Marrot, B.; Moulin, P. Reverse osmosis desalination: Water sources, technology, and today's challenges. *Water Res.* **2009**, *43*, 2317–2348.
8. *Desalination Plant Database*; Texas Water Development Board: Austin, TX, USA, 2014.
9. *2012 State Water Plan*; Texas Water Development Board: Austin, TX, USA, 2012.
10. Mickley and Associates. *Membrane Concentrate Disposal : Practices and Regulation*; U.S. Department of the Interior: Denver, CO, USA, 2006.
11. Rainwater, K.; Nash, P.; Song, L.; Schroeder, J. The Seminole Project: Renewable Energy for Municipal Water Desalination. *J. Contemp. Water Res. Educ.* **2013**, *151*, 50–60.
12. United States Department of Energy. *2012 Wind Technologies Market Report*; United States Department of Energy: Washington, DC, USA, 2012.
13. United States Department of Energy. *2013 Wind Technologies Market Report*; United States Department of Energy: Washington, DC, USA, 2013.
14. Electric Reliability Council of Texas (ERCOT). *Entity-Specific Resource Output*; ERCOT: Austin, TX, USA, 2012.
15. Sandia National Laboratories. *Electric Power Industry Need for Grid-Scale Storage Applications*; Sandia National Laboratories: Albuquerque, NM, USA, 2010.

16. Ma, Q.; Lu, H. Wind energy technologies integrated with desalination systems: Review and state-of-the-art. *Desalination* **2011**, *277*, 274–280.
17. Forstmeier, M.; Mannerheim, F.; D'Amato, F.; Shah, M.; Liu, Y.; Baldea, M.; Stella, A. Feasibility study on wind-powered desalination. *Desalination* **2007**, *203*, 463–470.
18. Zejli, D.; Benchrifa, R.; Bennouna, A.; Zazi, K. Economic analysis of wind-powered desalination in the south of Morocco. *Desalination* **2004**, *165*, 219–230.
19. Kershrnana, S.A.; Rheinl, J.; Gablerb, H. Seawater reverse osmosis powered Tom renewable energy sources— Hybrid wind/photovoltaic/grid power supply for small-scale desalination in Libya. *Desalination*, **2002**. *153*, 17–23.
20. United States Department of Energy. *2010 Solar Technologies Market Report*; United States Department of Energy: Washington, DC, USA, 2011.
21. BP Statistical Review of World Energy 2014. Available online: http://www.bp.com/content/dam/bp/pdf/Energy-economics/statistical-review-2014/BP-statistical-review-of-world-energy-2014-full-report.pdf (accessed on 20 April 2015).
22. Peterson, G.; Fries, S.; Mohn, J.; Muller, A. Wind and solar powered reverse osmosis desalination units: Description of two demonstation projects. *Desalination* **1979**, *31*, 501–509.
23. Headley, O. Renewable energy technologies in the Caribbean. *Sol. Energy* **1997**, *59*, 1–9.
24. Ghermandi, A.; Messalem, R. Solar-driven desalination with reverse osmosis: The state of the art. *Desalin. Water Treat.* **2009**, *7*, 285–296.
25. Weiner, D.; Fisher, D.; Moses, E.J.; Katz, B.; Meron, G. Operation experience of a solar- and wind-powered desalination demonstration plant. *Desalination* **2001**, *137*, 7–13.
26. Zhu, A., A. Rahardianto, P.D.C.; Cohen, Y. Reverse Osmosis Desalination with High Permeability Membranes—Cost Optimization and Research Needs. *Desalin. Water Treat.* **2010**, *15*, 256–266.
27. Gude, V.G. Energy storage for desalination processes powered by renewable energy and waste heat sources. *Appl. Energy* **2015**, *137*, 877–898.
28. Charcosset, C. Combining membrane processes with renewable energy technologies: Perspectives on membrane desalination, biofuels and biogas production, and microbial fuel cells. *Membr. Clean Renew. Power Appl.* **2014**, *1*, 44–62.
29. Chow, T. A review on photovoltaic/thermal hybrid solar technology. *Appl. Energy* **2010**, *87*, 365–379.
30. Skoplaki, E.; Palyvos, J. On the temperature dependence of photovoltaic module electrical performance: A review of efficiency/power correlations. *Sol. Energy* **2009**, *83*, 614–624.
31. Skoplaki, E.; Palyvos, J. Operating temperature of photovoltaic modules: A survey of pertinent correlations. *Renew. Energy* **2009**, *34*, 23–29.
32. Solimpeks Academy. *Volther Hybrid PV-T Panels*; Solimpeks Academy: Karatay, Turkey, 2010.
33. Mittelman, G.; Kribus, A.; Mouchtar, O.; Dayan, A. Water desalination with concentrating photovoltaic/thermal (CPVT) systems. *Sol. Energy* **2009**, *83*, 1322–1334.
34. El-dessouky, B.H.; Alatiqi, I.; Bingulac, S.; Ettouney, H. Steady-State Analysis of the Multiple Effect Evaporation Desalination Process. *Chem. Eng. Technol.* **1998**, *21*, 437–451.

35. Mittelman, G.; Kribus, A.; Dayan, A. Solar cooling with concentrating photovoltaic/thermal (CPVT) systems. *Energy Convers. Manag.* **2007**, *48*, 2481–2490.
36. Van Helden, W.G.J.; van Zolingen, R.J.C.; Zondag, H.a. PV thermal systems: PV panels supplying renewable electricity and heat. *Progr. Photovolt.: Res. Appl.* **2004**, *12*, 415–426.
37. Davis, T.; Cappelle, M. *Hybrid Photovoltaic/Thermal (PV-T) Systems for Water Desalination*; UTEP Center for Inland Desalination: Austin, TX, USA, 2013.
38. United States Department of Energy, National Renewable Energy Labotatory. *Installed Wind Capacity*; United States Department of Energy: Washington, DC, USA, 2014.
39. United States Department of Energy: National Renewable Energy Laboratory. *Dynamic Maps, GIS Data, and Analysis Tool: U.S. 50m Wind Resource Map*; United States Department of Energy: Washington, DC, USA, 2009.
40. Lopez, A.; Roberts, B.; Heimiller, D.; Blair, N.; Porro, G. US Renewable Energy Technical Potentials : A GIS-Based Analysis. *Contract* **2012**, *303*, 275–3000.
41. United States Department of Energy, National Renewable Energy Laboratory. *Dynamic Maps, GIS Data, and Analysis Tools: Solar Maps*; United States Department of Energy: Washington, DC, USA, 2014.
42. United States Department of Energy, National Renewable Energy Labratory. *The Open PV Project*; United States Department of Energy: Washington, DC, USA, 2013.
43. United States Department of Energy, National Renewable Energy Laboratory. *Dynamic Maps, GIS Data, and Analysis Tools: 10-Kilometer Solar Data*; United States Department of Energy: Washington, DC, USA, 2014.
44. Wogan, D.M.; Webber, M.E.; da Silva, A. A Framework and Methodology for Reporting Geographically and Temporally Resolved Solar Data: A Case Study of Texas. *J. Renew. Sustain. Energy* **2010**, *2*, 053107
45. Texas Water Development Board. *Groundwater Database*; Texas Water Development Board: Austin, TX, USA, 2009.
46. Al-Karaghouli, A.; Kazmerski, L.L. Energy consumption and water production cost of conventional and renewable-energy-powered desalination processes. *Renew. Sustain. Energy Rev.* **2013**, *24*, 343–356.
47. Klein, G.; Krebs, M. California's Water—Energy Relationship Final Staff Report. 2005. Available online: http://www.energy.ca.gov/2005publications/CEC-700-2005-011/CEC-700-2005-011-SF.PDF (accessed on 20 April 2015).
48. Semiat, R. Critical Review Energy Issues in Desalination Processes. *Environ. Sci. Technol.* **2008**, *42*, 8193–8201.
49. Texas Comptroller of Public Accounts. Liquid Assest: The State of Texas' Water Resources. 2009. Available online: http://www.window.state.tx.us/specialrpt/water/2009/PDF/96-1360-LiquidAssets.pdf (accessed on 20 April 2015).
50. Stillwell, A.S. The Energy-Water Nexus in Texas. Ph.D. Thesis, The University of Texas at Austin, Austin, TX, USA, 2010.
51. Moran, M.J.; Shapiro, H.N.; Boettner, D.D.; Bailey, M.B. *Fundamentals of Engineering Thermodynamics*, 7 ed.; Wiley: Hoboken, NJ, USA. 2010.

52. Environmental Proctection Agency. *Average Temperature of Shallow Groundwater*; Environmental Protection Agency: Washington, DC, USA, 2013.
53. Fudholi, A.; Sopian, K.; Yazdi, M.H.; Ruslan, M.H.; Ibrahim, A.; Kazem, H.A. Performance analysis of photovoltaic thermal (PVT) water collectors. *Energy Convers. Manag.* **2014**, *78*, 641–651.
54. Electric Reliability Coucil of Texas. *Abilene Solar Farm Entity-Specific Resource Output*; Electric Reliability Council of Texas: Austin, TX, USA, 2002.
55. Electric Reliability Council of Texas. *Sweetwater 1 Wind Farm Entity-Specific Resource Output*; Electric Reliability Council of Texas: Austin, TX, USA, 2010.
56. Kendrick, D.A.; Mercado, P.R.; Amman, H.M. *Computational Economics*; Princeton University Press: Princeton, NJ, USA, 2006.
57. Hardberger, A.; Kelly, M. *From Policy to Reality*; Environmental Defense Fund: NY, USA, 2008.
58. Mickley, M.C. *Membrace Concentrate Disposal: Practices and Regulation, Reclamation: Managing Water in the West*; Mickley and Associates: Boulder, CO, USA, 2006.
59. Foldager, R.A. Economics of Desalination Concentrate Disposal Methods in Inland Regions: Deep-Well Injection, Evaporative Ponds, and Salinity Gradient Solar Ponds. Ph.D. Thesis, New Mexico State University: Las Cruces, NM, USA, 2003.
60. United States Department of Energy, Energy Information Administration. *Annual Energy Review 2011*; United States Department of Energy: Washington, DC, USA, 2012.
61. Electric Reliability Council of Texas (ERCOT). *Historical RTM Load Zone and Hub Prices*; ERCOT: Austin, TX, USA, 2013.

Groundwater Quantity and Quality Issues in a Water-Rich Region: Examples from Wisconsin, USA

John Luczaj and Kevin Masarik

Abstract: The State of Wisconsin is located in an unusually water-rich portion of the world in the western part of the Great Lakes region of North America. This article presents an overview of the major groundwater quantity and quality concerns for this region in a geologic context. The water quantity concerns are most prominent in the central sand plain region and portions of a Paleozoic confined sandstone aquifer in eastern Wisconsin. Water quality concerns are more varied, with significant impacts from both naturally occurring inorganic contaminants and anthropogenic sources. Naturally occurring contaminants include radium, arsenic and associated heavy metals, fluoride, strontium, and others. Anthropogenic contaminants include nitrate, bacteria, viruses, as well as endocrine disrupting compounds. Groundwater quality in the region is highly dependent upon local geology and land use, but water bearing geologic units of all ages, Precambrian through Quaternary, are impacted by at least one kind of contaminant.

Reprinted from *Resources*. Cite as: Luczaj, J.; Masarik, K. Groundwater Quantity and Quality Issues in a Water-Rich Region: Examples from Wisconsin, USA. *Resources* **2015**, *4*, 323–357.

1. Introduction

The State of Wisconsin, United States, is located in the western Great Lakes region of North America (Figure 1). This region experiences humid continental climates with warm to hot summers, but cold winters [1]. Rainfall and snowfall are abundant, with total annual precipitation that varies significantly across the state, ranging from a high in the south of 96.72 cm (38.08 inches) to a low of 71.93 cm (28.32 inches) in the northeast [2]. The population of Wisconsin is just under 5.7 million people [3], with the largest density in the eastern and southeastern portions of the state.

Wisconsin is located in an unusually water-rich portion of the world, and it borders two of the Great Lakes, Lake Superior and Lake Michigan (Figure 1). It also contains 15,074 documented inland lakes [9], most of which were formed as great lobes of ice from the Laurentide Ice Sheet receded from the northern and eastern portions of the state during the Late Pleistocene Epoch about 13,000 years ago [10]. Wisconsin is also extremely fortunate to have abundant supplies of fresh groundwater in Paleozoic age sedimentary rocks and Pleistocene glacial sediments, which are present throughout a large portion of the state. Historically, very few areas in the region have faced water quantity limitations, but expanding water use, coupled with long-term aquifer drawdown, has resulted in some noteworthy water supply challenges in certain areas of the state.

About 88% of water withdrawal in Wisconsin is from surface water supplies, with the remaining 12% from groundwater [11]. Total water use statistics are skewed toward surface water withdrawals because of mostly non-consumptive water use for cooling purposes during power generation (74 percent). The largest users of surface water (excluding power generation) include paper production (33 percent) and municipal public supply (29 percent). The largest consumers of

groundwater include municipal water supply systems (37 percent) and agricultural irrigation (40 percent) [11]. It is estimated that 90% of groundwater withdrawal for irrigation purposes is consumed and not returned to the basin via surface water or groundwater [12].

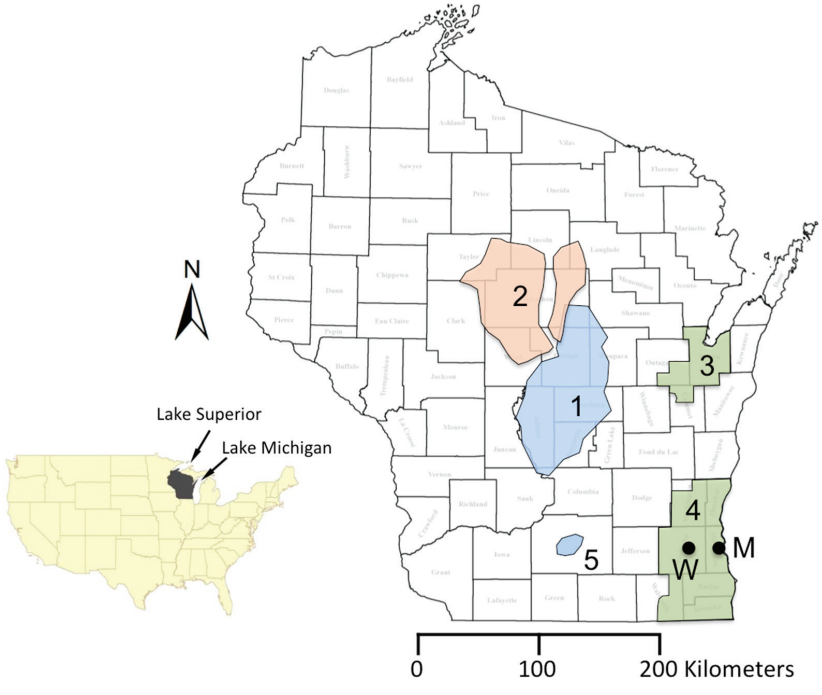

Figure 1. Map showing the location of Wisconsin counties with important regions of the state highlighted. Inset map shows the location of Wisconsin in the lower 48 contiguous United States. Numbered regions are as follows: (1) Central sand plain; (2) Groundwater deficient portion of north-central Wisconsin; (3) Northeast Groundwater Management Area; (4) Southeast Groundwater Management Area; (5) Area of declining water levels in Dane County. Lettered points refer to locations of Milwaukee (M) and Waukesha (W) [4–8].

In 2013, there were approximately 950 billion liters (250 billion gallons) of groundwater withdrawn, with the majority of water used for agricultural and municipal water supply (Table 1). There are approximately 800,000 small private wells statewide, plus an additional 14,000 high capacity wells that serve industry, municipal, and agricultural purposes as of 2013 [13]. Approximately 8408 of the high capacity wells are capable of producing above the state defined threshold of 265 liters per minute (70 gallons per minute), and the rest are statutory high capacity wells. Since 1950, nearly 60% of high capacity wells in Wisconsin have been installed for irrigation purposes [14].

Table 1. Total groundwater withdrawals by water use for Wisconsin in 2013 was approximately 950 billion liters (250 billion gallons) [11].

Water Use	Percentage of Total
Agricultural Irrigation	40%
Municipal Public Water	37%
Industrial	5%
Aquaculture	3%
Cranberry Production	4%
All other uses	11%

Wisconsin is also fortunate to have had relatively good groundwater quality throughout much of its history. A rigorous understanding of groundwater quality and quantity issues that began a century ago [15] has contributed to keeping groundwater safe and available. In most areas, abundant precipitation, thick aquifers, and relatively little saline groundwater have resulted in a high quality water supply for most of the state's residents [16]. However, ongoing land use changes, aquifer drawdown, and recognition of emerging contaminants over the past 25 years have shifted the focus of much of the groundwater research toward water quality issues. This article presents a review of the water quality and quantity issues faced in one of the most water-rich areas of the world.

2. Geologic Setting

Although regional climate is important, the geology and geologic history of Wisconsin play a critical role in understanding the water quality and quantity issues that the region faces. A general overview of the geology of Wisconsin is presented here for context, but the reader is directed toward other publications that provide a greater level of detail [17–24].

The physiographic setting of Wisconsin lies at the junction of the Superior uplands in the north, and several subsections of the Central Lowlands Province in the United States. A veneer of unconsolidated Quaternary deposits overlies bedrock throughout much of the region [24]. Bedrock consists of a complex array of eroded Precambrian rocks, overlain by a sequence of marine rocks related to ocean transgression-regression cycles. Bedrock units dip radially away from the Wisconsin Arch, toward the Michigan basin in the east, the Illinois basin in the south, and gently toward Iowa and Minnesota in the west. Wisconsin's geologic history is preserved in rocks and unconsolidated sediments from three distinctly different periods of time, with long intervals of erosion or nondeposition occurring between each [20].

2.1. Precambrian Geology

Rocks from the first of these three time intervals were deposited episodically over a long interval of Precambrian time from late in the Archean Eon (~2.8 billion years ago) to around 1 billion years ago. Many of these rocks consist of crystalline igneous and metamorphic rock, with significant amounts of sedimentary rocks that have been subjected to varying degrees of metamorphism after deposition. Rocks of the Precambrian "basement" are present beneath the entire state, but are concealed in the southern portion of the state by Paleozoic sedimentary rocks, and in much of the

northern portion of the state by Pleistocene sediments. While Precambrian rocks serve as important aquifers in parts of central and northwestern Wisconsin, most usage is restricted to domestic well use in areas with relatively low populations.

2.2. Paleozoic History

The second interval of Earth's history that is recorded in Wisconsin includes sedimentary rocks deposited during the Early to Middle Paleozoic Era. Rocks deposited during this interval consist mainly of sandstone, dolostone, and shale, and form the bedrock throughout much of the southern two-thirds of the state (Figure 2). Nearly all of these rocks are marine or marginal marine, deposited during some of the highest sea levels of the Paleozoic Era. These rocks range in age from Late Cambrian to Late Devonian, with the Devonian rocks only preserved along the Lake Michigan shoreline north of Milwaukee. Paleozoic sedimentary rocks range in thickness from 0 m thick to at least 700 meters (2300 feet) thick in parts of eastern and southeastern Wisconsin. These strata thicken significantly toward the ancestral Michigan basin, where younger Paleozoic and Mesozoic sedimentary rocks overlie them [25,26]. Key events in the history of development of Wisconsin's aquifers included formation of the ancestral Michigan basin to the east (Figure 2), as well as the Illinois basin to the south. Later fluid flow events emanating from these basins appear to have influenced the mineralogy of much of the Paleozoic bedrock, which has important implications for its present day groundwater quality [26].

Paleozoic rocks in Wisconsin and adjacent states are only slightly deformed, with gentle folding and faulting occurring during the Paleozoic Era (e.g., [25,26]). Subsidence of the Michigan basin, a classic intracratonic sedimentary basin, had the most pronounced effect on the structure of these rocks, with development beginning during the Late Cambrian and occurring simultaneously with sedimentation throughout the Paleozoic Era. The subsidence of the ancestral Michigan basin is centered over a portion of the Proterozoic Midcontinent rift system [25]. This subsidence resulted in a significant dip of the strata toward the center of the basin, which resulted in a concentric "bull's-eye" pattern on bedrock geologic maps (Figure 2). Paleozoic strata in eastern portions of Wisconsin typically dip eastward between about 5 and 7.5 m/km (25 and 40 ft/mi) [20].

Figure 3 presents a generalized stratigraphy of Paleozoic sedimentary rocks in Wisconsin, with only a generalized overview of the stratigraphy presented here. The lowermost Paleozoic rocks in Wisconsin are Middle to Upper Cambrian sandstones (~520 to 485 million years ago), which were deposited as sea level gradually rose to cover most of the North American craton [27]. They are exposed over a large portion of western and central Wisconsin, and they form the principal portion of the deep confined aquifer system in eastern and southern Wisconsin. These sandstones have average thicknesses of about 120 m [5,6,28,29]. These rocks have been extensively studied along the Mississippi River Valley in western Wisconsin (e.g., [27]), but their poor exposure beneath glacial sediments in eastern and southeastern Wisconsin has impeded research on these rocks, despite their regional importance as aquifers. A lack of economic deposits of petroleum or natural gas in the region has further limited our understanding of these units.

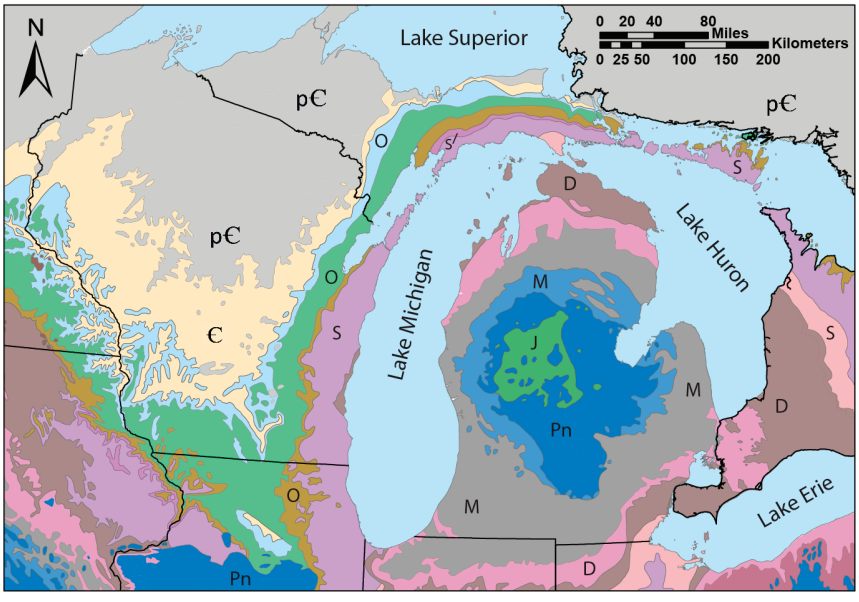

Figure 2. Simplified bedrock geologic map for the western U.S. Great Lakes region showing Wisconsin and Michigan, USA. Geologic systems of rock are as follows: pϵ = Precambrian, ϵ = Cambrian, O = Ordovician, S = Silurian, D = Devonian, M = Mississippian, Pn = Pennsylvanian, J = Jurassic. Modified from [20].

The Ordovician Period (485 to 443 million years ago) saw variable deposition of carbonate rocks, sandstones, and shale. Rocks of this age generally mimic the outcrop pattern of Cambrian rocks (Figure 2) and are exposed along a narrow horseshoe-shaped band stretching from the Mississippi River Valley in the west, south to the Illinois Border, and then northeastward along the eastern portion of the state where they border younger Silurian rocks. The lower half of the Ordovician section includes carbonate rocks of the Prairie du Chien Group, sandstones and minor shale of the Ancell Group, and carbonates from the Sinnipee Group (Figure 3). The vast majority of the carbonates in Wisconsin have been transformed from limestone to dolostone, with most limestone restricted to the southwestern portion of the state [26]. The most important aquifer within the Ordovician section is the Ancell Group, which consists mainly of the St. Peter Sandstone and a few other relatively thin units. The upper-half of the Ordovician section is dominated by the Maquoketa Shale, which is the most important regional confining unit and only present in eastern Wisconsin.

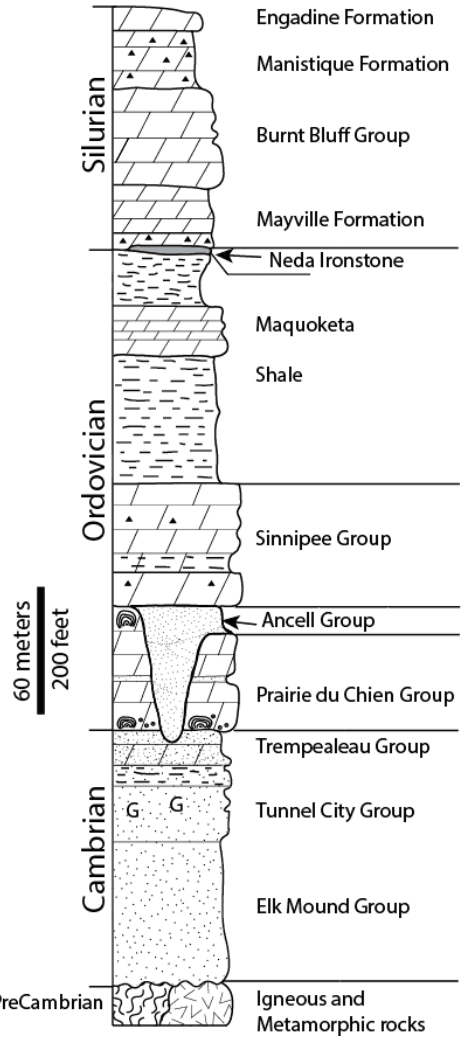

Figure 3. Simplified stratigraphic column for Paleozoic rocks in northeastern Wisconsin. Pleistocene sedimentary and younger Silurian and Devonian strata for southeastern Wisconsin are not shown here for simplicity, but can be found elsewhere [30,31].

The Middle and Late Paleozoic Era is recorded mainly in eastern Wisconsin by a sequence of Silurian (443 to 419 million years old) dolostone units as much as 240 m thick that were deposited in both open and marginal marine environments. These rocks form the backbone of the Niagara cuesta that forms the uplands of eastern Wisconsin. Numerous stratigraphic and bedrock investigations have been conducted on northeastern Wisconsin's Silurian rocks (see [20,31] and references therein). Younger Devonian rocks are only locally important along a narrow band near Lake Michigan and are not a focus of this article. There is a region-wide erosional disconformity throughout the Midwestern United States between the Late Paleozoic and the Jurassic Period, known

as “The Lost Interval” [32]. This interval is significant, despite the lack of strata from this period, because regional denudation and likely significant karst development occurred in certain carbonate rocks in the region during this time.

2.3. Quaternary History

The youngest of the three geologic intervals in Wisconsin was recorded during the later part of the Pleistocene Epoch of the Quaternary Period (2.6 million to 11,700 years ago). These sediments range in age from at least 780,000 years old in parts of central and northwestern Wisconsin, to about 13,000 years old, with the vast majority of these sediments deposited during the last three advances of ice lobes during the Wisconsin Glaciation (between about 32,000 and 13,000 years before present [10,24]). Only about three-fourths of Wisconsin was glaciated, leaving a region of the southwestern portion of the state known as “The Driftless Area.”

The absence of major mountain-building events in the region for at least 1.5 billon years, coupled with extensive Paleozoic deposition and several Pleistocene glacial advances, has resulted in a relatively gentle topography throughout most of Wisconsin. The maximum topographic relief in the state is less than 425 meters (1400 feet) [33]. The most significant local relief results from the erosional resistance of castellated mounds of well-cemented Cambrian quartz sandstone, along with several large quartzite monadnocks that result in hills up to 150 to 200 meters high. Additional topographic relief of up to 70 meters occurs along regional glacially sculpted erosional ridges, such as the Niagara Escarpment in eastern Wisconsin, and an extensive array of end moraines from lobes of the Laurentide ice sheet that invaded Wisconsin during the Late Pleistocene.

2.4. Hydrostratigraphy

The hydrostratigraphy in the state is relatively straightforward overall, but locally complex due to significant variation in the geology of Precambrian bedrock and Pleistocene glacial sediments. In contrast, the hydrostratigraphy of the Paleozoic rocks is relatively consistent throughout the region. Table 2 presents a generalized hydrostratigraphy for Wisconsin. In general, Precambrian basement rocks have relatively low porosity and permeability, with fracture flow providing the most significant permeability in most rocks, with the exception of some sandstones of the Midcontinent Rift System in northwestern Wisconsin [34]. In some areas, water is extracted principally from a single hydrostratigraphic unit. However, in some regions, multiple aquifers may be accessed by wells in close proximity. In southeastern Wisconsin, at least three aquifers are used. In other regions, such as the Niagara Escarpment region of northeastern Wisconsin, as many as 3 or 4 aquifers are used by domestic wells in close proximity. The well depth varies based on a number of factors, including well driller, water quality concerns, cost, and water quantity needs.

Paleozoic sedimentary rocks supply a large proportion of the water wells in the state. The most prolific bedrock aquifers include the Cambrian sandstones and the Ordovician St. Peter Sandstone (Ancell Group), which are present across at least half of the area of the state. These sandstones form the principal portion of the deep confined aquifer system in parts of Wisconsin and are about 120 m thick on average, but can be substantially thicker in some areas (e.g., [5,7,28]). Ordovician dolostones that overlie each of these sandstone aquifers (Figure 3, Table 2) form important aquifers for some domestic water wells, but the vast majority of high capacity wells in these areas are open to one or both of the sandstone aquifers.

Throughout a narrow band of eastern Wisconsin, and in parts of adjacent states, the overlying Late Ordovician Maquoketa Shale acts as a regional aquitard (e.g., [28,35,36]). East of this boundary, which is well defined in places by the topographic expression of the Niagara Escarpment [20], dolostones of Silurian age form the majority of the remaining bedrock stratigraphic section in eastern Wisconsin. In southeastern Wisconsin, the Silurian bedrock aquifer is particularly important in regions not served by municipal supplies [7]. These rocks typically contain well-developed karst features, especially in parts of east-central and northeastern Wisconsin where the thickness of unconsolidated sediments is low. Karst development in these rocks began as early as the Devonian Period, but the timing of most karst features is not well known. Recent radiometric age dates on bones and charcoal from caves in the region shows that sediment fills are at least 6000 to 8000 years old, suggesting that the karst development likely occurred prior to the Holocene [37,38]. The karst-enhanced fractured Silurian dolostones provide an important regional aquifer for residents east of the Niagara Escarpment, and many high-capacity wells are open to this aquifer system.

In eastern Wisconsin, the Cambrian-Ordovician aquifer is unconfined to the west of the Maquoketa boundary throughout eastern Wisconsin and into northeastern Illinois, with the primary recharge area to the west of the boundary [7,28,39,40]. Radiocarbon dating, stable isotope analysis and noble gas data for deep aquifer waters in southeastern and northeastern Wisconsin reveal ^{14}C ages for groundwater between 5000 and 26,000 years old [36,41].

The Pleistocene sediments in the region are divided into four major classes, including glacial till (ground and end moraines), glaciolacustrine (lake) sediments, outwash (sands and gravels), and pitted outwash with local ice contact deposits (e.g., [24]). The complex regional and stratigraphic variation of these deposits is beyond the scope of this article, but they are an important aquifer system, and they play a crucial role in some of Wisconsin's major groundwater quantity and quality problems. One portion of the Pleistocene sediments that is particularly important to describe is known as the "central sand plain" region, which covers a multi-county region in the central portion of the state. This region consists of thick glacial outwash overlying Precambrian and Paleozoic bedrock. This region has seen extensive development of groundwater resources for irrigation, and significant groundwater quality impacts have occurred there.

Table 2. Simplified hydrostratigraphy for Wisconsin (after [5–7,28]).

Geologic Age		Geologic Unit (Thickness, Meters)	Lithology	Hydrostratigraphic Unit
Cenozoic	Quaternary (Pleistocene)	Unconsolidated deposits (0–60 meters) Locally >150 m	Lacustrine silt and clay, glacial till, fluvial sand and gravel, and other deposits.	Local unconfined aquifer (sand and gravel) or regional confining unit (lacustrine clays and tills).
Paleozoic	Devonian		Black shale locally over limestone and dolostone.	Upper Aquifer; only present in southeastern Wisconsin along Lake Michigan Shoreline.
	Silurian	Undifferentiated (0–240 m)	Dolostone; fractured and karsted in many locations.	Upper Aquifer; Karsted in many locations of northeastern Wisconsin.
	Ordovician	Maquoketa Formation (0–150 meters)	Shale, dolomitic shale, and dolomite.	Confining Units; Sinnipee Group Carbonates are locally used as aquifers for domestic use.
		Sinnipee Group (120 meters)	Dolostone with some shale. Limestone in portions of southwestern Wisconsin.	
		Ancell Group (0–90 meters)	Silty sandstone, fine- to medium-grained sandstone, sandy shale.	Confined Deep Aquifer.
		Prairie du Chien Group (0–60 meters)	Dolostone with varying amounts of oolitic chert and minor interbedded sandstone.	Generally an aquitard relative to the adjacent sandstones in eastern Wisconsin; effective aquifer in western Wisconsin.
	Cambrian	Trempealeau Group (0–15 m)	Fine- to medium-grained sandstone with some silty glauconitic dolomite.	Confined Deep Aquifer.
		Tunnel City Group (30–46 m)	Fine- to medium-grained sandstone, silty sandstone to sandy dolomite. Abundant glauconite commonly observed.	
		Elk Mound Group (75–90 m)	Very-fine to coarse-grained sandstone.	
Precambrian	Precambrian	Undifferentiated	Crystalline rock, predominantly red granite, contains igneous and metamorphic rock. Limited sedimentary rocks (sandstones, dolostones).	Yields little to no water in many cases. Local aquifers, especially in Midcontinent Rift System rocks of northwestern Wisconsin.

3. Groundwater Quantity Concerns

3.1. Overview

Wisconsin receives on average about 25 cm (10 inches) of precipitation above and beyond the evapotranspiration demands of its climate and vegetation [42]. As a result, the state's rivers and streams receive the majority of streamflow from groundwater, and lake levels are often similar to the

local groundwater elevation. Wisconsin has limited regions with major groundwater quantity concerns compared to most regions of the world. Although Wisconsin is generally considered to be a water rich state, there is increasing attention being paid to issues of water quantity. In addition to the previously mentioned groundwater deficient areas, groundwater withdrawal effects are contributing to significant drawdown of confined aquifer systems as well as the effect of high capacity wells on lake levels and reduced streamflow and spring discharge (e.g., [4,43]).

Unlike western states that practice a prior-appropriation system of water regulation, many eastern states including Wisconsin follow what is known as a reasonable use doctrine [4]. The reasonable use doctrine historically has allowed a landowner to withdraw any amount of water as long as it goes towards some beneficial use on the overlying landscape. Water quantity concerns over the past two decades have compelled Wisconsin to revisit the way in which the state regulates groundwater. In 2003, the state passed Wisconsin Act 310 that legally recognized the interaction between surface and groundwater and the impact that individual wells may have on lakes, rivers, streams, springs and wetlands. The law allowed the state's regulatory agency to consider the environmental impact of a high capacity well located within 365 meters (1200 feet) of an Outstanding or Exceptional Resource Water or trout stream or springs with a flow greater than 1 cubic foot per second (0.0283 m^3/sec) [44]. This law also allowed for the designation of Groundwater Management Areas to encourage coordinated management and address problems related to groundwater pumping at a regional scale between state and local units of government. A Wisconsin Supreme Court Case in 2011 concerning Lake Beulah in southeastern Wisconsin found that the state had a general duty to consider the impact of proposed wells when presented with sufficient evidence of potential harm to any water of the state, regardless of its distance from a water body [45]. More recently in 2014, an administrative law judge ruled that the state must consider the "cumulative impacts" of existing wells and reasonable expected cumulative impacts of other users when making determinations regarding significant adverse environmental impacts [46]. It remains to be seen what effect this ruling will have on future groundwater management decisions.

In 2008, Wisconsin along with the other Great Lake states and two Canadian provinces ratified the Great Lakes Compact [47]. The agreement expanded high capacity well registration and reporting requirements and placed additional water conservation and efficiency goals on water users in the Great Lakes Basin [48]. In addition, it discourages the diversion of water outside the boundaries of the Great Lakes Basin; limited exceptions exist for straddling communities as long as water is returned to the basin. The Great Lakes Compact has had significant implications for the City of Waukesha (Figure 1), because it does not reside inside the boundaries of the Great Lakes basin, despite being located near Lake Michigan. The municipal water supply has seen increased levels of radium as a result of the significant drawdown in the confined aquifer. Limited options exist to expand groundwater use. As a result, the city hopes to partner with a community water system in the Great Lakes Basin to access Lake Michigan water. However, it must receive approval from ratifying states and provinces of the Compact if it is to be granted access.

3.2. Groundwater Management Areas in the Confined Sandstone Aquifer

Recent groundwater legislation, 2003 Wisconsin's Groundwater Protection Act 310, addressed concerns about groundwater as a resource and provided the Wisconsin Department of Natural Resources (WDNR) with additional groundwater management tools [5,6,29]. The WDNR has designated parts of northeastern and southeastern Wisconsin as Groundwater Management Areas (GMAs) due to the fact that water levels in the confined sandstone aquifers have declined by more than 150 feet from pre-development levels in the late 1800s [44] (Figure 1). In the Lower Fox River Valley in northeastern Wisconsin, this northeast GMA includes Brown County and portions of Outagamie and Calumet counties, while in Southeastern Wisconsin the southeast GMA includes Waukesha, Kenosha, Racine, Milwaukee, and Ozaukee counties, along with portions of Washington and Walworth counties.

Groundwater use in these regions began in the late nineteenth century. Flowing artesian wells were common in parts of eastern Wisconsin for wells that penetrated the Cambrian-Ordovician confined aquifer (Figure 3, Table 2). The Southeast GMA has experienced the greatest drawdown levels observed in the state, with water levels in the confined aquifer dropping as much as 150 meters (500 feet) by the year 2000 [49]. The major pumping center in southeastern Wisconsin has shifted westward from the city of Milwaukee to the city of Waukesha due to cessation of pumping by communities now using Lake Michigan water, along with increased pumping by growing communities farther away from the Lake Michigan shoreline. A recent model [49] predicts an additional 30 meters (100 feet) of drawdown between 2000 and 2020.

The Northeast GMA has also experienced significant drawdowns, with some areas of central Brown County dropping at least 120 meters (400 feet) between predevelopment conditions and 2005 [5,6,29]. The Northeast GMA contains two distinct cones of depression in the confined aquifer, one of which is located near Green Bay and De Pere in central Brown County, with the other located farther south near the "Fox Cities" region of Kimberly, Kaukauna, and Little Chute along the Fox River. The southern Fox Cities cone of depression has seen consistent drawdown during the last century. However, the northern cone has seen substantial changes in pumping as communities expanded and later switched to surface water supplies in 1957 and 2007.

Most recently, the opportunity to switch to surface water was possible due to state legislation passed in 1998, which allowed communities to combine efforts to address water problems. Six smaller communities surrounding Green Bay formed the Central Brown County Water Authority (CBCWA) in 1999. After evaluating options that included water quality and long term water quantity concerns, an agreement was signed by the CBCWA to purchase water from the City of Manitowoc's Public Water Utility about 65 miles to the southeast along the Lake Michigan shoreline. Two other communities decided to purchase their municipal water from the City of Green Bay beginning in 2006, with another community adding in 2011. These communities currently use their wells as a backup in case of pipeline interruptions, and some of the high capacity municipal wells in the region have been abandoned. The recent decisions to switch to surface water were driven by concerns regarding radium levels in groundwater (see Section 4.1.1 below).

The response to these communities switching from groundwater to surface water supplies has resulted in a dramatic recovery of the potentiometric surface in the confined aquifer of central Brown County. During 2006–2007, pumping in central Brown County decreased from about 60 million liters per day (16 million gallons per day) to about 16 million liters per day (4.2 million gallons per day). Water levels increased by as much as 60 meters (200 feet) in some parts of the region, resulting in some flowing artesian wells and a deep quarry flooding [5,6,29,50]. Water levels have continued to rise through early 2015. A more complete and up to date history of the northeastern GMA is forthcoming [29].

3.3. The Central Sand Plains

The central sand plains region is located near the center of Wisconsin (Figure 1). The soil properties make it unique from the surrounding areas of the state. Comprised of approximately 6400 km^2, the region is composed mainly of unconsolidated sandy deposits often >30 m thick with nearly level topography. The surface horizons average 93% sand and the subsurface horizons are 98% sand, which results in high infiltration rates and very little runoff [8]. As a result, most areas are extremely well drained and groundwater recharge is high [51]. Groundwater is intimately connected to surface waters, with baseflow representing upwards of 90% of annual streamflow of headwater streams [52]; while many of the region's kettle lakes are classified as groundwater flow-through systems with no surface water inlet or outlet.

Formed during the Pleistocene Epoch, the central sand plains region is sandwiched between the terminal moraine of the Green Bay Lobe of the Laurentide ice sheet and the driftless region, an area of the state untouched by the last ice age. As the glaciers advanced westward, the ice blocked the southern drainage route for glacial meltwater, and Glacial Lake Wisconsin was formed. Although the glacier never covered the central sand plains region, it served as the storage pond for the glacial meltwater and sediment. The glacier's eventual retreat reopened the southern drainage route and released the water of Lake Wisconsin southward, carrying with it some sediment, but leaving behind small amounts of clay, silt, and much of the sand that form the present day outwash plain [53].

It was observed early in Wisconsin's history that the central sand plain region was poorly suited for agricultural development, and as a result people were slow to settle in the region. The land in the sand plain was some of the last to be given away under the Homestead Act of 1862 [54]. Around the early 1900's wetland drainage districts were established, which taxed local landowners for the cost of the drainage efforts. Receiving little if any benefit from the draining of the wetlands, many farmers were left unable to pay the taxes on their land [54]. As a result, it was not uncommon for farmers to abandon their homesteads after only a few years of work.

In the early 1950's technological advances in irrigation and industrial fixation of nitrogen available as commercial fertilizer improved farming in the region. The area is well suited for irrigation; highly permeable soils sit upon large aquifers of easily accessible groundwater. Farmers who once relied solely on rainfall now watered crops with water that previously escaped below the plants' roots. Since 1950, over 3000 high capacity wells have been installed in the central sands region, mostly for irrigation purposes.

In 2012, approximately one-third of all groundwater withdrawals occurred in a three county area within the central sands [11]. Concerns over groundwater pumping go back decades when researchers first began studying the effects of high capacity wells on ground and surface waters. Weeks and Stangland [42] predicted that headwater streams would dry up in the summer of drought years and water levels at groundwater divides would be lowered by 1.2–1.5 m (4–5 ft) if 50% of the land in the region were to eventually be irrigated. More recently Kraft *et al.* [43] revisited this issue, and using modern groundwater modeling techniques the researchers concluded that present irrigation rates account for a 30%–40% reduction in annual streamflow of headwater streams and a 1.2 m decline of groundwater levels under steady-state model simulations.

Herein lies a major difference between water quantity concerns in arid climates *versus* more humid climates such as Wisconsin. At present, the current precipitation and evapotranspiration rates in the central sands region of Wisconsin do not suggest that the aquifer is in danger of running dry or being depleted in its entirety. Instead, the concern revolves around the effects irrigation is having on the upper portion of the aquifer that interacts intimately with the region's lakes, rivers, streams and wetlands. While the decline attributed to groundwater pumping is only a small portion of a >30 m thick aquifer, a 1–2 m decline in water levels is noticed by area residents who have expressed concern over low lake levels and reductions in streamflows in the region [55]. Balancing water use for irrigation, while maintaining the integrity of surface water ecosystems and property values of those businesses and homes that depend on lakes and rivers, is an ongoing groundwater management concern in Wisconsin [56]. The expansion of irrigation beyond the boundaries of the central sand plains region could result in similar concerns in other regions of the upper Midwestern United States.

3.4. Crystalline Bedrock

Groundwater yield can be limited to less than 7.5 liters per minute (2 gallons per minute) in portions of north-central Wisconsin where wells may extend into near-surface crystalline Precambrian rock as a groundwater supply (Figure 1). Water for public and industrial use in this region can be a limiting factor, and these aquifers have been classified as groundwater deficient [4,57]. Domestic wells in parts of central and northern Wisconsin may reach depths of 120 to 210 meters (400 to 700 feet). However, parts of northern Wisconsin have extensive Pleistocene cover that provides adequate water supply in most areas.

3.5. Groundwater Flooding

Several communities have been affected episodically by elevated groundwater levels leading to significant problems of oversupply of groundwater. The most noteworthy recent case was in Spring Green, Wisconsin. In 2008, about 1770 hectares (4378 acres) of land were flooded for over 5 months along the Wisconsin River outside of areas designated as floodplain by the U.S. Federal Emergency Management Administration (FEMA). This occurred as a result of large precipitation events during 2007 and 2008 [58], but the Wisconsin River did not overflow its banks at any time during the 2008 flooding. Overall, these cases are rare, but they have significant economic and human impact on a local scale.

4. Groundwater Quality Concerns

Groundwater quality has received significant attention over the past 25 to 30 years in Wisconsin. For example, recognition of a regional arsenic problem, new U.S. EPA maximum contaminant levels (MCLs), and a growing anthropogenic impact from non-point source land use activities have attracted the attention of regulators, academics, and the general public. Significant attention has been given to the study of arsenic levels and other quality issues. For example, during the period 2007–2010, Wisconsin health departments tested about 4000 rural drinking water supplies for coliform bacteria, nitrate, fluoride, and 13 metals as part of a state-funded program. The results were surprising, in that 47% of those wells exceed one or more health-based water quality standards [59].

This article focuses on problems specific to the region, and does not address ubiquitous problems such as leaking underground storage tanks, landfills, or localized industrial sites. Groundwater quality issues faced by the residents of Wisconsin are divided into both natural and anthropogenic sources. Naturally occurring contaminants are presented first below because an introduction to the geochemical and water-rock interaction history of these rocks provides an important lead-in to anthropogenic topics discussed later.

4.1. Naturally Occurring Inorganic Contaminants

It is important to recognize that the geochemical signature of an aquifer system is a function of the mineralogy of aquifer host rocks, as well as the source and history of fluids that have flowed through the aquifer. Both of these variables have had an effect on groundwater quality in Wisconsin, especially in the deep confined Paleozoic sandstone aquifers of eastern Wisconsin. Naturally occurring inorganic contaminants that have been recognized in Wisconsin include radium, arsenic, nickel, cobalt, fluoride, strontium, aluminum, and manganese. Some of these, such as radium and arsenic (along with associated metals nickel and cobalt) have been widely studied in the region since the 1980s. Some attention has been given to fluoride and strontium, but research on aluminum and manganese in Wisconsin's aquifers is not as well documented. The discussion below provides a general overview of each contaminant, along with its geologic distribution and relevant literature.

4.1.1. Radium in Sandstone Aquifers of Eastern Wisconsin

Radium is a chemical element with naturally occurring radioactive isotopes that are produced as part of the uranium-to-lead and thorium-to-lead decay series. Numerous regulatory agencies, including the World Health Organization (WHO) and the U.S. EPA have established drinking water limits for radium [60,61]. The limits used by the WHO are 1 Bq/L (27 pCi/L) for ^{226}Ra and 0.1 Bq/L (2.7 pCi/L) ^{228}Ra [60]. The MCL used by the U.S. EPA is 5 pCi/L (0.185 Bq/L) combined for both isotopes of radium. Radium is metabolized by the human body much like calcium. Long-term ingestion of radium over time can result in the accumulation of radium in the skeleton, which has the potential to increase the chance of bone and sinus cancer [62].

Two geologic regions of the United States have been identified as having notably high radium content in groundwater. One region includes the Piedmont and Coastal Plain provinces of New

Jersey, the Carolinas, and Georgia. The second region includes parts of Wisconsin, Minnesota, Iowa, Illinois, and Missouri [63]. Elevated dissolved radium is recognized as a significant water quality issue in the Cambrian-Ordovician aquifer system of eastern Wisconsin and northeastern Illinois [35,39,40,62,64]. However, one study did not find radium levels in Wisconsin Groundwater to be significantly associated with osteosarcoma [62]. In Wisconsin, more than two-dozen municipal wells exceed the EPA MCL for dissolved radium or gross alpha emissions [65], requiring them to solve the problem through water treatment options, source blending, or alternative water sources.

In eastern Wisconsin, the Cambrian-Ordovician aquifer is unconfined to the west of the Maquoketa boundary throughout eastern Wisconsin and into northeastern Illinois, with the primary recharge area to the west of the boundary [40]. Elevated radium activities of ≥5 pCi/L (≥0.185 Bq/L) are present throughout much of eastern Wisconsin, especially in locations where the aquifer transitions from unconfined to confined conditions (Figure 4). Weaver and Bahr [39,40] concluded that ^{226}Ra in the Cambrian-Ordovician aquifer of eastern Wisconsin originated from low levels of ^{238}U in the shaley portions of the aquifer. Grundl and Cape [35] provide the most recent assessment of the geochemical factors that control the radium activity in the deep aquifer. They considered three ultimate sources of radioactivity in the aquifer: (1) material in the aquifer solids themselves, either in shaley zones [39] or as rinds enriched in parent isotopes [66,67]; (2) in the Maquoketa Shale that overlies the aquifer or (3) uranium or thorium transported into the aquifer by deep-seated brines originating from the Michigan basin [68]. Unfortunately, they were not able to definitively identify the set of geochemical processes controls the radium activities in the confined portion of the aquifer [35].

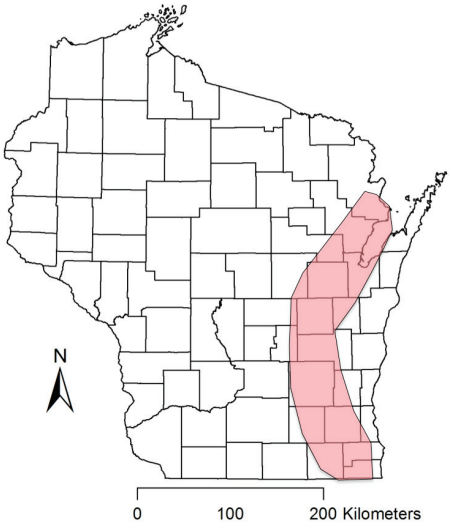

Figure 4. Region of the state with the majority of wells that exceed the U.S. EPA maximum containment levels (MCL) for combined Radium of 5 pCi/L (0.185 Bq/L). Pattern mimics the outcrop distribution of the western edge of the Michigan sedimentary basin (Figure 2) and reflects the region where water is drawn from the confined sandstone aquifers of eastern Wisconsin [65].

In 2000 December, the National Primary Drinking Water Regulations; Radionuclides; Final Rule was published [61]. The U.S. EPA promulgated a final radionuclide rule that required communities to analyze their water for ^{226}Ra, ^{228}Ra, uranium, and gross alpha emitters, and to assess the vulnerability for beta and photon activity. The most significant of these was radium, and an MCL of 5 pCi/L (0.185 Bq/L) was established for combined radium, with enforcement beginning during 2006. In 2006, 42 of Wisconsin's public water supply systems were in violation of the U.S. EPA MCL for combined radium. Three different strategies have been employed by different communities to tackle this problem, at a substantial cost to the public. These include water treatment systems, blending of water supplies, and switching to surface water supplies.

As described above, the most substantial radium-related project involved a switch from deep aquifer wells to surface water by numerous communities surrounding Green Bay, Wisconsin during 2006 and 2007 [5,6]. Some backup wells in the region still exceed the U.S. EPA MCL for combined radium, but are typically only in use when interruptions occur due to pipeline breaks. The initial cost of this pipeline was $80 million US Dollars in 2007, with substantial ongoing maintenance and repair costs [69]. The final cost was around $130 million US Dollars.

By 2009, some communities were still struggling to reach compliance. For example, the City of Fond du Lac, with only 43,000 residents, ended up spending $32.4 million US Dollars to upgrade its water supply [70]. The city also agreed to pay $35,000 US Dollars to settle claims with the Justice Department.

The City of New Berlin, a suburb of Milwaukee, got final approval from the Wisconsin DNR in 2009 to connect with the City of Milwaukee to use up to 8.1 million liters per day (2.142 million gallons per day) in areas outside the Great Lakes Basin to replace the volume supplied by deep aquifer wells that exceed the combined radium MCL. This was allowed because the City of New Berlin straddles the Great Lakes drainage divide, and all of the water used will return to Lake Michigan [71].

The City of Waukesha had radium exceedances as recently as 2011 and 2013 when pumps in one of the city's deep wells failed [72]. The city agreed to come into compliance with the standard at all times at each entry point by 2018. Waukesha blends water from both shallow and deep wells and uses Hydrous Manganese Oxide treatment plants to achieve compliance with drinking water standards [73]. The City of Waukesha has recently declared that it will not be able to achieve compliance by the court ordered 2018 date [74]. Waukesha currently has an application pending to divert water from Lake Michigan, despite the fact that it lies outside the Lake Michigan drainage basin.

4.1.2. Arsenic and Associated Heavy Metals

Dissolved arsenic has been recognized as a significant water quality problem that affects millions of people in parts of the world. Chronic consumption of high levels of arsenic can lead to several health problems, including lung, bladder and skin cancers. The most widely known region for arsenic contamination in groundwater is Bangladesh, where the situation has been described as a public health emergency (e.g., [75]). A similar, but less dramatic problem has been known in parts of Wisconsin for over two decades.

Discovery of the arsenic problem occurred in 1987 as part of a routine feasibility study for a landfill proposed in Winnebago County [76]. Over the past 28 years, several thousand wells have been analyzed for arsenic in parts of eastern Wisconsin. Arsenic concentrations vary from less than 1 µg/L to over 15,000 µg/L [77,78] over a region that includes several tens of thousands of private drinking water wells. In some townships, 20% or more of wells can exceed the 10 µg/L EPA MCL for arsenic. There are at least three regions in the state that contain elevated levels of dissolved arsenic in groundwater (Figure 5), each of which has a different potential geologic origin. These include the Paleozoic bedrock wells in eastern Wisconsin along the Fox River Valley, Pleistocene glacial sediment in southeastern Wisconsin, and wells in Precambrian bedrock with Pleistocene glacial sediment cover in Florence County (northern Wisconsin).

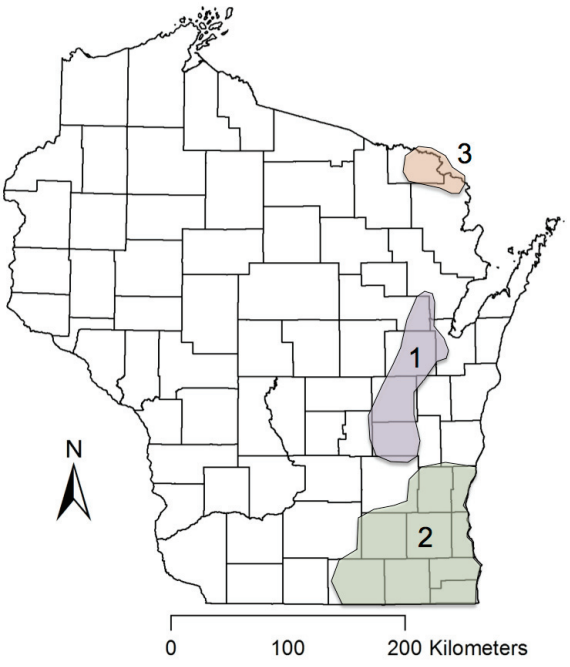

Figure 5. Three regions in the state have elevated arsenic in different aquifers. Region 1 represents the portion of the Paleozoic bedrock aquifer with elevated dissolved arsenic due to oxidation of sulfide minerals [78,79]. Region 2 represents elevated arsenic in the Pleistocene glacial sediments and the Silurian bedrock aquifer of southeastern Wisconsin [80]. Region 3 represents a region in Florence County with elevated arsenic in which Precambrian bedrock is overlain by Pleistocene glacial sediments [79].

The region in which this problem has been most thoroughly documented is in the Paleozoic bedrock of eastern Wisconsin (e.g., [76,78,81–84]). Much of this focus has been to characterize the distribution of arsenic and associated metals (Ni, Co, *etc.*) in well waters and aquifer rocks, primarily in parts of Winnebago and Outagamie Counties, but this problem extends from as far south as Fond du Lac County to as far north as the Michigan border in Marinette County, e.g., [59,76,77,84,86].

Arsenic concentrations as high as 15,000 µg/L have been encountered in wells open to the Paleozoic aquifer of eastern Wisconsin, and in some townships 20%–40% of the wells tested were above 10 µg/L (the EPA MCL for arsenic). Fewer wells have been tested for nickel and cobalt, but these metals are closely associated with arsenic in the region due to the host mineralogy of a regionally extensive sulfide cement horizon (SCH) at the top of the Ancell Group. One well in Outagamie County, Wisconsin had the following chemistry documented: pH = 2.05, As = 4300 µg/L, Co = 5500 µg/L, Cd = 220 µg/L, Cr = 84 µg/L, Ni = 11,000 µg/L, Al = 15,000 µg/L, and Pb = 400 µg/L [85].

Portions of this aquifer contain abundant sulfide mineralization associated with Cambrian and Ordovician sedimentary rocks (Figure 3). The most abundant sulfide-rich cement horizon (SCH) is a zone of pyrite, marcasite, and associated minerals that occurs near the interface of the St. Peter Sandstone (Ancell Group) and the Platteville Dolomite (Sinnipee Group) [26,78,86,87].

The SCH has been documented to occur across eastern Wisconsin from the Illinois border in the south to the Michigan border in the north [26,86]. The mineralogy and mechanisms of arsenic release differ in different settings. Oxidative release is thought to be the most important mechanism in eastern Wisconsin (e.g., [87]). Although most attention has been given to the St. Peter Sandstone aquifer, other units in the region, such as the Cambrian sandstones, also contain abundant sulfide mineralization. Oxidative release of arsenic and nickel during aquifer storage and recovery (ASR) testing has resulted in substantial volumes of groundwater contamination near test wells [85].

Another region of the state with significant arsenic problems is southeastern Wisconsin. This area has up to 150 meters of glacial till and outwash of Pleistocene age overlying Silurian age dolomite. This region has had arsenic concentrations up to 100 µg/L documented in portions of the lower sand and gravel aquifer beneath organic-rich glacial till units [80]. In contrast to the Paleozoic rocks of eastern Wisconsin, there appears to be a different mechanism for arsenic release in southeastern Wisconsin. The presence of reducing conditions, low sulfate concentrations, and solid-phase organic matter led Root *et al.* [80] to conclude that arsenic is released to ground water in the lower sand and gravel/dolomite aquifer via microbially mediated reductive dissolution of arsenic-bearing Mn and/or Fe-(hydr)oxides.

A third region with a recognized arsenic problem is Florence County (Figure 5). The origin of arsenic in this area is less understood, but dozens of wells are impacted in the region, and ongoing research is investigating the geologic mechanisms and stratigraphic relationships in the region.

The public health impact of high dissolved arsenic was recently investigated by Knobeloch *et al.* [77] in a study that associated arsenic-contaminated drinking water with the prevalence of skin cancer in eastern Wisconsin. They documented arsenic concentrations and surveyed several thousand residents using over 2200 wells in the region. Their results indicated that for residents over age 35 who had consumed arsenic-contaminated water for at least 10 years, those residents were significantly more likely to report a history of skin cancer than other residents.

In response to public health concern over arsenic in the Fox River Valley region of eastern Wisconsin, the Wisconsin DNR implemented special well casing requirements for wells in Winnebago and Outagamie counties that became effective on 1 October 2004. These requirements are in place to avoid the most sulfide-rich portion of the aquifer near the SCH. However, additional

requirements were included that limited the types of well construction methods and disinfection methods that can be used.

It is important to note that while much attention has been given to these two counties, the geologic strata and sulfide mineral distribution are similar throughout eastern Wisconsin [26,86]. Wells drilled in the same units in Marinette, Oconto, Brown, Shawano, and Fond du Lac counties have significant percentages of wells that exceed the 10 µg/L of arsenic in drinking water standard.

4.1.3. Fluoride Problems in Two Distinct Geologic Provinces

Fluoride at optimal levels (0.7 to 1.2 ppm) can reduce the incidence of dental caries. However, excess fluoride can produce dental fluorosis and negatively impact bone health, especially in children [88]. As such, the US EPA has set a MCL for dissolved fluoride of 4.0 mg/L, with a secondary (advisory) MCL of 2.0 mg/L. This value is intended to reduce the risk of severe enamel fluorosis and to minimize the risk of bone fractures and skeletal fluorosis in the adult population [59]. In 2011, the U.S. Department of Health and Human Services proposed to reduce the recommended level to 0.7 mg/L [89].

Wisconsin contains three distinct regions with elevated levels of dissolved fluoride above 1.2 mg/L in groundwater (Figure 6). One of these areas occurs in parts of Marathon County and the adjacent areas of central Wisconsin. Groundwater in this region is obtained principally from Precambrian crystalline bedrock aquifers and Quaternary glacial and alluvial sediments. A recent study focusing on Marathon County wells indicates that fluoride in this region ranges from <0.01 mg/L to at least 7.6 mg/L [90]. In that study, approximately 0.6% of the wells exceeded the EPA MCL of 4 mg/L, and 8.6% exceeded the secondary MCL of 2.0 mg/L. The source of fluoride in groundwater in this region appears to be fluorite and fluorapatite in felsic intrusive rocks, specifically syenite and Na-plagioclase bearing granites [90].

A second region of elevated fluoride occurs in the Cambrian and Ordovician confined aquifer of northeastern Wisconsin along the Fox River Valley and adjacent to the Bay of Green Bay. This anomaly has been known for more than 40 years [64,95], and a study by Krohelski [28] showed a mean concentration of 1.32 mg/L for the Ordovician and Cambrian sandstone aquifers in the region. While few wells appear to exceed the MCL of 4.0 mg/L, hundreds of wells likely exceed the secondary MCL of 2.0 mg/L, and most wells in the confined aquifer likely exceed the target value of 1.2 mg/L suggested by the U.S. EPA. The source of fluoride in this aquifer appears to be fluorite associated with Mississippi Valley-type mineralization in the region [26].

A third region is less well defined and less studied, but it extends along the Lake Michigan shoreline from Kewaunee County in the north to the Illinois border in the south. Many wells exceed the secondary MCL of 2.0 mg/L, and a few exceed 4.0 mg/L. Most of the wells with elevated fluoride appear to be drawing from both Pleistocene glacial sediments and Silurian dolomite units. It is likely that fluorite is also the source of this elevated dissolved fluoride because fluorite mineralization occurs in the Silurian rocks of eastern Wisconsin. More research on this topic is needed to better understand the stratigraphic distribution and origin of dissolved fluoride in eastern Wisconsin.

In Marathon and Lincoln counties (central Wisconsin), county health departments offer test kits for dissolved fluoride. Other municipalities, such as those in the Fox River Valley region, distribute notices to water utility customers advising them of elevated levels above the secondary MCL.

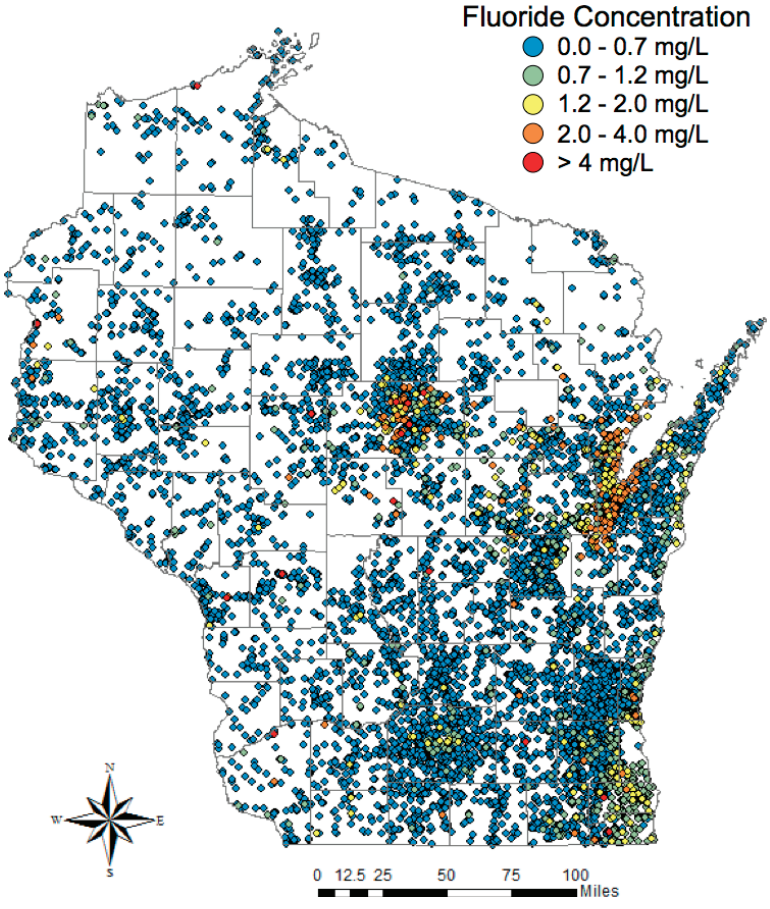

Figure 6. Map showing dissolved fluoride in Wisconsin aquifers. The highest concentrations are present in areas of shallow Precambrian bedrock of central Wisconsin. Another broad region of elevated fluoride occurs in the Cambrian-Ordovician confined aquifer of northeastern Wisconsin. A third region of elevated fluoride occurs in glacial sediments and Silurian bedrock in eastern and southeastern Wisconsin. Data sources include [91–94].

4.1.4. Dissolved Strontium

A region of high dissolved strontium (Sr) occurs in an arc-shaped band throughout eastern Wisconsin inland from the Lake Michigan shoreline where deep wells penetrate the Cambrian-Ordovician sandstone aquifer (Figure 7). Groundwater in parts of eastern Wisconsin contains dissolved Sr levels that exceed lifetime and short-term U.S. EPA Health Advisories of 4 mg/L and 25 mg/L,

respectively [64,92–94]. Hundreds of wells are impacted throughout this region, including an area of anomalously high dissolved Sr in parts of Brown, Outagamie, and Calumet counties.

At present, about 11,000 groundwater samples statewide have been analyzed for strontium [92,93]. Until recently, data regarding dissolved Sr in Wisconsin groundwater were limited, and it is now clear that elevated dissolved Sr is present in the deep aquifer throughout much of eastern Wisconsin. While limited evidence for high Sr in the region's groundwater was available for over 50 years [96], little attention was given to this problem until 2013 [92,93]. Affected wells include many municipal wells from the suburban Milwaukee metropolitan area north to Green Bay, with concentrations of strontium in groundwater drinking supplies reaching as high as 52 mg/L [96].

The source of the Sr appears to be the dissolution of heterogeneously distributed celestine ($SrSO_4$), and possibly strontianite ($SrCO_3$) cements in Cambrian and Ordovician rocks in the region [92–94]. These rocks were strongly impacted by dolomitization and mineralization associated with an ancient hydrothermal brine migration from the Michigan basin [26].

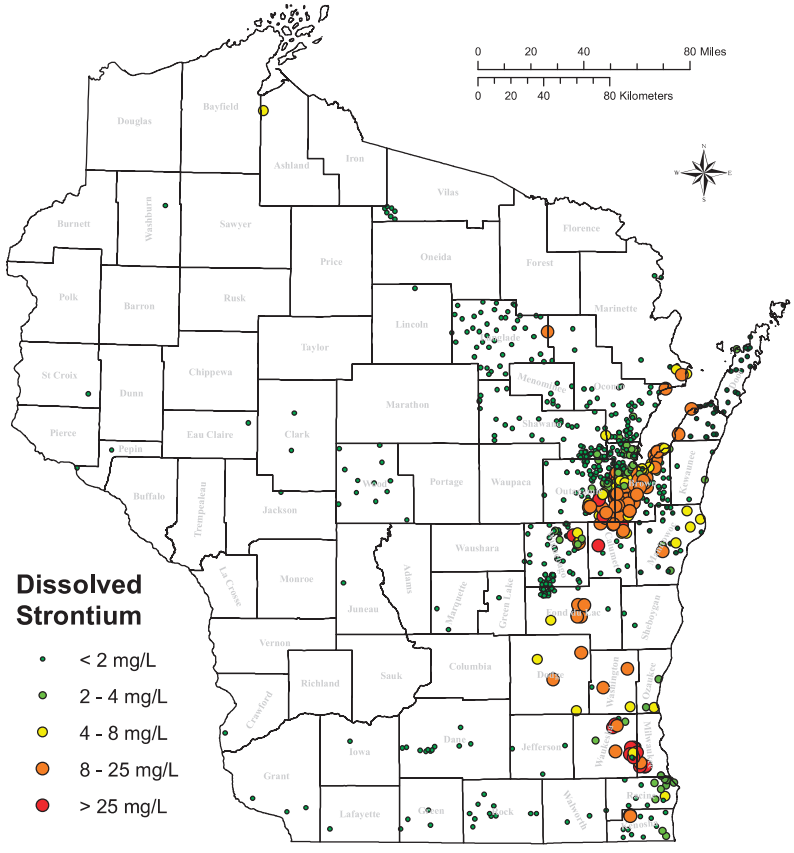

Figure 7. A broad arc-shaped region of eastern Wisconsin contains elevated dissolved strontium in the Cambrian-Ordovician aquifer. Limited data suggest additional wells in the Silurian bedrock east of this zone also contain elevated dissolved strontium above the EPA lifetime health advisory level of 4 mg/L [92–94].

Although the full spectrum of adverse human health effects from Sr ingestion is unclear, two health effects are documented in the literature. One of these is known as “strontium rickets”, which is a musculoskeletal disease in which bones are thicker and shorter than normal and can be deformed [97]. Another health effect linked to the ingestion of groundwater-derived strontium is tooth enamel mottling [98]. Recognition that dissolved Sr might be a more significant problem in Wisconsin than initially anticipated has prompted the recent addition of Sr to the State Lab of Hygiene water quality metals scan in the last several years. At present, there is no MCL in effect through the U.S. EPA, but there has been a preliminary determination by the EPA to regulate strontium in Drinking Water [99]. Treatment systems (standard water softeners or reverse osmosis systems) are very effective solutions, but the public is generally unaware of the Sr problem.

4.1.5. High Total Dissolved Solids

Most groundwater in Wisconsin has relatively low total dissolved solids. This is not surprising because the state also lacks any economic deposits of petroleum and natural gas, which are often associated with dense brines. While strong evidence for multiple ancient brine migrations is present in the Paleozoic sedimentary rocks in the region (e.g., [26,100]), these aquifers have been subsequently flushed of brine over millions of years prior to the Pleistocene Epoch. Some water has been documented by radiocarbon dating as being Late Pleistocene in age [36]. However, not all salts have been fully removed from the system.

Portions of the Cambrian-Ordovician aquifer system in eastern Wisconsin contain groundwater with elevated total dissolved solids (TDS). While a precise distribution of wells with high TDS is not available, the approximate region is roughly correlative with the Maquoketa Shale subcrop in eastern Wisconsin [64,93,94]. Values of total dissolved solids above 1000 mg/L have been reported mainly from the Cambrian-Ordovician confined aquifer of eastern Wisconsin [64,92,95], but significant regions of the Silurian aquifer of southeastern Wisconsin also have TDS values that exceed 1000 mg/L [7]. In addition, some wells in western and northwestern Wisconsin exceed this value [95]. Hundreds of wells are likely impacted by this problem, and it prevents a large part of eastern Wisconsin that has shallow aquifer contamination from accessing potable supplies of deep aquifer groundwater.

Dissolved boron (B) and lithium (Li) appear to be associated with elevated salinities [64,94]. In a recent study by Luczaj *et al.* [92], analysis of boron and lithium in selected samples has identified that these may also be important elements of concern in the deep aquifer system of northeastern Wisconsin. Two of 49 samples analyzed for dissolved B exceeded the MCL of 1000 µg/L. One sample was 3300 µg/L, over three times the MCL established by the State of Wisconsin. Although Li does not have an established MCL, concentrations varied dramatically in parts of the region from 1.7 µg/L to 305 µg/L. High levels of dissolved Sr, Li, B, and F have been reported elsewhere in carbonate rock on marginal parts of high salinity basins (e.g., [101]).

4.1.6. Other Noteworthy Problems

Several other noteworthy problems from naturally occurring contaminants are known in Wisconsin, including aluminum and manganese. The extent and cause of these problems is not fully understood, but they have variable origins in different parts of the state. One area of particular concern for manganese has been Taylor County in northern Wisconsin [102]. Elevated manganese and aluminum have been reported from several regions in the state [59], but a detailed analysis of most of these occurrences has not been completed.

4.2. Anthropogenic Contaminants

4.2.1. Nitrate

Nitrate is generally considered the most widespread groundwater contaminant in Wisconsin. Natural or background concentrations of nitrate-nitrogen in groundwater are typically less than 1 mg/L, and concentrations greater than this provide evidence of impacts from the use of nitrogen fertilizers, storage or spreading of animal waste and/or other bio-solids, or septic system drain fields. As nitrate, nitrogen is readily carried in the drainage that recharges groundwater. Previous estimates attribute 90% of nitrate in Wisconsin's groundwater to agricultural sources, 9% to septic systems and 1% to lawn fertilization [103]. The variety of nitrogen sources and the mobility of nitrate make it an ideal candidate to understand groundwater wells or aquifer systems that are susceptible to anthropogenic influences.

A statewide survey of private wells in Wisconsin showed 9% of wells exceeded the drinking water standard of 10 mg/L for nitrate-nitrogen [104]. The percentage of wells that exceeded the standard increased to 21% when limited to wells located in districts where greater than 75% of the area is cultivated. Additional information exists from voluntarily submitted private well data collected over a nearly 30-year period across the state. These data show similar exceedance rates to the statewide survey, revealing approximately 10% of wells exceed the nitrate standard [79]. Forty-two percent of all samples reported a concentration above 2 mg/L, which is generally considered conclusive evidence of anthropogenic influences. The amount of data collected through voluntary testing is significant and the spatial distribution is extensive (Figure 8). The patterns that emerge have allowed resource professionals to identify areas of concern and ground-truth existing models of groundwater susceptibility.

In Wisconsin, groundwater contamination susceptibility has previously been modeled as a function of surficial deposit type, depth to bedrock, type of bedrock and depth to groundwater [105]. Areas determined to have a high groundwater contamination susceptibility rating typically correlate well with areas of known groundwater nitrate concerns as evidenced by private well testing data in areas where sufficient data exists. Simply identifying areas that are susceptible should not be interpreted that groundwater quality is degraded. In order for groundwater to actually become contaminated there needs to exist a nitrogen source. Northern Wisconsin is an example of an area where the groundwater is rated as highly susceptible to groundwater contamination; however, nitrate above the drinking water standard is rare. The large percentage of forests and wetlands, combined

with low population densities in northern Wisconsin, results in very few nitrate impacted wells. Conversely just because there is a source of nitrogen does not guarantee significant groundwater nitrate impacts. Such is the case in eastern Wisconsin, where agriculture is often the dominant land use, but groundwater concentrations of nitrate are often found at background or natural levels. In these areas, a higher potential for denitrification, a greater use of drain tiles, and generally heavier texture soil types are potential explanations for the lack of nitrate found in groundwater in much of the area.

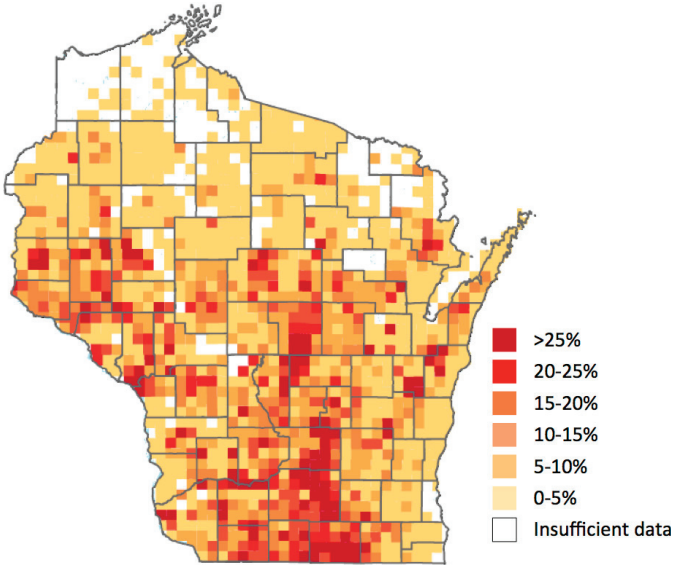

Figure 8. Map of Wisconsin showing the percentage of groundwater samples in each township above the 10 mg/L nitrate-N drinking water standard [79].

Much attention has been paid to the role of agricultural practices and the influence on ground and surface waters with respect to nitrate. Studies have affirmed that applying rates of nitrogen in excess of economic optimal rates exacerbate groundwater concerns; however many studies have shown that even at optimal rates of application, nitrate can leach at rates exceeding drinking water standards [106,107]. The groundwater nitrate pattern in Wisconsin is mostly explained by investigating the relationship between agricultural practices and a few soil or geologic characteristics. Three areas with significant nitrate impacts include: (1) regions of highly permeable sandy soils (central sands region and lower Wisconsin River valley), (2) shallow carbonate rock aquifer systems of eastern Wisconsin located along and east of the Niagara Escarpment, where solution-enlarged joints, sinkholes, and other karst features promote drainage of nitrate rich soil pore water from agriculturally managed soil horizons to groundwater in the unconfined dolostone aquifer, and (3) south-central Wisconsin where well-drained soils are extensively managed for high nitrogen input row crop production.

4.2.2. Pathogens

Pathogens are receiving increasing attention in Wisconsin. Recent work over the past 15 years in Wisconsin has revealed a complex problem with pathogens in a variety of geologic units from multiple sources. Bacterial contamination has been widely known from regions of the state with karst aquifers and heavy agriculture [108,109]. However, recent studies have found viruses in both municipal and domestic water supply wells drawing from a number of aquifer types. Viruses have been associated with leaking sewage systems in deep aquifers accessed by municipal wells, leaking septic systems in shallower wells in karst regions, and surface water contributions to municipal wells [110–117]. In one case, a restaurant well was contaminated by its own septic drainfield, leading to a norovirus outbreak that sickened 229 people [114].

The large number of dairy cows and other animals in the state mean that pathogenic contamination from manure is an ongoing concern. This is particularly true in areas where wells rely on the shallow carbonate rock aquifer such as eastern Wisconsin [108], but it is true in other regions as well [116]. Thin or absent soils overlying fractured, karsted dolomite rock allow surface water a direct conduit to groundwater with little to no ability to attenuate or filter contaminants such as bacteria or viruses. Anecdotal and documented evidence suggest "brown water" incidents (*i.e.*, sudden changes in water quality that occur during snowmelt or spring rains) have occurred for many years throughout Northeast Wisconsin (see also [117]). Between 2006 and mid-2014, sixty-four wells were replaced throughout Wisconsin due to confirmed contamination by livestock manure [118]; three-quarters of those wells were located in areas rated as having a significant to extreme vulnerability to groundwater contamination related to karst-type landscape features (e.g., sinkholes, fracture traces, surface rock outcrops, disappearing streams) [108].

The problem of pathogen contamination is widespread, and is not limited to shallow domestic wells. Nonetheless, disinfection of municipal water systems has the capability to limit the exposure of residents to pathogens like bacteria and viruses. Unfortunately, disinfection is not mandated for the municipal systems that supply groundwater to over 2 million residents of Wisconsin, although about 60% of the state's municipal groundwater systems do disinfect their water [119]. Recent studies in Wisconsin have suggested that public health could be improved by identifying municipal water systems that lack water treatment and are likely to transmit waterborne disease [116].

4.2.3. Pesticides

A survey of 398 private wells by the Wisconsin Department of Agriculture, Trade, and Consumer Protection estimated that 33.5% of wells statewide contain at least one detectable pesticide or pesticide metabolite [120]. Wells located in areas with a greater intensity of agriculture are more likely to contain detections of pesticides. The most frequently detected pesticides or pesticide metabolites in Wisconsin groundwater included metolachlor ESA, alachlor ESA, atrazine and metabolites of atrazine.

Wisconsin is unique in that it has a health-based groundwater standard of 3 parts per billion (ppb) for atrazine plus its three metabolites (diamino atrazine, deethyl atrazine, and deisopropyl atrazine), as opposed to just atrazine [121]. When concentrations of atrazine and its metabolites are detected in

a well above 3 ppb, an atrazine prohibition area may be established that prohibits future use of atrazine in a designated area around the well. Continued monitoring of wells in atrazine prohibition areas reveal that since 1995, concentrations of atrazine and its metabolites have slowly dissipated in most wells. It was estimated that following prohibition of atrazine it would take 11–17 years for atrazine and the metabolites to dissipate completely from wells [121].

4.2.4. Endocrine Disrupting Compounds

Recent research has addressed the prevalence of endocrine disrupting compounds (EDCs) in groundwater, which is an emerging class of contaminants. EDCs can originate from a wide variety of sources, including pharmaceuticals from leaky septic systems, land-applied manure, and estrogenic pesticides [109,122]. Historically, the best-studied EDC in Wisconsin has been atrazine and its metabolites [120,121].

Limited work has been done in Wisconsin regarding other EDCs, but these are likely to receive greater attention in the future because of their potential to cause physiological abnormalities and endocrine-related cancers in exposed organisms [109]. A recent study by Bauer *et al.* [109] in six northeastern Wisconsin counties showed that contamination of groundwater with EDCs, nitrate, and fecal bacteria is a common problem in karst areas of northeastern Wisconsin. Their study did not analyze specific endocrine disrupting compounds; rather, they used human breast cancer cells to evaluate the "estrogenicity" of the water [109].

4.3. Contaminants of Unresolved Origin

Boron and Molybdenum are two contaminants that have been recognized recently as having a significant impact on the water quality of parts of southeastern Wisconsin. The precise origin of the boron and molybdenum in groundwater is not completely understood, and disagreement exists regarding the source(s). The region of elevated molybdenum and boron values occurs in Racine, Kenosha, and Milwaukee counties in southeastern Wisconsin. Of 967 unique wells tested from 2010 to 2014, 45% of the wells exceeded the WDNR enforcement standard of 40 µg/L, and 22% exceeded the newly established Wisconsin Department of Health Advisory Level of 90 µg/L [123]. A smaller number of wells contained boron concentrations above 1000 µg/L, which is the WDNR enforcement standard. These wells are located in Pleistocene glacial sediments and underlying Silurian dolostone bedrock.

In a 2013 Report, the WDNR evaluated the possibility that three landfills, one of which was a coal fly ash landfill, could be the source of elevated boron and molybdenum in private wells nearby [124]. Water quality testing included stable isotopic analysis of boron and molybdenum, as well as tritium sampling. The WDNR concluded that a municipal and industrial landfill was not the source of molybdenum in private wells, but data were inconclusive as to whether or not a fly ash landfill was the source of molybdenum. Boron in most private wells appeared to be from sources other than the landfills, either natural or other anthropogenic sources. Tritium sampling showed that most private wells contained water without detectable tritium, suggesting that anthropogenic sources were not likely the source of molybdenum in most of the private wells analyzed. The elevated molybdenum

remains the largest mystery, especially because it is detected in wells spread across such a large region of the state.

A more recent study by the environmental group Clean Wisconsin [123] came to a different conclusion based on a regional analysis. They suggest that there is a correlation between beneficial coal fly as "reuse" sites and elevated levels of molybdenum in private wells. Wisconsin has the highest rate of "beneficial reuse" of coal fly ash in the United States, and concern has arisen from decades of unregulated disposal of coal fly ash beneath roads, buildings, and foundations. They suggest that widespread distribution of coal fly ash over several decades has led to the regional groundwater problem of elevated dissolved molybdenum. A recent 2014 U.S. EPA ruling continues to allow the beneficial reuse of coal combustion products, without the need to regulate it as a hazardous substance [125].

5. Conclusions

In general, groundwater quantity issues are most prominent in the central sands region of central Wisconsin and heavily populated parts of northeastern and southeastern Wisconsin that draw from confined aquifers. Some regions, such as the municipalities near Lake Michigan, are fortunate enough to have this resource available and have switched over to surface water resources when water quantity or quality issues have arisen.

Problems with groundwater quality, on the other hand, are more widespread and are difficult to solve. Groundwater quality issues originate through naturally occurring and anthropogenic sources, and they are strongly influenced by the regional geologic framework. The arsenic contamination problem in eastern Wisconsin has been addressed in some areas through well testing and special well casing requirements. Although significant problems remain, a greater public awareness has been established. Other contaminants, such as bacteria and nitrates, continue to be significant challenges. A few contaminants, such as viruses, EDCs, and strontium, might be considered emerging contaminants.

Acknowledgments

We would like to thank UW-Green Bay students Joseph Baeten and Josie Robertson for assistance with graphics related to their research on strontium and fluoride, respectively. Robert Smail contributed some helpful information on water use in the state. We also thank Elizabeth Luczaj and two anonymous reviewers for kindly reviewing this manuscript.

Author Contributions

John Luczaj's contribution includes researching the overall groundwater quantity and quality issues. Kevin Masarik focused on the groundwater quantity overview, issues related to the central sand plains, and sections covering nitrates, pesticides, and pathogens. Both parties worked on identifying and documenting the references and creating figures.

Conflicts of Interest

The authors declare no conflict of interest.

References

1. Rohli, R.V.; Vega, A.J. *Climatology*, 4th ed.; Jones & Bartlett Learning: Burlington, MA, USA, 2015; p. 443.
2. NOAA. National Weather Service Statewide Wisconsin Average Annual Precipitation Map—30 Year Average Precipitation 1981–2010. Available online: http://www.crh.noaa.gov/images/mkx/climate/avg_30_year_precip.png (accessed on 15 April 2015).
3. United States Census Bureau. United States Census—2010. Available online: http://www.census.gov/2010census/data/ (accessed on 15 April 2015).
4. Wisconsin Department of Natural Resources (WDNR). Status of Groundwater Quantity in Wisconsin. Available online: http://dnr.wi.gov/topic/Groundwater/documents/GCC/gw-quantity.pdf (accessed on 15 April 2015).
5. Luczaj, J.A.; Hart, D.J. *Drawdown in the Northeast Groundwater Management Area (Brown, Outagamie, and Calumet Counties, WI)*; Final report prepared for the Wisconsin Department of Natural Resources. Available online: http://wgnhs.uwex.edu/pubs/wofr200904/ (accessed on 15 April 2015).
6. Maas, J.C. Drawdown, Recovery, and Hydrostratigraphy in Wisconsin's Northeast Groundwater Management Area (Brown, Outagamie, and Calumet Counties). Master's Thesis, University of Wisconsin, Green Bay, WI, USA, December 2009.
7. Southeast Wisconsin Regional Planning Commission (SWRPC). Groundwater Resources of Southeastern Wisconsin: Technical Report Number 37. Available online: http://www.sewrpc.org/SEWRPCFiles/Publications/TechRep/tr-037_groundwater_resources.pdf (accessed on 15 April 2015).
8. Stites, W.; Kraft, G.J. Groundwater quality beneath irrigated vegetable fields in a north-central U.S. sand plain. *J. Environ. Qual.* **2000**, *29*, 1509–1517.
9. Wisconsin Department of Natural Resources (DNR). *Wisconsin Lakes*; Wisconsin Department of Natural Resources: Madison, WI, USA, 2009.
10. Syverson, K.M.; Colgan, P.M. The Quaternary of Wisconsin: A review of stratigraphy and glaciation history. In *Quaternary Glaciations—Extent and Chronology, Part II: North America*; Ehlers, J., Gibbard, P.L., Eds.; Elsevier Publishing: Amsterdam, The Netherlands, 2004; pp. 295–311.
11. Wisconsin Department of Natural Resources (WDNR). *Wisconsin Water Use: 2013 Withdrawal Summary*; Wisconsin Department of Natural Resources Water Use Section: Madison, WI, USA, 2014. Available online: http://dnr.wi.gov/topic/WaterUse/documents/WithdrawalReportDetail.pdf (accessed on 15 April 2015).
12. Ellefson, B.R.; Mueller, G.D.; Buchwald, C.A. *Water Use in Wisconsin: United States Geological Survey Open-File Report*; United States Geological Survey: Reston, VA, USA, 2000.

13. Smail, R.A. Written Communication regarding groundwater use in Wisconsin, 13 October 2014.
14. Center for Land Use Education (CLUE).Wisconsin Land Use Megatrends: Water. University of Wisconsin-Stevens Point and University of Wisconsin—Cooperative Extension. Available online: https://www.uwsp.edu/cnr-ap/clue/Documents/megatrends/WaterMegatrendsFINAL.pdf (accessed on 15 April 2015).
15. Weidman, S.; Schultz, A.R. *The Underground and Surface Water Supplies of Wisconsin*; Forgotten Books: London, UK, 1915.
16. Kammerer, P.A., Jr. *Ground Water Flow and Quality in Wisconsin's Shallow Aquifer System*; United States Geological Survey: Reston, VA, USA, 1995.
17. Dott, R.H., Jr.; Attig, J.W. *Roadside Geology of Wisconsin*, 1st ed.; Mountain Press: Missoula, MT, USA, 2004; p. 246.
18. La Berge, G.L. *Geology of the Lake Superior Region*; Geoscience Press, Inc.: Phoenix, AZ, USA, 1994; p. 313.
19. Larson, G.; Schaetzl, R. Origin and evolution of the Great Lakes. *J. Gr. Lakes Res.* **2001**, *27*, 518–546.
20. Luczaj, J.A. Geology of the Niagara escarpment in Wisconsin. *Geosci. Wis.* **2013**, *22*, 1–34. Available Online: http://wgnhs.uwex.edu/pubs/gs22a01/ (accessed on 15 April 2015).
21. Ojakangas, R.W.; Morey, G.B.; Green, J.C. The mesoproterozoic midcontinent rift system, lake superior region, USA. *Sediment. Geol.* **2001**, *141–142*, 421–442.
22. Schultz, G.M. *Wisconsin's Foundations: A Review of the State's Geology and its Influence on Geography and Human Activity*; UW Press: Dubuque, IA, USA, 1986; pp. 1–211.
23. Schulz, K.J.; Cannon, W.F. The Penokean orogeny in the Lake Superior region. *Precambrian Res.* **2007**, *157*, 4–25.
24. Syverson, K.M.; Clayton, L.; Attig, J.W.; Mickelson, D.M. *Lexicon of Pleistocene Stratigraphic Units of Wisconsin*; Technical Report; Wisconsin Geological and Natural History Survey: Madison, WI, USA, 2011; pp. 1–180.
25. Catacosinos, P.A.; Daniels, P.A., Jr.; Harrison, W.B., III. Structure, stratigraphy, and petroleum geology of the Michigan basin. In *Interior Cratonic Basins*; Leighton, M., Kolata, D., Oltz, D., Eidel, J., Eds.; American Association of Petroleum Geologists Memoir: Tulsa, OK, USA, 1990; pp. 561–601.
26. Luczaj, J.A. Evidence against the Dorag (Mixing-Zone) model for dolomitization along the Wisconsin arch—A case for hydrothermal diagenesis. *AAPG Bull.* **2006**, *90*, 1719–1738.
27. Runkel, A.C.; Miller, J.F.; McKay, R.M.; Palmer; A.R.; Taylor, J.F. High-resolution sequence stratigraphy of lower Paleozoic sheet sandstones in central North America: The role of special conditions of cratonic interiors in development of stratal architecture. *GSA Bull.* **2007**, *119*, 860–881.
28. Krohelski, J.T. *Hydrogeology and Ground-Water Use and Quality, Brown County, Wisconsin*; Wisconsin Geological and Natural History Survey: Madison, WI, USA, 1986; Volume 57, pp. 1–42.

29. Luczaj, J.A.; Maas, J.; Hart, D.J. A history of drawdown in the Cambrian-Ordovician confined aquifer system in northeastern Wisconsin. Manuscript in preparation.
30. Wisconsin Geological & Natural History Survey. *Bedrock Stratigraphic Units in Wisconsin*; Educational Series; Wisconsin Geological & Natural History Survey: Madison, WI, USA, 2011.
31. McLaughlin, P.I.; Mikulic, D.G.; Kluessendorf, J. Age and correlation of Silurian rocks in Sheboygan, Wisconsin, using integrated stable carbon isotope stratigraphy and facies analysis. *Geosci. Wis.* **2013**, *21*, 15–38.
32. Velbel, M. The "Lost Interval": Geology from the Permian to the Pliocene. In *Michigan Geography and Geology*, 1st ed.; Schaetzl, R., Darden, J., Brant, D., Eds.; Pearson Custom Publishing: Boston, MA, USA, 2009; pp. 60–68.
33. Moran, J.M.; Hopkins, E.J. *Wisconsin's Weather and Climate*, 1st ed.; University of Wisconsin Press: Madison, WI, USA, 2002; pp. 1–321.
34. Thorleifson, L.H. *Potential Capacity for Geologic Carbon Sequestration in the Midcontinent Rift System in Minnesota*; Open File Report for Minnesota Geological Survey: St. Paul, MN, USA, 2008, pp. 1–138.
35. Grundl, T.; Cape, M. Geochemical factors controlling radium activity in a sandstone aquifer. *Ground Water* **2006**, *44*, 518–527.
36. Grundl, T.; Magnusson, N.; Brennwald, M.S.; Kipfer, R. Mechanisms of subglacial groundwater recharge as derived from noble gas, ^{14}C, and stable isotopic data. *Earth Planet. Sci. Lett.* **2013**, *369–370*, 78–85.
37. Luczaj, J.A.; Stieglitz, R.D. Geologic history of New Hope Cave, Manitowoc County, Wisconsin. *Wis. Speleol.* **2008**, *June*, 7–17.
38. Wauters, G.J. Paleoecological Perspectives: The Brussels Hill Pit Cave Mammal Assemblage, with a Focus on Short-Tailed Shrews and Graphical Explorations of Holocene Paleomammalogy in Wisconsin. Master's Thesis, University of Wisconsin, Green Bay, WI, USA, 2013.
39. Weaver, T.R.; Bahr, J.M. Geochemical evolution in the Cambrian-Ordovician sandstone aquifer, eastern Wisconsin: 1. Major ion and radionuclide distribution. *Ground Water* **1991**, *29*, 350–356.
40. Weaver, T.R.; Bahr, J.M. Geochemical evolution in the Cambrian-Ordovician sandstone aquifer, eastern Wisconsin. 2. Correlation between flow paths and ground-water chemistry. *Ground Water* **1991**, *29*, 510–515.
41. Klump, S.; Grundl, T.; Purtschert, R.; Kipfer, R. Groundwater and climate dynamics derived from noble gas, ^{14}C, and stable isotope data. *Geology* **2008**, *36*, 395–398.
42. Weeks, E.P.; Stangland, H.G. *Effects of Irrigation on Streamflow in the Central Sand Plain of Wisconsin*; United States Geological Survey: Reston, VA, USA, 1971.
43. Kraft, G.J.; Clancy, K.; Mechenich, D.J.; Haucke, J. Irrigation effects in the Northern Lake States: Wisconsin central sands revisited. *Ground Water* **2012**, *50*, 308–318.
44. Groundwater Coordinating Council (GCC). Wisconsin Groundwater Coordinating Council FY 2013 Report to the Wisconsin State Legislature. Available online: http://dnr.wi.gov/topic/groundwater/documents/GCC/Report/WIgroundwaterLaw.PDF (accessed on 15 April 2015).

45. Supreme Court of Wisconsin, Lake Beulah Management District, Petitioner-Appellant-Cross-Respondent, Lake Beulah Protective and Improvement Association, Co-Petitioner-Co-Appellant-Cross- Respondent, v. State of Wisconsin Department of Natural Resources, Respondent-Respondent, Village of East Troy, Intervening-Respondent-Respondent- Cross-Appellant-Petitioner. 2011. Available Online: https://www.wicourts.gov/sc/opinion/DisplayDocument.pdf?content=pdf&seqNo=67353 (accessed on 15 April 2015).
46. Boldt, J.D. Case Nos. 1H-12-03, 1H-12-05, DNR-13-021 and NDR-13-027. State of Wisconsin, Division of Hearings and Appeals. 3 September 2014.
47. Council of Great Lakes Governors. Great Lakes-St. Lawrence River Basin Water Resources Compact (2008). Available online: http://www.cglg.org/projects/water-management/great-lakes-agreement-and-compact/ (accessed on 12 April 2015).
48. Karkkainen, B.C. The Great Lakes water resources compact and agreement: Transboundary normativity without international law. *William Mitchell Law Rev.* **2013**, *39*, 997.
49. Feinstein, D.T.; Hart, D.J.; Eaton, T.T.; Krohelski, J.T.; Bradbury, K.R. *Simulation of Regional Groundwater Flow in Southeastern Wisconsin*; Wisconsin Geological & Natural History Survey: Madison, WI, USA, 2004. Available online: http://wgnhs.uwex.edu/pubs/wofr200401/ (accessed on 15 April 2015).
50. Luczaj, J.A. The largest flowing artesian well in the state of Wisconsin is (sometimes) an abandoned deep quarry. In Proceedings of the American Water Resources Association—Wisconsin Section, 38th Annual Meeting, Wisconsin Dells, WI, USA, 13–14 March 2014. Available online: http://state.awra.org/wisconsin/2014meeting/Session3A4Luczaj.pdf (accessed on 15 April 2015).
51. Jakel, D.E. *Soil Survey of Adams County, Wisconsin*; USDA Soil Conservation Service: Washington, DC, USA, 1980.
52. Weeks, E.P.; Ericson, D.W.; Holt, C.L.R. *Hydrology of the Little Plover River Basin Portage County, Wisconsin and the Effects of Water Resource Development*; Water-Supply Paper for United States Geological Survey; United States Geological Survey: Reston, VA, USA, 1965.
53. Clayton, L. *Pleistocene Geology of Adams County, Wisconsin*; University of Wisconsin-Extension and Geological and Natural History Survey: Madison, WI, USA, 1987.
54. Goc, M.J. The Wisconsin Dust Bowl. *Wis. Mag. Hist.* **1990**, *73*, 163–201.
55. Prengaman, K. Groundwater War Pits Farmers Against Fish. Wisconsin Center for Investigative Journalism, 13 July 2013. Available online: http://wisconsinwatch.org/2013/07/groundwater-war-pits-wisconsin-farms-against-fish-2/ (accessed on 15 April 2015).
56. Wisconsin Department of Natural Resources (WDNR). Central Sands Strategic Analysis. Available online: http://dnr.wi.gov/topic/eia/cssa.html (accessed on 13 April 2015).
57. Bell, E.A.; Sherrill, M.G. *Water Availability in Central Wisconsin—An Area of Near-Surface Crystalline Rock*; Water-Supply Paper for United States Geological Survey: Reston, VA, USA, 1974.
58. Joachim, D.R.; Gotkowitz, M.B.; Potter, K.W.; Bradbury, K.R.; Vavrus, S.J.; Loheide, S.P. *Forecasting Impacts of Extreme Precipitation Events on Wisconsin's Groundwater Levels*; Open-File Report; Wisconsin Geological & Natural History Survey: Madison, WI, USA, 2011. Available online: http://wgnhs.uwex.edu/pubs/000897/ (accessed on 15 April 2015).

59. Knobeloch, L.; Gorski, P.; Christenson, M. Private drinking water quality in rural Wisconsin. *J. Environ. Health* **2013**, *75*, 16–20.
60. WHO. *Guidelines for Drinking Water Quality*, 4th ed.; World Health Organization: Geneva, Switzerland, 2011.
61. U.S. Environmental Protection Agency. *National Primary Drinking Water Standards*; Environmental Protection Agency: Washington, DC, USA, 2000; pp. 76708–76753.
62. Guse, C.E.; Marbbella, A.M.; George, V.; Layde, P.M. Radium in Wisconsin drinking water: An analysis of osteosarcoma risk. *Arch. Environ. Health* **2002**, *57*, 294–303.
63. Gilkeson, R.H.; Cowart, J.B. Radium, radon, and uranium isotopes in ground water from Cambrian–Ordovician sandstone aquifers in Illinois. In *Radon in Ground Water—Hydrogeologic Impact and Indoor Air Contamination*; Graves, B., Ed.; Lewis Publishers, Inc.: Chelsea, MI, USA, 1987; pp. 403–422.
64. Wilson, J.T. *Water-Quality Assessment of the Cambrian-Ordovician Aquifer System in the Northern Midwest, United States*; Scientific Investigations Report; United States Geological Survey: Reston, VA, USA, 2012. Available online: http://pubs.usgs.gov/sir/2011/5229 (accessed on 15 April 2015).
65. Wisconsin Department of Natural Resources (WDNR). Radium in Drinking Water. PUB-DG-008 2014. Available online: http://dnr.wi.gov/files/pdf/pubs/dg/dg0008.pdf (accessed on 15 April 2015).
66. Sturchio, N.C.; Banner, J.L.; BInz, C.M.; Heraty, L.B.; Musgrove, M. Radium geochemistry of ground waters in Paleozoic carbonate aquifers, midcontinent, USA. *Appl. Geochem.* **2001**, *16*, 109–122.
67. Gilkeson, R.H.; Cartwright, K.; Cowart, J.B.; Holtzman, R.B. *Hydrogeologic and Geochemical Studies of Selected Natural Radioisotopes and Barium in Ground Water in Illinois*; Report for Illinois Water Resources Center: Urbana, IL, USA, 1983, pp. 1–93.
68. Siegel, D.I. Sulfur isotope evidence for regional recharge of saline water during continental glaciation, north-central United States. *Geology* **1990**, *18*, 1054–1056.
69. Millard, P. Brown County Cities Find Water Crisis Solution in Manitowoc County. Available online: http://www.bizjournals.com/milwaukee/stories/2007/12/10/focus1.html?page=all (accessed on 15 April 2015).
70. Bergquist, L. Fond du Lac to Pay Settlement over Radium in Drinking Water. Available online: http://www.jsonline.com/news/wisconsin/37527669.html (accessed on 15 April 2015).
71. Wisconsin Department of Natural Resources (DNR). *DNR Approves New Berlin Request to Divert Lake Michigan Water*; Department of Natural Resources: Madison, WI, USA, 21 May 2009.
72. Behm, D. Waukesha Turns to More Radium-Laced Water after Well Pump Fails. Available online: http://www.jsonline.com/news/waukesha/waukesha-turns-to-radium-contaminated-water-after-well-pump-fails-b99108416z1-225570262.html (accessed on 15 April 2015).
73. Waukesha Water Utility Public Radium Notice. Letter to the Public (2014). Available online: http://www.ci.waukesha.wi.us/web/guest/redium (accessed on 15 May 2015).

74. Behm, D. Waukesha Concedes it Can't Meet Deadline for Radium-Free Water. Milwaukee Journal Sentinel, 19 November 2014. Available online: http://www.jsonline.com/news/waukesha/waukesha-concedes-it-can-meet-deadline-for-radium-free-water-b99393845z1–283255831.html (accessed on 15 April 2015).
75. Smith, A.H.; Lingas, E.O.; Rahman, M. Contamination of drinking-water by arsenic in Bangladesh: A public health emergency. *Bull. World Health Organ.* **2000**, *78*, 1093–1103.
76. Riewe, T.; Weissbach, A.; Heinen, L.; Stoll, R. Naturally occurring arsenic in well water in Wisconsin. *Water Well J.* **2000**, *49*, 24–29.
77. Knobeloch, L.M.; Zierold, K.M.; Anderson, H.A. Association of arsenic-contaminated drinking-water with prevalence of skin cancer in Wisconsin's Fox River valley. *J. Health Popul. Nutr.* **2006**, *24*, 206–213.
78. Schreiber, M.E.; Simo, J.A.; Freiberg, P.G. Stratigraphic and geochemical controls on naturally occurring arsenic in groundwater, Eastern Wisconsin, USA. *Hydrogeol. J.* **2000**, *8*, 161–176.
79. Center for Watershed Science and Education (CWSE) WI Well Water Viewer, University of Wisconsin-Stevens Point. Available online: http://www.uwsp.edu/cnr-ap/watershed/Pages/WellWaterViewer.aspx (accessed on 13 April 2015).
80. Root, T.L.; Gotkowitz, M.B.; Bahr, J.M.; Attig, J.W. Arsenic geochemistry and hydrostratigraphy in Midwestern U.S. glacial deposits. *Ground Water* **2010**, *48*, 903–912.
81. Johnson, D.M.; Riewe, T. Arsenic and Northeastern Wisconsin. *Water Well J.* **2006**, *60*, 26–31.
82. Burkel, R.S.; Stoll, R.C. Naturally occurring arsenic in sandstone aquifer water supply wells of Northeastern Wisconsin. *Groundw. Monit. Remediat.* **1999**, *19*, 114–121.
83. Schreiber, M.E.; Gotkowitz, M.B.; Simo, J.A.; Freiberg, P.G. Mechanisms of arsenic release to ground water from naturally occurring sources, eastern Wisconsin. In *Arsenic in Ground Water*; Welch, A., Stollenwerk, K., Eds.; Kluwer Academic Publishers: Boston, MA, USA, 2003; pp. 259–280.
84. Gotkowitz, M.B.; Schreiber, M.S.; Simo, J.A. Effects of water use on arsenic release to well water in a confined aquifer. *Ground Water* **2004**, *42*, 568–575.
85. Johnson, D. Written communication, 28 August 2008.
86. Luczaj, J.A.; McIntire, M. Geochemical characterization of MVT mineralization in eastern Wisconsin Paleozoic sedimentary rocks: Implications for groundwater quality. Manuscript in preparation.
87. Thornburg, K.; Sahai, N. Arsenic occurrence, mobility, and retardation in sandstone and dolomite formations of the Fox River Valley, Eastern Wisconsin. *Environ. Sci. Technol.* **2004**, *38*, 5087–5094.
88. Ozsvath, D.L. Fluoride and environmental health: A review. *Rev. Environ. Sci. Biotechnol.* **2009**, *8*, 59–79.
89. Tiemann, M. *Fluoride in Drinking Water: A Review of Fluoridation and Regulation Issues*; Congressional Research Service: Washington, DC, USA, 2013; pp. 1–21.
90. Ozsvath, D.L. Fluoride concentrations in a crystalline bedrock aquifer Marathon County, Wisconsin. *Environ. Geol.* **2006**, *50*, 132–138.

91. Wisconsin Department of Natural Resources (WDNR). Groundwater Retrieval Network. Available online: http://prodoasext.dnr.wi.gov/inter1/grn$.startup (accessed on 20 October 2014).
92. Luczaj, J.A.; Zorn, M.; Baeten, J. *An Evaluation of the Distribution and Sources of Dissolved Strontium in the Groundwater of Eastern Wisconsin, with a Focus on Brown and Outagamie Counties*; Final Report Submitted to the UW Water Resources Institute: Madison, WI, USA, 15 November 2013.
93. Baeten, J. Spatial Distribution and Source Identification of Dissolved Strontium in Eastern Wisconsin's Cambrian-Ordovician Aquifers. Master's Thesis, University of Wisconsin, Green Bay, WI, USA, 2013.
94. Luczaj, J.A.; Baeten, J.; Zorn, M. Distribution and Sources of Dissolved Strontium in the Groundwater of Eastern Wisconsin. Manuscript in preparation.
95. Holt, C.; Skinner, E.L. Ground-water quality in Wisconsin through 1972. *Wis. Geol. Nat. Hist. Surv. Inform. Circular* **1973**, *22*, 1–148.
96. Nichols, M.S.; McNall, D.R. Strontium content of Wisconsin municipal waters. *J. Am. Water Works Assoc.* **1957**, *49*, 1493–1498.
97. Özgür, S.; Sümer, H.; Koçoğlu, G. Rickets and soil strontium. *Arch. Dis. Child.* **1996**, *75*, 524–526.
98. Curzon, M.E.J.; Spector, P.C. Enamel mottling in a high strontium area of the USA. *Community Dent. Oral Epidemiol.* **1977**, *5*, 243–247.
99. U.S. Environmental Protection Agency (USEPA). EPA Makes Preliminary Determination to Regulate Strontium in Drinking Water (20 October 2014). Available online: http://yosemite.epa.gov/opa/admpress.nsf/6427a6b7538955c585257359003f0230/327f339e63facb5a85257d77005f4bf9!OpenDocument (accessed on 15 April 2015).
100. Bethke, C.M.; Marshak, S. Brine migrations across North America—The plate tectonics of groundwater. *Annu. Rev. Earth Planet. Sci.* **1990**, *18*, 237–315.
101. Klimas, A.; Mališauskas, A. Boron, fluoride, strontium, and lithium anomalies in fresh groundwater of Lithuania. *Geologija* **2008**, *50*, 114–124.
102. Oberle, S. Written communication, 22 June 2011.
103. Shaw, B. Nitrogen contamination sources: A look at relative contributions. In Proceedings of the Nitrate in Wisconsin's Groundwater: Strategies and Challenges Conference, Stevens Point, WI, USA, 10 May 1994.
104. Department of Agriculture, Trade and Consumer Protection (DATCP), Agricultural Chemicals in Wisconsin Groundwater (April 2008). Available online: http://datcp.wi.gov/uploads/Environment/pdf/ARMPub180.pdf (accessed on 15 April 2015).
105. Schmidt, R.R. *Groundwater Contamination Susceptibility Map and Evaluation*; Wisconsin's Groundwater Management Plan Report; Wisconsin Department of Natural Resources: Madison, WI, USA, 1987.
106. Masarik, K.; Norman, J.; Brye, K. Long-term drainage and nitrate leaching below well-drained continuous corn agroecosystems and a prairie. *J. Environ. Prot* **2014**, *5*, 240–254.

107. Randall, G.W.; Huggins, D.R.; Russelle, M.P.; Fuchs, D.J.; Nelson, W.W.; Anderson, J.L. Nitrate losses through subsurface tile drainage in conservation reserve program, alfalfa, and row crop systems. *J. Environ. Qual.* **1997**, *26*, 1240–1247.
108. Erb, K.R.; Stieglitz, R. *Final Report of the Northeast Wisconsin Karst Task Force*; University of Wisconsin—Extension: Madison, WI, USA, 2007; pp.1–46.
109. Bauer, A.C.; Wingert, S.; Fermanich, K.J.; Zorn, M.E. Well water in karst regions of northeastern Wisconsin contains estrogenic factors, nitrate, and bacteria. *Water Environ. Res.* **2013**, *85*, 318–326.
110. Borchardt, M.A.; Bertz, P.D.; Spencer, S.K.; Battigelli, D.A. Incidence of enteric viruses in groundwater from household wells in Wisconsin. *Appl. Environ. Microbiol.* **2003**, *69*, 1172–1180.
111. Borchardt, M.A.; Haas, N.L.; Hunt, R.J. Vulnerability of drinking-water wells in La Crosse, Wisconsin, to enteric-virus contamination from surface water contributions. *Appl. Environ. Microbiol.* **2004**, *70*, 5937–5946.
112. Borchardt, M.A.; Bradbury, K.R.; Gotkowitz, M.B.; Cherry, J.A.; Parker, B.L. Human enteric viruses in groundwater from a confined bedrock aquifer. *Environ. Sci. Technol.* **2007**, *41*, 6606–6612.
113. Hunt, R.J.; Borchardt, M.A.; Richards, K.D.; Spencer, S.K. Assessment of sewer source contamination in drinking water wells using tracers and human enteric viruses. *Environ. Sci. Technol.* **2010**, *44*, 7956–7963.
114. Borchardt, M.A.; Bradbury, K.R.; Alexander, E.C., Jr.; Kolberg, R.J.; Alexander, S.C.; Archer, J.R.; Braatz, L.A.; Forest, B.M.; Green, J.A.; Spencer, S.K. Norovirus outbreak caused by a new septic system in a dolomite aquifer. *Ground Water* **2011**, *49*, 85–97.
115. Borchardt, M.A.; Spencer, S.K.; Kieke, B.A.; Lambertini, E.; Loge, F.J. Viruses in non-disinfected drinking water from municipal wells and community incidence of acute gastrointestinal illness. *Environ. Health Perspect.* **2012**, *120*, 1272–1279.
116. Uejio, C.K.; Yale, S.H.; Malecki, K.; Borchardt, M.A.; Anderson, H.A.; Patz, J.A. Drinking water systems, hydrology, and childhood gastrointestinal illness in central and Northern Wisconsin. *Am. J. Public Health* **2014**, *104*, 639–646.
117. Erb, K.R.; Ronk, E. Documenting the regional impacts of karst task force recommendations on 'brown water incidents' in Northeast Wisconsin, USA. *Resources* **2015**, under review.
118. Chern, L. Written communication, 8 April 2014
119. Gotkowitz, M.B.; Liebl, D.S. Municipal drinking water safety, the link between groundwater, pathogens, and public health. *Wis. Geol. Nat. Hist. Surv. Educ. Ser.* **2013**, *053*, 1–4.
120. Wisconsin Department of Agriculture, Trade, and Consumer Protection. Wisconsin groundwater quality: Agricultural chemicals in Wisconsin groundwater. *Agric. Resour. Manag.* **2008**, *180*, 21. Available online: http://datcp.wi.gov/uploads/Environment/pdf/ARMPub180.pdf (accessed on 15 April 2015).
121. Wisconsin Department of Agriculture, Trade, and Consumer Protection. Fifteen Years of the DATCP Exceedence Well Survey 2010. Available online: http://datcp.wi.gov/uploads/Environment/pdf/FifteenYearsoftheDATCPExceedenceSurvey.pdf (accessed on 15 April 2015).

122. Benotti, M.J.; Trenholm, R.A.; Vanderford, B.J.; Holady, J.C.; Stanford, B.D.; Snyder, S.A. Pharmaceuticals and endocrine disrupting compounds in U.S. drinking water. *Environ. Sci. Techol.* **2009**, *43*, 597–603.
123. Cook, T.; Mathewson, P.; Nekola, K. Don't Drink the Water—Groundwater Contamination and the "Beneficial Reuse" of Coal Ash in Southeast Wisconsin. Clean Wisconsin, (November 2014). Available online: http://www.cleanwisconsin.org/wp-content/uploads/2015/02/dont-drink-the-water-report-clean-wisconsin.pdf (accessed on 15 April 2015).
124. Lourigan, J.; Phelps, W. Caledonia groundwater molybdenum investigation Southeast Wisconsin—2013. Wisconsin Department of Natural Resources: Madison, WI, USA, 2013. Available online: http://dnr.wi.gov/files/PDF/pubs/WA/WA1625.pdf (accessed on 15 April 2015).
125. United States Environmental Protection Agency (USEPA). Hazardous and Solid Waste Management System; Disposal of Coal Combustion Residuals from Electric Utilities. Available online: http://www.gpo.gov/fdsys/pkg/FR-2015-04-17/pdf/2015-00257.pdf (accessed on 15 April 2015).

MDPI AG
Klybeckstrasse 64
4057 Basel, Switzerland
Tel. +41 61 683 77 34
Fax +41 61 302 89 18
http://www.mdpi.com/

Resources Editorial Office
E-mail: resources@mdpi.com
http://www.mdpi.com/journal/resources

MDPI • Basel • Beijing • Wuhan • Barcelona
ISBN 978-3-03842-205-1
www.mdpi.com